UNIVERSITÄT
DUISBURG
ESSEN

Highway Embankment Constructed on Soft Soil Improved by Stone Columns with Geosynthetic Materials

Dissertation
Submitted for the degree of
Doctor of Engineering

By

Mohamed Basheer Dardeer Elsawy,
Aswan, Egypt

Institute of Geotechnical Engineering,
Department of Civil Engineering,
Faculty of Engineering,
Duisburg-Essen University

Essen, 2010

Date of Submission:	**May 20, 2010**
Date of Examination:	**October 4, 2010**
Reviewers:	**Prof. Dr.-Ing. W. Richwien**
	Prof. Dr.-Ing. C. Boley

Acknowledgements

I would like to present great thanks to my supervisor, Prof. W. Richwien, for the patient guidance, encouragement and advice who has provided throughout my time as his student. I have been extremely lucky to have a supervisor who cared so much about my work, and who responded to my questions and queries so promptly. Special thanks to Prof. K. Lesny for her great assistance.

I would also like to thank all the members of staff at Geotechnical Engineering institute who helped me a lot. Their kindness and generosity will stay in my memory forever. The financial suppor provided by the Egyptian Ministry of Higher Education for my stay in Germany are is also gratefully acknowledged.

While it is not possible to give acknowledgements to all those who assisted me, I have to give special thanks to my family whose prayers and moral support enabled me to successfully pursue my study.

In vielen Gebieten stehen weltweit entlang der Flüsse und der Küsten weiche Böden an. Das Bauen auf diesen Böden ist schwierig, weil sie nur eine geringe Festigkeit haben und sich unter Last stark zusammendrücken. Die Baugrundverbesserung der anstehenden Böden durch Steinsäulen hat sich in den letzten Jahrzehnten als eine effektive Methode erwiesen, auf Böden dieser Art leichte Konstruktionen wie Dämme von Verkehrsanlagen sicher zu gründen.

Die Steinsäulen beziehen ihre Tragfähigkeit aus der Bettung, die sie aus dem umgebenden Boden erfahren. Allerdings muss der umgebende Boden zur Aktivierung dieser Bettung eine Mindestfestigkeit haben, weil andernfalls die Stützung nicht zur Aufnahme der Lasten reicht. Um die Dispersion der Steinsäulen in den umgebenden Boden zu vermeiden, werden die Säulen in sehr weichen Böden von einer geosynthetischen Membran eingehüllt. Die Tragfähigkeit der Steinsäulen wird so gesteigert, ihre Gebrauchstauglichkeit und Wirtschaftlichkeit ergibt sich aus den lateralen und vertikalen Formänderungen während der Konsolidierung. Daher werden Ansätze zur Abschätzung dieser Verformungen und ihrer Dauer benötigt.

Im Rahmen dieser Dissertation wird das Verformungsverhalten von nicht ummantelten und ummantelten Steinsäulen in einem weichen bindigen Boden (Bremerhavener Klei) mit FE Berechnungen grundsätzlich untersucht. Zunächst wird der Einfluss des Säulendurchmessers und des Säulenabstands sowie der Ummantelung und ihrer Festigkeit und Steifigkeit auf das Tragverhalten untersucht. Die Ergebnisse zeigen, dass nicht ummantelte Säulen mit einem kleineren Durchmesser und kleinem Abstand eine größere Tragfähigkeit haben als solche mit großem Durchmesser und großem Abstand. Mit der Ummantelung steigt die Tragfähigkeit dramatisch, zugleich nimmt die Setzung ab. Dieser Effekt wird mit steiferen Ummantelungen noch gesteigert. Wenn die Säulen nur teilweise ummantelt werden, nimmt ihre Tragfähigkeit mit der Länge der Ummantelung zu. Grundsätzlich ist der durch die Ummantelung erzielbare Zuwachs der Tragfähigkeit nach der Konsolidierung größer als unmittelbar nach der Lastaufbringung, die Konsolidierungsdauer wird deutlich verkürzt.

Im zweiten Teil der Arbeit wird das Setzungsverhalten von ummantelten und nicht ummantelten Steinsäulen unter einer beispielhaften Dammschüttung analysiert. Für den umgebender Boden werden die Kennwerte von zwei realen und in der Literatur umfassend dokumentierten Böden angesetzt, es sind dies der Bremerhavener Klei und der Hamburger Schlick. Variiert werden der Säulendurchmesser, der Säulenabstand, die Art der Ummantelung (teilweise oder ganz) und die Steifigkeit der Ummantelung. Die verwendeten Rechenansätze werden anhand der Messergebnisse aus einem Anwendungsfall überprüft und ergeben eine gute Übereinstimmung.

Es kann gezeigt werden, dass Steinsäulen die Tragfähigkeit der Gründung erhöhen, sie reduzieren die Setzungen und beschleunigen die Konsolidation. Setzungen und Konsolidationsdauer sind umso kleiner bzw. kürzer, je dichter die Säulen angeordnet sind. Demgegenüber ist der Säulendurchmesser für die Setzungsgröße und die Dauer der Konsolidierung von nur untergeordneter Bedeutung.

Die Ummantelung der Säulen hat eine weitere Steigerung der Tragfähigkeit und Reduktion der Setzungen proportional zur Steifigkeit der Ummantelung zur Folge.

Stichworte: Steinsäulen, weicher Ton, Ummantelung, Geogitter, Konsolidierung

Great areas all over the world, particularly along the rivers and the seas, are covered with soft clay. Construction on soft natural soil is considered a risk due to its low shear strength and high compressibility. Stone columns are an effective improvement method for soft soils under light structures such as rail or road embankments. The stone columns derive their load carrying capacity from the passive earth pressure resistance developed against the bulging of the column which thereby depending on the shear strength of the surrounding soil. To avoid dispersion of the stones into the clay and to improve the stone columns as reinforcing elements, geosynthetics are used as an encasement of the stone columns. Increasing lateral and vertical deformations over the consolidation time controls the serviceability state and affects the economy of the embankments. Therefore, additional efforts to predict the long-term behavior of the reinforced soft soil with ordinary and encased stone columns foundation are required.

In this research full scale stone columns in Bremerhaven clay, are analyzed using the finite element program Plaxis. Firstly, the stone columns are only loaded to investigate the effect of varying parameters like spacing distance between columns, column diameter, geogrid encasement and stiffness of the geogrid, and encasement depth on the behavior of the stone column in short and long term conditions. The results showed that the ordinary stone columns with narrower spacing distances and smaller diameters have a greater bearing capacity and show smaller settlement as well as lateral bulging than wider spacings and greater diameters of stone columns. When using geogrids as encasement for stone columns, a huge increase in the bearing capacity of the stone column as well as a huge reduction in the bulging occurs. More improvement occurs in the behavior of the encased stone columns with increasing encasement stiffness in both short and long term conditions. The bearing capacity of the partially encased stone columns increases with increasing encasement depth. The increase in the bearing capacity in long term is more significant than that in short term conditions under working loads.

Secondly, the non-reinforced and the reinforced soft clay with ordinary and encased stone columns have been loaded by a highway embankment fill. Two types of soft clay have been used which are the Bremerhaven clay and the Hamburg clay. The analysis is performed to study the effect of spacing distance between columns, column diameter, geogrid stiffness and encasement depth on the behavior of the reinforced soft soils during and after the consolidation. A case history of an embankment constructed on the reinforced soft soil with stone columns is also simulated and gave a good agreement. Using stone columns in soft clay reduces the settlement and the production of the initial pore water pressure and accelerates the consolidation time to minimum values. The smaller the spacing distance between the columns is, the faster the consolidation is and the smaller the settlement, the bulging of the column and the generated excess pore water pressure are. The construction time of the reinforced clay decreases also with decreasing diameter of the column. But the settlement has no significant decrease with decreasing diameter of the column. Once the stone columns are encased with geogrid under embankment loads, the consolidation time, the settlement, the column bulging and the excess pore water pressure are reduced with a high degree. Further reduction occurs in the deformation and the excess pore water pressure with increasing stiffness of the encasement.

Keywords: stone columns, soft clay, encasement, geogrid, consolidation

Contents

Symbol	Dimension	Meaning
Latina Symbols		
A_c	[L²]	Cross sectional area of the column
A_e	[L²]	Cross sectional area of the unit cell
A_s	[L²]	Cross sectional area of the surrounding soil
a_s	[1]	Area replacement ratio
B	[L]	Half width of the plain strain unit cell
b_c	[L]	Half width of the wall in the plain strain unit cell
C	[1]	Material constant
c	[F/L²]	Cohesion
$c`_r$	[L²/T]	Modified coefficient of radial consolidation
$c`_v$	[L²/T]	Modified coefficient of vertical consolidation
C_c	[1]	Compression index
c_r	[L²/T]	Coefficient of radial consolidation
C_s	[1]	Swelling index
c_u	[F/L²]	Undrained shear strength
c_v	[L²/T]	Coefficient of vertical consolidation
C_α	[1]	Secondary compression index
d	[L]	Diameter of the stone column
d_e	[L]	Diameter of the unit cell
E	[F/L²]	Elasticity modulus
e	[1]	void ratio
E_0	[F/L²]	Initial Elasticity modulus
E_{50}	[F/L²]	Secant modulus at 50 % strength
E_c	[F/L²]	Elasticity modulus of the stone column
E_{gp}	[F/L²]	Modulus of elasticity of the granular pile
E_{gpi}	[F/L²]	Modulus of elasticity of the granular pile at a depth z_i
E_s	[F/L²]	Elasticity modulus of the soil
E_{ur}	[F/L²]	Unloading and reloading Elasticity modulus
H	[L]	Thickness of the soil
h	[L]	Encasement depth
J	[F/L]	Stiffness of the geosynthetic materials
k_h	[L/T]	Horizontal permeability
K_o	[1]	Coefficient of earth pressure at rest
k_v	[L/T]	Vertical permeability
L	[L]	Length of the stone column
m_{vc}	[L²/F]	Coefficient of compressibility of the stone material
m_{vs}	[L²/F]	Coefficient of compressibility of the surrounding soil
N	[1]	Diameter ratio
n	[1]	Number of geosynthetic layers
n_s	[1]	steady stress concentration ratio

Symbole	Dimension	Meaning
P	[F/L²]	Applied pressure
p´	[F/L²]	Effective mean stress
$p´_o$	[F/L²]	Initial effective mean stress
q	[F/L²]	Applied load
r_c	[L]	Radius of the stone column or the drain well
r_e	[L]	Radius of the unit cell
R_s	[1]	Ratio between the total settlement of the reinforced clay with ordinary stone columns and the non-reinforced clay
$R_{s(NR)}$	[1]	Ratio between the total settlement of the reinforced clay with encased stone columns and the non-reinforced clay
$R_{s(R)}$	[1]	Ratio between the total settlement of the reinforced clay with encased columns and the reinforced clay with ordinary columns
R_t	[1]	Ratio between the consolidation time of the reinforced clay with ordinary stone columns and the non-reinforced clay
S	[L]	Spacing distance
s	[L]	Settlement
SC_{accel}	[1]	Participation of stress concentration in the consolidation acceleration
s_{max}	[L]	Maximum settlement
s_{NR}	[L]	Settlement of the reinforced soil with ordinary stone columns
s_R	[L]	Settlement of the reinforced soil with encased stone columns
t	[T]	Time
T	[F/L]	Hoop tension forces in geosynthetic materials
$T`_r$	[1]	Modified time factor of the radial consolidation
$T`_v$	[1]	Modified time factor of the vertical consolidation
t_c	[T]	Time up to the end of the primary consolidation
T_r	[1]	Time factor of the radial consolidation
T_v	[1]	Time factor of the vertical consolidation
u_h	[L]	Lateral bulging of the column
$u_{h(max)}$	[L]	Maximum lateral bulging of the column
$u_{h(NR)}$	[L]	Lateral bulging of the ordinary stone column
$u_{h(R)}$	[L]	Lateral bulging of the encased stone column
u_o	[F/L²]	Original pore water pressure
U_r	[1]	degree of radial consolidation
U_{rv}	[1]	degree of radial and vertical consolidation
U_v	[1]	degree of vertical consolidation
v	[L]	Vertical displacement
x	[L]	Horizontal distance from the column centreline
y	[L]	Depth under the top of the column
z	[L]	Depth in soil

Symbole	Dimension	Meaning
Δu	[F/L²]	Excess pore water pressure
Δu_i	[F/L²]	Average maximum initial excess pore water pressure
Greeks Symbols		
α	[1]	Rate of the increase of the modulus of elasticity of the granular pile with depth
γ	[F/L³]	Soil unit weight
γ_d	[F/L³]	Dry soil unit weight
γ_{wet}	[F/L³]	Wet soil unit weight
$\dot{\varepsilon}$	[1/T]	Strain rate
ε_1	[1]	Vertical strain
ε_a	[1]	Axial strain
ε_c	[1]	Strain up to the end of the primary consolidation
ε_v	[1]	Volumetric strain
κ^*	[1]	Modified swelling index
λ^*	[1]	Modified compression index
μ^*	[1]	Modified secondary compression index
ξ	[1]	Poisson ratio factor
σ	[F/L²]	Applied average stress
σ'_r	[F/L²]	Effective radial stress
σ'_{ro}	[F/L²]	Initial effective radial stress
σ'_v	[F/L²]	Effective vertical stress
σ'_{vo}	[F/L²]	Initial effective vertical stress
σ_1	[F/L²]	Major stress, (maximum vertical stress in triaxial test)
σ_3	[F/L²]	Minor stress, (confining pressure in triaxial test)
σ_c	[F/L²]	Stress in the column
σ_{cs}	[F/L²]	Steady stress in the column
σ_h	[F/L²]	Horizontal stress
σ_s	[F/L²]	Stress in soft clay ground
σ_{ss}	[F/L²]	Steady stress in the surrounding soil
σ_v	[F/L²]	Total vertical stress
$\sigma_{v(f)}$	[F/L²]	Average final total vertical stress
$\sigma_{v(i)}$	[F/L²]	Average initial total vertical stress
φ	[1]	Friction angle
ψ	[1]	Dilatancy angle
ν	[1]	Piossan ratio
ν_c	[1]	Poisson ratio of the stone
ν_s	[1]	Poisson ratio of the surrounding soil

Abbreviations	
ESC	Encased stone columns
I.Wr	Improvement width ratio
OSC	Ordinary stone columns
sc	Stone columns
SCF	Stress concentration factor or ratio
SP	Settlement plate

with: F... Force,
L... Length,
T... time

1 Introduction

1.1 Engineering background

Great areas all over the world, particularly along the rivers and the seas, are covered with thick soft alluvial and marine clay. As increasing developments on these areas recently, a lot of buildings and industry structures are being constructed. Construction on soft natural soil is considered a risk and poses major problems to geotechnical engineers due to its low shear strength and high compressibility. A lot of soil improvement methods have been used to deal with soft soil problems. The improvement methods of the soft soil include replacement, preloading, sand drains and preloading, vacuum pressure and preloading, dynamic compaction, lime stabilization, geosynthetic reinforcement and stone or gravel columns. The stone column method is the most effective to soft soil improvement. Stone columns have higher drainage ability and stiffness than sand drains. Therefore, ground reinforcement by stone columns solves the problems of the soft soil by providing advantage of reduced settlement and accelerated consolidation process. Another advantage of this method is the simplicity of its construction.

The use of stone columns as a method of soft soil improvement has been successfully implemented around the world. The stone column technique was developed in Germany about 60 years ago. In 1939, Steuermann claimed that using stone columns could double the bearing capacity of a soft soil site. Hughes and Withers (1974) reported that stone columns were well known in France in the 1830's and were used to support heavy foundations of ironworks at the artillery arsenal in Bayonne. Hence, Stone columns have been regularly used in Europe since 1950's and in North America since 1972.

Technique of stone columns to improve the mechanical properties of marginal soils is well established. The carrying capacity of the stone columns depends mainly on the lateral support. The lateral support is provided by the native soft soil and depends on its shear strength. The stiffness of the stone column also plays an important role in the increase of the stress concentration within the column, which leads to increase the bearing capacity of the improved ground.

1.2 Current research topics

In order to achieve the engineering and the economical purposes, investigations into the stone columns reinforced soft soil technique have received a great deal of interest in the recent years. A detailed review of the existing research is given in this thesis. The major topics of these publications are:

- Experimental standard and modified triaxial tests of stone columns surrounded with soft soil;
- Experimental models in laboratory taken in consideration failure modes of the long and the short stone columns;
- Stone column stiffness role in soft ground settlement reducing;
- Experimental models loading tests in laboratory conducted on geosynthetic reinforced stone columns;

- Analytical analyses and numerical simulation on stone columns reinforced soft soil foundations.

With the efforts of many investigators all over the world during the last two decades a large quantity of research was carried out on these topics. A great deal of experimental data and theoretical analyses explained the stone columns–soft soil improvement technique and its effect on the bearing capacity of the soft soil. The influence of the geosynthetic reinforced stone column–soft soil improvement technique on the behavior of the soft soil and the stone column was also explained. Most past researchers studied the stone columns technique only in the short term conditions. A lot of soil models were used in the theoretical analyses in order to calculate the displacements and the bearing capacity of the improved ground. Most of the analytical and the numerical analyses used elastic models for soft soil and stone materials in spite of the behavior of these soils are elasto-plastic. The generated heave in short term conditions wasn't also studied and it needs to be illustrated. Some researchers studied the stone columns bulging but the variation of bulging with column diameter and spacing between columns especially in long term conditions was not explained. Hence, the behavior of the reinforced soft soil with ordinary and encased stone columns foundation needs to be studied in long term conditions.

Although a great number of the experimental and the theoretical investigations on these subjects were conducted, the present design methods are empirical and only limited information is available on the design of the stone columns. This is due to the used models have small dimension and are studied in short term conditions. Full scale models are used in the current research. Most of researchers also used the geotextile encasement material although the geogrid encasement has the greater stiffness. The influence of the geogrid confinement on the bearing capacity and the lateral bulging of the stone columns is not clear particularly in long term conditions. The influence of the stiffness of the encased stone column on load sharing and stress concentration is also far from clear. The stress concentration needs to be studied during the consolidation. Finally, the role of the stress concentration in the acceleration of the consolidation needs also to be explained.

1.3 Scope and methods of the present research

Based in the engineering and the research background mentioned above, ordinary and encased stone columns with geogrid materials are used for reinforcing soft soil in undrained and drained conditions. The stone columns-soft soil foundation system is studied in this research, to investigate the improvements in the behavior of the reinforced soft ground. The effect of geogrid encasement on the stiffness, the bearing capacity, and the bulging of the stone column is also investigated. Numerical Plaxis 9 program is used to model the soft soils, the stone material, the highway embankment fill, and the geogrid materials. The specific objectives of this research are as follows:

a. Numerical analyses of a unit cell of a stone column and the surrounding soft soil have been conducted to study the effect of the ordinary and the encased stone column on the behavior of the reinforced soft soil foundation in short and long term conditions. The current study is conducted on soft soil considering following parameters:

- Spacing between columns and diameter of the column,

- Loading type, (loading stone column only and loading entire area),
- Loading conditions (undrained and consolidation conditions),
- Soft soil type (Bremerhaven clay and Hamburg clay), and
- Geogrid encasement, stiffness of the geogrid encasement, and encasement depth

b. FEM simulation for a case of study for an embankment resting on reinforced soft soil with ordinary stone columns is carried out. The numerical analyses results should be compared with the field measurements and should give a good agreement. The encased stone columns have been also used to reinforce the soft soil in the FEM analyses to imply the influence of the encasement on the behavior of the stone columns-soft soil foundation.

This research contains the following chapters,

In Chapter 1 the practical background, scope and research objective are outlined briefly.

Chapter 2 includes development of the stone columns concept, and its effect on the behavior of the soft soil. This chapter also introduces the literature review of the experimental and theoretical studies of the ordinary stone columns and the encased stone columns with geosynthetic materials, which reinforced soft soil.

Chapter 3 contains a brief description of Plaxis program, the element types for soil and geogrid material, and the constitutive models for the used soils.

Chapter 4 concerns with the numerical modelling and the selection of parameters of the unit cell parts. The results of the reinforced Bremerhaven clay by ordinary and encased stone columns under column loading only are discussed.

Chapter 5 continues with the results discussions of the non-reinforced and the reinforced Bremerhaven clay by stone columns under loads of an embankment.

Chapter 6 discusses also the results of the non-reinforced and the reinforced Hamburg clay by stone columns under loads of an embankment.

Chapter 7 indicates the results discussions of the reinforced Bremerhaven and Hamburg clay by ordinary stone columns with various spacings and diameters under loads of an embankment.

Chapter 8 presents the results discussions of the reinforced Bremerhaven and Hamburg clay by encased stone columns under loads of an embankment.

Chapter 9 shows the results of the modeling parts of a case of study of an embankment resting on reinforced soft soil by ordinary and encased stone columns.

Chapter 10 introduces the summery and the conclusion of this work based on the numerical study and the observations.

List of reference is given at the end of the thesis.

2 Soft Soil Engineering and State of The Art in Soil Improvement Using Stone Columns and Geosynthetic

2.1 General

The special nature of soft soil deposits are arguably the most interesting soil to work with from the viewpoint of geotechnical engineering. Soft soils are fairly widespread all over the world and the places of them are in important cities. There are two main problems encountered when undertaking civil constructions in soft soil deposits, excessive settlement and low shear strength. Due to large void ratio and inherent compressibility of such clays, consolidation and displacements can be noticeable under construction loads and continue long time after implementation of the structure. Low shear strength is particularly hazardous when constructing large embankment on soft clay base, facilitating potential circular or sliding failure planes. Hence, the need to ground improvement schemes is very necessary. Ground improvement by stone columns is considered to be a very effective method to improve soft soil properties.

A lot of research on stone columns to reinforce soft soil were previously carried out by many investigators all over the world. These research discussed the stone column effect on the enhancement of the properties of the soft soil. The stone columns cause an increase of the bearing capacity of the soft soils, and enhance the drainage and the dissipation of the excess pore water pressure.

2.2 Construction techniques on soft Soil

Soft soils are usually located near most river estuaries and harbor areas all over the world. But still, these areas are chosen to be developed. All structures built on soft soil are incompatible with weak foundation soil conditions. However, some techniques could be taken to overcome the problem, such as:

a) Drive deep foundations through the unsuitable soils,
b) Excavate and replace the soft soils with suitable soils,
c) Stabilize the soft soils with injected additives,
d) Construct in stages and wait until natural consolidation occurs,
e) Treat the soft soil by dewatering.

Additionally, there are some improvement techniques such as:

a) Geosynthetic reinforcement,
b) Fibre reinforcement,
c) Preloading with or without vertical drains,
d) Micro or mini piles,
e) Vacuum preloading method,
f) Dynamic compaction,
g) Lime columns,
h) Stone columns.

Ground reinforcement by stone columns method is the most effective technique due to it solves the soft soil problems by providing advantage of reduced settlement and accelerated consolidation process. Another advantage of this method is the simplicity of its construction. Within this research, the construction on soft soil will be treated by using non-reinforced and reinforced stone columns with geosynthetic materials.

2.3 Geosynthetic materials

Polymeric reinforcement materials are a subset of a much larger recent development in civil engineering materials: *geosynthetics*. ASTM has defined a *geosynthetic* as a planar product manufactured from a polymeric material used with soil, earth, or other geotechnical-related material as an integral part of a civil engineering project, structure or system. There are few developments that have had such a rapid growth and strong influence on so many aspects of civil engineering practice as geosynthetics. In 1970, there were only five or six geosynthetics available, while today more than 600 different geosynthetic products are sold throughout the world. The use of a geosynthetic can significantly increase the safety factor, improve performance, and reduce costs in comparison with conventional design and construction alternates.

2.3.1 Types and manufacture

Most geosynthetics are made from synthetic polymers such as polypropylene, polyester, polyethylene, polyamide, PVC, etc. These materials are highly resistant to biological and chemical degradation. Natural fibers such as cotton, jute, bamboo, etc., could be used as geotextiles and geogrids, especially for temporary applications, but with few exceptions they have not been promoted or researched as widely as polymeric geosynthetics. A convenient classification system for reinforcement materials is given in Diagram 1. Brief descriptions of the geosynthetic materials are provided in the following sections.

- *Geotextiles* the majority of today's geotextile fabrics are made from polypropylene, polyethylene, or polyester polymer fibers or yarns. Geotextiles are typically used to provide separation, soil reinforcement, drainage, filtration of soil particles, and a combination of these functions.
- *Geogrids* are reinforcement geosynthetics formed by intersecting and joining sets of longitudinal and transverse ribs with resulting open spaces called "apertures". These products are available for soil reinforcement in one direction (uniaxial), and also in two directions (biaxial).
- *Geonets* are primarily plastic material with continuous ribs oriented in a grid pattern with openings typically smaller than that of geogrids.
- *Geomembranes* are low permeability geosynthetics used as fluid barriers.
- *Geocomposite* is formed from a combination of geosynthetic materials such as geotextiles bonded to geonets. Each component of these "hybrid" materials has a specific function.

2.3.2 Functions and fields of application of the geosynthetic materials

Geosynthetic applications are usually defined by their primary or principal function. In a number of applications, in addition to the primary function, geosynthetics usually perform one or more secondary functions. It is important to consider both the primary and secondary functions in the design computation and specifications. The main functions of geosynthetic materials are filtration, drainage, separation, packing, protection, erosion control, sealing and reinforcement.

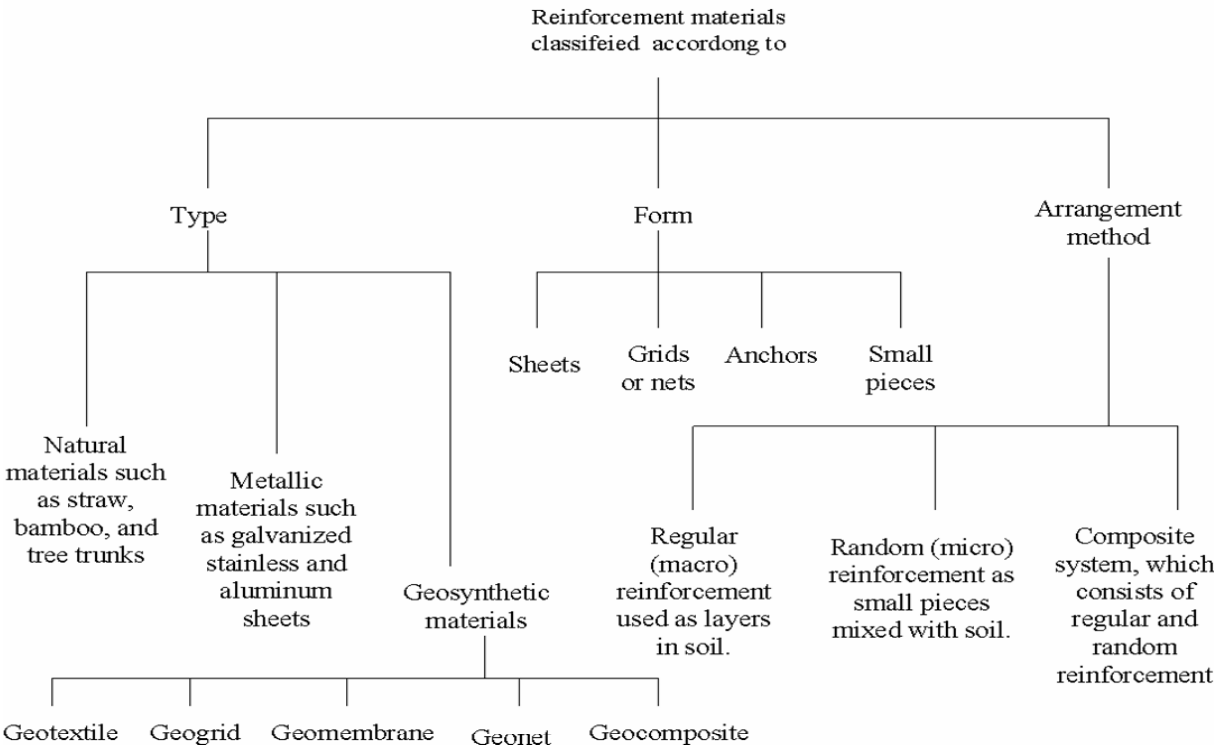

Diagram 2-1 Classification of the reinforcement materials

When used for reinforcement purposes, geotextiles, geogrids and composites are placed below or between soil layers and around columns to take up tensile forces and thereby improve their mechanical properties. The experimental works which were conducted proved that the concept of soil reinforcement increases the shear strength of soil and reduces the settlement, depending on the stiffness of reinforcement material. The use of geosynthetic reinforced soil structures has been successfully practiced for more than 30 years. The types of application fields are as the following, (Koerner, 2000).

- Paved and unpaved roads and parking lots, Fig. 2-1-a.
- Repair of Paved Roads and Parking Lots, Fig. 2-1-b.
-Railway roads and airport runway, Fig 2-1-c.
-Embankments and slopes, Fig. 2-1-d.
- Reinforcing Retaining Walls and Bulkheads, Fig. 2-1-e.
- Dams, Fig. 2-1-f.
- Tunnels, Fig. 2-1-g.
- Beneath Structures Foundations, Fig. 2-1-h.

The production cost of geosynthetics is low compared to other materials used for soil reinforcement, such as steel and other man-made materials. The reasons for the increased implementation of geosynthetics as soil reinforcement include the following:

- Deformability and high tensile strength,
- Ability to produce geosynthetic in different shapes, and strength and
- Ability to bond and interlock with soil particles and hence ensure composite action.

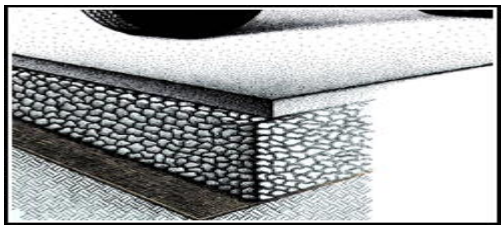

Fig. 2-1-a Reinforcement of subgrade soil for paved and unpaved roads

Fig. 2-1-b Repair of paved roads by placement a layer of geotextile under the new pavement

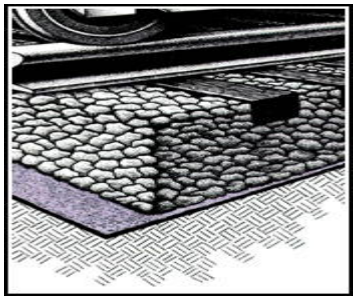

Fig. 2-1-c Geotextile sheet used as reinforcement in railway road

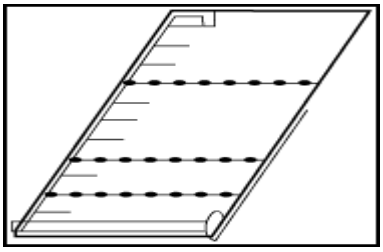

Fig. 2-1-d Geogrid used to reinforce the steep embankment

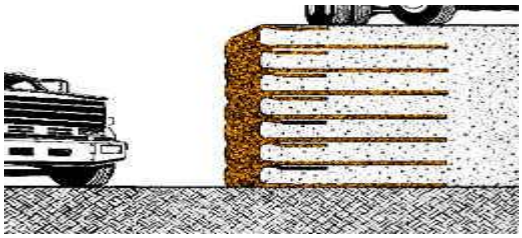

Fig. 2-1-e Reinforced Soil Retaining Walls

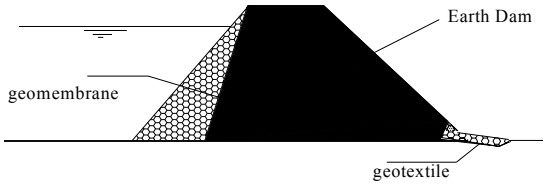

Fig. 2-1-f Geosynthetic use for Earth, earth-rock, and Roller compacted concrete dam waterproofing

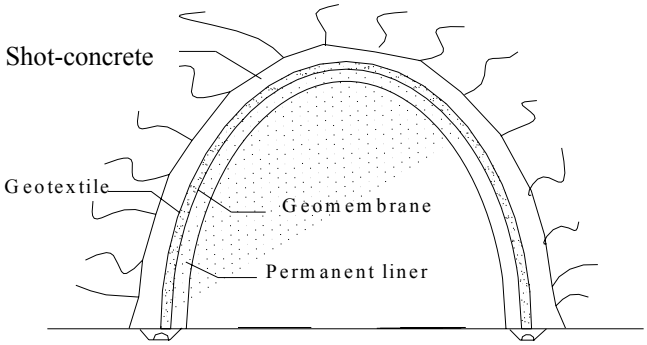

Fig. 2-1-g Geosynthetic Use for Tunnel Waterproofing

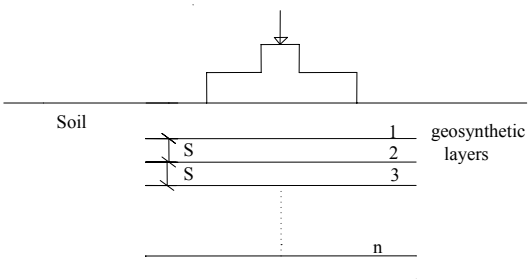

Fig. 2-1-h Geosynthetic use for reinforcement the poor soil under footing

Fig. 2-1 Geosynthetic applications (Koerner, 2000)

2.4 Stone columns

Stone columns are an extension of the vibro-compaction method used to treat cohesive soils, which was conceived in Germany in the mid of 1930s. Within the past 30 years, the value of stone columns to reinforce cohesive soils for foundation has been generally recognized. The stone column technique, developed mainly in Europe, now is increasingly used in many regions in the world primarily for embankments and road works. Among the various methods for improving soft ground conditions, stone columns are considered one of the most versatile and cost-effective ground improvement techniques. Stone columns have been used extensively in weak deposits to increase the load carrying capacity, reduce settlement of structural foundations and accelerate consolidation settlements due to the reduction in flow path lengths.

2.4.1 Stone column installation

A stone column consists of crushed rock with particles size less than one-seventh of the stone column diameter. Stone columns are normally installed in a triangular, squared or hexagonal pattern, as shown in Fig. 2-2.

2.4.1.1 Installation methods

The following methods are commonly used to install stone columns,

Replacement method involves replacing in-situ soil with stone column materials. A vibratory probe (vibroflot), accompanied by a water jet, is used to create the holes for the columns. This technique is suitable when the ground water level is high and the in-situ soil is relatively soft.

Displacement method is utilized when the water table is low and the in-situ soil is firm. It involves using a vibratory probe, which uses compressed air, to displace the natural soil laterally. Figure 2-3 depicts the different construction stages of installation.

Case-Borehole or rammed columns method is also used. In this method, the piles are constructed by ramming granular materials in the pre-bored holes in stages using heavy falling weight, (Bergado et al., 1991).

The grain size of the stone column material is one of the main controlling parameters in the design of the stone columns. Hence, the influence of column material in the performance of stone column was studied through laboratory experiments on model stone columns installed in clay by Dipty and Girish (2009). Five reinforcement materials were studied: stones, gravel, river sand, sea sand and quarry dust. It was found that stones are the most effective material and gravel is more effective than the other materials.

It is common knowledge that bulging and subsequent failure of granular piles mainly occur due to high stress concentration near top of the granular pile. Stresses near top of the treated ground are significantly influenced by the presence of granular mat as well as the cross-sectional area of the granular piles. After installing stone columns, a blanket of sand or gravel of 0.3 m or more in thickness is usually placed over the top. This blanket

works both as a drainage layer and also to distribute uniform stresses under the structure, (Ali and Abolfazle, 2005 and Shahu, 2006**)**.

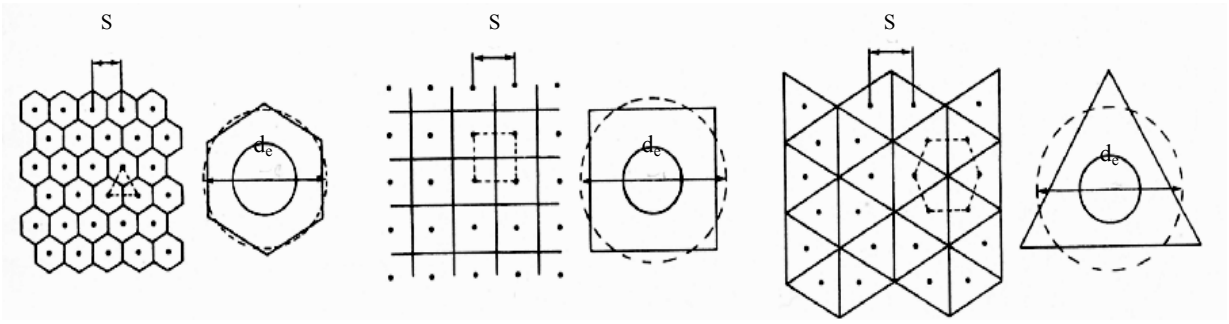

$d_e = (2\sqrt{3}/\pi)^{1/2} .S = 1.05.S$ $d_e = (4/\pi)^{1/2} .S = 1.13.S$ $d_e = (3\sqrt{3}/\pi)^{1/2} .S = 1.29.S$

(a) Triangular Orientation (b) Square Orientation (c) Hexagonal Orientation

Fig. 2-2 Orientation of stone columns and influence area of the unit cell (Weber, 2008)

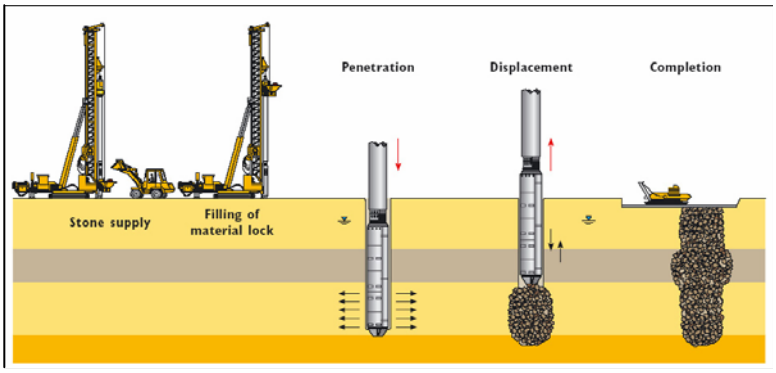

Fig. 2-3 Dry bottom feed installation method (Keller, 2002)

2.4.1.2 Installation effects

The route towards a failure condition in any column depends on the initial stress state in the column and in the surrounding soil, and this depends very strongly on the installation process used to create the stone columns, (Wood et al., 2000).

The installation of stone columns disturbs soft soil especially when using displacement method and changes the soft soil properties dramatically. The soil adjacent to the column is displaced during column installation. The soil displacement leads to an increase in the horizontal stress, the stress state and the stiffness of the soil for a distance ranged from 4 times and 8 times the column diameter around the single column and the columns group, respectively. Pore water pressure in the surrounding soil increases substantially during the construction of the stone column as well as the coefficient of earth pressure increases. The pore water pressure dissipates in days or weeks as the soft soil consolidates and gains strength. The values of the coefficient of earth pressure increase and range from 1.1 to 2.5. The coefficient of earth pressure depends mainly on the spacing between adjacent stone columns and the type of installation equipment as well as the soil type and the adopted installation procedure. A reorientation of the clay

particles in direct contact with stone column occurs. Beside the compaction and high density of the clay around the columns, the permeability is reduced decreasing drainage performance of the improved soil. A lot of researchers studied and toke in consideration the installation influence of the stone column on the properties of the surrounding soft soil (Kirsch, 2006, Elshazly et al., 2006, Xu et al., 2006, Elshazly et al., 2007, Wehr et al., 2007, Elshazly et al., 2008, Weber, 2008 and Satibi, 2009).

The installation of the vibro stone column into the ground was modeled numerically by the theory of cylindrical cavity expansion in which along the border of the cylindrical hole, the soft soil is subjected to a radial displacement to form the stone column. As the process of stone column installation is relatively quick in soft soil, undrained cavity expansion is most applicable. Kirsch (2008) studied the individual and the global installation effects for loading a group of 25 stone columns on the soil properties. Both effects were modeled numerically by using cavity expansion. Both effects cause an increase in the stress state and an improvement in the surrounding soil.

Guetif et al. (2007) simulated the case history of the Damiette project by using cavity expansion method. Along the thickness of the soft clay layer a numerical procedure called "Dummy materials" as an elastic material was performed to simulate the installation which was represented by a cylindrical hole occupied by vibro-probe radius of 0.25 m having a weakest young modulus of 20 kPa. Then, along the border of the cylindrical hole, the soft soil was displaced radially until the horizontal expansion reached the column radius of 0.55 m. The main conclusions of this contribution, based on Mohr Coulomb's behavior adopted for the soft clay and stone materials, are as follows:

I. Immediately after column installation, high excess pore pressure values, (Δu) were developed in the surrounding clay with unchanged effective mean stress, (p') as shown in Fig. 2-4 and Fig. 2-5. The effective vertical stress, (σ'_v) had a minor decrease while the effective radial stress, (σ'_r) increased in soft clay during the column installation. However, in the material of the column, the effective mean stress increased to about four times with respect to that predicted in soft clay.
II. After a period of 11 months, during which the primary consolidation in the soft clay has taken place, the predictions are:
– A quasi-total dissipation of excess pore water pressure occurred with a significant increase of the effective mean stress caused by the increase of effective radial stress, as depicted in Fig. 2-6 and Fig. 2-7.
– The effective vertical stress, remaining almost unchanged, resulted for an increase of the coefficient of lateral earth pressure at rest.
– Initial soil improvement at a distance equivalent to six times the column radius was taken place.

Most experienced practitioners are aware that the installation of stone columns into soft soil can generate a degree of surface heave, particularly if the construction control is inadequate and the ground overworking takes place. Therefore, heave is rarely measured. Geduhn et al. (2001) observed that the installation of four stone columns led also to the heaving of the soft soil between the columns grid. Castro (2007) also observed a zone of surface heave with a maximum value of 290 mm following

installation of a test group of seven columns. Nonetheless, the few case studies where heave was recorded are of interest as they showed that the amount of heave is a function of column size, spacing, extent and construction method. Single column, rows and small groups of columns exhibit less heave than large grid of columns. It also appears that the closer the column spacing for any given column arrangement is, the greater the magnitude of the heave is, (Egan et al., 2008).

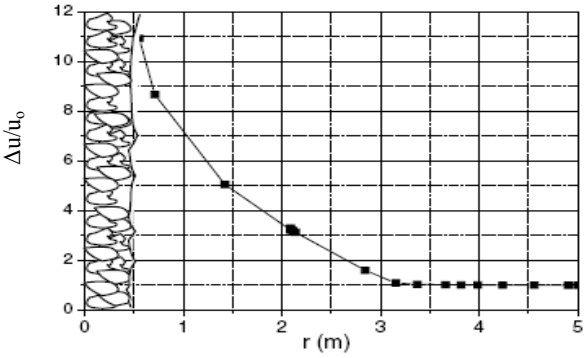

Fig. 2-4 Variation of normalized pore pressure in soft soil before consolidation with distance from the column (Guetif et al., 2007)

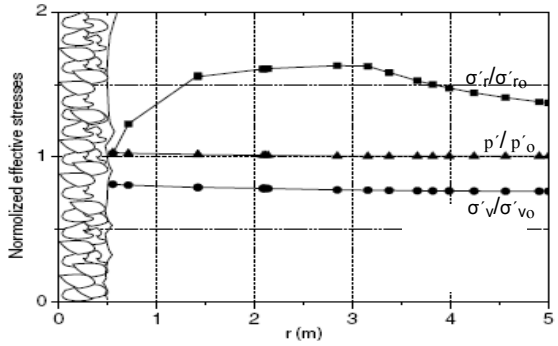

Fig. 2-5 Variation of normalized effective stress in soft soil before consolidation with distance from the column (Guetif et al., 2007)

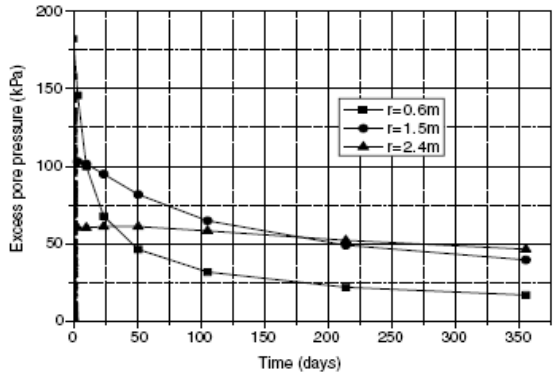

Fig. 2-6 Variation of excess pore pressure with time in soft clay during consolidation (Guetif et al., 2007)

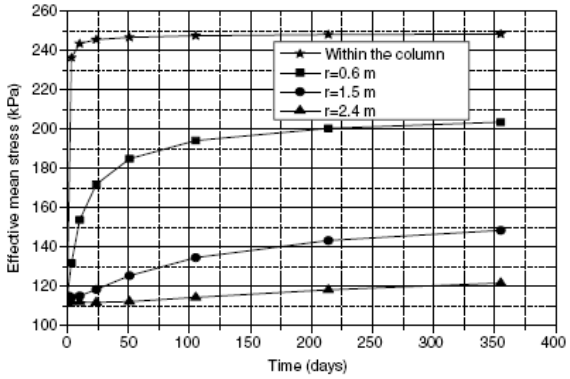

Fig. 2-7 Variation of effective mean stress with time at mid-width of soft clay at radii 0.6 m, 1.5 m and 2.4 m (Guetif et al., 2007)

2.4.2 Engineering behavior of the composite ground

2.4.2.1 Unit cell

The triangular, squared or hexagonal pattern installation of stone columns experiences different influence areas of the stone column as a unit cell. The unit cell is defined as a cylinder with an influence zone diameter (d_e) enclosing surrounding soil and one stone column. In the unit cell technique the triangular, the squared or the hexagonal influence area is converted to an equivalent circular influence area with diameter d_e, as indicated previously in Fig. 2-2.

Bergado et al. (1996) presented a theory to determine the stability of ground reinforced with stone columns. The theory is based on the stress concentration in the granular pile. Figure 2-8 illustrates a diagram of the composite ground. Each stone column is separated into its own unit cell, as shown in fig. 2-8-a.

The area replacement ratio is the ratio of the granular pile area (A_c) over the whole area of the equivalent cylindrical unit cell.

$$a_s = A_c / (A_c + A_s) \quad (2.1)$$

This ratio can also be expressed in terms of the stone column diameter (d) and spacing (S). The area replacement ratio for stone columns installed in a square and equilateral triangular pattern is respectively.

$$a_s = (\pi / 4)(d / S)^2 \quad (2.2)$$
$$a_s = (\pi / 2\sqrt{3})(d / S)^2 \quad (2.3)$$

2.4.2.2 Load sharing and stress concentration

The distribution of the stress in the column (σ_c), soft clay ground (σ_s) and average stress (σ) is illustrated in Fig. 2-8-b. Studies have shown that when ground reinforced with stone column is loaded, stress concentrations develop in the column accompanied by reduction in stress in the surrounding clayey ground. This can be explained by the fact that, when loaded, the vertical settlement of the stone column and surrounding soil is approximately the same, causing generation of stress concentration in the column, which is stiffer than the surrounding cohesive soil. A stress concentration factor or ratio (SCF) is used to express the distribution of the vertical stress within the unit cell.

$$SCF = \sigma_c / \sigma_s \quad (2.4)$$

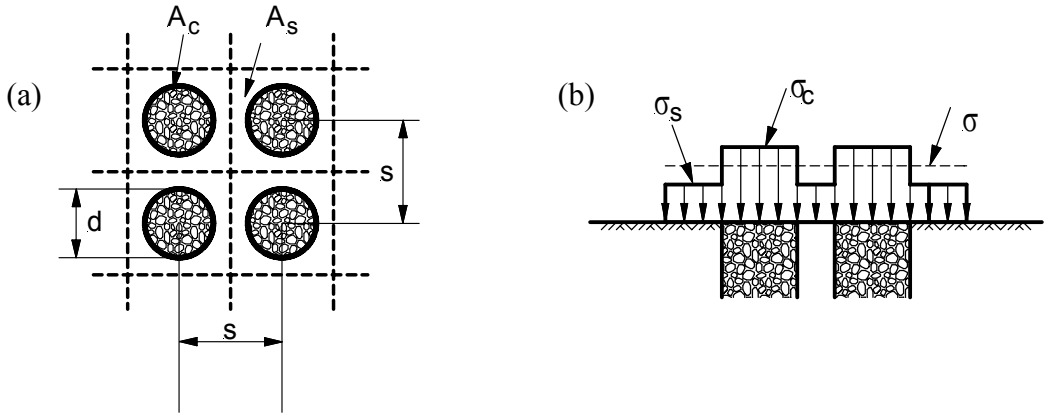

Fig. 2-8 Diagram of composite ground (Bergado et al., 1996)

The relative stiffness of the stone column and the surrounding soil is influenced on the magnitude of the stress concentration. The average stress (σ) over the unit cell area is given by:

$$\sigma = \sigma_c a_s + \sigma_s(1 - a_s) \quad (2.5)$$

The stress in the stone column (σ_c) and the stress in the surrounding clayey ground (σ_s) are then given as follow:

$$\sigma_c = (SCF.\ \sigma) / (1 + (SCF - 1)\ a_s) = \mu_c \sigma \quad (2.6)$$

$$\sigma_s = (\sigma) / (1 + (SCF - 1)\, a_s) = \mu_s \sigma \quad (2.7)$$

Analytical study

As mentioned above, the applied load is divided between the stone column and the surrounding soil relative to their stiffness values. Therefore, the stone column carries the most applied load due to its higher stiffness. The modular ratio is defined as the ratio between the elasticity modulus of the stone column and the elasticity modulus of the soil, (E_c / E_s) which represents the stiffness ratio. Depending on that, the final stress concentration ratio is equal to the constrained modular ratio in case of a lateral confinement and an elastic behavior of the stone column. However, this is in contradiction with experience: the modular ratio is usually in the range 10–50, while the stress concentration ratio measured in actual cases is much lower, in the range 2–10. In fact the column is not confined and it has a lateral displacement. Additionally, the behavior of the column is elstoplastic because the lateral bulging of the column is a result from its yielding.

Shahu et al. (2000**)** presented a simple theoretical approach to analyze soft ground reinforced by non-homogeneous granular piles with granular mat on top based on the unit cell concept. The modulus of elasticity of the non-homogeneous granular pile (E_{gp}) increases with depth, α. While the modulus of elasticity of the homogeneous granular pile is constant with depth.

$$E_{gpi} = E_{gp} (1+\alpha z_i/H) \quad (2\text{-}8)$$

Where α is defined as the rate of the increase of the modulus of elasticity of the pile E_{gp} with depth, E_{gpi} is the modulus of elasticity of granular pile at a depth z_i, and H is the thickness of the soil. A parametric study was also carried out to evaluate the relative influence of various parameters on the effect of non-homogeneity of the granular pile on treated ground process. The results showed that the variation of stress concentration factor with depth tends to become more uniform as the rate of variation of the granular pile stiffness with depth increases, as shown in Fig. 2-9. The higher the area replacement ratio is, the higher the increase in the stress concentration factor is. The values of the stress concentration factor are high because the stone column and the soil behave linearly and the lateral displacement of the stone column is prevented in the theoretical approach of Shahu et al. (2000**).**

Castro 2008, and Castro and Sagaseta (2008a) and (2008b) studied analytically the influence of the horizontal deformation and plastic behavior of the column on the distribution of stresses between soil and column which is pointed out in Fig. 2-10. With lateral confinement the stress concentration factor SCF starts from zero and reaches a final value equal to the confined modular ratio *(Ec/Es=40)*. This is not realistic, as commented above. The consideration of radial deformations, keeping elastic behaviour, reduces this final value to 25. Plastic strains in the column reduce further the final value of SCF to about 5 which is in the actual range.

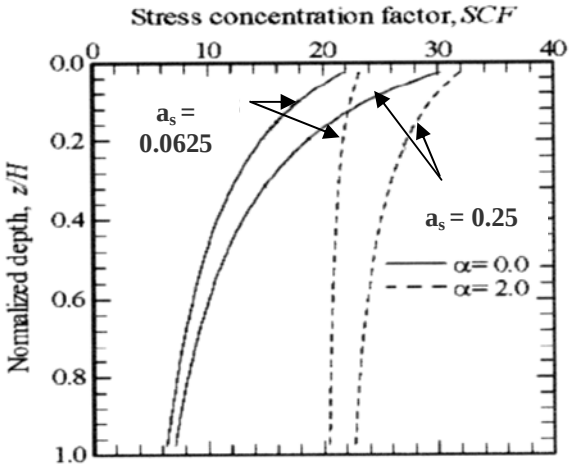

Fig. 2-9 Effect of area ratio on stress concentration factor of non-homogeneous granular pile (Shahu et al., 2000)

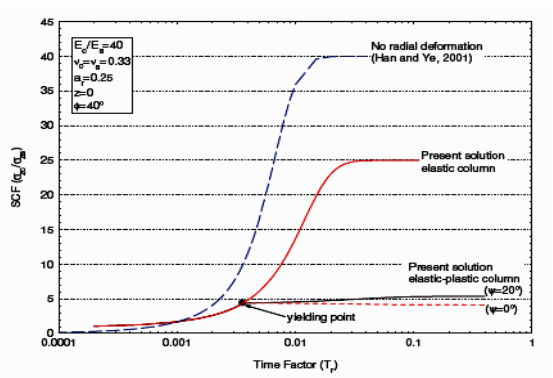

Fig. 2-10 Influence of radial deformation and plastic strains on stress concentration factor (Castro, 2008)

Deb (2007) developed a simple generalized mechanical foundation model for granular bed-stone column-improved soft soil, which incorporates the nonlinear behavior of the granular fill and soft soil. Parametric studies for a uniformly loaded strip footing have been carried out to show the effects of various parameters on the total as well as the differential settlement and the stress concentration ratio. It has been observed that the presence of granular bed on the top of the stone columns helps to transfer stress from soil to stone columns and reduces total as well as differential settlement. The results also indicated that when the modular ratio increases, the stress concentration ratio increases. As spacing distance between columns increases, more stress is also transferred from soil to stone columns.

Experimental studies

Stewart and Fahey (1994) conducted a number of centrifuge tests to study the load share between the stone columns and the surrounding soft clay due to construction of an iron ore stockpiles imposing a surface load up to 500 kPa. The results of the tests proved that the loading on the surrounding soft soil is partially carried by the stiffer columns. This results in less stress being on the soft clay, and therefore leads to smaller settlement. Stress concentration factors of about 4 were estimated from the centrifuge tests. In addition, a confined compression test was performed on a stone column and surrounding clay as a unit cell. The loads were applied through a stiff steel plate. The results

suggested that stress transfer from the clay to the column is mainly dependent on consolidation around the column. The stress concentration factor in a confined compression test was found to be increase with increasing loading from about 2 to about 3.5. This is general trend agreed with a numerical analysis using elasto-plastic soil models.

Kirsch and Sondermann (2003) concluded that the stress concentration is depending on various parameters such as the loading type (Flexible or rigid), the surcharge, the material parameters of column and soil, and the geometrical dimensions. They performed numerical and analytical analyses for an embankment resting on soft soil reinforced with stone columns and compared their results with the measurements at another embankment site in Kuala Lumpur. The columns were installed using a square pattern at 2.2 m. The result of approx. SCF = 2.6 was compared well with the results of the practical embankment. The value of SCF = 2.8 was measured for the same column pattern and the same surcharge of 120 kN/m².

Mckelvey et al. (2004) examined the load-sharing mechanism of the composite clay/granular column material by analysing pressures measured beneath a square rigid footing. Variations in the stress concentration ratio as the applied footing pressure increased are presented in Fig. 2-11. Initially in TS-11 and TS-13 (two identical tests on long columns) the columns seemed to take a large proportion of the applied load (SCF > 4). In contrast, stress concentration ratio SCF was less than 2 in the shorter column test TS-14 immediately after the loads were applied. Short columns appear to provide less resistance to loading compared with long columns, which show some resistance to punching.

In practice, columns are not loaded to failure, and working loads are considerably smaller than the ultimate bearing capacity. Examining a possible operational region, shown by the shaded area in Fig. 2-11, it appears that the stress distributions underneath the footing supported on the stone columns are significantly different between short and long columns. At higher loadings, beyond the possible working range, the stress ratio appeared to approach a constant value (approximately = 3), regardless of the column length. This observation agrees well with previously reported data, particularly from field studies. Barksdale and Bachus (1983) suggested that typical values of SCF usually fall within the range 2.5–5. Based on a case study of a footing supported on long columns with 10 m long and 0.75 m in diameter, Greenwood (1991) and Han & Ye (1991) reported that the stone columns carried a high percentage of the load as the loading progressed. In this case, the stress concentration ratio was initially as high as 25, reducing to 5 at higher loadings. In contrast, Bell et al. (1986) examined the stress concentration ratio underneath a footing supported on short columns (less than 4 m). The value of SCF increased from as low as 1.24 to 3 as the loading progressed.

Weber (2008) carried out centrifuge tests for an embankment resting on reinforced soft soil with stone columns. The results emphasized that the stress concentration in the stone column is not only load dependent but also dependent on column depth. Small loads give stress concentrations up to 8, which decrease with depth, while high loads result in a constant distribution of stress concentration over depth with values between 2.5 and 4.

Castro and Sagaseta (2009) also found that the stress concentration factor in the range of 3-6 from the field measurements for an embankment with 10 m height constructed on reinforced soft soil with stone columns.

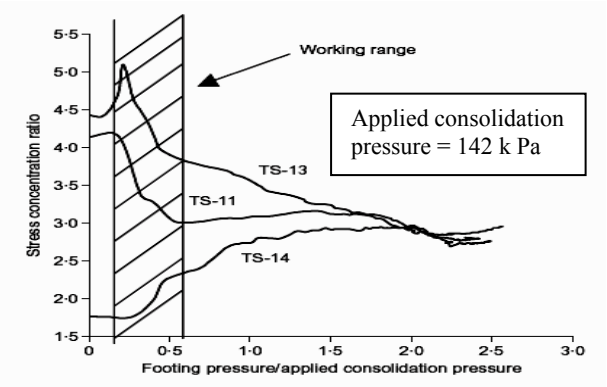

Fig. 2-11 Variation in the stress concentration ratio as the applied foundation load increased (Mckelvey et al., 2004)

2.4.3 Mechanism and performance of ordinary stone columns

The presence of the column creates a composite material of lower overall compressibility and higher shear strength than in-situ soil. Confinement, and thus stiffness of the stone, is provided by the lateral stress within the weak soil. When an axial load is applied at the top of a single stone column, an extension of the column diameter is produced beneath the surface. This extension in turn, increases the lateral stress within the clay, which provides an additional confinement for the stone column. An equilibrium state is eventually reached, resulting in a reduction in the vertical displacement, when compared with the untreated ground.

2.4.3.1 Experimental studies

Cho et al. (2005) carried out centrifuge tests to investigate the settlement reduction effect of a sand compaction pile (SCP) and a gravel compaction pile (GCP). Numerical analyses by the finite element method (FEM), which simulate the test conditions, also were carried out to compare the test results with those of the analyses. Settlements of SCP and GCP were measured during the centrifuge test for different area replacement ratios. The results of the study showed that GCP is more effective than SCP.

Field tests

Mitchell and Huber (1985) performed 28 field load tests on individual stone columns constructed in soft estuarine deposits during the installation of 6,500 stone columns. The stone columns reinforced soft soils were used to support a large wastewater treatment plant. All stone columns extended completely through the soft soil layer which ranged from 9 m to 15 m. The diameter of stone columns ranged from 0.5 m to 0.75 m. The column spacings ranged from a 1.2 m x 1.5 m pattern to a 2.1 m x 2.1 m pattern. The results of the load tests showed that the existence of the stone column led to a reduction in settlements to about 30 %-40 % of the values on the un-improved ground.

Han and Ye (1991) presented the results of full scale load tests on stone columns reinforced soft soil in coastal areas. Sixteen stone columns were used in soft soil having

a length of 14 m and an average diameter of 0.85 m, and arranged in triangular pattern. The treated ground with stone columns and untreated ground were loaded. It was found that the stone columns increase the bearing capacity to two times the untreated ground. It is very effective for the composite ground with stone columns to decrease the production of the initial excess pore water pressure and to keep the foundation stable.

Christoulas et al. (2000) described the results of two instrumented axial loading tests on large scale model stone columns. Kaolin clay was used to simulate natural soil conditions. Two columns were constructed with average diameter of 0.17 m in a cubic pit with 1.5 m edge. The results of the experimental tests provided support of that the upper part of the column bulged along a length of about 2.5-3.0 column diameter. The experimental data of this study suggested that the ultimate load corresponds to settlements approximately equal to 35 % of the stone column diameter.

Laboratory tests

Hughes and Withers (1975) and Hughes et al. (1975) studied the behavior of single stone columns. They used laboratory radiography to observe the deformations occurring in and around a column loaded within cylindrical chamber containing clay. They concluded that stone column bulging deformation occurred with a depth of four column diameters, measured from the column surface. The capacity of the stone columns can be assumed by observing behavior of bulging of the stone columns as they expanded radially into the surrounding soil (Wood et al., 2000).

Wood et al. (2000) performed model tests to determine the mechanisms of response for beds of clay reinforced with stone columns subjected to surface footing loads. An exhumation technique was used to discover the deformed shapes of the stone columns. The laboratory model tests showed that there was significant interaction between the footing and the individual stone columns within a group. As a consequence, the load-settlement relationships for neighboring columns in different locations would be different. This will be pessimistic in design of the stone column reinforced foundations to neglect increasing stiffness towards the centre of the group. The kinematic constrains that the base of a rough footing imposes, push the load to greater depths toward the center of the footing. Based on the study of Wood et al. (2000), the following failure modes of stone columns have been proposed,

a. The bulging failure of a stone column takes place, when it is not prevented from expanding radially by adjacent columns, Fig. 2-12-a.
b. The bearing capacity failure plan occurs in the head of the column, Fig. 2-12-b.
c. If the stone column has a little lateral restraint and is subjected to high loads, it may fail by a diagonal shear plane, Fig. 2-12-c.
d. A short stone column can fail by penetration through an underlying soft clay layer, Fig. 2-12-d.
e. The compression failure happens when the stone column is long, Fig. 2-12-e
f. A slender stone column can fail by bending if it is laterally loaded, Fig. 2.12.f

Bae et al. (2002) investigated also the failure mechanism and various parameters of the behavior of end-bearing single and group stone columns by laboratory loading tests. Results of the laboratory tests were verified by FEM analyses. From the laboratory tests

and the FEM analyses results, single stone column showed the bulging failure mode in the depth of 1.6 to 2.8 times the column diameter. The major failure mode of stone columns group is conical failure. The conical failure angle in short columns is smaller than that in long columns. The results also showed that the bearing capacity of the stone column is affected by the undrained shear strength of the surrounding soil, the spacing distance between columns and the installation of mat.

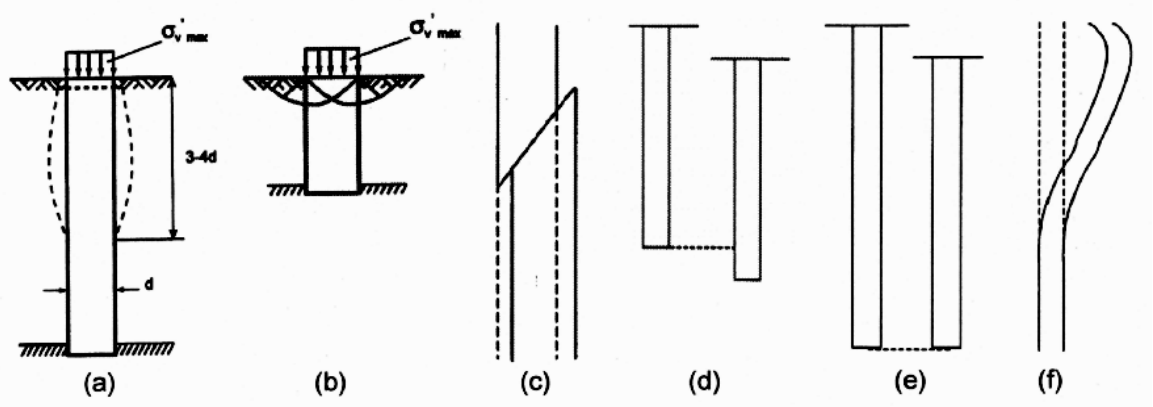

Fig. 2-12 Failure modes of stone columns (Wood et al., 2000)

Mckelvey et al. (2004) carried out a series of laboratory model tests on a consolidated clay bed using two different materials: (a) "transparent material" with 'clay like' properties, and (b) speswhite kaolin clay. The transparent material was prepared by mixing fumed silica in an oil blend of mineral spirits and crystal light liquid paraffin. The tests on the transparent material, probably for the first time, permitted visual examination of deforming granular columns during loading. Foundation loading was conducted on transparent material samples. Three sand columns, 25 mm in diameter, were installed in a triangular arrangement beneath the circular footing (100 mm in diameter) and in a row beneath the strip footing to depths of 150 mm and 250 mm. But for the foundation loading of kaolin clay tests, four sand columns, 25 mm in diameter, were installed in a square arrangement beneath a model pad footing (90 mm x 90 mm) to depths of 150 mm and 250 mm (L/d of 6 and 10).

The presence of the granular columns significantly improved the load-carrying capacity of the soft clay. However, columns longer than about six times their diameter did not seem to show further increases in the load capacity. The results of the tests showed that columns can fail in three different ways: bulging, punching and bending. Punching is more prevalent in short columns whilst bending failure is predominant in 'perimeter' columns located beyond the centre of the footing. Bulging was more generally common in long columns, as shown in Fig. 2-13. Beneath the rigid footing, the central column in the stone columns group deformed or bulged uniformly, while the edge columns bulged away from the neighbouring columns as also shown in Fig. 2-13. This was also stated by Wood et al. (2000), Kirsch (2004), Sivakumar et al. (2004) and Sivakumar et al. (2007).

Black et al. (2006) used an advanced testing method to examine the settlement of footings supported on granular columns. A relatively large sample size of 300-mm diameter and 400-mm high was used. The results indicated that, at a footing displacement of 10 mm the load carrying capacity of the non-reinforced deposit was

1.25 kN. This increased to 1.4 kN and 1.6 kN which represents an increase of 12 and 28 % for the composite samples of T2 and T3, respectively. Where the column T2 is with length of 125 mm and T3 is with length 250 mm samples, respectively with the same column diameter of 25-mm. In relation to the settlement consideration, the sample with no column exhibited a footing settlement of 6.5 mm at a foundation load of 1 kN. This settlement reduced to 4.5 mm and 2.2 mm which reduced settlements correspond to settlement reduction factors of 0.69 and 0.34 for T2 and T3, respectively at the same loading condition. Therefore, the test results proved that the length of the columns effect is more significant in settlement reduction than in increase of the load-carrying capacity.

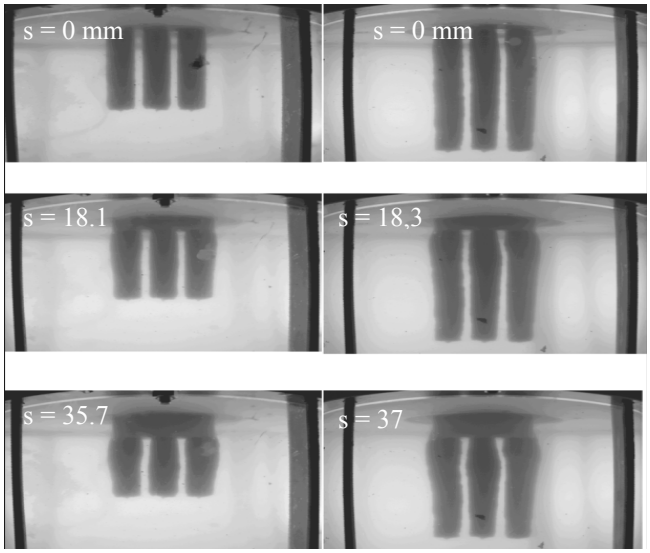

(a) (b)

Fig. 2-13 Photographs of sand columns beneath circular footing at beginning, middle and end of foundation loading process: (a) 150 mm length; (b) 250 mm length (Mckelvey et al., 2004)

Ambily and Gandhi (2007) carried out a detailed experimental study on the behavior of single column and group of seven columns by varying parameters like spacing between the columns, undrained shear strength of the clay, angle of internal friction of the stones and loading type. Laboratory tests were carried out on a column of 100 mm diameter surrounded by soft clay of different consistencies. The tests were performed with both of an entire equivalent area loaded and a column only loaded. During the experimental tests, the actual stress on the column and the clay were measured by fixing pressure cells in the loading plate. The finite-element analyses were performed by using axisymmetric analyses. The numerical results were compared with the experimental results which showed good agreements. The following conclusions were drawn based on this study:

1. When the column area alone was loaded, the failure was by bulging with maximum bulging at a depth of about 0.5 times the diameter of the stone column.
2. As spacing increases, the axial capacity of the column decreases and settlement increases up to spacing ratio of 3, beyond which the change is negligible.
3. The load-settlement behavior of a unit cell with an entire area loaded is almost linear and it is possible to find the stiffness of the improved ground, Fig. 2-14.

4. Single column tests with an entire unit cell area loaded compared well with the group test results. Hence the single column behavior with unit cell concept can simulate the field behavior for an interior column when a large number of columns are simultaneously loaded, as illustrated in Fig. 2-15.
5. Stiffness improvement is found to be independent on the shear strength of the clay and depends mainly on column spacing and the friction angle of the stone.

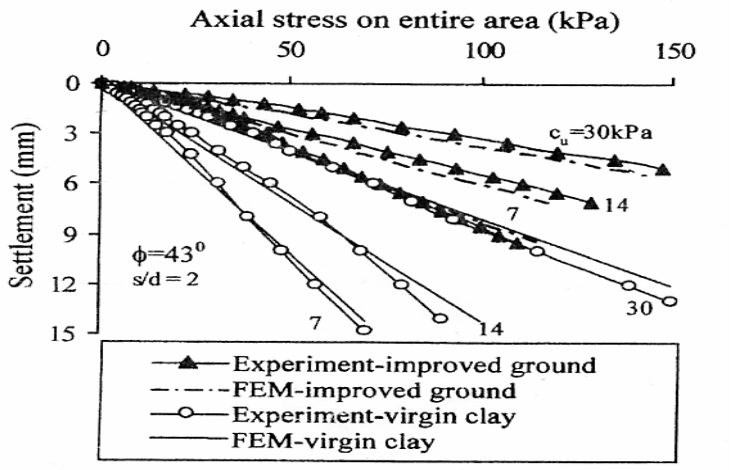

Fig. 2-14 Stress-settlement behavior under entire area loading (Ambily and Shailesh, 2007)

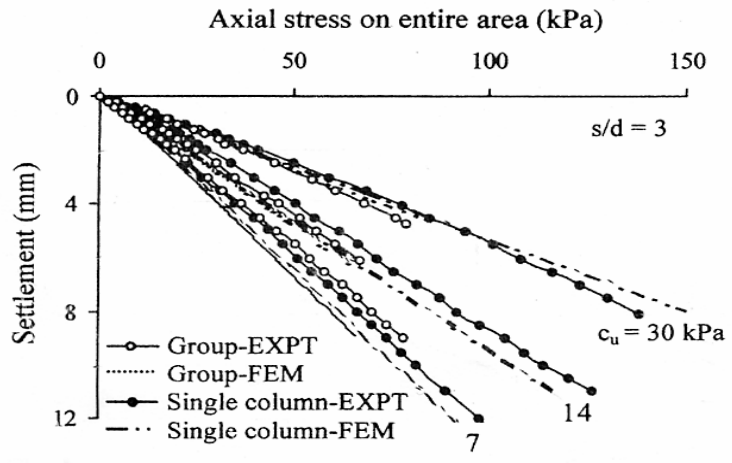

Fig. 2-15 Comparison of group column test and single column test (Ambily and Shailesh, 2007)

Triaxial Laboratory tests

Hughes and Withers (1974) carried out one of the earliest and most influences pieces of research on granular columns. They postulated that a granular column in the ground would behave that like a column in a triaxial cell that was confined by a radial stress, (Black at el., 2007).

Li et al. (2000) studied the interaction between granular columns and surrounding soil systematically by means of laboratory triaxial tests. The stress–strain relationships of gravel and clay in conventional triaxial compression tests showed that the volumetric strain of gravel is negative, i.e. its volume deformation is dilatation while the volumetric strain of clay is positive. The different volumetric strains of the two kinds of material

are significant. The different volumetric strain may cause a strong lateral interaction between the column and the surrounding soil by increasing radial stress.

Modified triaxial tests were also conducted in order to simulate a typical element of composite ground. The sample consisted of a gravel column in the centre surrounded with unsaturated Baihepu clay. In these tests, the vertical stress on gravel column, the radial stress on the inner surface of gravel column and surrounding clay, and the volumetric strain of the gravel column were measured. The tests results showed that the radial contact stress in the interface is higher than the confining pressure in the testing cell, which resulted from the dilatation of the gravel when loaded, as depicted in Fig. 2-16. The comparison of these tests results with the results of conventional triaxial tests of clay and gravel under the same confining pressure showed that the strength of gravel is higher and the strength of clay is lower in the composite samples, as demonstrated in Fig. 2-17.

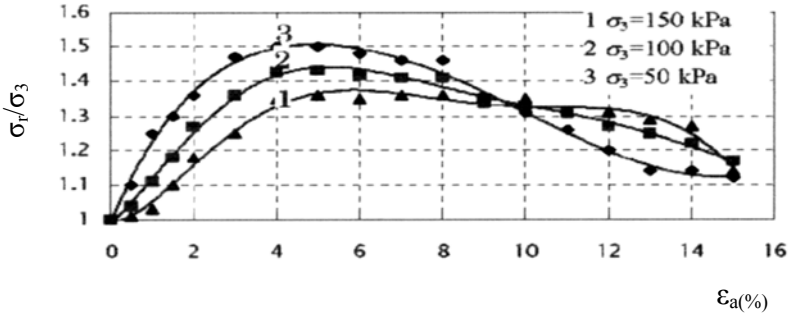

Fig. 2-16 Radial contacting stress on the interface of gravel column and surrounding soil (Li et al., 2000)

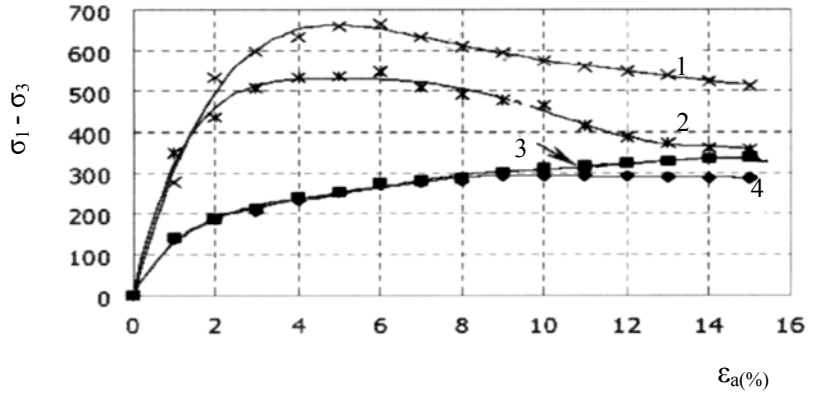

1. Axial stress of gravel column in composite sample.
2. Axial stress of gravel in triaxial tests.
3. Axial stress of clay in triaxial tests.
4. Axial stress of clay in composite sample.

Fig. 2-17 Axial stress-strain curves of gravel and clay in different tests at a confining pressure of, σ_3 = 100 kPa (Li et al., 2000)

Black et al. (2007) conducted an experimental study in which samples of soft kaolin clay (100 mm in diameter and 200 mm in height) were reinforced with vertical columns of sand and tested under triaxial conditions. Samples were reinforced with either a single column of sand of 32 mm diameter or three columns of sand with diameter of 20 mm. The columns were installed in the clay to depths of 120 and 200 mm. It was found that the undrained shear strength of samples containing full-depth columns was greatly improved compared with that of the unreinforced samples.

Andreou et al. (2008) performed triaxial compression tests on specimens of non-reinforced and reinforced soft Kaolin clay with granular columns. The specimens had a 200 mm high and a 100 mm in diameter and the column diameter was 20 mm. The results suggest that the response of a soft foundation soil reinforced by granular columns to vertical loading is highly dependent upon the drainage conditions, the material of the stone column and the loading rate of the soil. The results also proved that as the confining pressure increases, the strength of the reinforced soil decreases.

2.4.3.2 Theoretical studies

Laboratory research, testing and field studies undertaken over the last years have contributed to the understanding of the conventional stone column behavior. This has led to the development of empirical, analytical and numerical techniques used to assess column capacity and load-settlement behavior. In the following sections, a brief description of the design methods for assessment of settlement reduction is introduced.

Greenwood curves

Greenwood (1970) was the first to introduce design curves to assess settlement reduction associated with the use of conventional stone columns. The empirical curves were derived from column groups placed under widespread loads on uniform soft soils. They represents settlement reduction as a function of column spacing and the undrained shear strength of the natural soil (for c_u = 20 kPa and 40 kPa). Later, Greenwood and Kirsch (1983) presented updated curves as a function of area ratio, as illustrated in Fig 2-18. The curves have limited use as a detailed design tool.

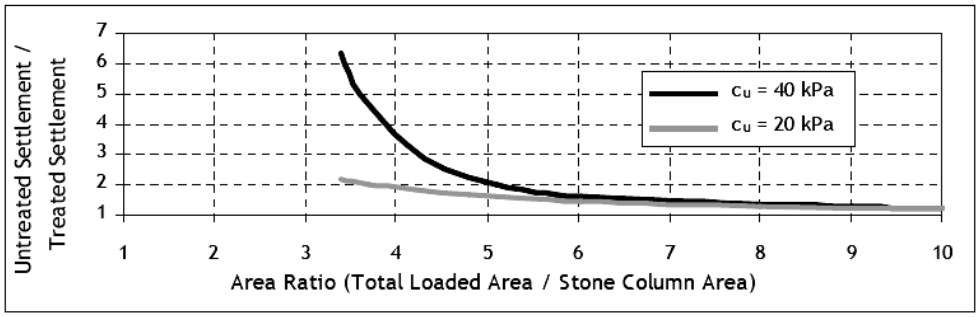

Fig. 2-18 Greenwood curves (modified from Greenwood and Kirsch, 1983)

Priebe method

Priebe (1976) proposed a method for assessing settlement reduction based on the unit cell, elastic theory and Rankine earth pressure theory. In this model, the stone column was assumed to be incompressible and surrounded by an elastic material. Soil settlement occurred when lateral pressure in the column exceeded the confining pressure in the surrounding soil. Priebe generated a series of design curves where the basic settlement improvement factor was plotted against the area ratio for a range of granular materials. The improvement factor is the ratio between the settlement of the untreated and the treated ground with stone columns. An example of these design curves is presented in Fig. 2-19. Using this method, a conventional calculation for untreated soil settlement is undertaken and divided by the improvement factor. Following criticism of aspects of the

technique, Priebe (1995) presented a revised version which included consideration of column compressibility, modular ratio of column and soil, confinement from overburden and solutions for single and strip footings. Although the Priebe method has been used extensively, it has a limitation in settlement estimation, (Bouassida et al., 2008).

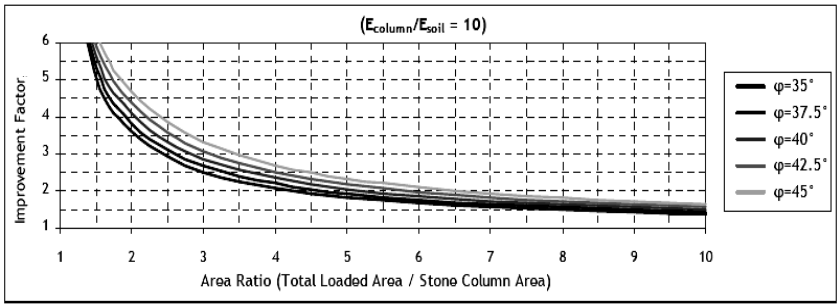

Fig. 2-19 Priebe design curves (modified from Priebe, 1995)

Numerical methods

Numerical methods are probably the most theoretically suitable to modeling stone column treated ground. Gniel and Bouazza (2007) reported that Balaam et al. (1977) used finite element and finite difference methods to explore stone column behavior, resulting in publication of design curves used to assess settlement reduction. This work was continued by Balaam and Booker (1981; 1985) and Balaam and Poulos (1983). Recently, sophisticated models have been used to better model soft soil behavior and its interaction with loaded columns such as the study of Lee and Pande (1998), Tan and Oo (2005) and Tan et al. (2008).

Balaam and Booker (1985) also studied the settlement of a rigid foundation supported by a layer of clay, which was stabilized with stone columns. The results of an analytic solution for the settlement, assuming no yield occurs in the clay or columns were presented. Later, this solution was used to develop an interaction analysis, which considered yielding within the stone columns. The solutions were obtained from the analysis of a 'unit cell'. In order to check the validity of these assumptions elasto-plastic finite element analyses were performed and the agreement between the two methods was very good. The results were plotted as a settlement correction factor, which equals to the actual settlement and the elastic settlement ratio of the foundation. The results showed that the most significant corrections to the elastic settlement occur when the columns are closely spaced and the stone column-soft soil modular ratio is high.

Alamgir et al. (1996) presented a simple theoretical approach to predict the deformation behavior of uniformly loaded soft ground reinforced by columnar inclusions. The approach incorporated the free strain condition, the distribution of shear stress and the load sharing between column and soil. A simple deformation model of the column soil system was assumed. The results were validated by the finite element analyses. The predictions showed that the effects of spacing and modular ratios on the distribution of the shear stress, the load sharing between the column and the soil and the settlement of the ground are significant. However, the Poisson's ratio of the soil has little influence.

Poorooshasb and Meyerhof (1997) introduced elastic analyses to study the settlement reduction of a raft foundation resting on reinforced soft soil with end bearing stone columns. The results of the analyses showed that the factors that most severely affect the performance of a stone column foundation scheme are the spacing and degree of compaction of the material in the columns which, in turns, control their strength and stiffness.

2.5 Consolidation rate of improved ground by stone column

A number of publications were written on the development of theoretical solutions for estimating bearing capacity and settlements of reinforced soft soil with stone columns (Aboshi 1979, and Priebe 1995). Field observations showed that stone columns accelerate the consolidation rate in the soft soil. Field pore water pressure measurement under an embankment indicated that a homogenous clay stratum without stone columns area only completed 25 % primary consolidation when that clay with stone columns area completed 100 % primary consolidation, (Munfakh et al. 1983). Han and Ye (1992) reported that the rates of settlement of two similar buildings, one on an unreinforced foundation and the other on stone columns reinforced foundation in the same site, reached 66 % and 95 %, respectively in the same time of 480 days. The acceleration of the consolidation rate is accredited to the stone column for providing a drainage path and relieving excess pore water pressures by transferring load from the surrounding soft soil to the stone column.

Barron (1947) proposed a known solution which dealt with consolidation of fine grained soil by vertical drain. The average rate (or degree) of consolidation in the radial direction is

$$U_r = 1 - \exp^{-[8/F(N)]T_r} \tag{2-9}$$

Where $F(N) = \left[N^2/\left(N^2-1\right)\right]\ln(N) - \left(3N^2-1\right)/\left(4N^2\right); N = d_e/d$ diameter ratio; $T_r = c_r t/d_e^2$ time factor in a radial flow; r_c and r_e = radii of drain well and its influence zone, respectively, as defined in Fig. 2-20 and d and d_e = diameters of a drain well and its influence zone, respectively.

The solution of Barron (1947) dealt with the consolidation of fine-grained soils by vertical drain. Stone columns and vertical drain have two major differences. First, stone columns have the larger drainage ability. Barron's solution ignored the effect of stiffness difference between the vertical drain and the surrounding soil on the consolidation rate. However, the stone columns are much stiffer than vertical drains and carry a substantial part of the applied load. Second, the stone columns have a smaller diameter ratio (influence diameter/column diameter) than drain wells. Typical diameter ratios for stone columns range from 1.5 to 5. However, the values for well diameter ratios used by Barron (1947) ranged form 5 to 100.

Han and Ye (2001) presented a simplified method for computing rate of the consolidation of the soft soil around stone columns considering stiffness ratio. Although stone columns and surrounding soil were assumed linearly elastic in thier study, in

reality, they have a nonlinear behavior. Stone columns act as drain wells where vertical and radial flows are similar to those of Terzhagi 1D solution and the Barron solution for drain wells in fine grained soils, respectively. The following relationship is still applicable to calculate time rate and settlement of the stone column improved ground:

$$U_{rv}=1-(1-U_r)(1-U_v) \tag{2.10}$$

Where,
U_{rv} = degree of consolidation (both radial and vertical direction)
U_r = degree of consolidation (radial direction only)
U_v = degree of consolidation (vertical direction only)

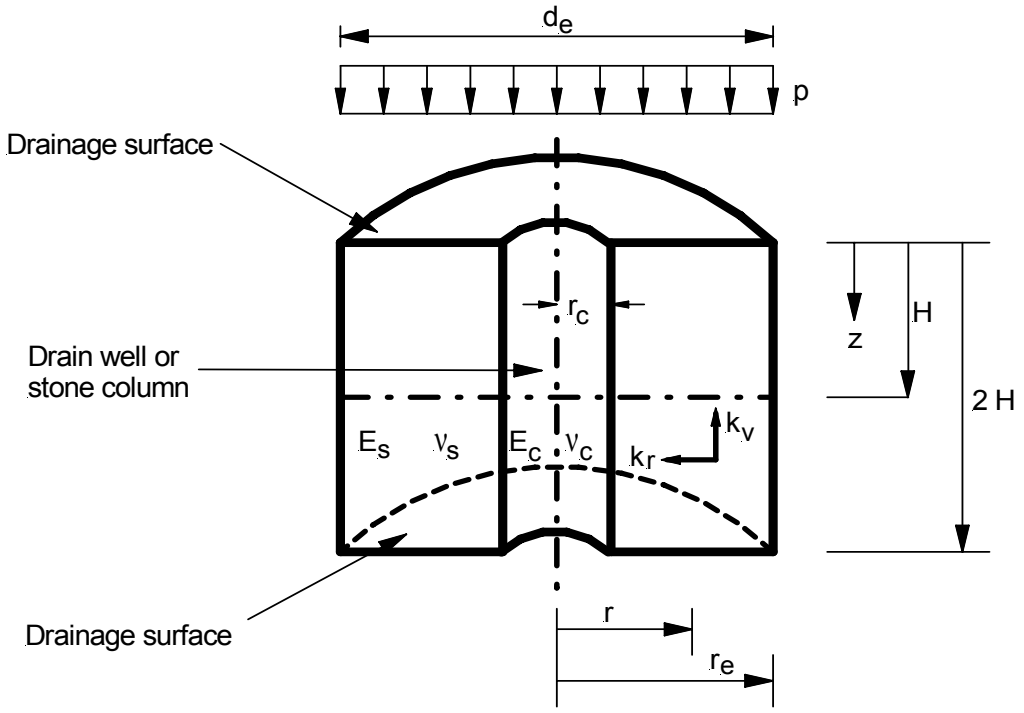

Fig. 2-20 Definition of terms for modelling (Han and Ye, 2001)

An approximate solution can be obtained as follows:

$$U_{rv}=1-\frac{8}{\pi^2}\exp^{-[8/F(N)]T_r'-\{\pi^2/4\}T_v'} \tag{2.11}$$

Where $T_r'=c_r't/d_e^2$, a modified time factor in the radial flow; $T_v'=c_v't/H^2$, a modified time factor in the vertical flow; and H = thickness of soil from a free/draining horizontal surface to an impervious one.

Based on the assumption that all the applied loads at the time t = 0 are carried by the excess pore water pressures within the surrounding soil, then $\overline{\sigma_c'}=\overline{\sigma_s'}=0$. When consolidation of the surrounding soil is complete, the effective stress within the stone column and the surrounding soil finally become steady state and equal to the total stress.

$$n_s = \frac{\sigma_{cs}}{\sigma_{ss}} = \frac{m_{vs}}{m_{vc}} = \xi \frac{E_c}{E_s} \tag{2.12}$$

In which σ_{cs} and σ_{ss} = steady stress in column and soil, respectively; m_{vs} and m_{vc} = coefficients of compressibility of surrounding soil and stone material, respectively; E_c and E_s = elastic module of column and surrounding soil, respectively; ξ = a Poisson ratio factor ; where $\xi = \frac{(1+\nu_s)(1-\nu_c)(1-2\nu_s)}{(1+\nu_c)(1-\nu_s)(1-2\nu c)}$ where ν_c and ν_s = Poisson ratios of the stone and the surrounding soil, respectively, n_s = steady stress concentration ratio as the consolidation is complete. The stress concentration ratio values mostly refer to steady-stress concentration ratio. However, the stress concentration ratio, SCF can also be defined as the ratio of the stress on the columns to that on the soil at certain time t. The modified coefficients of consolidation can also expressed using steady stress concentration ratio,

$$c_r' = c_r\left(1 + n_s \frac{1}{N^2 - 1}\right);$$

$$c_v' = c_v\left(1 + n_s \frac{1}{N^2 - 1}\right) \tag{2.13}$$

Where N = a diameter ratio, as defined before.

The new solutions demonstrate stress transfer from the soil to stone columns and dissipation of excess pore water pressures due to drainage and vertical stress reduction during consolidation. Ignoring consolidation due to vertical flow, the calculated average total stress on the soil and columns for the case N = 3 and n_s = 5 are plotted in Fig. 2-21. In this figure, the average total stress σ_s and σ_c are normalized by the applied pressure, p. The results demonstrate that the stress on columns increases with time, while the stress in soil decreases. This stress transfer process from the soil to columns is called “stress concentration”. The stress transfer or concentration process can also be presented in terms of the stress concentration ratio, as shown in Fig. 2-22.

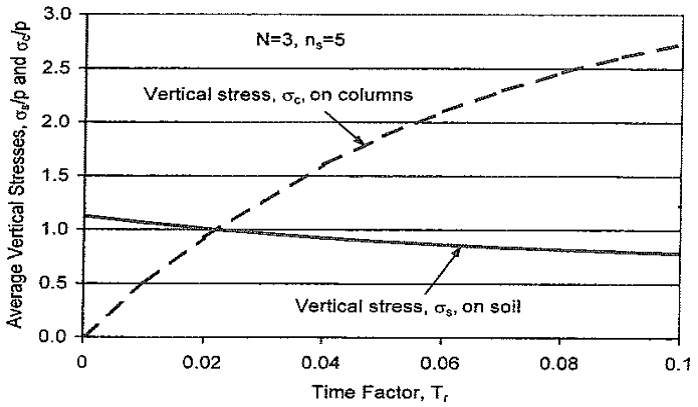

Fig. 2-21 Vertical stress on soil and columns with time, N = 3 and n_s =5 (Han and Ye, 2001)

The stress concentration ratio increases with time and approaches the steady-stress concentration ratio (n_s = 5 in this case), which is in agreement with the finding from several laboratory and field studies (Juran and Cuermazi 1988; Han and Ye 1991; Lawton 1999). This proposal method indicated the general trend that the steady-stress concentration ratio increased with the applied load. At larger loads than the yield load of the stone columns, the steady-stress concentration started to decrease.

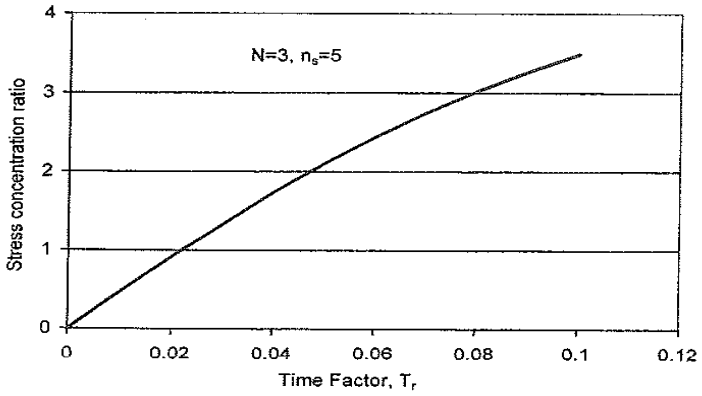

Fig. 2-22 Stress concentration ratio with time, N = 3 and n_s =5 (Han and Ye, 2001)

In Han and Ye (2001) study however, no lateral displacement was assumed in the theoretical development. Therefore, the dissipation of excess water pressures depends on two factors, drainage and reduction of vertical stress. The dissipation of excess pore water pressure, due to vertical stress reduction, is about 40 % of the total dissipation for this special case, as shown in Fig. 2-23. The contribution of vertical stress reduction to the dissipation of excess pore water pressures explains why stone columns are more effective than drain wells in accelerating consolidation rate of the soft clays.

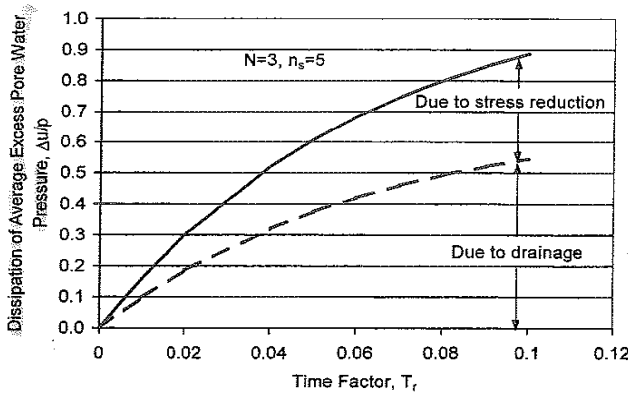

Fig. 2-23 Dissipation of excess pore water pressure, N = 3 and n_s = 5 (Han and Ye, 2001)

The comparison between the results of the simplified method and the numerical study of Balaam and Booker (1981) for all cases indicated that the computed rate of consolidation by numerical method is greater than that by the simplified method at the beginning of the consolidation. However, it is reversed when the rate of consolidation is greater than approximately 40 %. These discrepancies can result from the different assumptions used in the numerical and simplified methods.

In the numerical study, the lateral displacement is permitted. However, the lateral displacement is not allowed in the development of the simplified method. The lateral displacement in the numerical study tends to reduce the excess pore water pressures at the beginning of the loading, so that it accelerates the rate of consolidation. When more stress is transferred onto the stone column with time, however, the lateral displacement from the stone towards the soft soil in the numerical study tends to increase the excess pore water pressures, so that it slows down the process of consolidation. The difference between the rate of consolidation from the numerical analysis and the simplified method is diminished with an increase of the diameter ratio, N, as shown in Fig. 2.24.

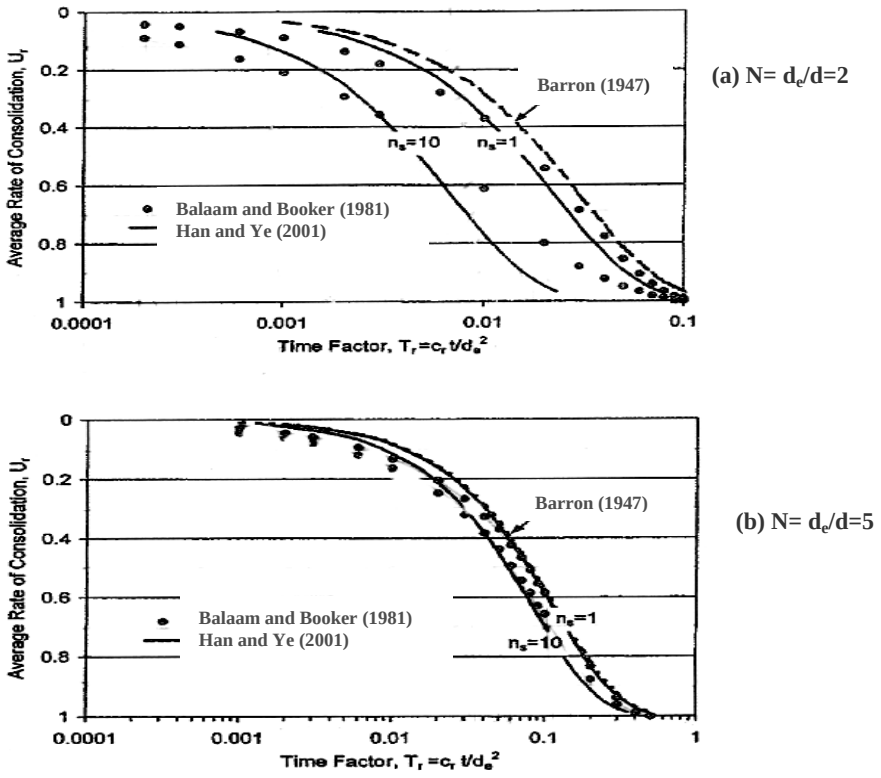

Fig. 2-24 Rate of consolidation of stone column reinforced foundations (Han and Ye, 2001)

Poorooshasb and Meyerhof (1997) also modified the Barron's equation to include the effect of stress concentration. Since the coupled effect of deformation and dissipation of pore water pressure has been incorporated in the FEM code Plaxis which uses Biot's (1941) system of differential equations solved by integration over time, the stress concentration effect is automatically taken in consideration in the PLAXIS analysis of the unit cell of the stone column-soft soil, (Malarvizhi and Ilamparuthi, 2007).

Bergado and Long (1994) presented the use of the Finite Element Method (FEM) for embankments simulation. Based on revised Cam clay model for 2-D consolidation analysis, two test embankments were constructed on soft Bangkok clay improved by granular piles and vertical drains. The embankments have 4 m height. The soft clay which has 8 m depth is over-lained by a medium stiff clay layer. In 2-D plane strain model, the vertical drains and Granular piles were converted into continuous walls. The

analyses results showed that granular piles imply more acceleration of consolidation and more reductions in the total settlement of the soft clay than vertical drains, as shown in Fig. 2-25.

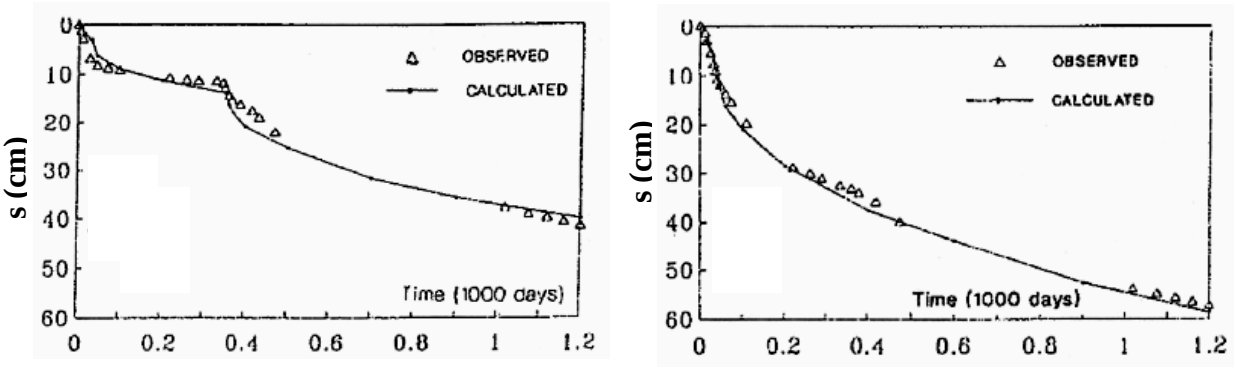

Fig. 2-25 Total settlement-time relationship of reinforced soft clay by (a) Granular piles and, (b) Vertical drain (Bergado and Long, 1994)

Raju and Hoffman (1996) and Raju (1997) reported the behavior of very soft soil with shear strength less than 10 kPa in terms of settlements and consolidation rates when improved using stone columns. Stone columns were carried out at seven interchanges and overpasses in the new Shah Alam Expressway (in Malaysia) to treat soft soils underneath approach embankments and reinforced walls. In all over 900,000 linear meters of stone columns were installed in predominantly very soft soils. The performance of the treatment is assessed based on measured settlements at the Kinrara and Kebun interchanges. The Kinrara site with slime soil has stone columns with diameter of 1.2 m, spacing 1.8 m and a depth down to 17 m under an embankment with a height of 7.5 m. At Kebun site with very soft marine clay, stone columns with 1.1 m diameter were installed at 2.2 m spacing to a depth of 12 m under another embankment with a height of 2.6 m.

The measured settlements which were in the order of 25 cm at Kinrara and 40 cm at Kebun compared to values over 1.0 m in untreated areas employed improvement factors of 4 and 2.5, respectively. The settlement behavior of the two types of soft soils related to their shear strength was distinctly different. The slime consolidated very quickly. Over 75 % of the settlement occurred during construction and then, no significant settlements were measured after a period of about 3 months, as shown in Fig. 2-26. In comparison, the marine clay took much longer time to consolidate. Over 75 % of the total settlement occurred after completion of embankment construction. A period of about 6 months was required for the settlements to stabilize. This behavior is understandable when looking at the values of the coefficient of consolidation and the highly plastic nature of the marine clay.

2.6 Stone columns-soft soil reinforcement system under embankment

Terzaghi and Peck (1967) stated that the instability of embankment constructed on soft soil foundations is mainly of two types: a) where the embankment sinks into the

foundation soils and b) failure by spreading. Hence, stone columns reinforced soft soils of embankment foundation have been used as a more effective method to prevent sinking and spreading failure. Therefore, this reinforced system is being, which improves the performance of an embankment over it by increasing shear strength and bearing capacity as well as decreasing consolidation settlement and lateral displacement.

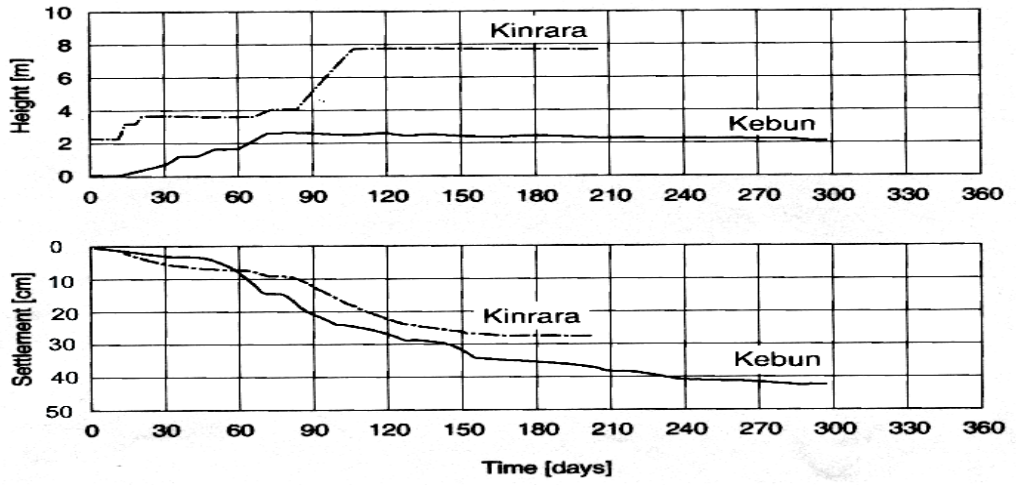

Fig. 2-26 Embankment height and settlement versus time plot at Kinrara and Kebun sites (Raju, 1997)

Cheung and Wagner (1998) investigated the construction of the South Eastern Arterial Road project in Auckland, a 4 m high geogrid reinforced embankment with steep side slopes (1H:4V). The embankment is underlain by soft ground and is in close proximity to three adjacent structures. The site is underlain by a 22 m thick layer of alluvium clay. Stone columns were installed along the edges of the embankment to strengthen its foundations and reduce the influence of ground displacement on the adjacent buildings. A layer of woven geotextile was placed at the base of the embankment. Stone columns of 90 cm diameter were arranged in four rows at 2 m centre to centre around the perimeter of the embankment. Wick drains were used in the central part of the embankment where stone columns were not installed. The embankment was constructed in two stages. Embankment settlement responses were monitored.

Measurements of settlement gauges installed in the non-reinforced zone of the embankment indicated ground settlements of 100 mm under 2 m of the light weight fill. The embankment settlement rate became very small within six months after construction. Within the stone column reinforced zone, ground settlements of 40 mm to 70 mm were measured under the 4 m high embankment load. At a distance of about 2 m outside the embankment area, no detectible ground deformation was recorded in the deformation surveys.

Samieh (2002) investigated numerically the behavior of an earth embankment on a 11 m thick soft clay layer reinforced with stone columns and compared the predicted and monitored responses. This analysis was performed by two dimensional numerical analyses by using Plaxis in which the stone columns were modelled as continuous walls. The parameters considered were stone column depth and extend the improvement area after embankment toe.

The results showed that the maximum settlement occurred at the embankment centreline while the maximum horizontal displacement occurred in the zone near the embankment toe and somewhat below the ground surface. Also the stress concentration ratio at any depths ranged from 2.6 to 3.0. A decrease of the stone column length, using floating stone column system, led to an increase of the embankment settlement. However, the horizontal displacement was not remarkably affected. A decrease of the improvement width along the embankment base led to a decrease of the settlement under the improved zone and to an increase of the settlement under unimproved zone below the embankment, as shown in Fig. 2-27-a. Also, with decreasing improvement width the horizontal displacement was decreased and this decrease was remarkable for I.Wr below 0.75, as depicted in Fig. 2-27-b. The improvement width ratio (I.Wr) is defined as the ratio between the width along which the stone columns are constructed and the embankment base width. Installation of stone column beyond the embankment toe had nearly no influence on the embankment deformational response.

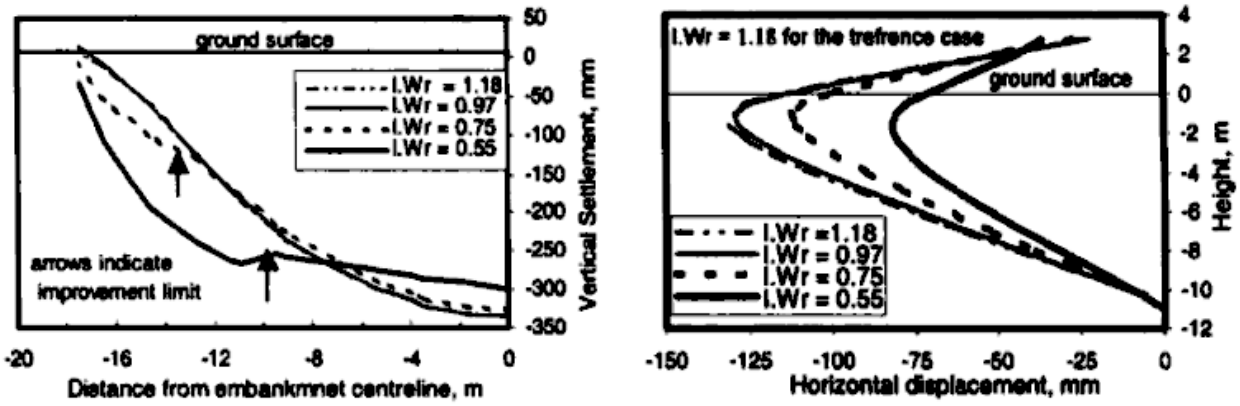

a. Vertical displacement profile

b. Horizontal displacement profile at mid of slope

Fig. 2-27 Effect of ground improvement width on the embankment deformational response (Samieh, 2002)

Weber (2006) investigated the behavior of a base reinforced embankment constructed on a soft clay layer, which is improved with stone columns. Centrifuge tests were performed in order to gain a deeper understanding of the interaction problem within the structure. The centrifuge tests were performed at 50–times gravity. The model represented a prototype structure of a 7 m clay layer depth with a compaction pile grid spacing of 1.7 m x 1.7 m and an average pile length of 5 m with a 0.6 m pile diameter. The model embankment produced an overburden pressure of about 90 kPa, representing a prototype embankment constructed of sand of about 5 m in height. The test was conducted in a modeling container, which was divided into 2 sections to permit comparison to be made on the soil with the same provenance and stress history. In one section, the soft clay was improved with sand compaction piles, while in the other section, the clay was not improved.

Due to the ground improvement in this centrifuge test, a factor of settlement reduction of 2.0 was measured. The acceleration of consolidation time t_{90} was measured with a factor of 5.0 for the described test. This showed that the factor of ground improvement

for settlement reduction does not coincide with the factor of accelerated consolidation time. The reason for that is probably the floating pile construction and ongoing consolidation in the lowest third of the clay layer, which was not improved.

Saroglou et al. (2008) presented the ground improvement using stone columns for the construction of a new highway road from Keratea to Lavrio, in Attika peninsula, Greece. An embankment of maximum height of 3 m was constructed on subsoil comprises of soft clays of low plasticity with intercalations of silty to clayey sands of medium density with gravel. Using stone columns with a depth of 14 m reduced the total settlement from 14 cm to 7 cm and accelerated the consolidation time from 16 months to a period of 4 months.

Borges et al. (2009) conducted a parametric study to investigate the influence of several factors on the behavior of the soft soils reinforced with stone columns under embankment loads: the replacement area ratio, the deformability of the column, the thickness of the soft soil, the deformability of the fill and the friction angle of the column material. The confined axisymmetric cylindrical unit cell was used. The analyses were performed by a finite element program that incorporates the Biot consolidation theory. The results confirmed that increasing replacement area ratio or stiffness of the column material significantly reduces settlements and horizontal displacements and accelerates the consolidation.

2.7 Reinforced stone columns with geosynthetic materials

The technique of ordinary stone columns to improve the mechanical properties of marginal soils was well established. However, the use of stone columns is usually associated with excessive deformation due to lack of lateral support from the surrounding soil. The lateral support is expressed by means of the undrained shear strength. According to German regulations, stone columns can be applied, if soft soils have undrained shear strength of c_u = 15 - 25 kN/m^2. In contrast to conventional techniques, encased granular columns can be used as a ground improvement and bearing system in very soft soils, for example peat or sludge with undrained shear strengths $c_u <$ 2 kN/m^2, (Kempfert, 2003).

The lack of lateral support causes large lateral deformation (bulging) in the upper part in the stone column and excessive settlements which lead to failure by bulging. When an embankment is constructed on the soft ground reinforced with ordinary stone columns, lateral spreading of ground occurs beneath the embankment. The lateral spreading reduces the confinement of the stone column. Therefore, further developments of the stone column technique include the reinforcement of the column using either horizontal layers of reinforcement or encasing individual stone column by geosynthetics.

2.7.1 Reinforced stone column with layers of geosynthetic

The degree of decreasing bulging and increasing bearing capacity depends on the number of the reinforcement layers, the spacing between layers and the angle of shearing resistance of the granular column. Based on numerical analysis, Madhav et al. (1994)

suggested that the greater the number of the reinforcement layers and the closer the spacing, the lesser will be the bulging.

Sharma et al. (2004) performed loading tests to investigate the improvement in load-carrying capacity of a granular pile in soft clay by using geogrid reinforcement as layers. The experimental program consisted of 14 plate load tests on soft soil bed alone without granular piles, and granular piles (alone) in soft soil bed and on composite ground (both granular piles and clay bed). In all the tests the diameter of the granular pile (d) was fixed 60 mm and length (L) at 300 mm. The top geogrid layer was placed at 10 mm. The number of geogrid layers (n) was varied as 2, 3, 5 and the spacing (s) as 10, 15, 20 mm. Load tests were conducted in a test tank using proving ring and a loading frame as shown in Fig. 2-28. After the test was finished, the diameter of the deformed portion (bulge) of the granular pile was measured by carefully exhuming clay. The results of the laboratory tests indicated that the load-carrying capacity improved further when the granular pile was reinforced by geogrid. The behavior of the pile was better with an increase in the number of geogrids and a decrease in the spacing between the geogrids, as shown in Fig. 2-29. The bulge diameter and the bulge length decreased on the reinforced granular pile with increasing number of geogrid layers and decreasing spacing distance.

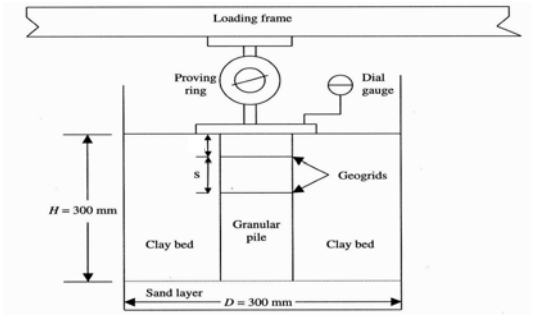

Fig. 2-28 Experimental setup (Sharma et al., 2004)

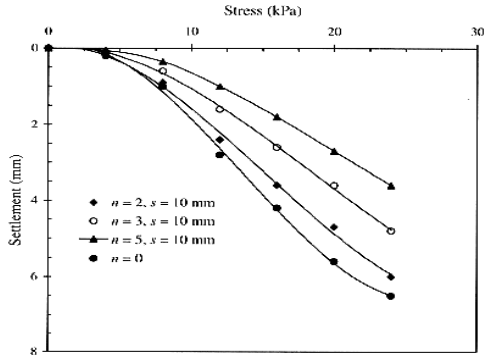

Fig. 2-29 Effect of number of geogrids, n on stress-settlement response of composite ground (Sharma et al., 2004)

2.7.2 Encasing stone column with geosynthetic materials

The past researchers proved that the encasement materials provide a greater lateral support to the stone columns than using reinforcement layers. Hence, using geosynthetic material with high stiffness as confinement around the stone column to prevent large bulging, ground spreading as well as excessive settlement under high load levels is more effective.

The radial support is guaranteed through the confining effect of the coating surrounding soft soil, because the geosynthetic experiences ring tension forces. On the basis of the interaction between cover filling, columns, geosynthetic and soft layer, the foundation system shows a flexible and a self regulating bearing behavior. The existence of geosynthetic around granular column causes the possibility of an enormous settlement reduction, acceleration of the settlement rate as well as increasing shear strength of the surrounding soft soil and bearing capacity of the whole system. This confirms that the encased stone columns are very effective in very soft clays, (Geduhn et al., 2001 and Malarvizhi and Ilamparuthi, 2004).

The encasement, besides increasing strength and stiffness of the stone column, prevents the lateral squeezing of stones when the column is installed even in extremely soft soils, thus enabling quicker and more economical installation. Encasement materials prevent also the mixing of fine grained soil with stone material which has a negative effect on the stone column drainage efficiency during the consolidation process, (Murugesan and Rajagopal, 2006).

2.7.2.1 Experimental studies

Al-Joulani (1995) carried out triaxial and uniaxial tests in which natural and reinforced stone columns with polymer sleeves were tested under controlled conditions. The effect of different variables on the stone column behavior was investigated. These variables included type of polymer sleeve, type of column aggregate, confining pressure and loading condition. The specimens were tested under static and cyclic loading conditions. This study showed that using polymer sleeves to confine stone columns would be effective in increasing stiffness and in reducing vertical and lateral deformation of these columns. The stiffness of a stone column can be given as the secant modulus. The polymer sleeves increased the secant modulus, at 10 % of axial strain, between 1.5 and 3 times as compared to corresponding module for the natural columns.

The coefficient of earth pressure at rest, K_o of the reinforced specimens was found to be less than that for the non-reinforced specimens. The K_o value of the granular material in this research was 0.34. The K_o values for sleeve reinforced columns ranged from 0.26 to 0.20 depending on geogrid type. The mobilized tensile stress in the grid sleeves decreased with an increase of the confining pressure. Therefore, the maximum tensile stresses in the sleeves were mobilized in stone columns tested under uniaxial stress conditions.

Malarvizhi and Ilamparuthi (2004) performed load tests on soft marine clay bed stabilized with a single stone column and reinforced stone column having various slenderness ratios and using different types of encasing material. Three types of geogrid with different tensile strengths were used as encasement for the stone columns which were (net1), (net2) (net3). The stiffness of net2 is greater than that of net1 but net3 has the greatest stiffness. The net3 geogrid has a maximum tensile strength of 7.68 kN/m. Load tests were conducted on single columns of 30 mm diameter. Loading was done on a plate of 72 mm diameter, which placed over the clay filled in the tank of size 300 mm diameter and 280 mm in height. Loading was done over clay alone, clay stabilized by stone column and clay stabilized with stone column encased within geogrids. The results of the tests indicated that:

1. Encasing stone column with geogrids resulted in an increase of load carrying capacity irrespective of whether the column is end-bearing or floating, as shown in Fig. 2-30. The ultimate bearing capacity of reinforced stone column and ordinary stone column treated beds are three times and two times that of the untreated bed, respectively.
2. The ultimate load capacity of the reinforced column increases with increasing stiffness of the reinforcement.
3. The modular ratio of the reinforced columns and clay (end-bearing) increases with the increase in settlement irrespective of the type of encasing material, however, the increase is negligible in case of ordinary stone column and net1 encased stone column. But the increase is appreciable and the modular ratio is 17 to 25 for the settlement between 5 and 20 mm, as illustrated in Fig. 2-31.

Gniel and Bouazza (2008) performed small-scale laboratory tests of model sand columns in order to investigate the effect of geogrid encasement on stone columns. A cylindrical tank as a unit cell was used which had a diameter of 155 mm and height of 310 mm. the unit cell consisted of a sand column with diameter of 50 mm and the surround Kaolin clay. In conjunction with this, a numerical modeling study was undertaken to further understand the interaction between the geogrid, column material and surrounding soil. Particular emphasis was placed on comparing behavior of the partially encased columns to fully encased columns. Results indicated a significant reduction in vertical column strain with an increased percentage of encased length.

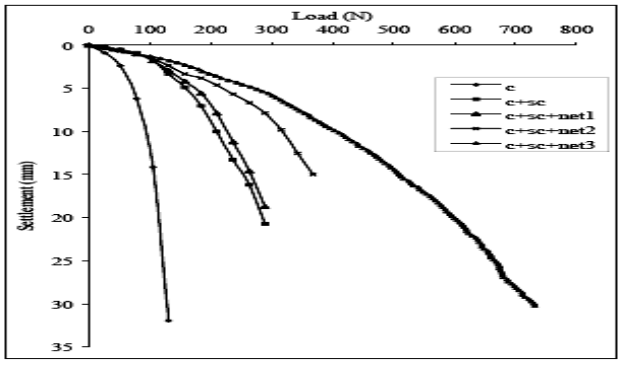

Fig. 2-30 Load versus Settlement of composite bed with various encasements (Malarvizhi and Ilamparuthi, 2004)

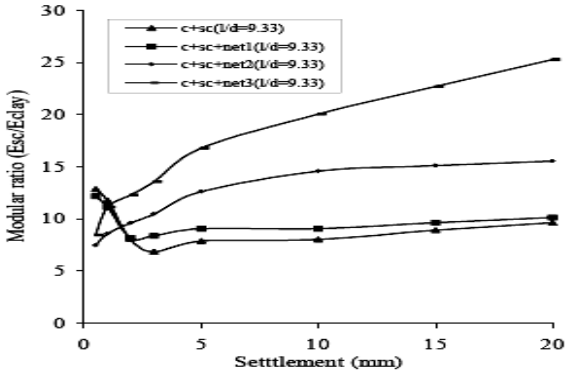

Fig. 2-31 Variation of Modular ratios with settlement (Malarvizhi and Ilamparuthi, 2004)

Murugesan and Rajagopal (2008) and Murugesan and Rajagopal (2009) presented the results from a laboratory based studies on the performance of the encased stone columns. The laboratory studies consisted of load tests on stone columns with and without encasement in a clay bed formed in unit cell tank with two different dimensions. The influence of parameters such as the diameter of the stone column and stiffness of the geosynthetic encasement were also investigated. Four different types of geosynthetics were used namely woven geotextile, nonwoven geotextile, soft grid-1 with fine mesh and soft grid–2 with coarse mesh which have ultimate tensile strength values of 20, 6.8, 2.5 and 1.5 kN/m, respectively. The major conclusions drawn from this study are as follows:

- Load-settlement response of geosynthetic encased stone columns generally shows linear behavior not indicating any catastrophic failure unlike the conventional stone columns.
- The improvement in the load capacity due to encasement depends upon the diameter of the stone column. Lesser the diameter more would be the improvement. This is in line with the findings from earlier published literature.

2.7.2.2 Theoretical studies

Malarvizhi and Ilamparuthi (2006) used a finite element analysis of a geogrid encased stone column with appropriate models to simulate the experimental conditions. Mohr Coulomb model and Soft Soil model were used for modeling stone column and the clay soil, respectively in Plaxis program. The clay is treated as an undrained material and the stone as a drained material. The column and the clay-bed were modeled as axi-symmetric. Three different geogrids were used for encasing columns net1, net2 and net3 with tensile strength of 15, 40, and 60 kN/m, respectively. Tests were conducted on single column of 30 mm, 40 mm and 60 mm diameter formed in a clay-bed of 400 mm diameter and 300 mm deep on a standard loading frame as a strain-controlled test. The diameter of the loading plate used was 2d (d – diameter of the stone column) of adequate thickness and rigidity. Based on the experimental and numerical studies, the following conclusions were drawn:

1. For a particular settlement, the load intensity of the stabilized bed with smaller diameter columns is higher than the larger diameter columns, as shown in Fig. 2-32.
2. The hoop stress generated in the geogrid was responsible for the increase in load capacity of the encased stone columns. The stiffer the geogrid is, the more the developed hoop stresses are and consequently, the higher is the load carrying capacity.
3. The composite effect of the stones and the geogrid contributes to the higher stress concentration ratio of the columns. For a smaller diameter of encased stone column, the stress concentration is higher. The increase in stress concentration is more in the columns encased with stiffer geogrid materials, as depicted in Fig. 2-33.

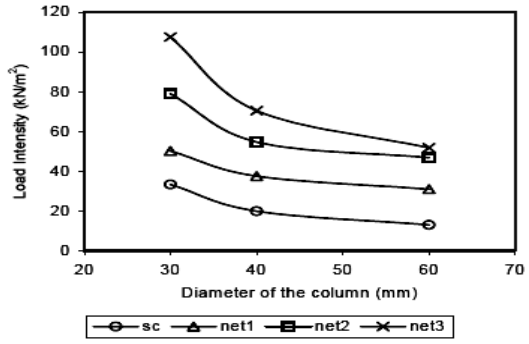

Fig. 2-32 Load intensity versus size of the column for a settlement of 10 mm (Malarvizhi and Ilamparuthi, (2006)

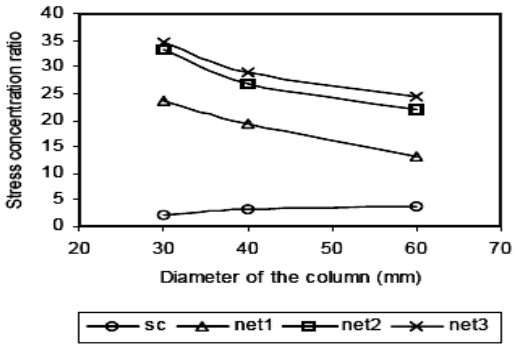

Fig. 2-33 Stress concentration ratio versus size of the column (Malarvizhi and Ilamparuthi, (2006)

Murugesan and Rajagopal (2006) studied the improvement in the load capacity of the stone column by encasement through a parametric study using finite element analysis in short term. The stone columns and soft soil were modelled as hyperbolic non-linear

elastic materials while the geosynthetic encasement was modelled as a linear elastic material. Initially, the analyses were performed by applying uniform pressure on the stone column portion alone in order to directly assess the influence of the confinement effects due to encasement. Later, analyses were performed by constructing layers of soil above the stone-column reinforced foundation soil. Detailed parametric analyses were performed. All cases were idealised through axi-symmetric modelling. The foundation soil in all the cases is assumed to be a 5 m thick soft clay layer underlain by a rigid hard stratum. Based on the results obtained from this study, the following conclusions were made:

1. The load capacity and the stiffness of the stone column can also be increased by all-round encasement by geosynthetic as shown in Fig. 2-34. By geosynthetic encasement, it was also found that the stone columns were confined and the lateral bulging was minimised.
2. The confining pressures generated in the stone columns are higher for stiffer encasements.
3. The hoop tension forces developed in the encasement were significant within a depth equal to approximately twice the diameter of the stone column as shown in Fig 2-35.
4. The performance of encased stone columns of smaller diameters is superior to that of larger diameter stone columns because of mobilisation of higher confining stresses in smaller stone column.

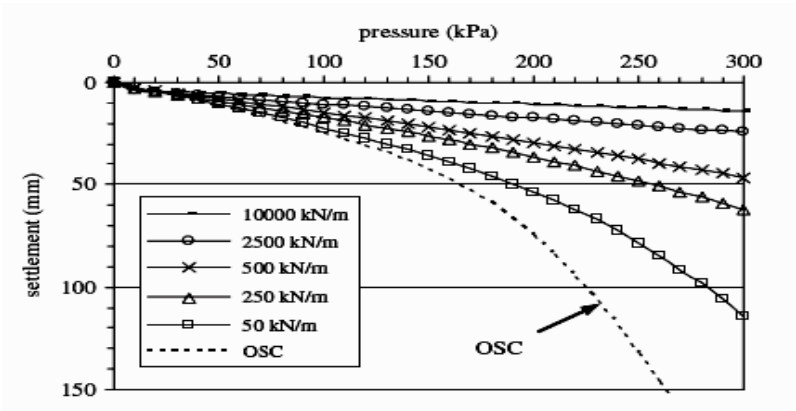

Fig. 2.34 Response of 1 m diameter stone columns with different encasement stiffness values (Murugesan and Rajagopal, 2006)

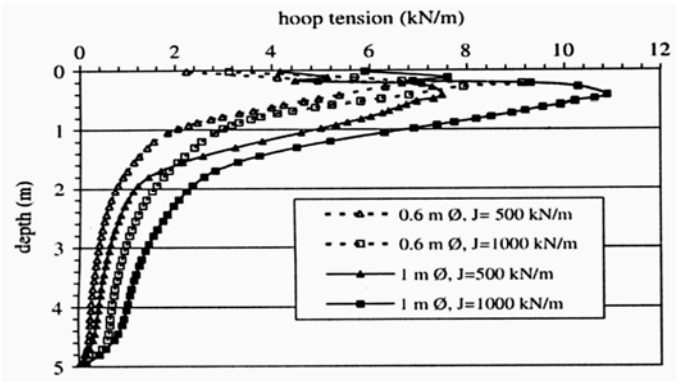

Fig. 2-35 Hoop tension forces developed in two sizes of stone columns (Murugesan and Rajagopal, 2006).

Malarvizhi and Ilamparuth (2007) also performed an axisymmetric FEM analyses on a single ordinary and encased stone column stabilized clay bed to bring out the influence of the various column parameters. The parametric study on stone columns involved varying of *L*/*d* ratio (L= length of the column; d = diameter of the column) and stiffness of geogrid. A stone column with 1 m diameter and 10 m length was modelled in a clay bed of 20 m thick. The numerical analyses showed the following results:

1- The mobilised hoop forces in the geogrid increased with increasing surcharge pressure and geogrid stiffness, as depicted in Fig. 2-36.
2- Encasing stone column increased the stress concentration on the column which increased with increasing geogrid stiffness causing reducing stress on clay and reducing settlement, as shown in figure 2-37.
3- The parametric study showed that the bearing capacity increase of ordinary and encased stone columns stabilized clay bed is not effective beyond l/d ratio of 10 and geogrid stiffness over 2000 kN/m, respectively.

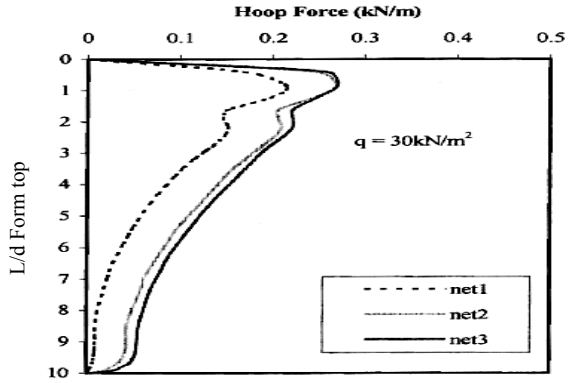

Fig. 2-36 Variation of hoop forces in encasements (Malarvizhi and Ilamparuth, 2007)

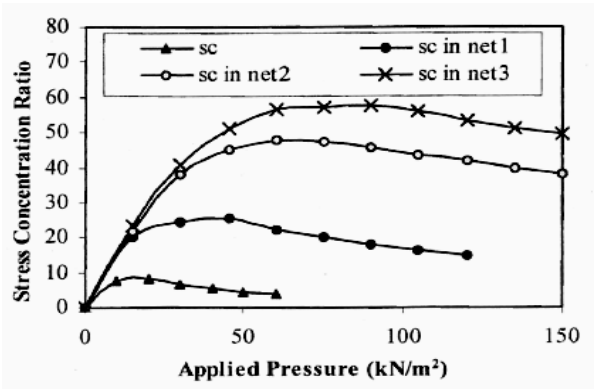

Fig. 2-37 Stress concentration ratio in column (Malarvizhi and Ilamparuth, 2007)

Zhang and Lo (2008) presented the findings of a series of numerical studies on the behavior of geosynthetic encased stone columns in very soft clay deposits and surcharged by embankment type loading. Oh et al. (2007) observed settlement of a trial embankment built on very soft clay strengthened with ordinary stone columns which indicated that the stone columns were not adequately effective in reducing settlement. Earlier work showed that the very softy clay could not provide adequate confining stress to the stone columns. For this reason, an alternative concept utilizing geosynthetic encasement was examined numerically. The development of settlement with time after the completion of stone column installation was performed. The unit cell idealization was used. Lo et al. (2007) found that the settlement after 10 years for the ordinary stone columns was 0.80 m. The study of Zhang and Lo (2008) showed that the settlement of the encased stone column is reduced to about 0.225 m by encasing stone column.

Khabbazian et al. (2009) carried out 3D finite element analyses to simulate the behavior of a single geosynthetic-encased stone column in a soft clay soil using computer program Abaqus. The thickness of the clay soil and the length of the stone column are assumed to be 5 m. The results of the analyses indicated that improving parameters of

stone column materials (friction angle and stiffness) increases the load-carrying capacity of a given stone column; however, it is more efficient to select encasement with higher stiffness rather than to improve the stone column material.

2.8 Geosynthetic encased sand columns

Using sand columns in supporting soft ground is not sufficient in some cases. Hence, it is better to encase the sand columns. When sand columns are inserted into bearing layer, the radial supporting of sand columns is strengthened by using geotextile materials.

The applied load distributed between the surrounding soil, and the cross sectional area of the column. From the loading tests, the effect of the geotextile coating on the column causes the stabilization of the column through ring tension forces in the geotextile. The mobilizing of these ring tension forces depends on the interaction between column and geotextile. The settlement and the excess water pressure decrease rapidly as well as the shear strength increases, (Kempfert, 1996 and Kempfert et al., 1997).

Raithel (1999) carried out well monitored, large scale and rational symmetric model tests of geotextile coated sand columns under static and cyclic loading. Analytical solution was performed also for the geotextile coated sand columns. The results showed that the settlement is depended mainly on the area replacement ratio and the stiffness of the geotextile.

Raithel and Kempfert (2000) developed a numerical and an analytical calculation model for the design of the geotextile coated sand columns foundation system. The numerical analysis was split up into two separate models. By the examination of a single column, according to the 'unit cell concept' and the use of an axial symmetric calculation model, the ring tension forces for the design were derived. To investigate the deformation behavior of the whole system of a dam foundation, a large scale model was used. The coating can not be simulated directly, because the columns must be substituted by walls of equal area ratio. The results showed that large settlements and strains in the geotextile were observed when using analytical model compared to the numerical analyses, especially immediately after loading, as illustrated in Fig. 2-38-a. It can also be shown that the ring tension forces and the settlement definitely depend on the stiffness of the geotextile and the area ratio of the column grid, as shown in Fig. 2-38-b.

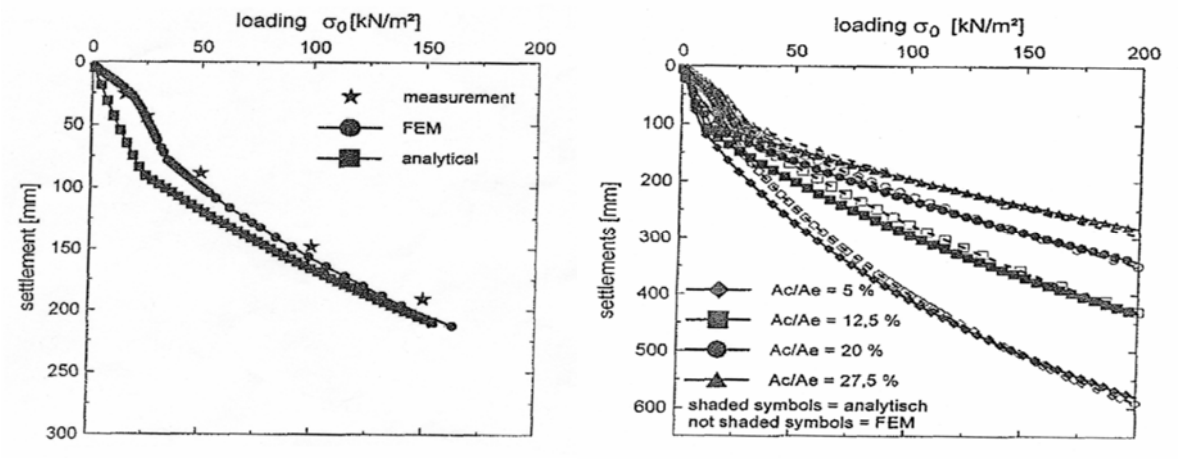

(a) (b)

Fig. 2-38 Load-settlement curves of (a) Comparative calculation-large scale model test and, (b) parametric study: variation of area ratio A_c/A_e for J = 1000 kN/m (Raithel and Kempfert, 2000)

Kempfert et al. (2002) studied geotextile encased sand columns (GEC) under a dike in the Elbe River, Hamburg (2001/2002), instead of the original concept of using sheet piles on a length of 2500 m and 40 m depth. The dike was constructed on a polder area which contains a soft soil layer with a thickness of 7-15 m. The engineering concept used encased sand columns by circular-woven geotextile. Over 60 000 geotextile-encased columns were installed with a diameter of 80 cm, which were sunk to the bearing layers at depths of between 4 and 14 m below the base of the dyke. Raithel et al. (2004) explained the theoretical background of the GEC bearing system for this project of the Elbe River. The processes both for the design and the preparation of the earth statically calculations were presented. Numerical calculations were also used for the GEC-System using Plaxis program. Generally, an axial symmetric model according to Raithel (1999) and Raithel and Kempfert (2000) was used for calculating and designing geotextile encased column foundation. In comparison with the original concept, the foundation and ground improvement GEC system achieved the following:

- Eliminated 35,000 tons of steel, since sheet wall was not necessary
- Saved 150,000 sq. m of tidal mud-flat reclamation;
- Used 1,100,000 sq. m less sand to fill up the dike (steeper slope, large settlement reductions);
- Shortened construction time for the dike from 3 years to 8 months;
- Produced a dramatic settlement reduction and high settlement acceleration.

2.9 Discussion

Past researchers especially in the last two decades discussed the improvement mechanism of soft soil with stone columns. Although the studies were performed by using experimental small and somewhat large models, the full scale reflects the real behavior of the studied cases. The past research also contained FEM analyses and analytical solutions of the stone columns reinforced soft soil. Although most of the used FEM analyses and analytical solutions included elastic behavior for the soft soil and the column material, the behavior of these materials are elastoplastic. Most of the past

studies were performed in undrained conditions in spite of the long term stability is more important when dealing with soft soil. The experimental and theoretical studies indicated that stone columns are most often used in soft clay soils to: 1) reduce and accelerate detrimental ground settlement, and 2) increase the bearing capacity of the site. The generated heave in short term conditions wasn't studied and it needs to be illustrated.

The bearing capacity of the improved site is governed by the degree of the lateral bulging of the stone column that occurs during loading. Some researchers studied the stone columns bulging but the variation of bulging with column diameter and spacing between columns especially in long term was not explained. The past researchers discussed that the stress concentration and load transferring within stone columns increase with increasing stone column stiffness. But the stress concentration in the stone columns and reducing stress in the surrounding soil correlation with the applied loads along the consolidation process need to be illustrated. The role of the stress concentration on acceleration of the consolidation needs also to be outlined.

The past researchers explained that the geosynthetics industry has responded to the instability of stone columns need by developing casing of the stone column. The types of geosynthetic that fulfill this function are either geotextile 'socks' or geogrid tubes that enclose the stone or granular material of the column. By installing geosynthetic in conjunction with the stone column, there exists a method to prevent the lateral bulging of the column during loading, thereby maximizing bearing capacity of the improved ground. Most the past research and projects used geotextile to encase the stone columns. In spite of the geogrid material has a higher stiffness than the geotextile material. But the geogrid material has the greater openings which permit the mixing of the soft soil with stone materials. Composite section of geogrid / geotextile has been used in the current study to gain the advantage of higher stiffness of the geogrid and the advantage of preventing mixing and keeping drainage ability of the stone column.

Although the past research performed on the encased stone columns also were in short term conditions, the role of the encasement stiffness in the soft soil heave is far from clear. Therefore, the behavior of geogrid-stone columns reinforcement system in soft soil foundations during and after consolidation time is also far from clear. The bearing capacity, the settlement, the differential settlement and the bulging as well as the stress distribution within the geogrid casing is still poorly understood especially in long term conditions which have great influences on the performance of the geogrid-stone column reinforced soft soil foundation. The degree of that foundation system improvement is depended on several variables: the stiffness of the geogrid casing; the depth of encasement; the diameter of the stone column; the volume of soft soil around the stone column; the loading level and; the loading conditions. Naturally, it is essential to understand those components of the encased stone column system to enhance the system performance and to be effective throughout its service life.

3 Finite Element Modeling

3.1 General

The finite element method has been applied to geotechnical engineering problems since 1960's, having been developed a decade earlier for applications in structural engineering and continuum mechanics. The name finite element was, however, first coined in a paper by Clough (1960), in which the technique was presented for plane stress analysis. Since then, a large amount of research has been devoted to this technique and a number of research papers and text books have been published on this subject. The method is now firmly established as an engineering tool of wide applicability. The main advantage of the method is that it can be applied to the materials exhibiting non-linear stress-strain behavior. In the current research the finite element program of Plaxis has been used.

3.2 PLAXIS program

This study discusses the reinforced soft soil with ordinary and encased stone column under embankment loads, which was carried out by (Plaxis 9) computer program. Development of Plaxis began in 1967 at the Technical University of Delft as an initiative of the Dutch Department of Public Works and Water Management. The initial brief was to develop an easy-to-use finite element code for the analysis of a river embankment on soft soil of low lands in Holland. In subsequent years, Plaxis was extended to cover the most other areas of geotechnical engineering.

Plaxis is a finite element package specially intended for the analysis of deformation and stability in geotechnical engineering projects. Plaxis Version 9 is a two-dimensional finite element code and is available commercially to conduct analysis of deformation and stability for a variety of geotechnical problems. The program can be used in plane strain as well as in axisymetric modeling. Geotechnical applications require advanced constitutive models for the simulation of the non-linear and time - dependent behavior of soils. In addition, since soil is multi-phase material, special procedures are required to deal with hydrostatic and non-hydrostatic pore pressure in soil. The input of soil layers, structures, loads and boundary conditions based on convenient drawing procedures (CAD), which allows a detailed accurate modeling of real situations is achieved. From this geometry model a finite element mesh is automatically generated. Plaxis program consists of four main parts, Input, Calculation, Output, and Curves part. In the following sections a brief description of the Plaxis program parts will be mentioned.

3.3 Finite elements and nodes

To deal with accuracy in geotechnical problems, Plaxis program contains various types of elements and nodes (Plaxis Manual, 2008). The following paragraphs contains the types which used in the current analyses,

3.3.1 Soil element

During generation of the mesh, clusters are divided into triangular elements. Plaxis provides two types of triangular elements, 6-nodes element which contains six nodes and 15-nodes element which contains fifteen nodes, as shown in Fig. 3-1. During the finite elemet calculation, displacements are calculated at those nodes. Users can preselect nodes for the generation of the load-displacement curves. In the other hand, stress is calculated at individual points which called stress points rather than at the nodes. A 15-nodes triangular element contains twelve stress-points while a 6-nodes triangular element contains three stress points, as shown in Fig. 3-1.

The non-reinforced and the reinforced soft soil with ordinary and encased stone columns under embankment have been modelled as 2D (two dimensions) analysis as axisymetric and plane strain problems, 15-nodes triangular element was selected.

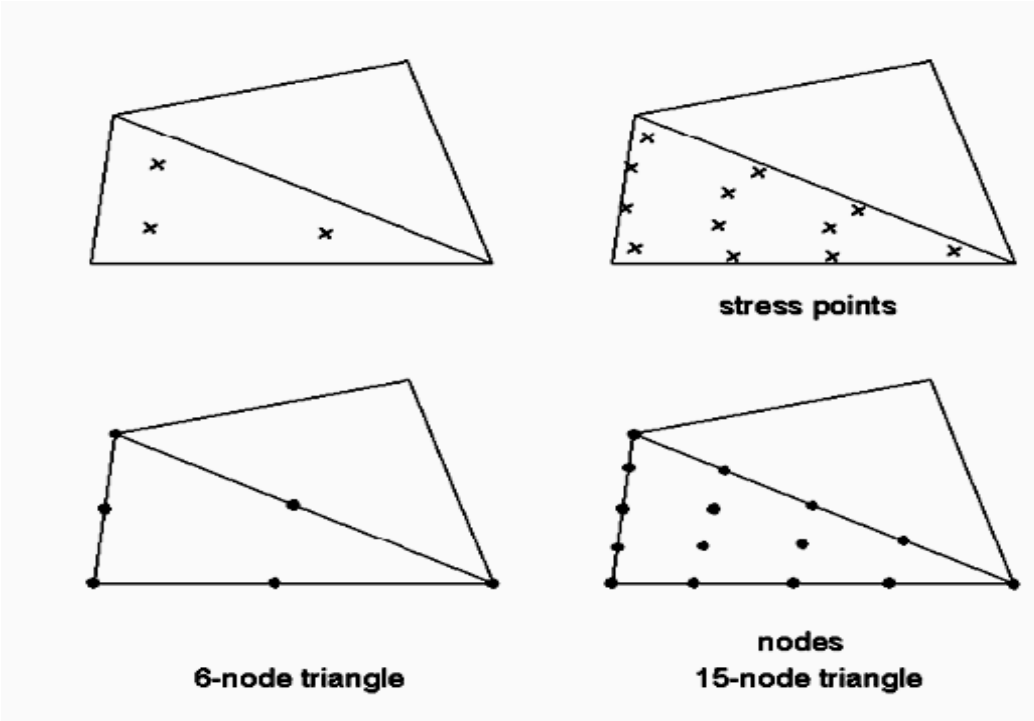

Fig. 3-1 Distribution of nodes and stress points in soil element

3.3.2 Geogrid element

Geogrids are slender objects with a normal stiffness but no bending stiffness. Geogrid can only sustain tensile force and no compression. Therefore, the only material property of the geogrid which needs to be specified is the axial stiffness, J = EA. The geogrid element is defined by three nodes when the 6-nodes soil elements are used. Whereas when the 15-nodes are used, the geogrid element is defined by five nodes. In the current research 5-node geogrid elements are used in combination with 15- node soil elements. Axial forces are calculated at the stress points. The location of the stress points corresponds to the location of the nodes. The geogrid element is used to simulate the encasement material in the current research.

3.4 Input program

In the Input program of Plaxis the geometry is given by entering different soil layers, structural parts, and external loads etc. A choice between various available material models: Linear model, Mohr-Coulomb, Hardening Soil, Hardening Soil Model with Small-Strain Stiffness, Soft Soil and Soft Soil Creep, is made at the input for each material. The material is given relevant material properties, such as stiffness and density, which are assigned to elements together with appropriate boundary conditions. Also the model in whole is assigned boundary conditions. When the model is complete, a mesh is generated and initial stresses and pore water pressures are initiated before moving to the Calculation program.

3.4.1 Modeling of soil behavior

Plaxis 9 supports different models to simulate the behavior of the soil. These models are briefly mentioned in the following sections. In the other hand, the Mohr-Coulomb model and the Soft Soil Creep model which are used in the current study are also mentioned in more detail.

- ***Linear Elastic Model (LE)***

This model represents Hooke's law of isotropic linear elasticity. The model involves two elastic stiffness parameters, namely Young's modulus, E and Poisson's ratio, ν. This model is very limited for the simulation of the soil behavior.

- ***Hardening Soil Model (HS)***

This is an elastoplastic type of hyperbolic model, formulated in the framework of friction hardening plasticity. It is a hardening model that does not account for softening due to soil dilatancy and de-bonding effects. This model can be used to simulate the behavior of sand, gravel and overconsolidated clays.

- ***Hardening Soil Model with Small-Strain Stiffness (HSsmall)***

It is a modification of the above hardening soil model that accounts for the increased stiffness of soils at small strains. At low strain levels most soils exhibit a higher stiffness and this stiffness varies non-linearly with strain. The advanced features of the HSsmall model are apparent in working load conditions.

- **Soft Soil Model *(SS)***

This model can be used to simulate the behavior of the soft soils such as normally consolidated clay and peat. The model performs best only in case of primary compression.

- **Mohr Coulomb Model *(MC)***

It is also an elastic perfectly plastic model. The Mohr-coulomb model requires a total of five parameters, which are generally familiar to most geotechnical engineers and which can be obtained from basic tests on soil samples. These parameters are Young's modulus, E, Poisson's ratio, ν, Friction angle, φ, Cohesion, c, and Dilatancy angle, ψ.

Young's modulus (E)

Plaxis uses the young's modulus as the basic stiffness in the elastic model and the Mohr-Coulomb model. A stiffness modulus has the dimension of stress. The values of the stiffness parameter adopted in a calculation require a special attention as many geo-materials show non-linear behavior from the beginning of loading. For soils, the initial slope is usually indicated as E_0, and secant modulus at 50 % strength is denoted as E_{50}, as shown in Fig. 3.2. For materials with a large linear elastic range it is realistic to use E_0, but for loading of soils E_{50} is generally used. Considering case of unloading problems, as in tunnels and excavations, E_{ur} is used instead of E_{50}. E_{ur} is defined as the unloading and reloading elasticity modulus. Plaxis offers a special option of layers in which the stiffness increases with depth.

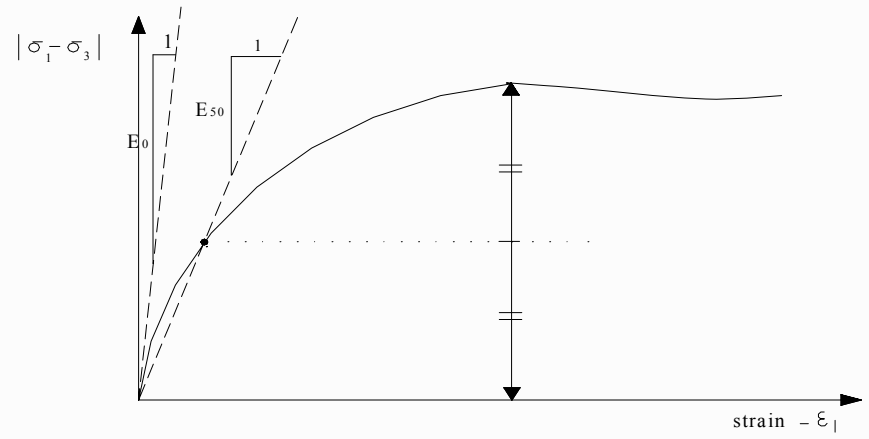

Fig. 3-2 Definition of E_0 and E_{50} for standard drained triaxial test results

Poisson's ratio (ν)

The selection of a Poisson's ratio is particularly simple when the elastic model or the Mohr-Coulomb model is used for gravity loading. For this type of loading Plaxis should give realistic ratios of $K_0 = \sigma_h / \sigma_v$ as both models will give the well-known ratio of $\sigma_h / \sigma_v = \nu / (1 - \nu)$. For one-dimensional compression it is easy to select Poisson's ratio that gives a realistic value of K_0: Hence, ν is evaluated by matching K_0. In many cases, the value of ν is ranged between 0.3 and 0.4. In general, such values can also be used for loading conditions other than one-dimensional compression.

Cohesion (c)

The cohesive strength has the dimension of stress. Plaxis can handle cohesion-less soils (c = 0), but some options will not perform well. Plaxis offers a special option of layers in which the cohesion increases with depth.

Friction angle (φ)

The friction angle, φ is entered in degrees. The friction angle largely determines the shear strength by means of Mohr's stress circle, as shown in Fig. 3-3. The Mohr-Coulomb failure criterion proves to be better for describing soil behavior than the

Druker-Prager approximation, as the latter failure surface tends to be highly inaccurate for axisymetric configurations.

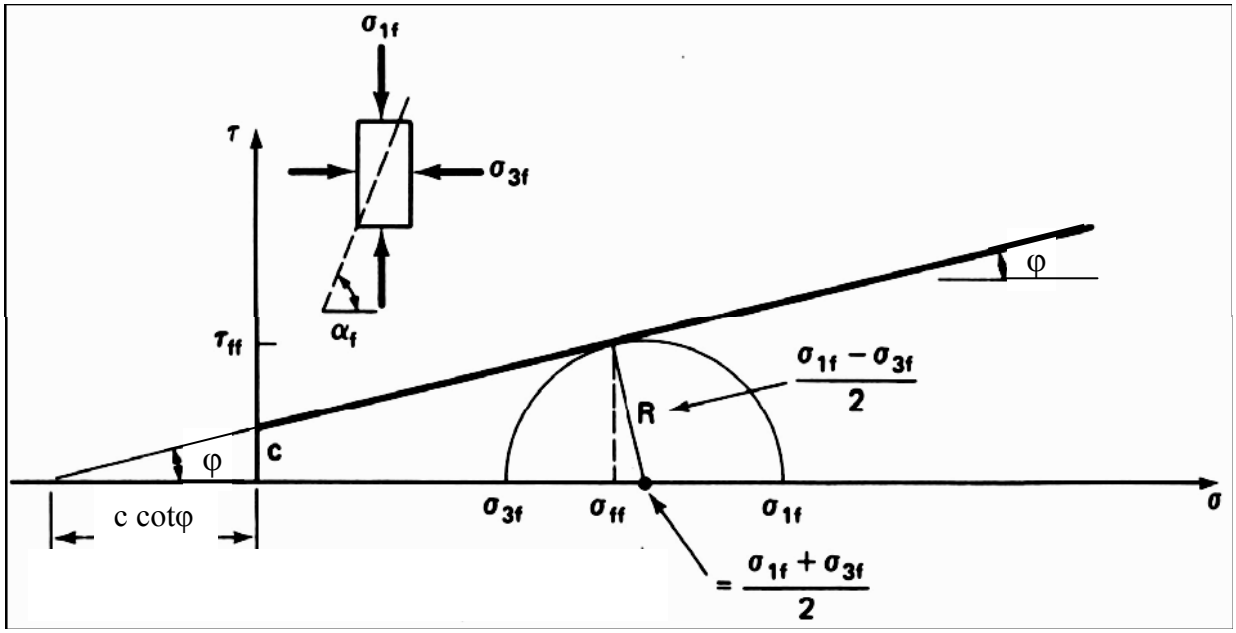

Fig. 3-3 Mohr coulomb failure envelope with one Mohr failure circle

Dilatancy angle (ψ)

The dilatancy angle, ψ is specified in degrees. Apart from heavily over-consolidated layers, clay soils tend to show little dilatancy ($\psi = 0$). The dilatancy of sand depends on both the density and the friction angle. A small negative value of ψ is only realistic for extremely loose sands.

- **Soft Soil Creep Model *(SSC)***

The Hardening Soil model doesn't account the creep and the stress relaxation. In fact, all soils exhibit some creep and the primary compression is thus followed by a certain amount of secondary compression.

The high degree of compressibility, creep and the secondary compression are dominant in soft soils such as normally consolidated clay, silt and peat. These are best demonstrated by oedometer test data. Therefore, Plaxis implemented a model under the name of Soft Soil Creep which is a relatively new model and it has been developed for application of settlement problems of foundations, embankment, etc. The proper initial soil conditions are essential when using Soft Soil Creep Model. It also includes data on the pre-consolidation stress to take in consideration the effect of over-consolidation. Some basic characteristics of the Soft Soil Creep model are:

- Stress dependent stiffness (Logarithmic compression behavior)
- Distinction between primary loading and unloading-reloading
- Secondary (time dependent) compression

- Memory of pre-consolidation
- Failure behavior according to Mohr Coulomb criterion

The full description of the Soft Soil Creep model and the above soil models is stated in the Manual of Plaxis 9, (2008). In the current study, the Soft Soil Creep is used to simulate the Bremerhaven clay and the Hamburg clay. The Soft Soil Creep Model requires the following main parameters:

- Failure parameters as in the Mohr-Coulomb model:

Cohesion, c
Friction angle, φ
Dilatancy angle, ψ

- Parameters of the Soft Soil Creep model:

Modified compression index, λ*
Modified swelling index, κ*
Modified secondary compression index, μ*

These parameters can be obtained both from an isotropic compression test and an oedometer test. When plotting logarithm of the stress as a function of strain, the plot can be approximated by two straight lines, as shown in Fig. 3-4. The slope of the normal consolidation line gives the modified compression index, λ* and the slope of the unloading or swelling line can be used to compute the modified swelling index, κ*. There is a difference between the modified indices λ* and κ* and the original Cam-Clay parameters λ and κ. The later parameters are defined in terms of the void ratio, e instead of the volumetric strain, ε_v. The parameter μ* can be obtained by measuring volumetric strain on the long term and plotting it against the logarithm of time, as shown in Fig. 3-5.

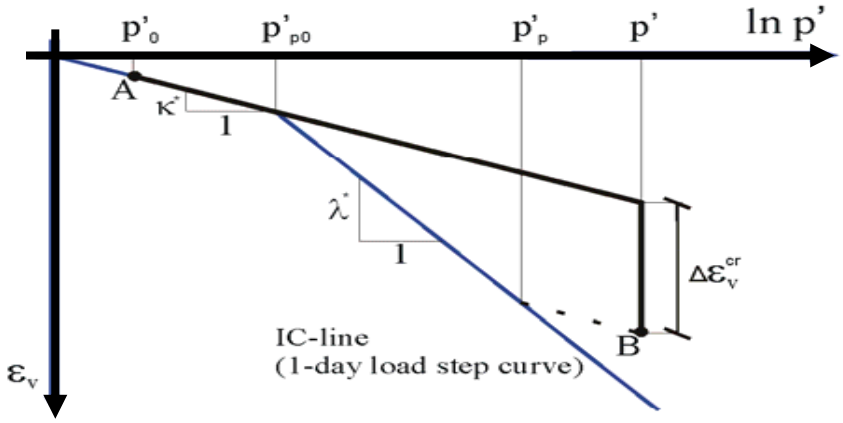

Fig. 3-4 Idealized stress-strain curve from oedometer test with division of strain increments into elastic and a creep component

Relationship to Cam-Clay parameters:

$$\lambda^* = \lambda / (1+e) \qquad \kappa^* = \kappa / (1+e)$$

Relationship to internationally normalized parameters:

$$\lambda^* = C_c / 2.3(1+e) \qquad \kappa^* \approx 2C_s / 2.3(1+e) \qquad \mu^* = C_\alpha / 2.3(1+e)$$

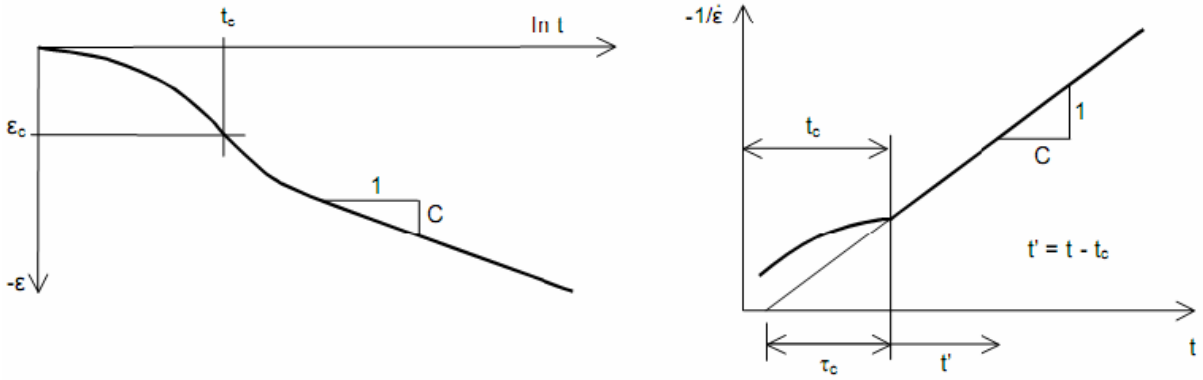

Fig. 3-5 Consolidation and creep behavior in standard oedometer test, (Manual of Plaxis 9, 2008)

3.4.2 Types of soil behavior

In principle, all model parameters in Plaxis are meant to represent the effective soil response, i.e. the relation between stresses and strains of the soil skeleton. An important feature of the soil is the presence of pore water. Pore pressure significantly influences the soil response. To enable incorporation of the water-skeleton interaction in the soil response Plaxis offers for each model a choice of three types of behaviour:

- ***Drained behavior***

Using this setting no excess pore water pressure is generated. This is clearly the case for dry soils and also for full drainage due to high permeability as in sand or a low rate of loading. This option may also be used to simulate long-term soil behaviour without the need to model the precise history of the undrained loading and consolidation.

- ***Undrained behavior***

This setting is used for a full development of excess pore water pressure. This occurs when a soil has low permeability as in clays or under a high rate of loading. The undrained behavior is usually followed by consolidation in loading phases.

- ***Non-porous behavior***

Using this option neither initial nor excess pore-water pressure is taken into account. Application for this option may be found in modelling of concrete and rock or structural behaviour. Non-porous behavior is often used in combination with linear elastic model.

3.4.3 Model generation

As mentioned above, two types of material elements have been used to model the reinforced soft soil with ordinary and encased stone column using geogrid material which studied in this research.

- Soil elements have been used to simulate the stone column material; the surrounding soft soil, the blanket layer and the embankment fill in both of the unit cell and the whole embankment modelling. The soft foundation soil has been modeled (in undrained and consolidation, and drained conditions) by the Soft Soil Creep Model. The stone column material, the blanket layer and the embankment fill have been modeled by the Mohr Coulomb Model in drained conditions.
- Geogrid elements have been used to simulate the geogrid encasement. Three different geogrid materials are used as encasement. The axial stiffness, EA values are 400, 600 and 800 kN/m.

- **Geometry and boundary conditions**

When setting up the geometry of the models, each model was divided into four clusters. The first and the second cluster represent the foundation soil and the stone column. While the third and the forth cluster represent the blanket fill layer and the embankment fill. However, the forth cluster was divided into sub-clusters to represent the stages of the embankment construction. The geometry of each model was controlled by the following conditions,

- Applying uniform load on the stone column portion only as a distributed load.
- Loading entire area of the stone column and the surrounding soft soil by applying embankment loads in intervals.
- The volume of the surrounding soft soil has been varied to investigate the influence of spacing distance between columns on the behavior of the soft soil foundation.
- The volume of the stone column has been varied to investigate the influence of the column diameter on the behavior of the soft soil foundation
- Ordinary and encased stone columns are used to reinforce the soft soil to study the effect of encasement on the behavior of the soft soil foundation.
- Different encasement stiffness and depths are used to study the effect of them on the performance of the stone columns.

Half of the model is selected to reflect the effect of symmetry. The standard fixities are assigned to the boundary conditions which is available in Plaxis.

- **Mesh generation**

Plaxis uses unstructured mesh, which is generated automatically with options for global and local mesh refinement. Plaxis provides five choices of mesh density ranged from very coarse mesh to very fine mesh. In this research medium mesh was chosen. Mesh was refined in zones which stresses and strains are expected to be high i.e. the upper part of the stone column and the surrounding soil.

- **Initial conditions**

Once the geometry of the model has been created and the finite element mesh has been generated, the initial situation must be specified. Plaxis provides an option to specify the initial conditions. This option consists of two modes: one mode for the generation of the initial water pressure and the other mode for the specification of the initial geometry configuration and the generation of the initial effective stresses. In this research, the water table has been set to be at the surface of the soft foundation soil.

3.5 Calculation

After generation of a finite element model, calculation can be executed and calculation type has to be specified in this step.

3.5.1 Types of calculations

Choices between different ways of analysis the actual problem are made in the Calculation program. Distinction is made between three basic types of calculations, a plastic calculation, Consolidation analysis and Ph-c reduction (safety analysis).

- ***Plastic calculation*** should be selected to carry out an elastic-plastic deformation analysis in which it is not necessary to take excess pore pressures with time into account. The plastic calculation does not take time effect into account, except when the Soft Soil Creep model is used.

- ***Consolidation analysis*** should be selected when it is necessary to analyze the development or the dissipation of excess pore pressures in water-saturated clay-type soils as a function in time. Plaxis allows for true elastic-plastic consolidation analyses. In general, a consolidation analysis without additional loading is performed after an undrained plastic calculation. It is also possible to apply loads during a consolidation analysis. Varying time spans can be considered by choosing *Consolidation* and then enter the desired number of days. If full consolidation analysis is wanted, *Minimum Pore Pressure* should be selected, where all excess pore pressure is reduced. The plastic calculation and the consolidation analyses have been used in the current study.

- **Phi-c reduction (safety analysis)** can be executed by reducing shear parameters. A safety analysis can be performed after each individual calculation phase and thus for each construction stage to calculate the safety factor. However, the Phi-c reduction cannot be used as a starting condition for another calculation phase because it ends in a state of failure.

3.5.2 Loading types

After specifying calculation type, the loading has to be specified. The following types of loading can be selected:

- ***Staged construction*** is the most important type of loading. In this Plaxis feature it is possible to change the geometry and load configuration by deactivating or reactivating loads, volume clusters and structural objects as created in the geometry input. Staged

construction enables an accurate and a realistic simulation for various loading, construction and excavation processes. The option can also be used to reassign material data sets and to change the water pressure distribution in the geometry. To carry out a stage construction calculation, it is first necessary to create a geometry model that includes all the objects that need to be used during the calculation. Objects that are not required in the start of the calculation should be deactivated in the initial geometry configuration. A stage construction can be executed in Plastic calculation or in Consolidation analysis which both of them have been used in the current research.

- *Total multipliers* type is used to specify the ultimate values of external loads. When the total multiplier loading is selected, the ultimate values of external loads will be applied exactly at the end of calculation.

- *Incremental multiplier* type is selected when the external load is applied incrementally. Before entering a load increment, an increment of time can be entered. Increments of time are not relevant when using plastic calculation except when time-dependent models are used. The input of time increments is essential when using consolidation analysis.

3.6 Output

When the calculations are completed the results can be viewed in the Output program.
A large amount of data can be obtained from a finite element calculation such as stresses, pore pressures and displacements for soils, and displacement and forces for geogrid material.

3.7 Curves

In the Calculation program there is an option to pre-select points of interest in the model. If such a point is pre-selected, the displacement, the stress or the pore pressure of the point for each iteration, step or time can be viewed in the sub program Curves. The results can be viewed in either a table or as a graphic curve.

4 Behavior of the Geosynthetic Reinforced Stone Columns - Soft Soil Foundation System

4.1 Introduction

The soft soil is reinforced by ordinary and encased stone columns to study the behavior of soft soil-stone column foundation system. The FEM package of Plaxis 9 program analysis has been used to provide all the valuable information, which is required to understand this foundation behavior. This analysis can predict the complete response of the geogrid reinforced stone column-soft soil foundation system. In the following sections, the modeling of the stone columns, the soft soil and the geogrid, and the discussion of the results of the parametric study are presented. The discussion contains the effect of the spacing between columns, the column diameter, the encasement, the encasement stiffness and the encasement depth on the behavior of the stone columns. The behavior of the system has been investigated for undrained and drained conditions.

4.2 Numerical modeling and selection of parameters

In order to make realistic predictions of the behavior of the geogrid reinforced stone column-soft soil system, two types of soil are used, stone for the columns and Bremerhaven clay as a soft soil. The Mohr Coulomb model in Plaxis 9 program is used for the stone columns material and the Soft Soil Creep model is used to describe the behavior of the Bremerhaven clay. The properties of the stone columns material were adopted from the study of Ambily and Gandhi (2007) and the properties of Bremerhaven clay were adopted from the study of Geduhn (2005). The stone column material is modeled in drained condition while the surrounding soft soil is modeled in undrained and drained conditions. The properties of these soils are tabulated in Table 4-1. In the current research, the “unit cell” analyses have been conducted using axisymmetric conditions, so the shear strength parameters of the triaxial test are used directly.

A wide variety of geosynthetic materials such as woven and non-woven geotextiles, geogrid, geomembrane and geo-composites are used in foundation engineering. In the present work, the geogrid reinforcement is used as encasement for stone columns. As known, the geogrid has stiffness values greater than geotextile. Three types of geogrid materials are used in this research, Secugrid 20/20 Q1, and Secugrid 30/30 Q1. The other type is a geogrid/nonwoven geotextile composite which is called Combigrid 40/40 Q1 151 GRK 3 (Naue GmbH). The Combigrid 40/40 includes a geogrid covered by a geotextile to allow drainage without mixing soft soil with stone particles. The geotextile is arranged in such a way that it would not contribute either to vertical or lateral stiffness of the encased stone column. The properties of these materials are tabulated in Table 4-2.

The geogrid encasement is modeled as a linear elastic continuum element with a series of one-dimensional bare (line) elements having no bending stiffness. The axial stiffness modulus of the reinforcement is defined as the tensile force per unit width per unit strain. The geogrid stiffness (J = EA) has been calculated at a strain of 2 % where the geogrid is under working stress conditions.

Table 4-1 Properties and shear strength parameters used for the soil.

Parameter	**Symbol**	**Stone Soil, (Ambily and Gandhi, 2007)**	**Bremerhaven clay, (Geduhn, 2005)**[1]
Material model	Type	Mohr-Coulomb	Soft Soil Creep
Loading	Condition	Drained	Undrained and drained
Wet soil unit weight	γ_{wet}, (kN/m^3)	19	15
Horizontal permeability	k_h, (m/day)	12	2x10^{-4}
Vertical permeability	k_v, (m/day)	6	1x10^{-4}
Young's modulus	E, (kN/m^2)	55,000	-
Poisson's ratio	ν (-)	0.3	-
Modified compression index	λ^* (-)	-	0.203
Modified swelling index	κ^* (-)	-	0.025
Modified secondary compression index	μ^*	-	0.007
Cohesion	c`, (kN/m^2)	0	5
Friction angle	φ` °	43	37.75
Dilatancy angle	ψ°	10	0

1) After Richwien, 1981.

Table 4-2 Properties of the geogrid materials

Property	**Unit**	**Secugrid 20/20 Q1**	**Secugrid 30/30 Q1**	**Combigrid 40/40 Q1**
Raw material	-	Polypropylene (PP), white		
Mass per unit area	g/m^2	155	200	240
Max. tensile strength, md / cmd*	kN/m	20 /20	30 /30	40 /40
Elongation at nominal strength, md / cmd*	%	8 / 8		
Tensile strength at 2% elongation, md / cmd*	kN/m	8 / 8	12 / 12	16 / 16
Axial stiffness at 2% elongation, J	kN/m	400	600	800
Aperture size, md x cmd*	mm x mm	33 x 33	32 x 32	31 x 31

Based on md = machine direction and cmd = cross machine direction

4.3 Finite element model

4.3.1 Finite element mesh

The used finite element model for the reinforced soft soil with stone column as a unit cell is shown in Fig. 4-1-a. The unit cell consists of one stone column with a specific diameter, (d) and the surrounding soft soil. The unit cell area depends on the orientation of the columns. In this research the square orientation method is used which having a

square influence zone around the column, as mentioned in Chapter 2. This square zone is approximated and converted to a circle zone with the same area. Where the diameter of the influence area of the unit cell is d_e = 1.13 (S), S: spacing distance between columns. The radius of the unit cell (d_e/2) in this model is extended from the column centerline to the outer border of the unit cell. In this unit cell analyses technique, the soft soil layer with 6.0 m depth is reinforced with stone columns. The system is simulated as axisymetric model. Half of the foundation is selected to reflect the effect of symmetry. The nodes on the lateral boundaries have been restrained in the x – direction only but the nodes on the bottom boundary have restrained in both x and y – directions. The finite element mesh was generated automatically with 15-node elements, as shown in Fig. 4-1-b.

4.3.2 Analysis Procedure

The reinforced soft soil with ordinary and encased stone columns has been investigated by using an elastic perfectly plastic finite element analysis which involves a number of iterations.

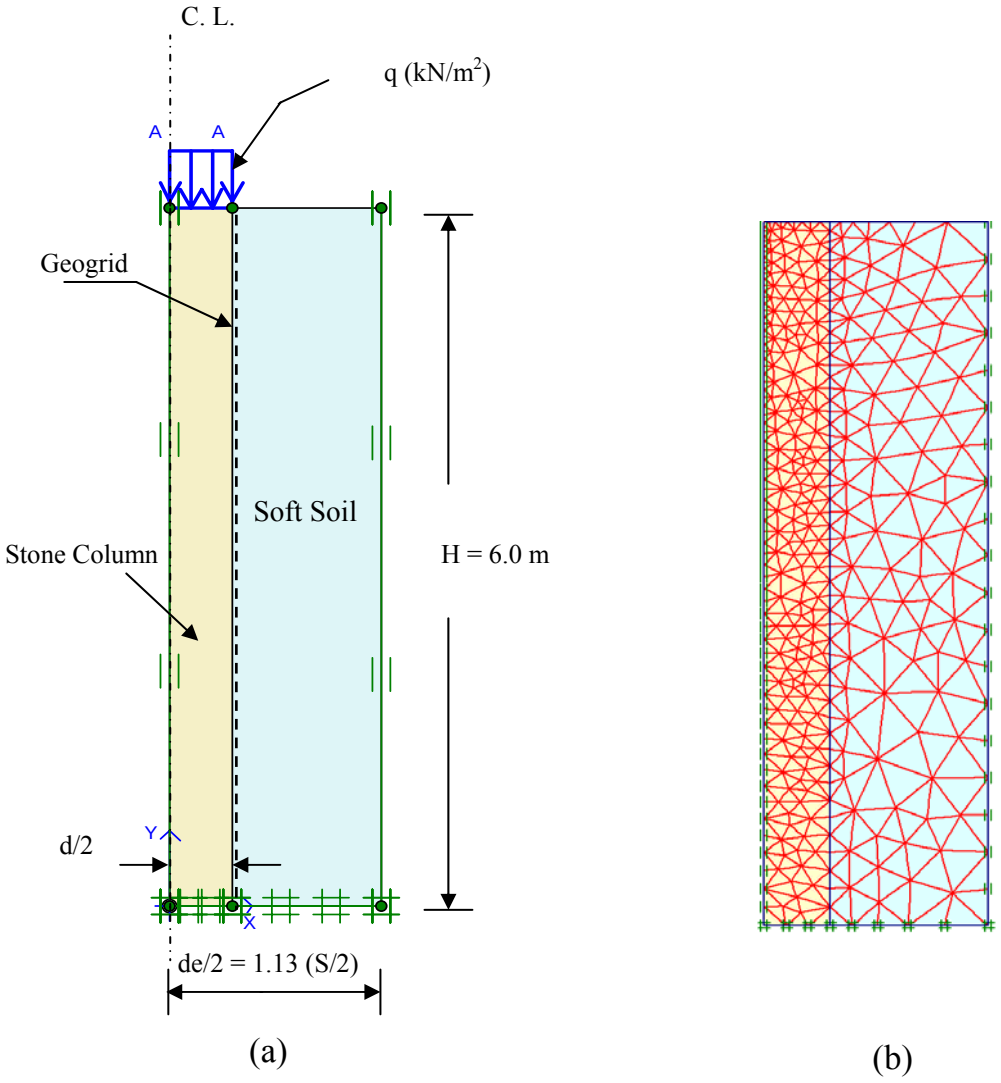

Fig. 4-1 Model of the unit cell (a) Model parts, (b) FEM mesh

When a load is applied on the soft soil–stone column foundation system, the load is divided relatively between the stone column and the surrounding soil according to their stiffness. As known, the stone column has greater stiffness than the soft soil. Therefore, the stone column carries a high percentage from the load.

Hence, this part of the current research contains the stone column loading only to study the effect of spacing between columns, column diameter, geogrid encasement, geogrid stiffness and encasement depth on the behavior of the stone columns in undrained and drained conditions of the surrounding soft soil. The ordinary and the encased stone columns were loaded by a vertically distributed load in intervals until failure.

Table 4-3 presents all cases of study which have been computed by Plaxis 9 program. This table contains four groups which will be discussed in the following paragraphs.

Table 4-3 Parametric study

Group No.	Column diameter, d (m)	Spacing ratio between Columns (S/d)	Geogrid Encasement			Surrounding soft soil conditions
			Name	Stiffness, J (kN/m)	Depth ratio (h/d)	
A	1.0	2 3 4	-	-	-	Undrained and Drained
B	0.6 1.0 1.4	2	-	-	-	
C	0.6	2	Secugrid 20 Secugrid 30 Combigrid 40	400 600 800	10	
D	0.6	2	Combigrid 40	800	1 2 3 4 5 6 8 10	

4.4 Discussion of the results

Firstly, the stone column with a diameter (d) of 1.0 m and a spacing ratio (S/d) of 3.0 has been loaded until failure. Fig. 4-2 shows the load-settlement relationship of the stone column loaded in undrained conditions. Initially, there is a small increase in settlement with increasing load which continues linearly until the yield point is reached at a load of 150 kPa. Beyond this point the plastic phase starts with a larger increase in settlement with loading. The rate of the settlement increases until failure is reached

where the settlement increase at approximately constant load. The limit state occurs at a load of 200 kPa. Therefore, a load of 180 kPa has been chosen to be applied in all the further calculations in undrained conditions to compare between the results of the studied cases.

The lateral displacement, (u_h) along the stone column-soft soil interface at section I-I was calculated under column loads of 40, 80, 120, 150, 160 and 180 kPa. The column displaces laterally into the soft soil in the upper part near the ground surface. The displacement rate increases with increasing load up to 150 kPa. Larger loads result a large increase in the lateral displacements because the stone column transfers from the elastic to the plastic stage, as shown in Fig. 4-3. The lateral bulging gradually increases up to a maximum value which occurs approximately at a depth of 15 % of the column diameter. Below that, the lateral bulging values decrease gradually with depth. The values of the lateral bulging approach zero below a depth that equals two times the column diameter (2d) for all load levels.

The load-settlement relationship of the stone column was also computed in drained conditions, as shown in Fig. 4-4. The relation starts with a slight increase in settlement with loading until the load approximately equals 60 kPa. Then, the rate of settlement increases with loading and the load-settlement relationship behaves approximately linearly. Depending on this linear relation, the modulus of elasticity of the whole system can be determined. The load-settlement curve continues and doesn't indicate a clear failure. So, the limit state is considered in this case at a settlement of 20 % of the stone column height. The limit state load is 358 kPa at a settlement of 120 cm. In comparison to the undrained conditions, the bearing capacity of stone column in drained conditions is higher. This is because the increase in the shear strength of the soft soil due to consolidation. The consolidated soft soil provides a stronger lateral support to the stone column which leads to the increase of the bearing capacity of the stone column. At similar load levels, the settlement in drained conditions is greater than that in undrained conditions.

The lateral displacement along the stone column-soft soil interface was calculated under column loads of 60, 120, 150, 180 and 300 kPa, as shown in Fig. 4-5. The column displaces laterally into the soft soil with loading especially in the upper part. This displacement starts with a small value near the surface and gradually increases with depth until it reaches a maximum value at a depth of half of the column diameter (0.5 d). Then, the lateral displacement decreases gradually along the column to reach zero at the column base. The lateral bulging along the stone column increases with increasing load.

In comparison of drained with undrained conditions, the maximum values of lateral bulging transfer to greater depths and the lateral bulging distributes along the whole depth of the stone column. This phenomenon is due to stress transfer to greater depths when loaded in drained conditions. The stress transfer increases with increasing load.

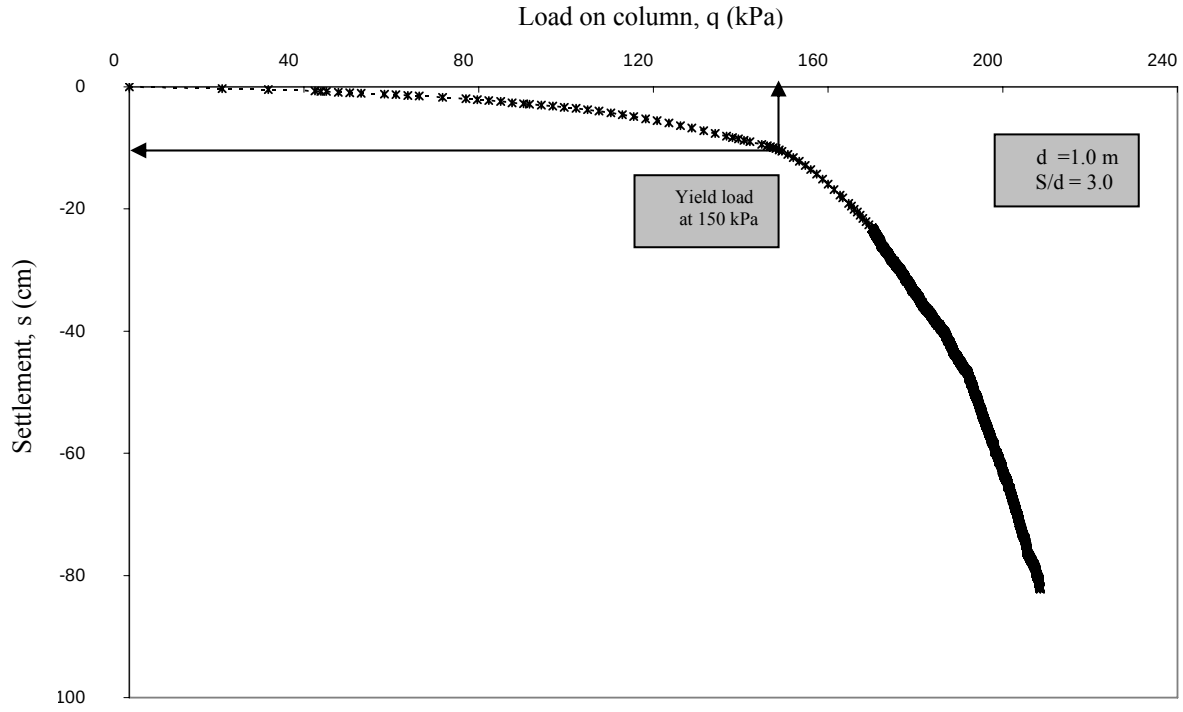

Fig. 4-2 Stone column-load settlement relationship under undrained conditions

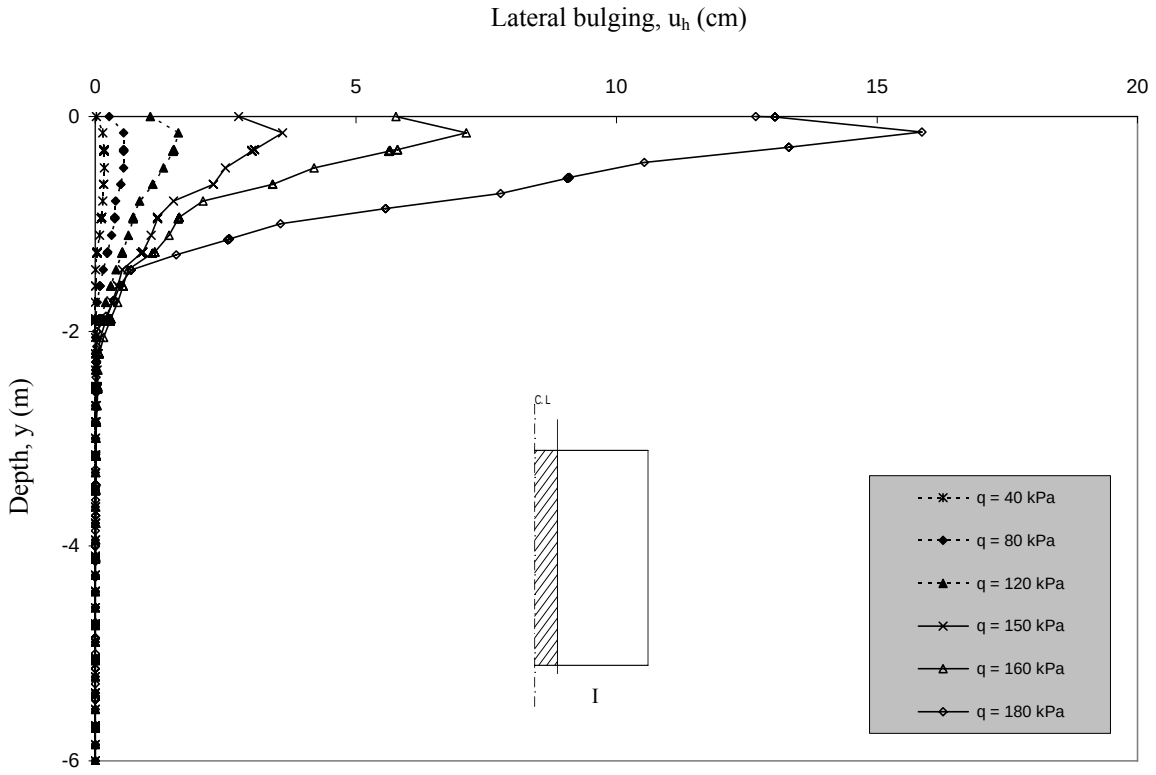

Fig. 4-3 Lateral bulging observed in the stone column-soft soil interface for various column load levels, q under undrained conditions

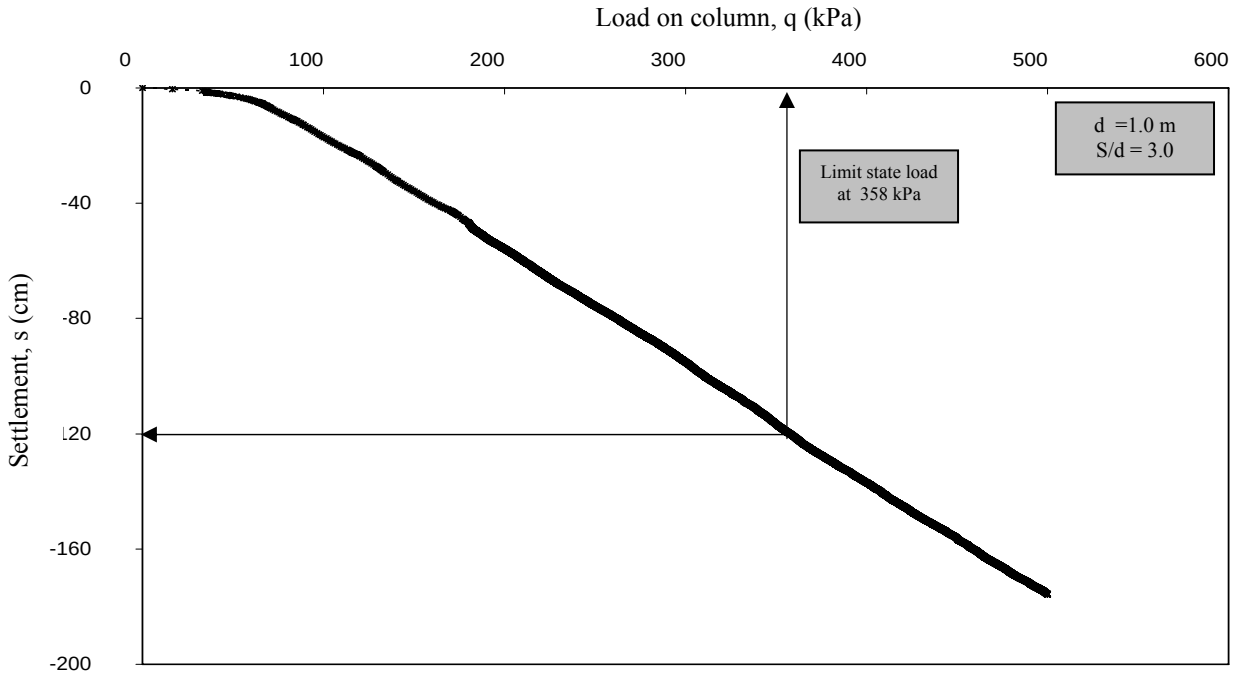

Fig. 4-4 Stone column load-settlement relationship under soft soil drained conditions

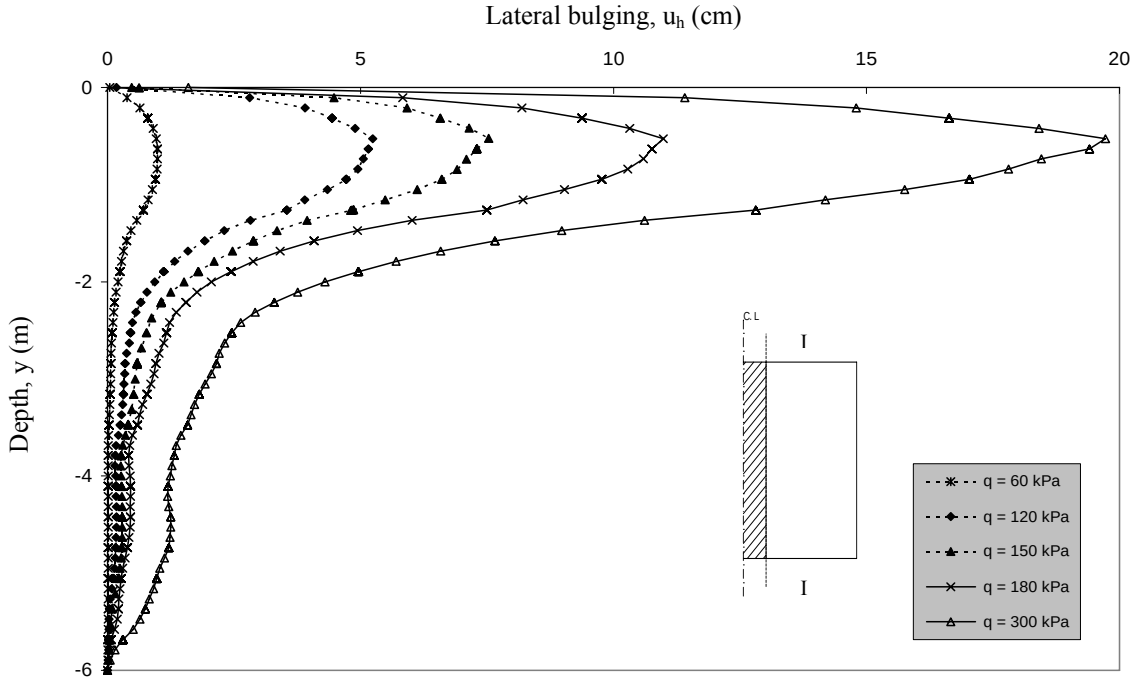

Fig. 4-5 Lateral bulging observed in the stone column-soft soil interface for various column load levels, q under drained conditions

Fig. 4-3 and Fig. 4-5 indicate that, the lateral bulging of the stone column in undrained conditions is smaller than that in drained conditions for loads smaller than 150 kPa. For example at a load of 120 kPa, the maximum lateral bulging is 1.6 cm in undrained conditions and 5.2 cm in drained conditions. For loads larger than the load of 150 kPa, the lateral bulging of the stone column in undrained conditions is greater than that in drained conditions. For example at a load of 180 kPa the maximum lateral bulging is 15.9 cm in undrained conditions and 11.0 cm in drained conditions. This is because the stone column yields at load of 150 kPa in undrained conditions.

4.4.1 Group (A): Effect of spacing between columns (S)

The unit cell technique with various geometric dimensions is used to study the effect of spacing between columns on the column behavior. So, ordinary stone columns with diameter 1.0 m have been loaded with varying surrounding soft soil volume in undrained and drained conditions. The spacing to diameter ratios are S/d = 2, 3, and 4. The load-settlement behavior of the stone columns for all spacing ratios is the same in undrained and drained conditions, as shown in Fig. 4-6 and Fig. 4-7, respectively. The bearing capacity of the stone column increases with decreasing spacing distance between the columns, as tabulated in Table 4-4. So, the highest bearing capacity is occurred when the least spacing (S/d = 2) is used in undrained and drained conditions. Also the modulus of elasticity of the stone column increases with decreasing spacing distance in drained conditions, as shown in Table 4-4.

The lateral bulging, (u_h) values at the stone column-soft soil interface and the vertical displacements at the surface were calculated at the load of 180 kPa. The lateral bulging of the stone column increases with increasing spacing distance in undrained conditions. The values of the lateral bulging disappear below a depth that equals two times the column diameter (2d) for all the column spacing ratios, as shown in Fig. 4-8.

The lateral bulging of the stone column in drained conditions increases with increasing spacing distance in the upper part of the column while the lower parts of the column contain somewhat small lateral displacements. These lower horizontal displacement values increase with decreasing spacing distance between columns. This is due to the stress in the stone column transfer downwards while the consolidation process develops. So, if the spacing distance between the columns is reduced, more stress is transferred to greater depths due to the greater confinement from the nearly neighbor columns. At the same spacing ratio, the lateral displacement of the stone columns in undrained conditions is greater than that in drained conditions at the upper part as shown in Fig. 4-8. This is due to the shear strength of the soft soil increases after consolidation which leads to increasing lateral support of the column.

Table 4-4 Bearing capacity results for a column diameter of 1.0 m.

Spacing ratio, (S/d)	**Undrained Conditions**	**Drained Conditions**	
	Settlement at 160 kPa load, (cm)	**Settlement at 300 kPa load, (cm)**	**Modulus of Elasticity, E (kPa)**
2	13.2	66.9	2317
3	15.0	95.1	1526
4	19.2	105.9	1362

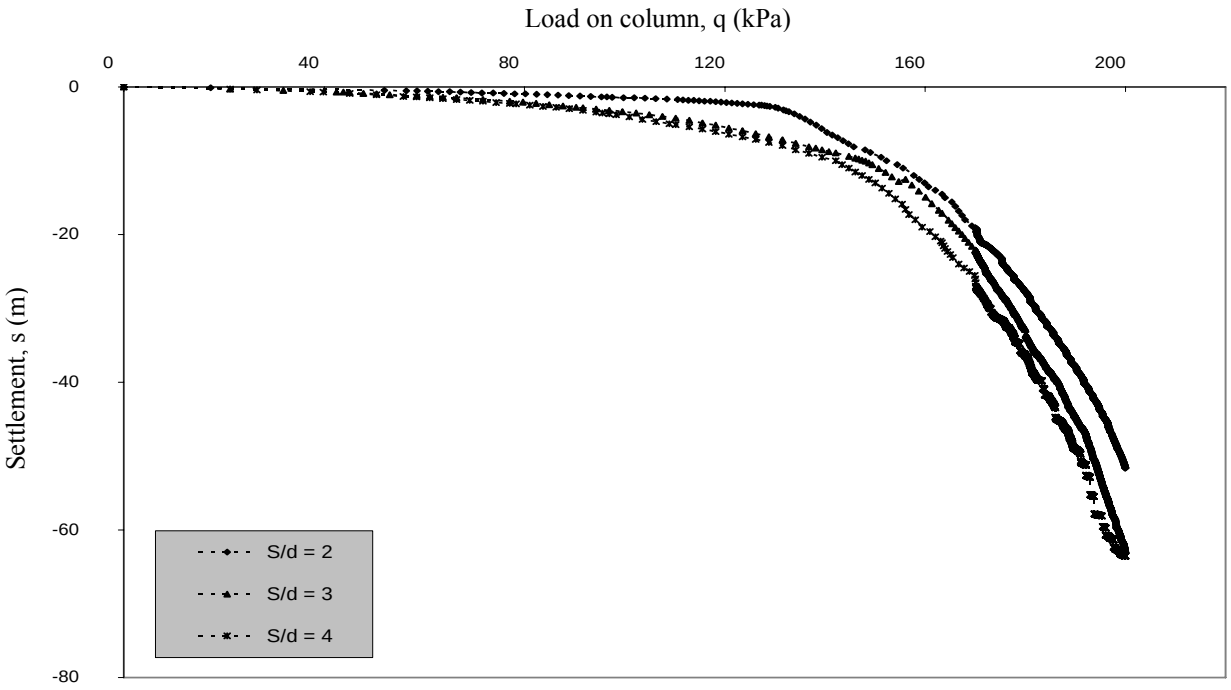

Fig. 4-6 Effect of stone column spacing on the load-settlement relationship in undrained conditions with diameter d = 1.0

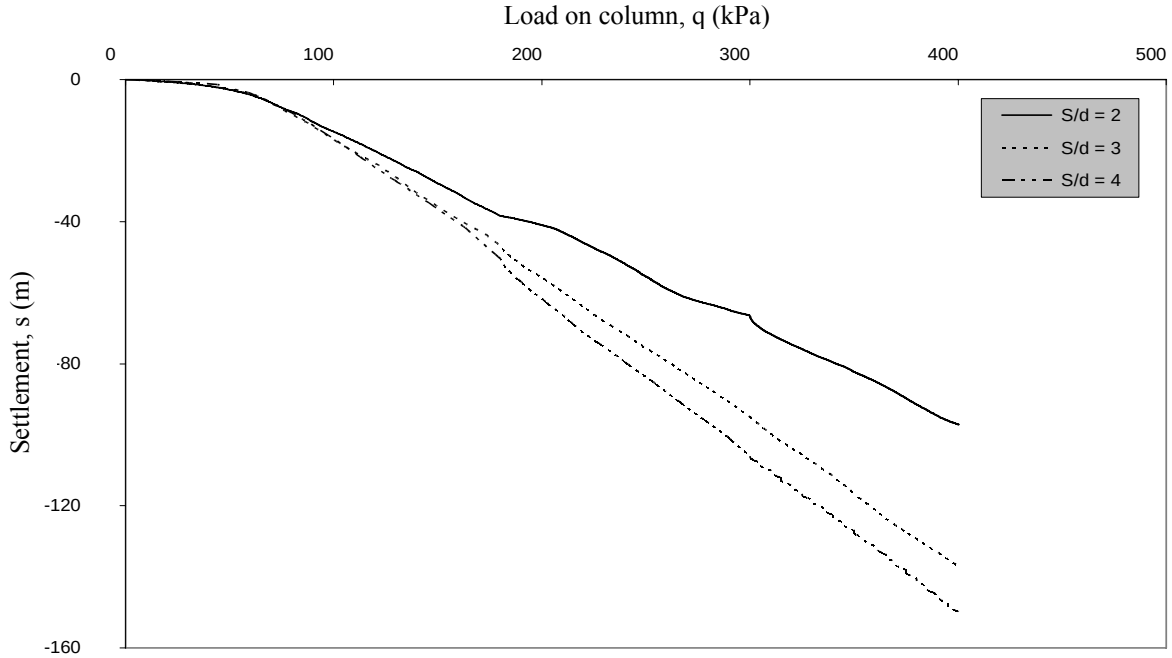

Fig. 4-7 Effect of stone column spacing on the load-settlement relationship in drained conditions with diameter d = 1.0

Fig. 4-9 shows the vertical displacements distributed at the surface for a distance from the stone column centerline to the outer edge of the unit cell. Firstly in undrained condition, the settlement of the stone column is approximately constant across its diameter. The settlement gradually decreases beside the stone column and converts to heave. The maximum value of the heave is near the column generating a high differential vertical displacement between the stone column and the surrounding soft soil. Then the heave decreases gradually with distance away from the column. The settlement increases with increasing spacing distance but the heave decreases with

increasing spacing distance. This phenomenon is due to the stress overlap occurring between the closed columns as well as due to constant volume in undrained loading condition. When two narrow standing columns are loaded, they are displaced downwards and laterally causing lateral displacement in the surrounding soft soil on both sides. So, the soft soil between these two columns must be displaced upward with a significant distance to keep the overall soft soil volume constant. The volume of the soft soil between narrow spacing columns is more stressed and less than that between wide spacing columns. Hence, the soft soil heave in the narrow spacing columns is greater than that in the wider spacing distances.

Secondly, in drained conditions the stone columns have an approximately constant settlement across the diameter. The settlement decreases gradually in soft soil causing a high differential settlement between the stone column and the surrounding soft soil. The settlement of the stone column increases with increasing spacing distance between the columns while the settlement in the soft soil decreases with increasing spacing distance. Therefore, the differential settlements increase with increasing spacing distance between the columns, as shown in Fig. 4-9. The soft soil between the closed columns shows the maximum settlement because the volume of the soft soil between the columns is more confined and more stressed than that in the cases of larger spacing distances. This causes more settlement during the consolidation process. The settlement of stone columns in drained conditions is greater than that in undrained conditions for all spacing ratios while the soft soil heave in undrained condition converts to settlement in drained conditions as shown in Fig. 4-9.

From the above discussions the spacing ratio of S/d = 2 is better than the greater spacing ratios in increasing stone column bearing capacity and also in decreasing stone column bulging.

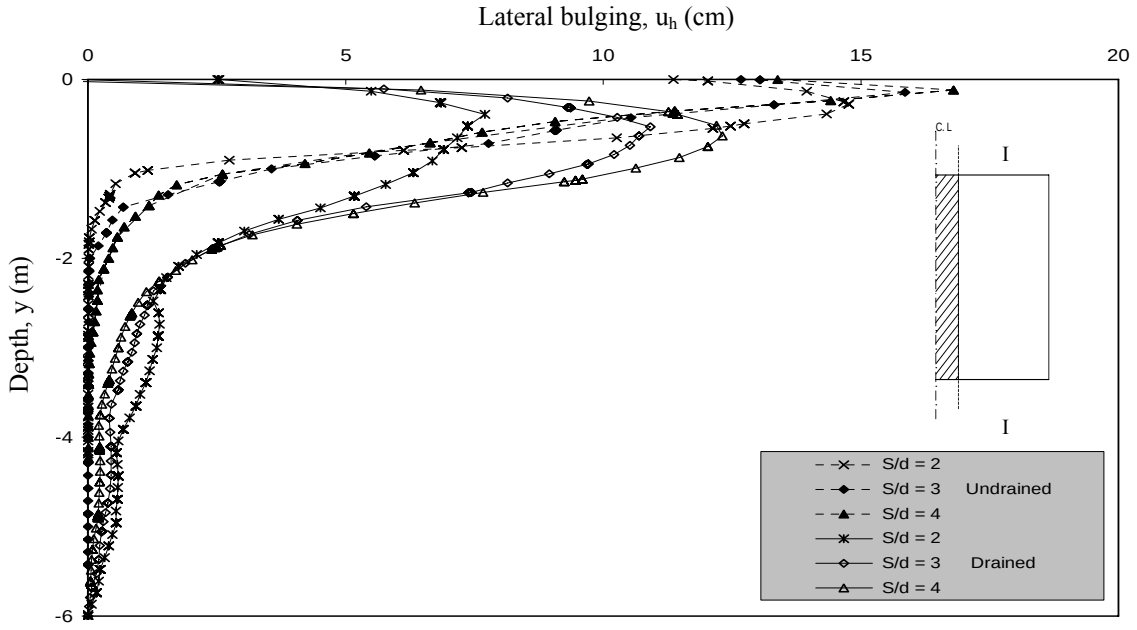

Fig. 4-8 Effect of stone column spacing on the lateral bulging for a column load of 180 kPa with a diameter 1.0 m in undrained and drained conditions

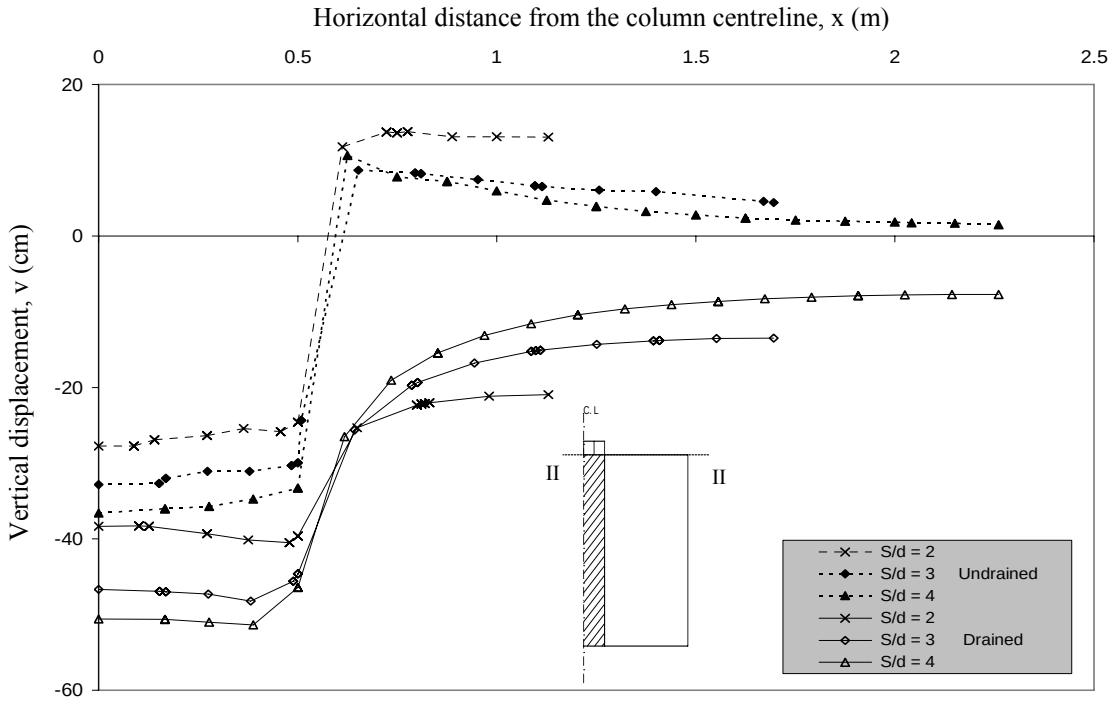

Fig. 4-9 Effect of stone column spacing on the vertical displacements for a column load of 180 kPa with a diameter 1.0 m in undrained and drained conditions

4.4.2 Group (B): Effect of stone column diameter (d)

Stone columns with the same spacing distance ratio S/d of 2 and different diameters d = 0.6, 1.0 and 1.4 m have been loaded in undrained and drained conditions. Fig. 4-10 and Fig. 4-11 show the load-settlement relationships of the stone columns in undrained and drained conditions, respectively. The load-settlement relationships for three diameters show the same development. The bearing capacity of the stone column increases with decreasing column diameter in undrained and drained conditions. But the bearing capacity increase in long term is greater than that in short term. The difference between the bearing capacity of the stone column with diameter of 1.0 m and 1.4 is greater than the difference between the bearing capacity of the stone column with diameter of 0.6 m and 1.0 m especially in long term. The stone column with a diameter d of 0.6 m has the highest bearing capacity of the studied cases in both short and long term conditions.

The lateral displacement at section I-I and the vertical displacement at section II-II were calculated under a load of 180 kPa. The lateral displacement significantly increases with increasing diameter of the stone column in undrained and drained conditions, as shown in Fig. 4-12. Hence, the stone column with a diameter of 0.6 m has the smallest lateral displacement. This behavior occurs due to the fact that the stone columns with smaller diameters are more confined by the surrounding soil and the near stone columns. The lateral displacement increasing rate is greater in short term than that in long term.

The stone column settles when loaded in undrained conditions. This settlement is converted to heave in soft soil. The settlement of the stone column and the heave of the soft soil increase with increasing stone column diameter values and also the differential vertical displacements increase as shown in Fig. 4-13. Beside the confinement effect the constant volume has also an influence on the vertical displacements of the stone

column. At the same spacing ratio, the settlement of the stone column and the lateral displacement in soft soil increase within increasing column volume. Therefore, the stone column with a greater diameter and volume experiences a greater lateral displacement which leads to increasing heave in the surrounding soft soil to keep its undrained volume constant.

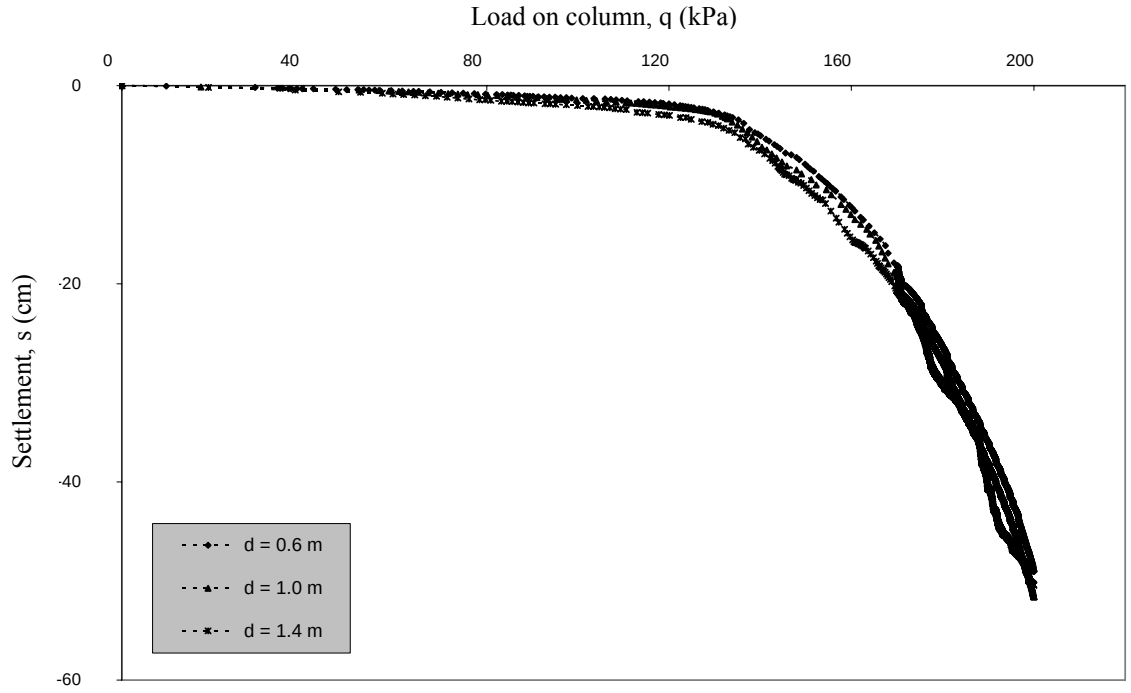

Fig. 4-10 Effect of the stone column diameter on the load-settlement relationship in undrained conditions with a spacing ratio of S/d = 2.0

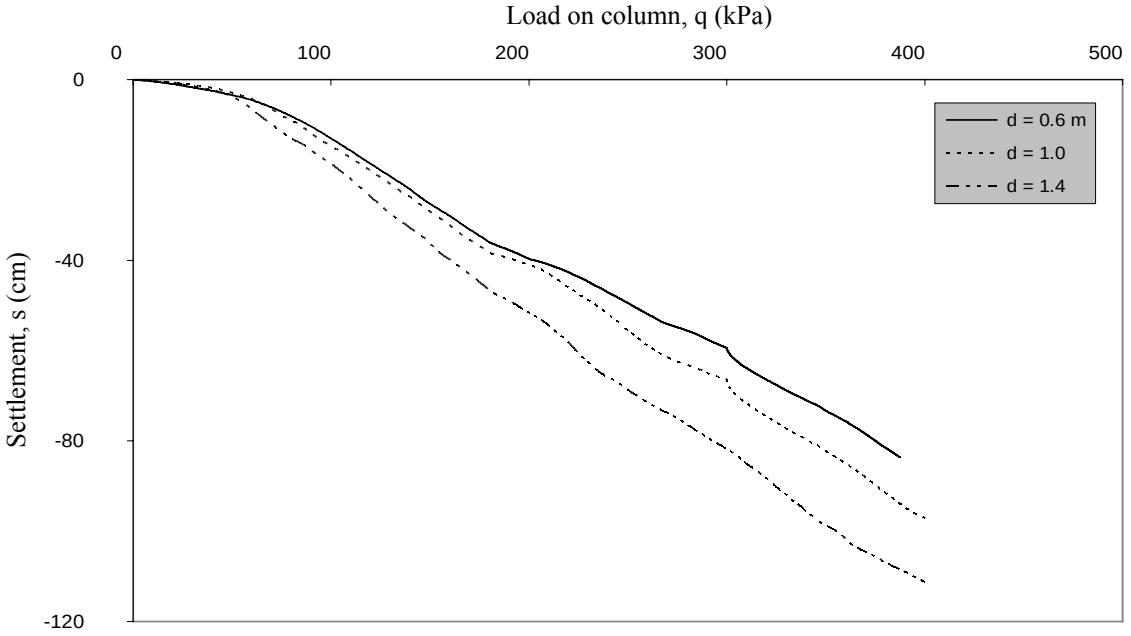

Fig. 4-11 Effect of the stone column diameter on the load-settlement relationship in drained conditions with a spacing ratio of S/d = 2.0

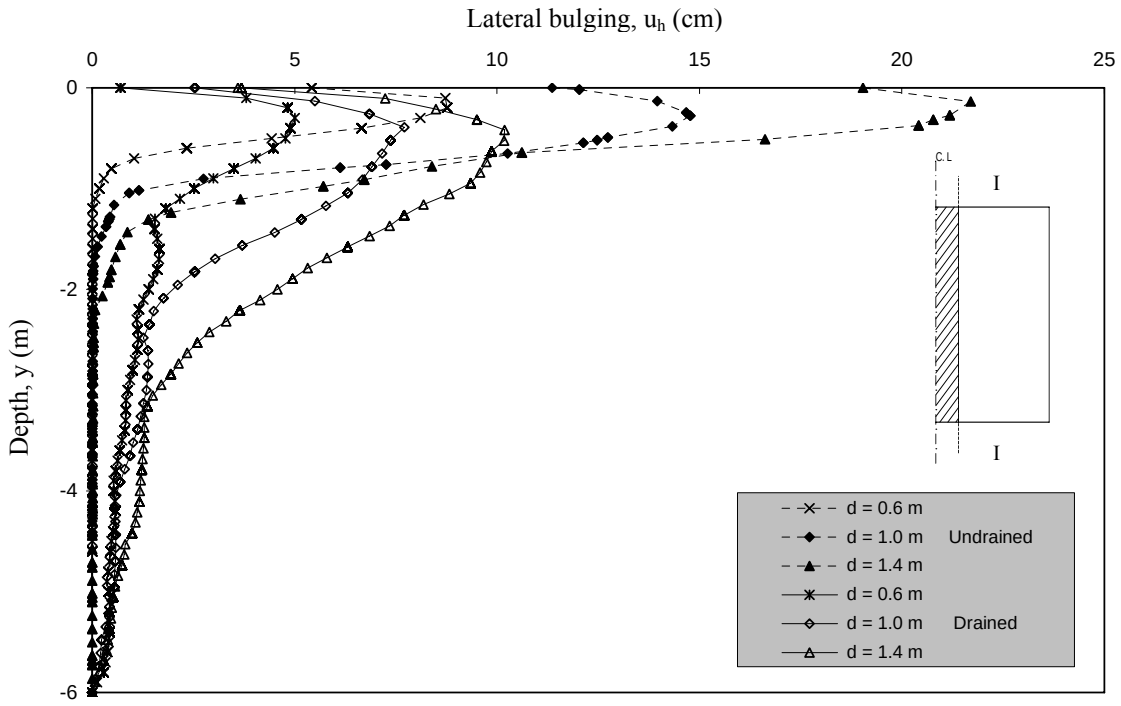

Fig. 4-12 Effect of the stone column diameter on the lateral displacement under a column load of 180 kPa in undrained and drained conditions with S/d = 2.0

Fig. 4-13 also includes the settlement of the stone column and the surrounding soft soil in drained loading conditions. The stone column settles under the applied load. The settlement decreases sharply in the surrounding soft soil. The settlement in the stone column increases with increasing column diameter while the settlement in the surrounding soft soil has a slight reduction with increasing column diameter. So, the differential settlement increases with increasing stone column diameter.

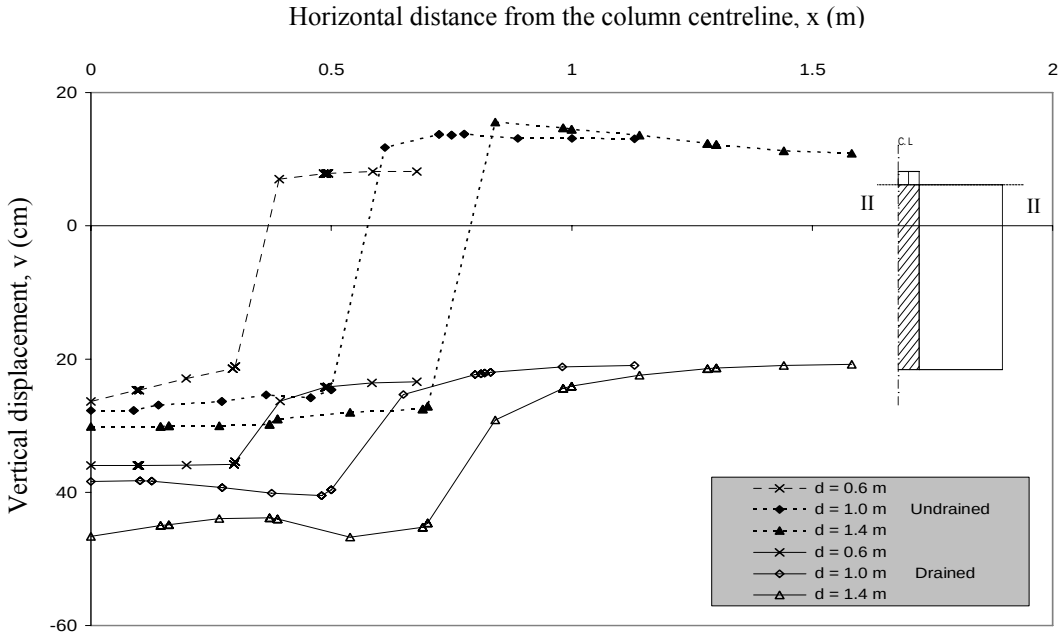

Fig. 4-13 Effect of the stone column diameter on the vertical displacement under a column load of 180 kPa in undrained and drained conditions

This phenomenon occurs because the stresses overlap between the columns. When the stone columns have smaller diameters at the same spacing ratio S/d, the soft soil volume is smaller between these columns. Thus volume between the columns is higher stressed than in case of larger diameters of columns. Therefore, the soft soil in case of small diameters of columns experiences a greater consolidation settlement than in case of larger diameters of columns.

Discussion

The above results indicate that the bearing capacity of the ordinary stone column increases with decreasing spacing distance between columns as well as with decreasing stone column diameter in undrained and drained conditions. But the increase of the bearing capacity in long term is greater than that in short term. The settlement and the lateral bulging of the stone column increase with increasing column diameter and spacing distance between the columns in short and long term conditions. The column diameter effect on the lateral bulging of the stone column is greater than that on the settlement, especially in short term as shown in Fig. 4-12.

Fig. 4-14 shows the relation between the maximum lateral bulging of the stone column and the column spacing ratio values under a column load of 180 kPa. The maximum lateral bulging increases with increasing spacing ratio and column diameter. These lateral bulging values in undrained conditions are greater than those in drained conditions. The rate of the lateral bulging increase is the smallest at stone column diameter of d = 0.6 m but this rate becomes greater with diameters of d = 1.0 m and 1.4 m. Fig. 4-15 shows the relation between the maximum settlement in the stone column and the column spacing ratio values under a column load of 180 kPa. The maximum settlement also increases with increasing spacing ratio and column diameter. The settlement values and the settlement rate in drained conditions are greater than those in undrained conditions. The settlement increase rate is also the smallest at stone column diameter of d = 0.6 m but this rate is so greater with diameters of d = 1.0 m and 1.4 m.

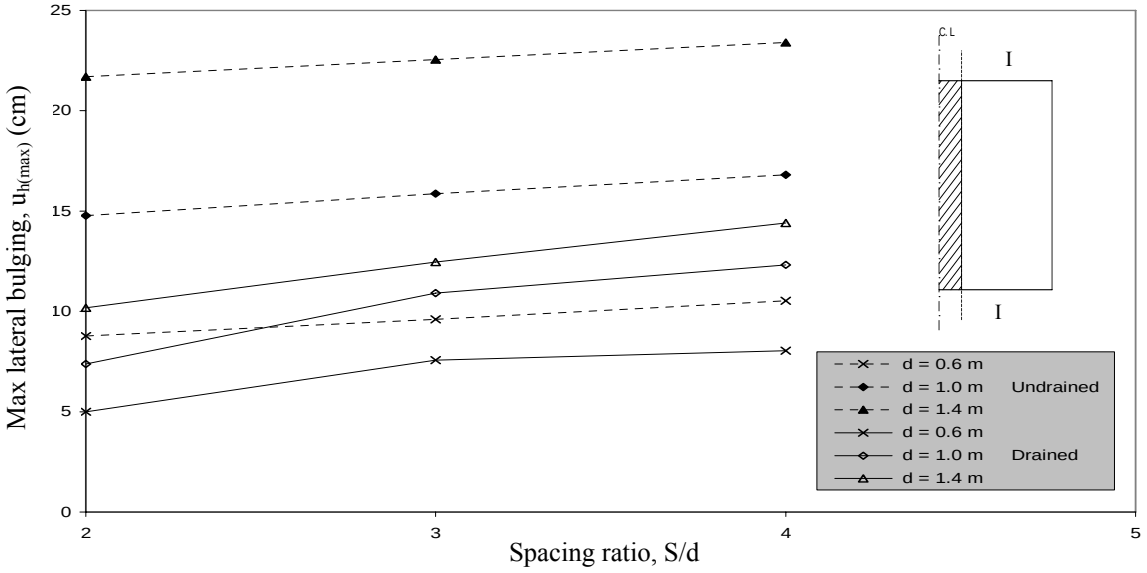

Fig. 4-14 Maximum lateral bulging of the stone column and spacing ratio relationship under a load of 180 kPa in undrained and drained conditions

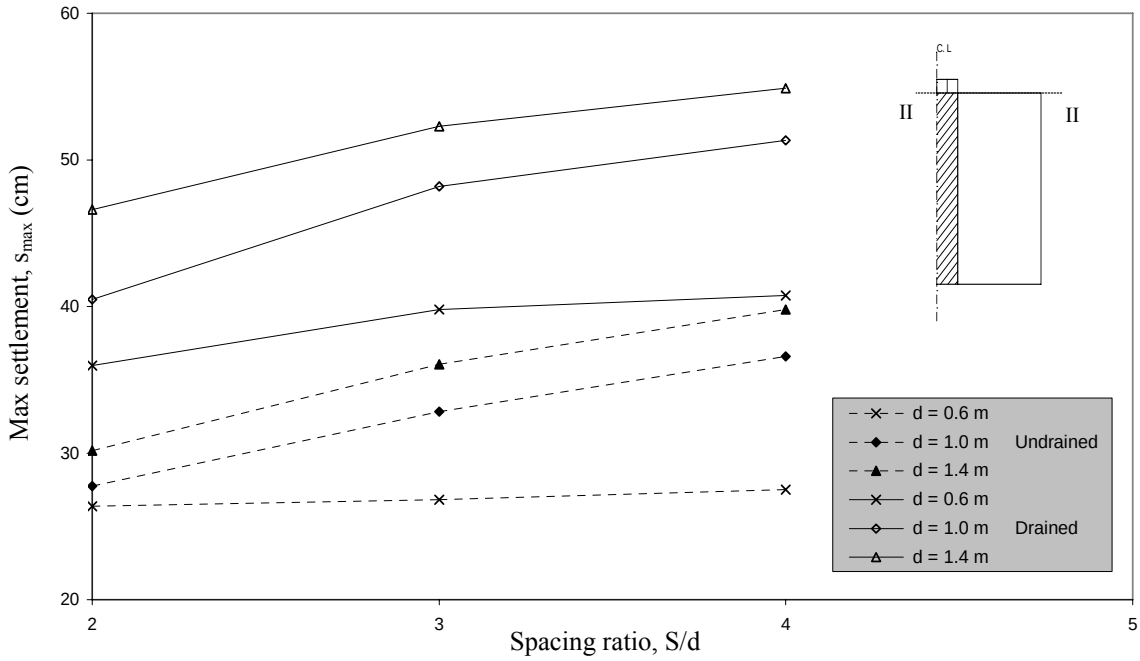

Fig. 4-15 Maximum settlement of the stone column and spacing ratio relationship under a load of 180 kPa in undrained and drained conditions

The above discussion concludes that a stone column with a diameter of d = 0.6 m and a spacing ratio of S/d = 2.0 provides the greatest bearing capacity. It has also the smallest stone column settlement as well as the lowest lateral bulging in undrained and drained conditions in comparison with the other cases.

4.4.3 Group (C): Effect of geogrid encasement and stiffness (J)

The geogrid materials have been put around the stone column as encasement which is illustrated in Fig. 4-1-a. Ordinary (OSC) and encased (ESC) stone columns with diameter of 0.6 m and spacing ratio of 2 have been loaded until failure occurs in undrained and drained conditions. Three different geogrid materials are used: Secugrid 20/20 Q1 with stiffness of 400 kN/m, Secugrid 30/30 Q1 with stiffness of 600 kN/m and Combigrid 40/40 Q1 with stiffness of 800 kN/m, as shown in Table 4-3.

Undrained conditions

When the stone column is encased with geogrid materials, a huge increase in the bearing capacity occurs. The bearing capacity of the stone column increases with increasing geogrid stiffness as shown in Fig. 4-16. This huge increase in the bearing capacity of the stone column is due to the increase of the column confinement with geogrid materials. These encasement materials provide also a stronger lateral support by generating radial tension forces. The stone column confinement increases with increasing geogrid stiffness which leads to an increase of the overall stiffness of the encased stone column. Fig. 4-16 indicates that the load-settlement relationship becomes linearly over a larger range of load with increasing geogrid stiffness. The initial elasticity modulus of the stone column also increases with increasing geogrid stiffness. The initial elasticity modulus of the ordinary stone column is 47385 kPa, and it increases to 54010 kPa for Secugrid 20, to 65465 kPa for Secugrid 30 and finally to 73195 kPa for Combigrid 40.

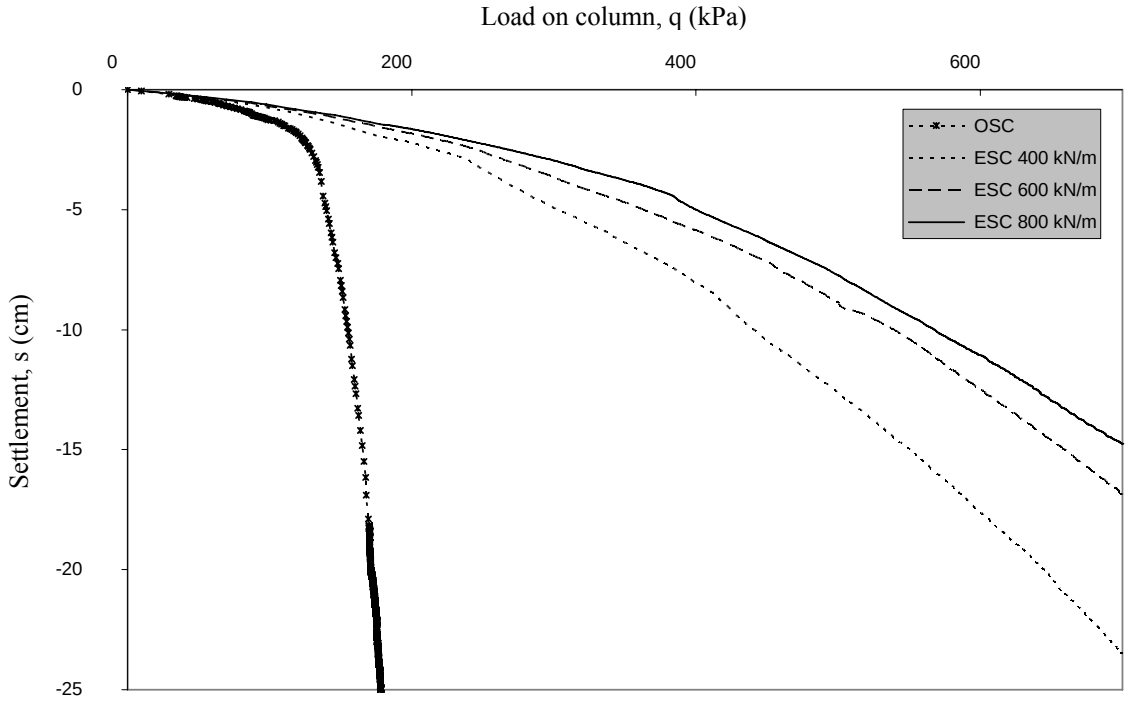

Fig. 4-16 Effect of the geogrid encasement stiffness on the load settlement behavior of the stone column in undrained conditions, d = 0.6 and S/d = 2.0

The vertical displacements at the stone column-soft soil surface and the lateral displacement along the stone column-soft soil interface were calculated at a column load of 180 kPa in undrained conditions. A huge reduction in the stone column settlement occurs and the soft soil heave disappears when encasing stone column with geogrid materials, as shown in Fig. 4-17. The differential vertical displacement also decreases with encasement. A small decrease in the vertical displacement occurs with increasing geogrid stiffness under 180 kPa load but this reduction increases with increasing load as shown in Fig. 4-16. Fig. 4-18 shows also a huge reduction in the lateral bulging of the stone column with encasement. The lateral bulging decreases with increasing geogrid stiffness. This reduction also increases with increasing applied loads on the encased stone columns as shown in Fig. 4-19.

Fig. 4-20 shows the distribution of the radial hoop tension forces which have been generated in geogrid encasement under a column load of 180 kPa in undrained conditions. The tension forces start with a value in the surface and gradually increase with downward direction until a maximum value at a depth of 15 % of the column diameter is reached. Below that, the values decrease gradually to reach zero at a depth of 4.5 times the column diameter. The lateral displacements of the stone column are prevented by geogrid material which works as a lateral support to the stone column. When the column tries to displace, radial tension forces are generated in the geogrid encasement. So, the development of the hoop tension forces looks like that of the horizontal displacement of the stone column. The more the horizontal and vertical displacements of the encased stone column are reduced, the more the hoop tension forces are generated. The hoop tension forces increase with increasing geogrid stiffness as shown in Fig. 4-20.

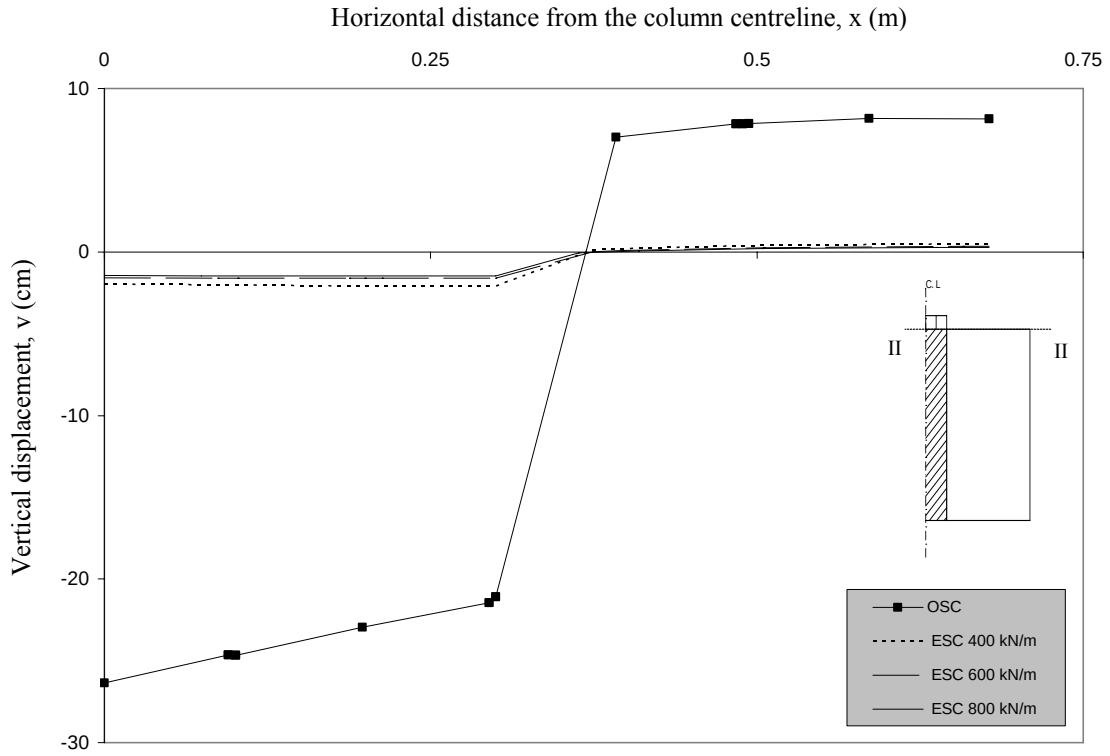

Fig. 4-17 Effect of geogrid encasement stiffness on the vertical displacement at a column load of 180 kPa in undrained conditions, with d = 0.6 and S/d = 2.0

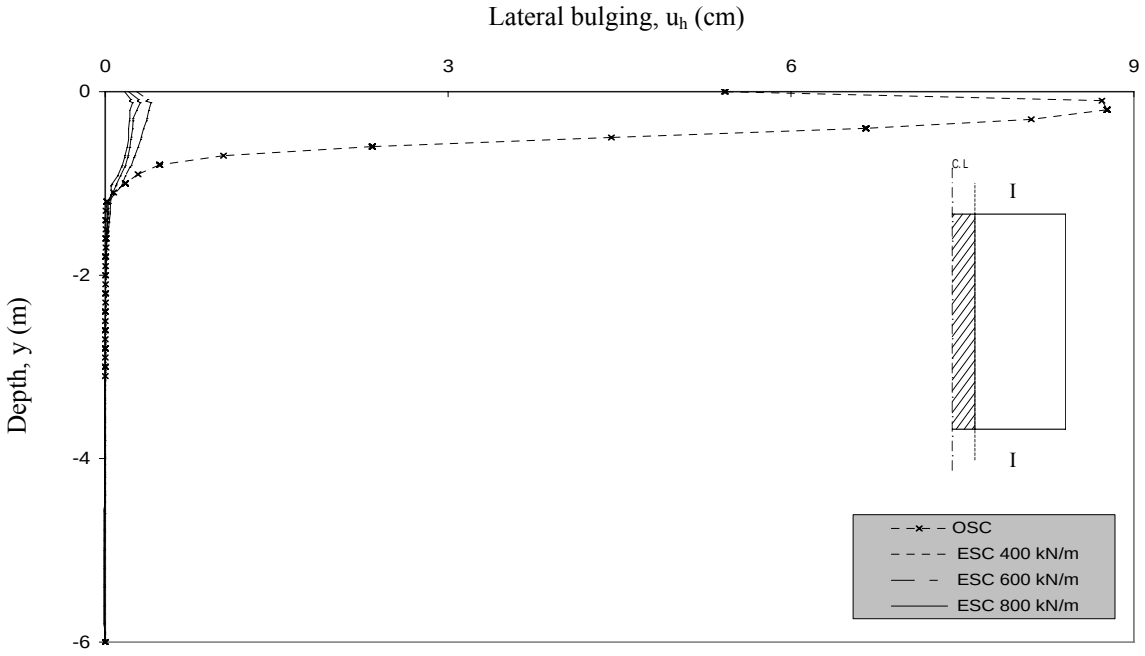

Fig. 4-18 Effect of geogrid encasement stiffness on the lateral bulging at a column load of 180 kPa in undrained conditions, d = 0.6 and S/d = 2.0

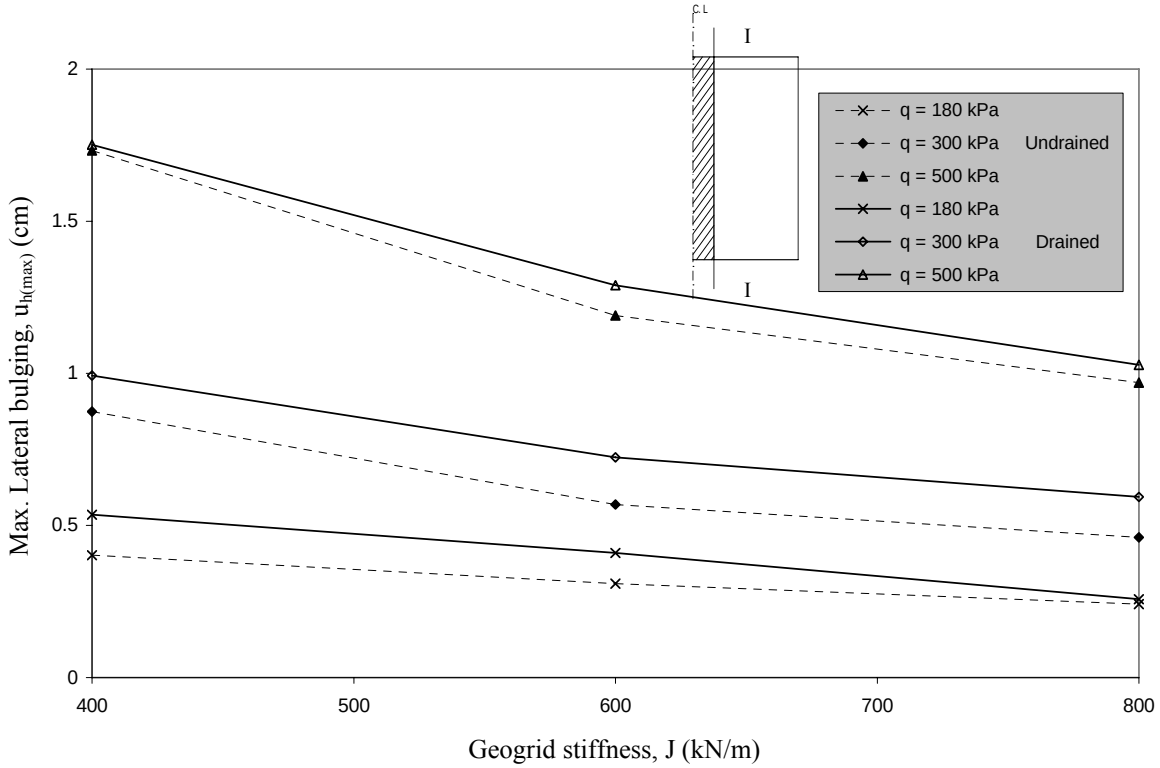

Fig.4-19 Effect of geogrid stiffness on the maximum lateral bulging under various load levels in undrained and drained conditions

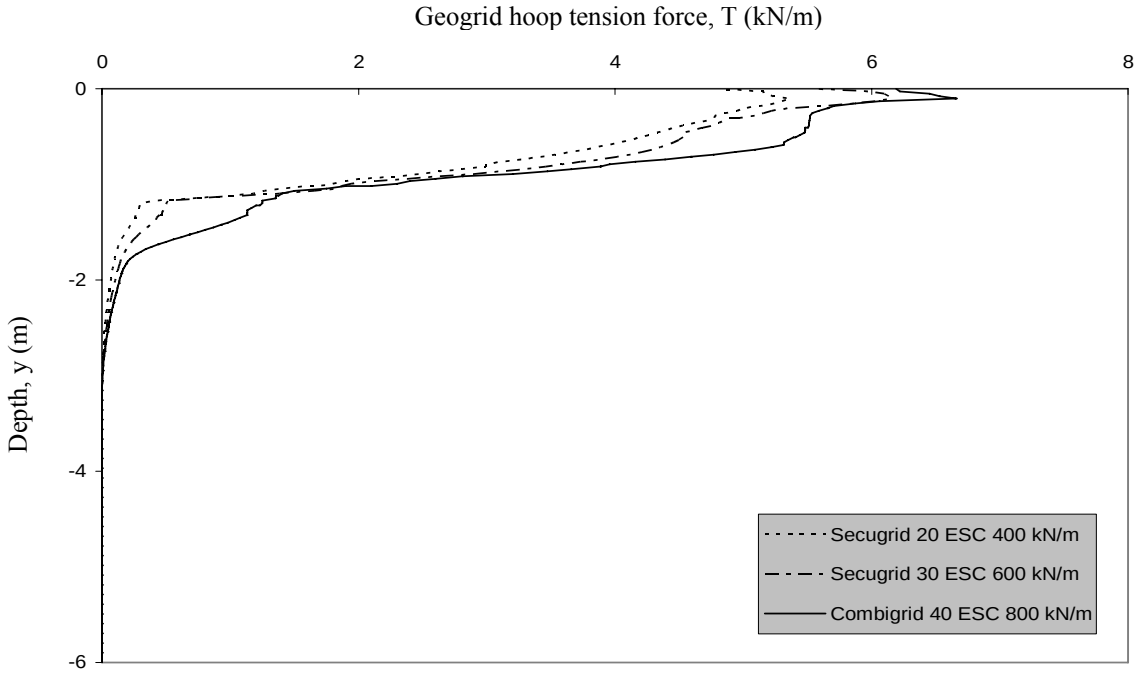

Fig. 4-20 Effect of geogrid stiffness on the encasement hoop tension force under 180 kPa load in undrained conditions

Drained conditions

When the stone column is encased with geogrid materials and loaded until failure in drained conditions, a huge increase in the bearing capacity also occurs. The bearing capacity of the encased stone column increases with increasing geogrid stiffness especially at the higher loads as shown in Fig. 4-21. The load-settlement relationship of the encased stone column is approximately linear and no yield point occurs. While consolidation ongoing, the encasement provides a stronger lateral support for the stone column by generating radial tension forces. The confinement of the stone column increases with increasing geogrid stiffness which leads to an increase in the overall stiffness of the encased stone column. The encased stone column stiffness in soft soil can be expressed by the elasticity modulus which can be obtained from Fig. 4-21. The elasticity modulus of the ordinary stone column is 3200 kPa, and it increases to 5539 for Secugrid 20, to 9707 kPa for Secugrid 30 and finally to 11722 kPa for Combigrid 40.

The vertical displacement at the stone column-soft soil surface and the lateral displacement along the stone column-soft soil interface were calculated for a column load of 300 kPa in drained conditions. A huge reduction in the settlement of stone column and the surrounding soft soil occurs when the geogrid materials are used to encase stone columns, as shown in Fig. 4-22. The differential settlements also decrease with encasement. The settlement of the encased stone column and the soft soil decreases with increasing geogrid stiffness values. The settlement reduction degree of the encased stone columns increases with increasing geogrid stiffness and applied loads as shown in Fig. 4-21. The differential settlements between the encased stone column and the surrounding soft soil also decrease with a large degree when the geogrid stiffness increases. The differential settlement approximately disappears when using a geogrid encasement with stiffness of 800 kN/m, as shown in Fig. 4-22.

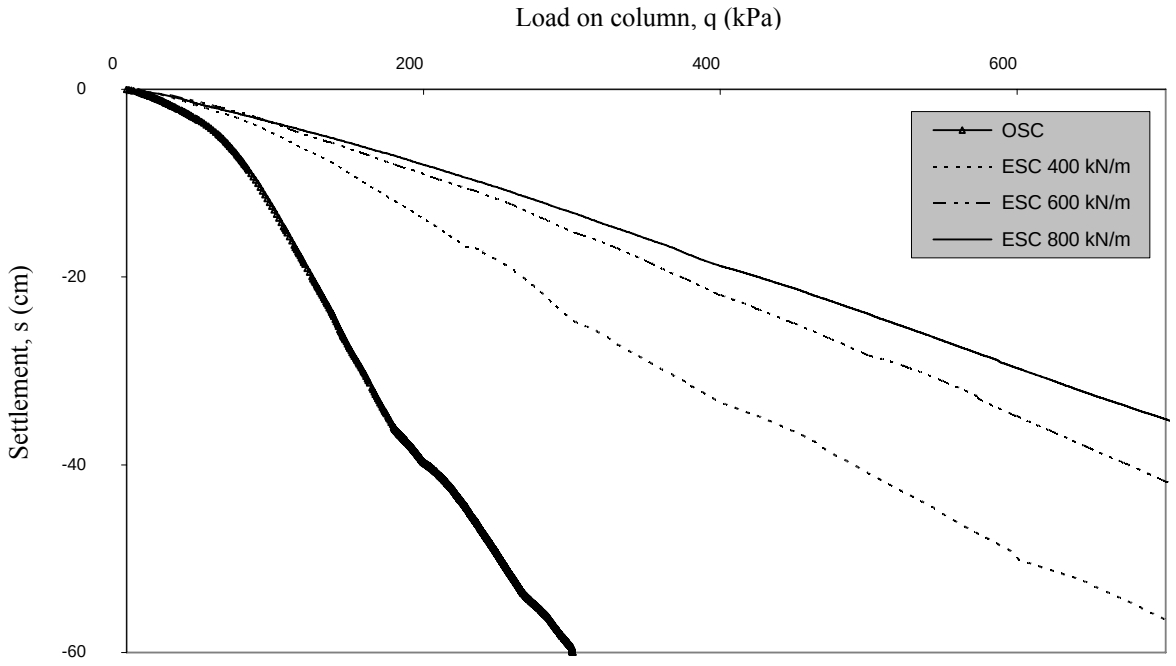

Fig. 4-21 Effect of geogrid encasement stiffness on the load-settlement relationship of the stone column under drained conditions, d = 0.6 and S/d = 2.0

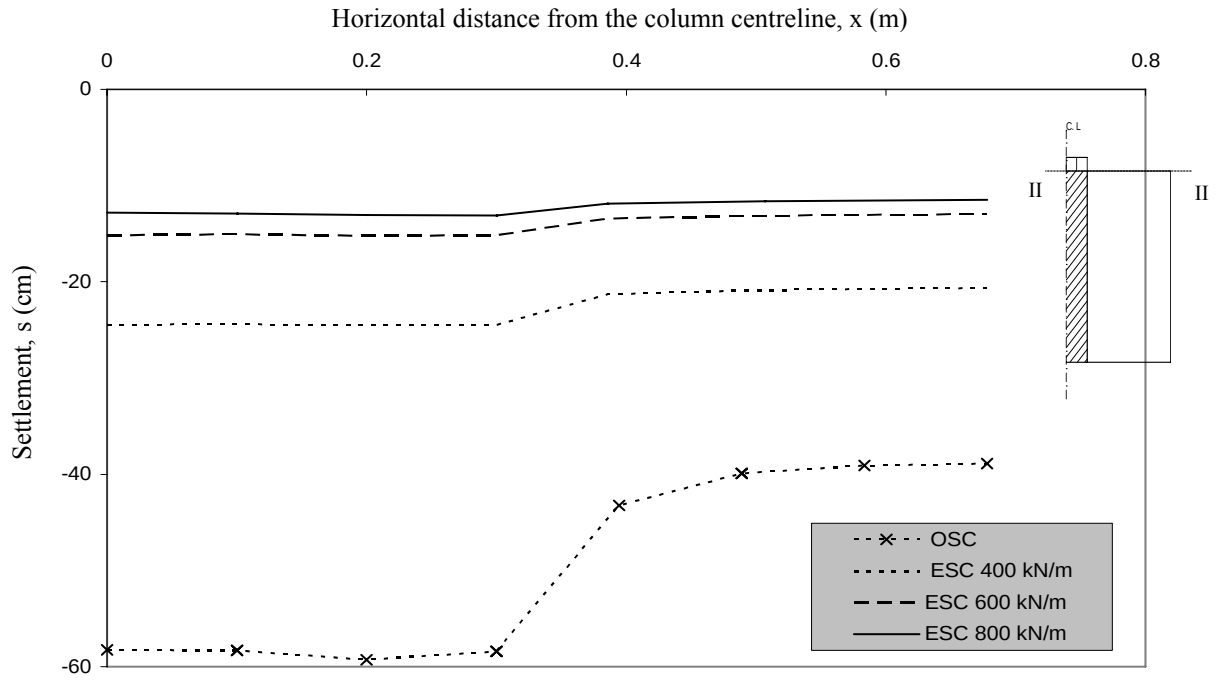

Fig. 4-22 Effect of geogrid encasement stiffness on the settlement in section II-II at a column load of 300 kPa in drained conditions, d = 0.6 and S/d = 2.0

Huge reductions also occur in the lateral displacement when using encasement as shown in Fig. 4-23. These huge reductions of the lateral bulging are due to the confinement from the encasement of stone column which provides a stronger lateral support than that in the ordinary stone column. The lateral bulging of the encased column starts with a value in the surface which increases gradually downward to reach a maximum value at a depth of half the column diameters, (0.5 d). Below that the lateral bulging values decrease gradually to reach a zero value at the column base. The encasement makes the lateral displacement distribution along the column more organized due to more stress transfer within lower depths. The lateral displacement of the encased stone column decreases with increase of the geogrid stiffness values. This reduction of the lateral bulging increases with increasing column load as shown in Fig. 4-19. At the same load the maximum lateral bulging values of the encased column in long term are greater than those in short term for all geogrid stiffness values as depicted in Fig. 4-19.

Fig. 4-24 shows the radial hoop tension forces in geogrid materials distributed along the stone column under a column load of 300 kPa. The hoop tension forces start with a value at the surface. Below that, the hoop tension forces increase downwards until they reach a maximum value at a depth of approximately 0.7 d, then they decrease gradually to reach zero at the column base. The hoop tension force distribution is similar to that for the lateral bulging of the stone column. The hoop tension force increases with increasing geogrid encasement stiffness as shown in Fig. 4-24. The degree of improvement in the encased stone column-soft soil foundation behavior increases with increasing hoop tension forces in the encasement material. In comparison with the undrained conditions, the hoop tension forces in drained conditions extend to lower depths due to the stress transfer within downward direction.

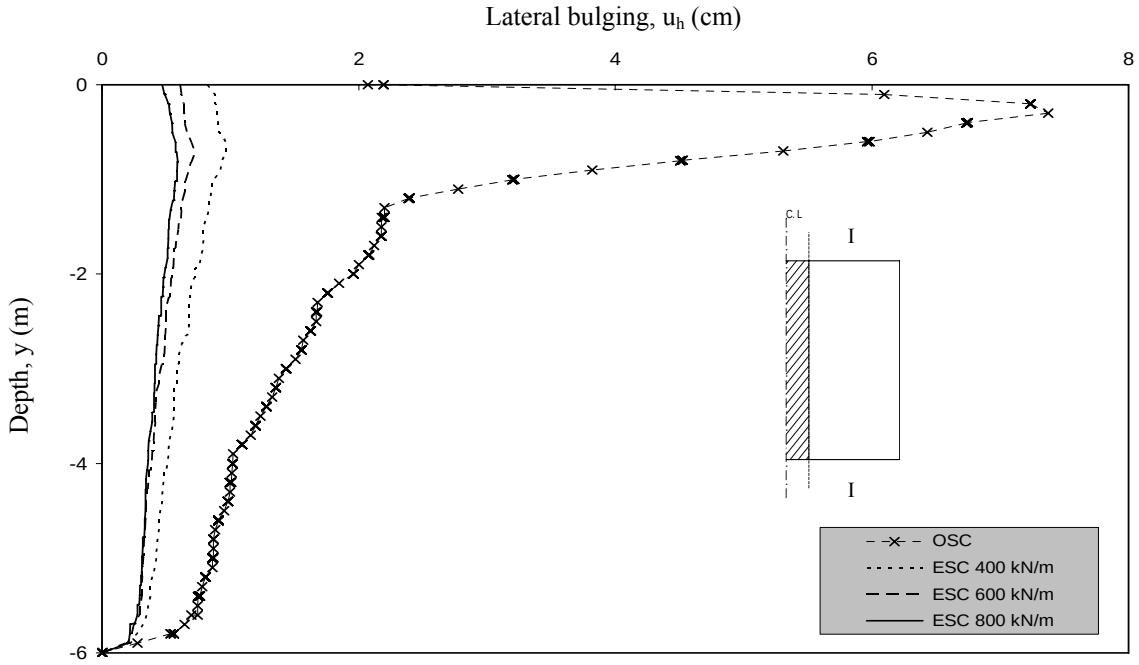

Fig. 4-23 Effect of geogrid stiffness on the lateral displacement of the stone column at a load of 300 kPa in drained conditions

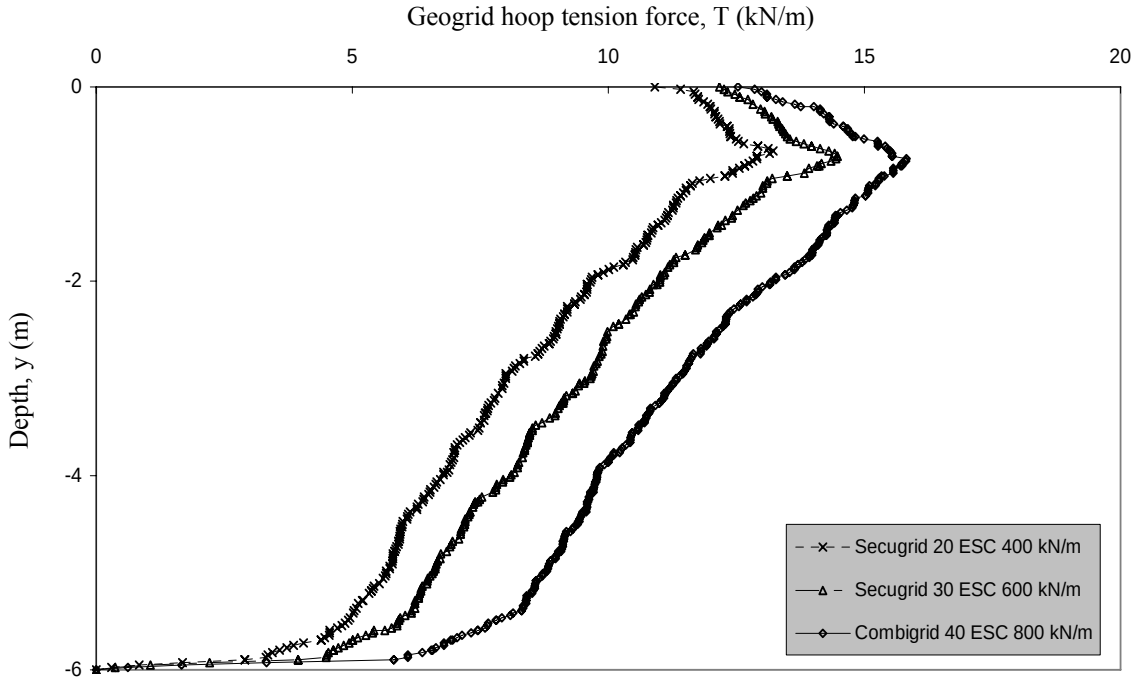

Fig. 4-24 Effect of geogrid stiffness on the encasement hoop tension force at a load of 300 kPa in drained conditions

Discussion

The above results indicated that when the encased stone column is loaded, a huge increase in the bearing capacity and a huge reduction in the lateral and the vertical displacements occur. The bearing capacity of the encased stone column increases with increasing geogrid encasement stiffness. The lateral displacement and the settlement of the stone column also decrease with increasing encasement stiffness values which cause

also a reduction on the vertical displacements in the surrounding soft soil. These improvements are more effective with increasing load level.

Fig. 4-25 shows the development of the ratio of the maximum lateral bulging of the encased and the ordinary stone column $(u_{h(R)}/u_{h(NR)})_{max}$ with increasing load for various encasement stiffness values in undrained and drained conditions. The maximum lateral bulging ratio of the stone column decreases with increasing load and encasement stiffness in both short and long terms. The lateral bulging ratio starts with values in drained conditions smaller than those in undrained condition until approximately a load of 150 kPa. Beyond that the lateral bulging ratios become smaller in undrained conditions. The greatest lateral bulging reduction of the stone column occurs at high loads and high encasement stiffness values. The reduction rate in undrained conditions is greater than that in drained conditions.

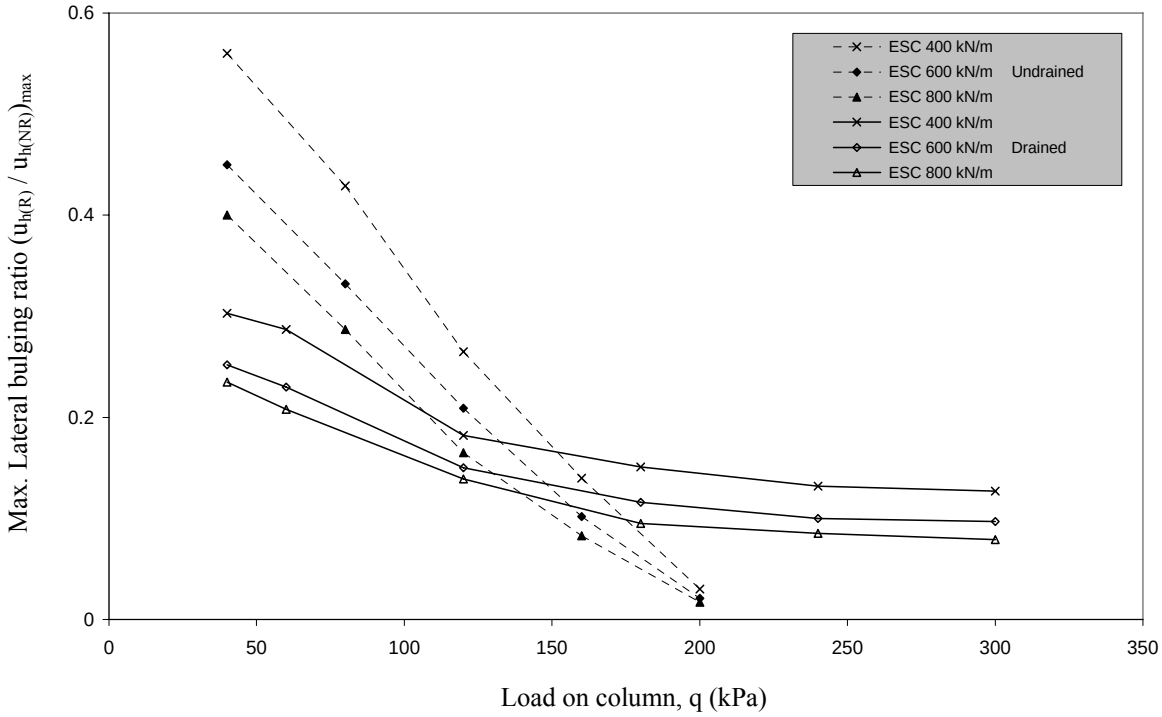

Fig. 4-25 Maximum lateral bulging of ordinary and encased stone columns ratio and load relationship for various encasement stiffness values in short and long terms.

Fig. 4-26 shows also the relationship of the ratio of the maximum settlement of the encased and the ordinary stone column $(s_R/s_{NR})_{max}$ with load for various encasement stiffness values in undrained and drained conditions. The maximum settlement ratio of the stone column decreases with increasing load as well as increasing encasement stiffness in both short and long term conditions similar to the maximum lateral bulging ratio behavior as shown in Fig. 4-25. The maximum settlement reduction ratio starts with values in drained conditions smaller than those in undrained conditions until approximately a load of 150 kPa. Beyond that the settlement reduction ratio becomes smaller in undrained conditions. The greatest settlement reduction of the stone columns occurs at high load levels and high encasement values. The reduction rate in the undrained conditions is greater than that in drained conditions.

The geogrid encasement effect in stone column lateral bulging is more effective than that in stone column settlement especially in long term as shown in Fig. 4-25 and Fig. 4-26. The encasement material provides a strong lateral support for the stone column which leads to increase its load carrying ability. Hence, the encased stone column performance becomes better with increasing geogrid stiffness. Therefore, the more effective case in the analysed cases is the encased stone column with the highest geogrid stiffness of 800 kN/m.

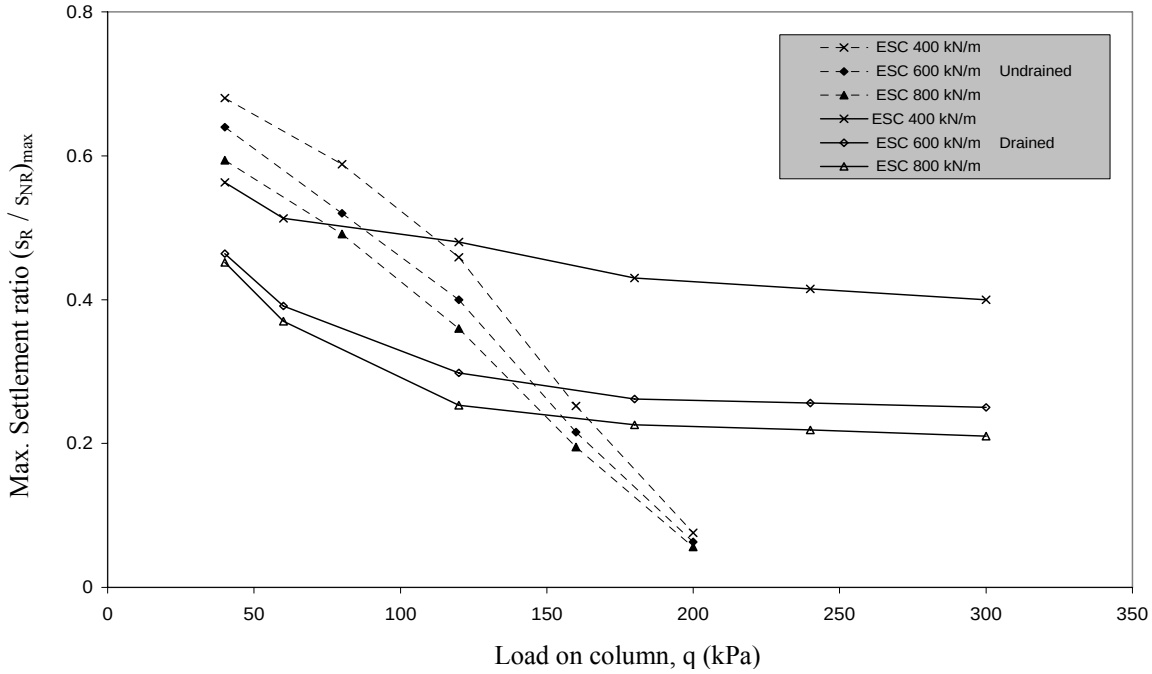

Fig. 4-26 Maximum settlement of ordinary and encased stone columns ratio and load relationship for various encasement stiffness values in short and long terms.

4.4.4 Group (D): Effect of encasement depth (h)

The encased stone columns with various encasement depths have been loaded in undrained and drained conditions. The analyses have been carried out using stone columns with a diameter of 0.6 m, a spacing ratio of S/d = 2 and a geogrid stiffness of 800 kN/m. The encasement depth to column diameter ratios of h/d = 1, 2, 3, 4, 5, 6, 8 and 10 have been used to investigate the influence of the encasement depth on the stone column behavior.

Undrained conditions

The bearing capacity of the encased stone columns increases with increasing encasement depth as shown in Fig. 4.27. The increase in the bearing capacity is greater at the higher loads. The highest bearing capacity occurs when the full encased stone column is used.

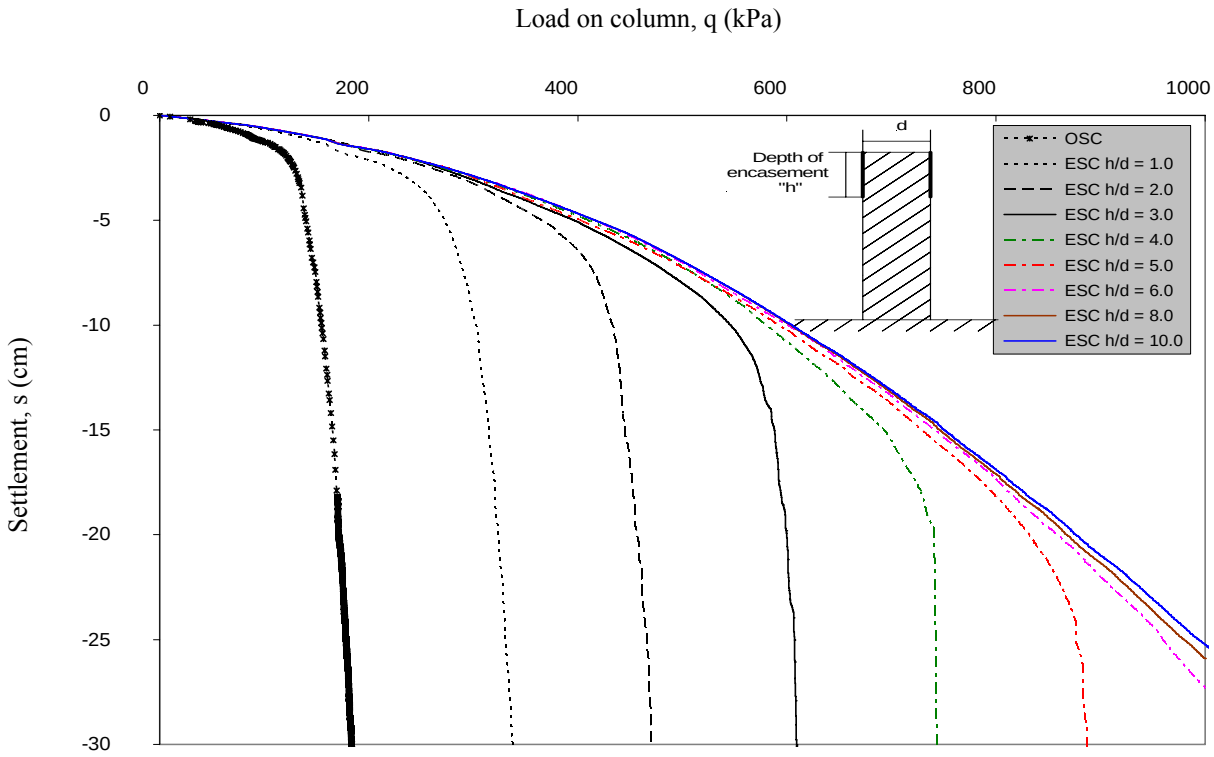

Fig. 4-27 Effect of geogrid encasement depth on the load-settlement behavior of the stone column in undrained conditions, d = 0.6 m, S/d = 2.0 and J = 800 kN/m

Loads have been applied on the partially and the full encased stone column up to a load of 300 kPa which acts as a working load. The encasement beyond a depth equal to twice the diameter of the column doesn't lead to further improvement in the bearing capacity of the stone columns as shown in Fig. 4.28. Similar results were stated by Murugesan and Rajagopal (2006).

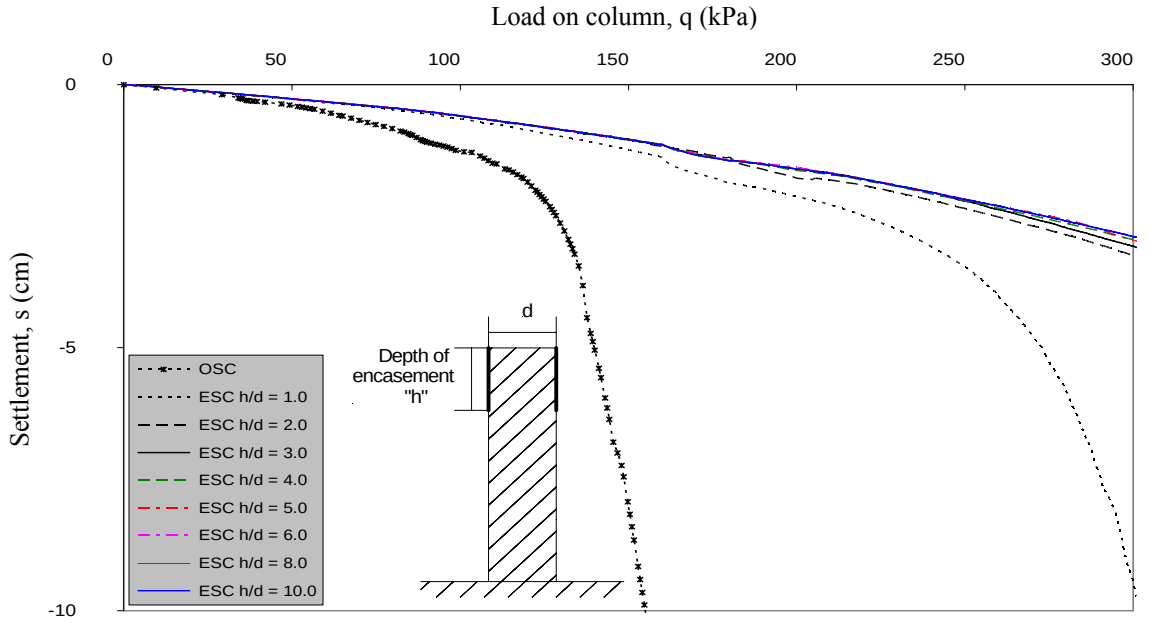

Fig. 4-28 Effect of geogrid encasement depth on the load-settlement behavior of the stone column in undrained conditions up to a load of 300 kPa, d = 0.6 m, S/d = 2.0 and J = 800 kN/m

The vertical displacements at the ground surface and the bulging of the stone columns have been calculated under the column load of 300 kPa. The settlement in the stone column and the heave in the soft soil decrease with increasing depth of the encasement. When the stone column is encased with a depth equal to the column diameter, the settlement and the heave are higher than those with deeper encasement, as shown in Fig. 4-29. Then, the settlement and the heave decrease sharply with increasing encasement to a depth equal twice the column diameter. Beyond the depth of h/d = 2, there is no significant reduction in the settlement and the heave.

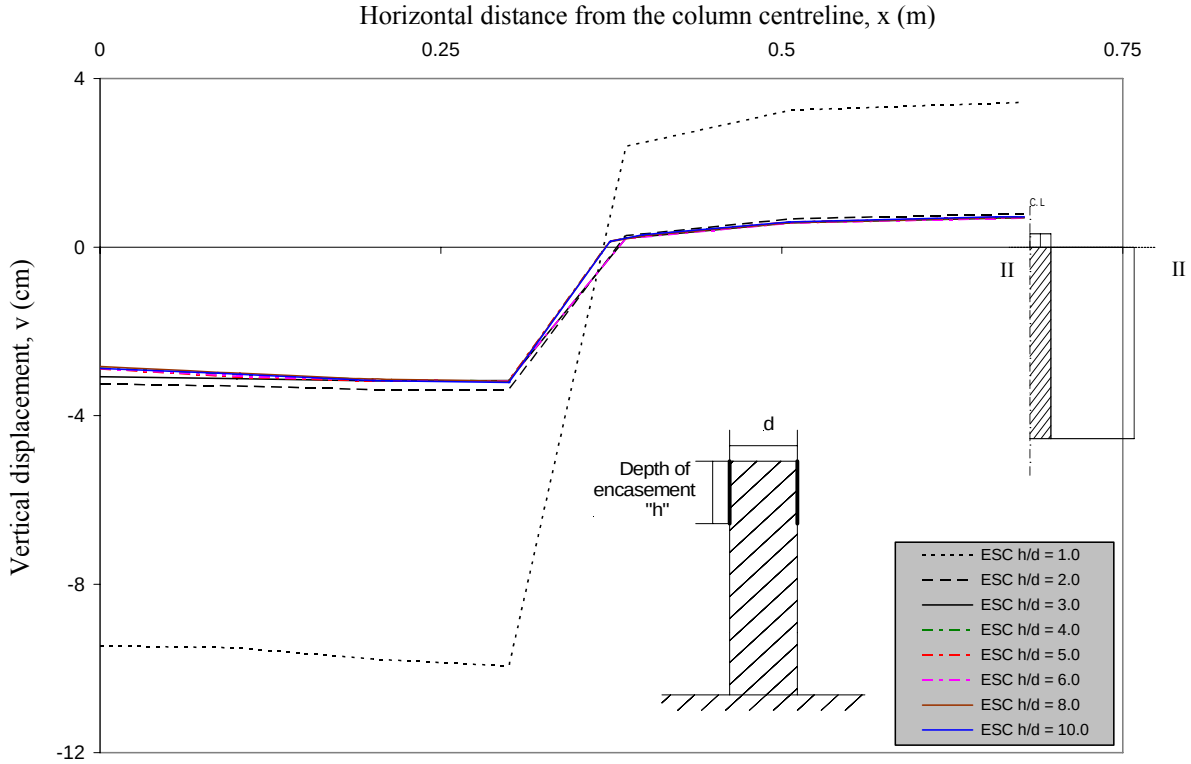

Fig. 4-29 Vertical displacement at the surface of the encased column with various depths of geogrid under a column load of 300 kPa in undrained conditions.

The lateral bulging of the partly and the full encased stone columns is also investigated. The lateral bulging decreases with increasing depth of the encasement. It is well established from Fig. 4-30 that the bulging of the stone column is predominant up to a depth equal to 2-2.5 times the diameter of the column. Hence, the partly encasement of the stone columns with a depth of 3 times the diameter of the column, h/d = 3 is sufficient to reduce the bulging of the column to minimum values and to provide the required confinement of the column. When the stone columns are reinforced by encasement depth smaller than h/d = 3, larger lateral displacements of the column occur at the end point of the encasement. Largely differentially lateral displacements are also generated at the encasement end. This phenomenon is clear especially when using encasement depth of h/d = 1, as shown in Fig. 4-30.

Fig. 4.31 shows the hoop tension forces distribution along the column for various encasement depths. The development of the hoop tension forces looks like that of the column bulging. The hoop tension forces distributions are the same for depths larger

than h/d = 3. At encasement depths shallower than h/d = 3, there are peak values in the hoop tension forces at the end point of the encasement where there is a largely differentially lateral displacement. The encased stone column with encasement depth of h/d = 1 implies the highest peak value of tension forces at the end point of the encasement as shown in Fig. 4-31. Because the upper zone of the stone column is the more loaded zone and contains the maximum bulging of the column. Hence this upper zone needs to be confined.

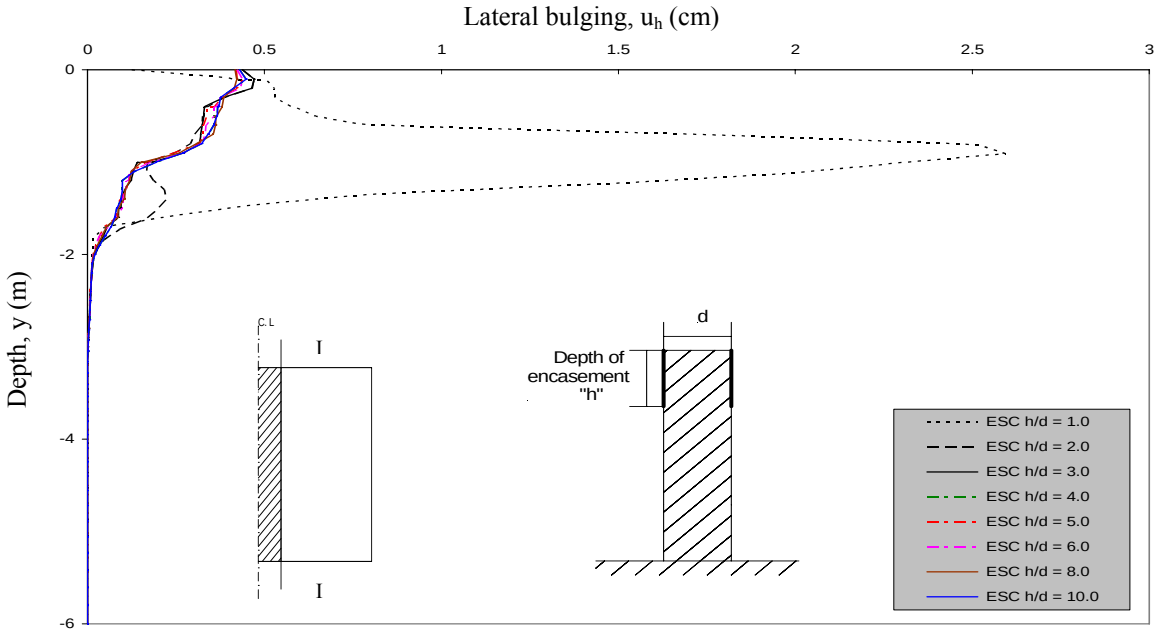

Fig. 4-30 Lateral bulging of the encased stone column with various encasement depths for a column load of 300 kPa in undrained conditions

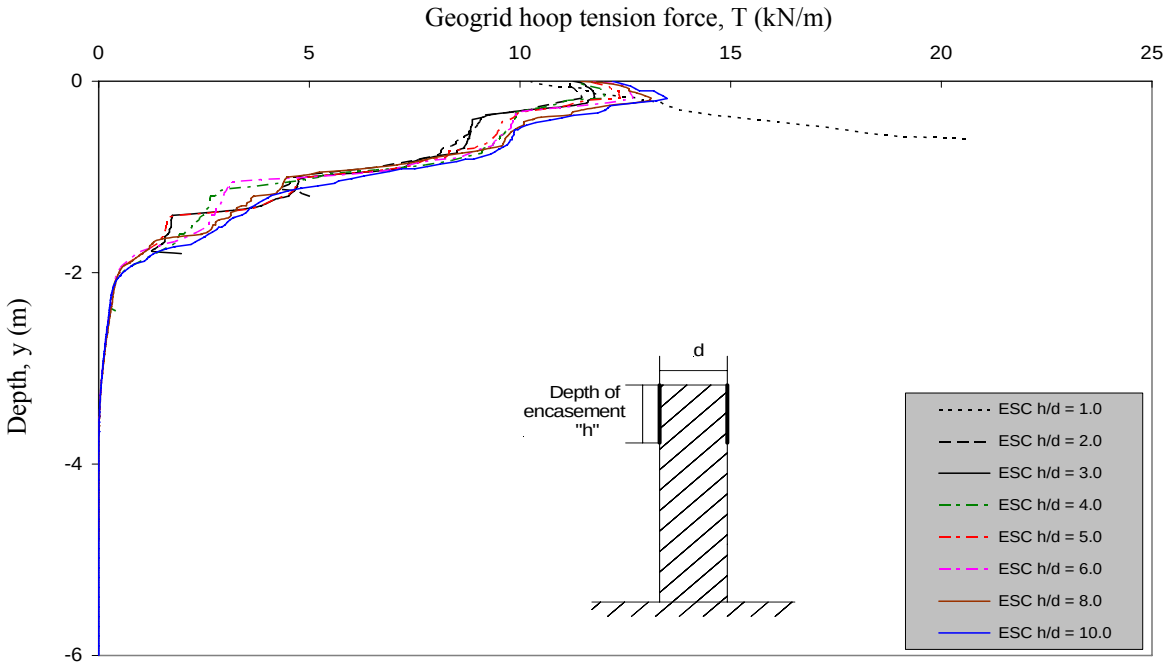

Fig. 4-31 Effect of geogrid depth on the hoop tension forces of the encasement under a column load of 300 kPa in undrained conditions

Drained conditions

The partially and the full encased stone columns have been also studied in drained conditions. When using encasement depth ratio of h/d = 1, the stone column has a large increase in the bearing capacity. The increase in the bearing capacity of stone columns continues with increasing encasement depth, h/d. The rate of the increase is significant at higher loads as shown in Fig. 4-32. Loads have been applied on the partially and the full encased stone column up to a load of 300 kPa which acts a working load. The bearing capacity of the encased stone column increases also with increasing encasement depth, as illustrated in Fig. 4-33.

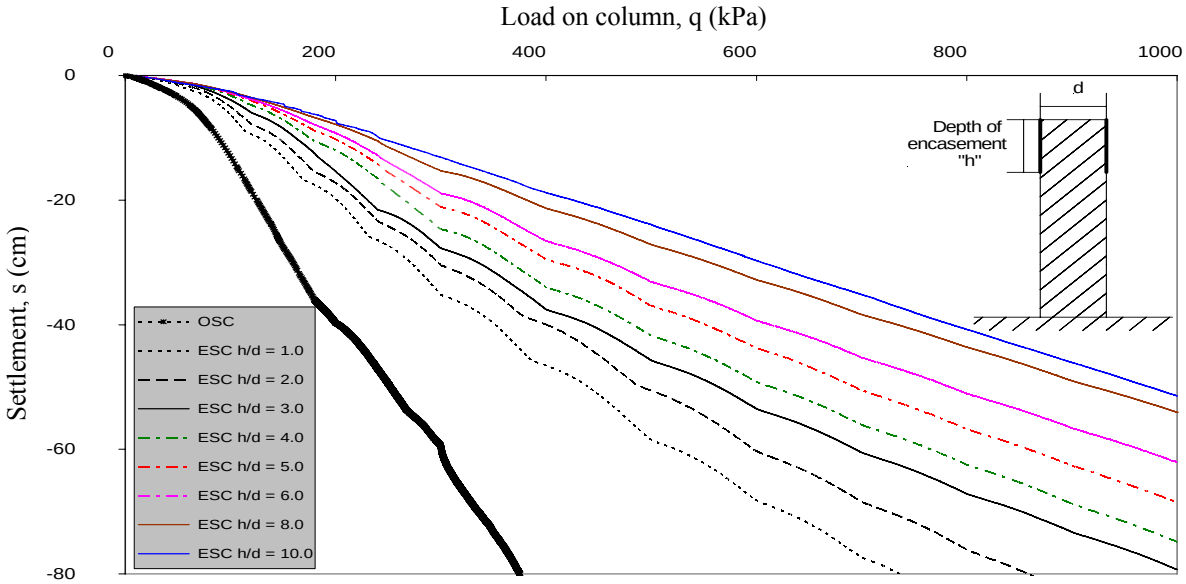

Fig. 4-32 Effect of geogrid encasement depth on the load-settlement behavior of the stone column in drained conditions, d = 0.6 m, S/d = 2.0 and J = 800 kN/m

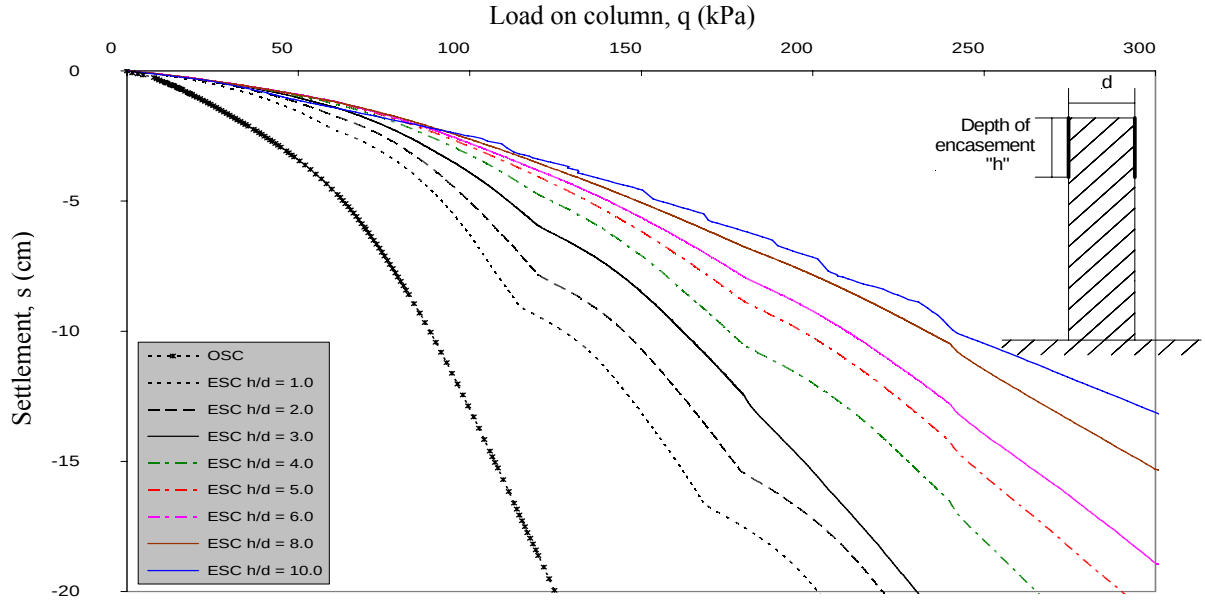

Fig. 4-33 Effect of geogrid depth on the load-settlement behavior of the stone column in drained conditions under a load of 300 kPa, d = 0.6 m, S/d = 2.0 and J = 800 kN/m

The settlement and the lateral bulging of the stone column and the hoop tension forces in the encasement were also calculated under a column load of 300 kPa. The settlement in the stone column and in the soft soil decreases with increasing encasement depth, as illustrated in Fig. 4.34. The differential settlement between the stone column and the surrounding soft soil also decreases with increasing depth of the encasement. The settlement and the differential settlement reduce to the minimum when encasing stone column with the complete depth h/d = 10, as shown in Fig. 4.34.

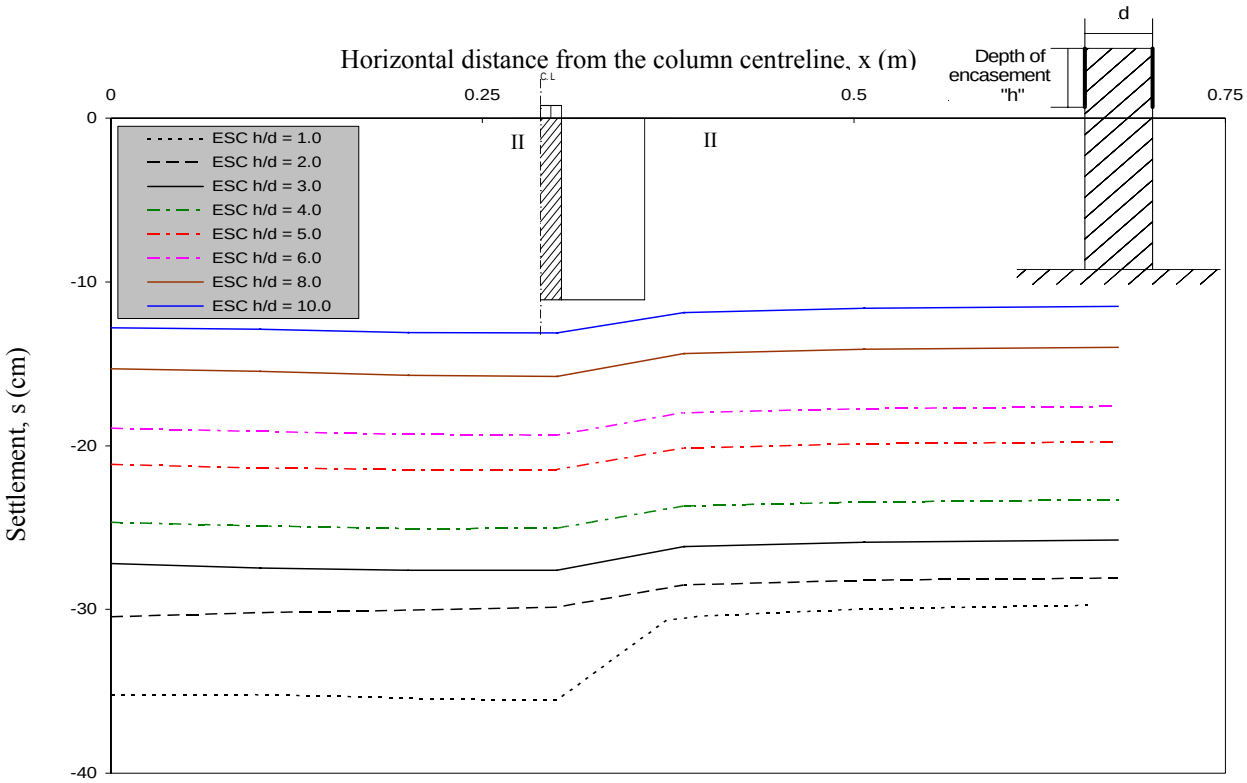

Fig. 4-34 Settlement at the surface of the encased column with various depths of geogrid under a column load of 300 kPa in drained conditions, d = 0.6 m, S/d = 2.0 and J= 800 kN/m

It was well established that the lateral bulging is distributed along the stone column when it is loaded in drained conditions. Hence, the encasement is required to a depth that equals the depth of the stone column. Fig. 4.35 shows the distribution of the bulging of the encased stone column through its depth using various encasement depths. The bulging of the column reduces to minimum values in all the column depth when the column is encased completely, h/d = 10. When the stone column is partially encased, its bulging in the encased zone is slightly smaller than that of the full encased column case, while the non-encased zone has so higher values of the column bulging. The non-encased zone in the column starts with a maximum value which generates a largely differential bulging at the end point of the encasement. Below the end point of the encasement, the bulging values decrease gradually with depth until it reaches zero at the column base, as shown in Fig. 4.35. The shallower the encasement depth is, the higher the bulging values are in the non-encased zone of the stone column. Therefore, the non-encased zone has the largest bulging in the stone column when the encasement depth is the smallest.

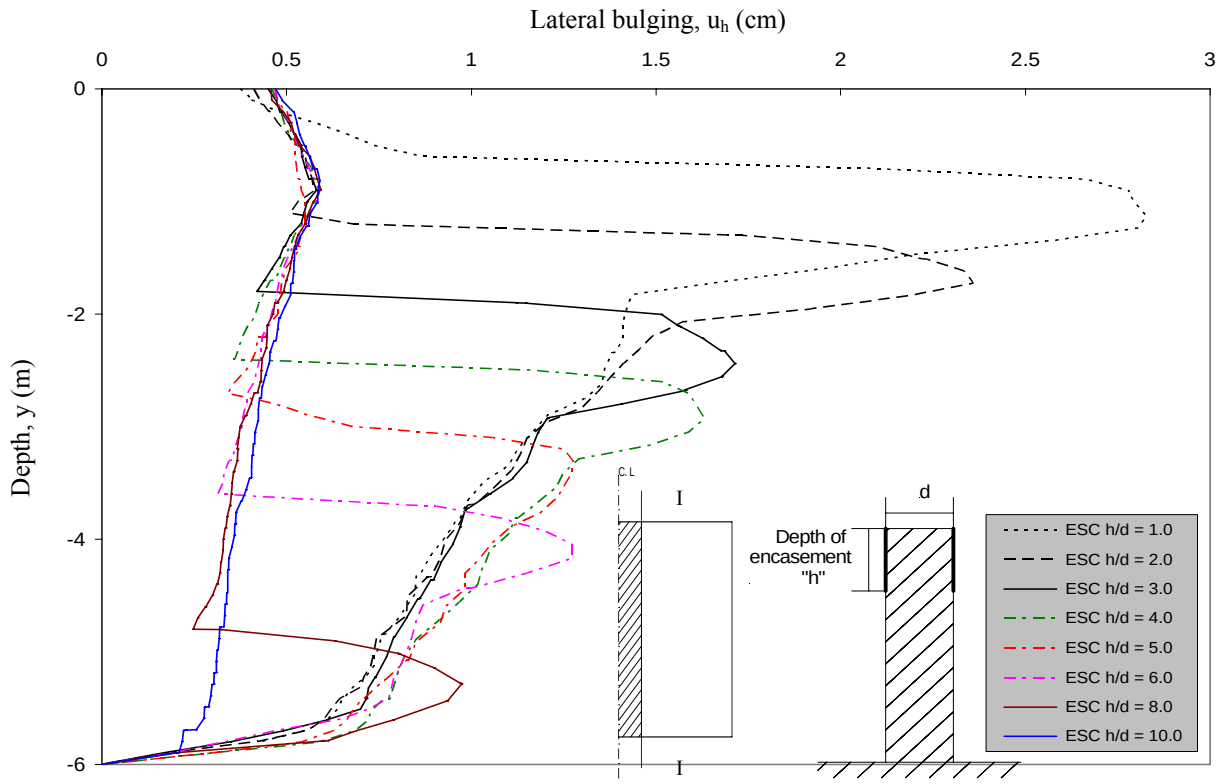

Fig. 4-35 Lateral bulging of the encased stone column with various encasement depths for a column load of 300 kPa in drained conditions, d = 0.6 m, S/d = 2.0 and J= 800 kN/m

The distribution of the hoop tension force of the geogrid as a partial encasement of the stone column is shown in Fig. 4-36 under a column load of 300 kPa. The full encasement induces a value of hoop tension force at the ground surface. Then the tension force values increase with depth until they reach a maximum value at a depth of 1.25 times the column diameter. Beyond this depth, the tension forces decrease gradually until they reach zero at the base of the column. Under the same load in comparison with undrained conditions, the encasement in drained conditions has the larger tension forces and the distribution of the tension forces extends to lower depths.

The distribution of the hoop tension forces is similar to that of the stone column bulging. When the stone column is reinforced by partially encasement, the tension forces are implied in the encased part of the column. The tension forces in the partial encasement of the stone column are smaller than those of the full encasement. While the end point of the partial encasement has a peak value of tension force which is larger than that of the full encasement at the same location. This is because the end point of the partial encasement is free and subjected to lateral stress from the stone column where there is a large differential lateral displacement. The shallower the encasement is, the higher the peak value of the tension force at the end point of the encasement is, as illustrated in Fig. 4.36. The smallest encasement depth which equals the column diameter experiences the highest peak value of the tension forces at the end point of the encasement.

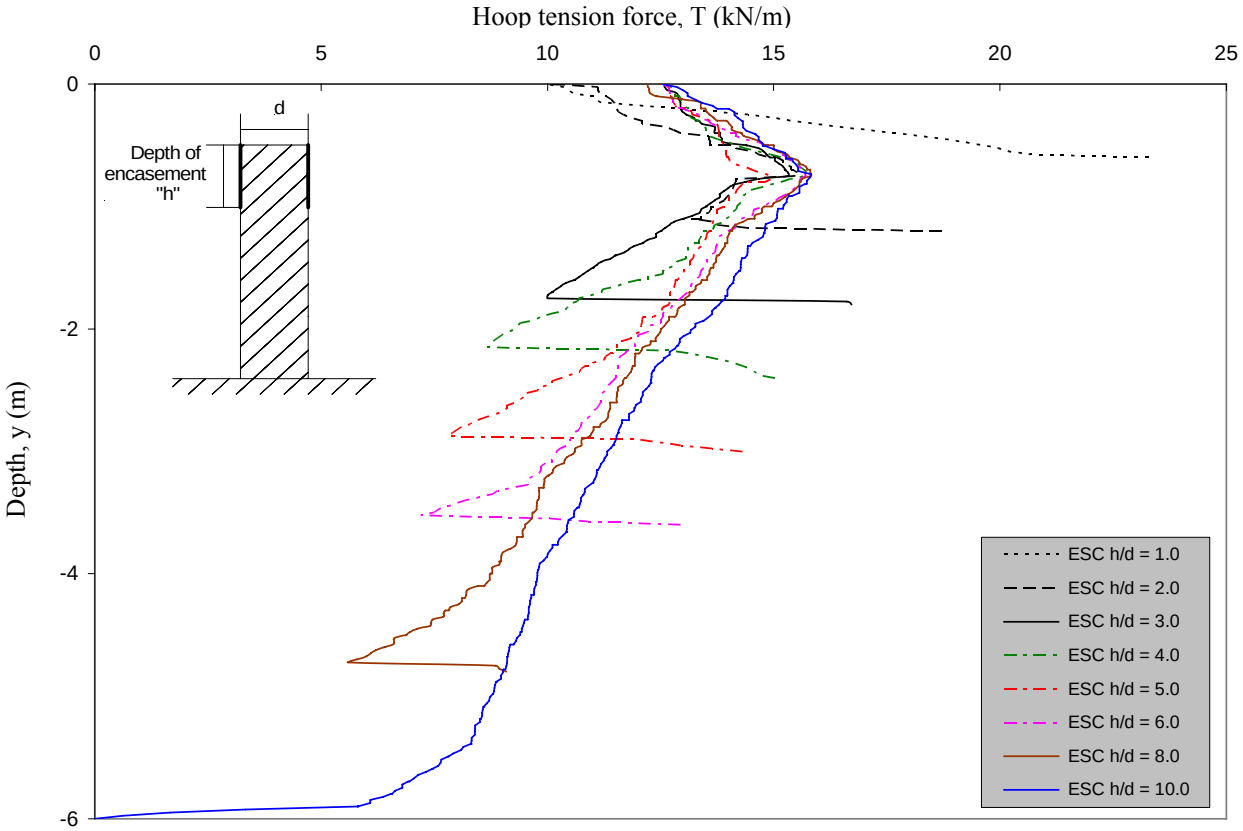

Fig. 4-36 Effect of geogrid depth on the hoop tension forces of the encasement under a column load of 300 kPa in drained conditions, d = 0.6 m, S/d = 2.0 and J = 800 kN/m

Discussion

The bearing capacity of the partially encased stone columns increases with increasing encasement depth in undrained and drained loading conditions. When the working load of 300 kPa is applied on the encased stone columns in undrained conditions, the increase of the bearing capacity beyond an encasement depth that equals three times the column diameter is not significant. Therefore, the encasement depth of three times the column diameter is sufficient to minimize the values of the settlement and lateral bulging of the stone column as well as the heave of the soft soil and the differential vertical displacement.

When the work stress load of 300 kPa is applied in drained conditions, the bearing capacity of the encased stone column increases with increasing depth of the encasement. The deeper the encasement of the stone column is, the greater the bearing capacity is and the smaller the settlement, the differential settlement and the lateral bulging are. Therefore, full encasement of the stone column leads to the optimum performance of the encased stone columns.

5 Behavior of the Reinforced Bremerhaven Clay with Stone Columns under Embankment Fill

5.1 Introduction

The non-reinforced and the reinforced Bremerhaven clay with stone columns have been loaded by a highway embankment fill to study the effect of stone columns on the behavior of the soft soil. The FEM package of Plaxis 9 program analysis has been used to provide all the valuable information, which is required to understand this foundation behavior. The behavior of the system has been investigated through the consolidation process. In the following sections, the modeling of the non-reinforced soft soil and the stone columns surrounded by soft soil, and the discussion of the results of the parametric study are presented. The discussion contains the effect of stone column on settlement, consolidation time, excess pore water pressure and stress in the soil.

5.2 Numerical modeling and selection of parameters

The Bremerhaven clay layer with 6.0 m depth is used as a soft soil. A blanket layer of compacted sand which has 30 cm thickness is used as a drainage layer. The clay layer has also a permeable sand layer in the bottom. So the non-reinforced clay layer has two way of drainage path in the vertical direction while the reinforced clay with stone column has drainage paths in both the vertical and the horizontal directions. The current analyses consider that the entire area of the non-reinforced and the reinforced Bremerhaven clay has been loaded with the sand fill as embankment loads. The sand used in the embankment fill and in the blanket layer is the same. Under embankments or large uniformly loaded areas, it is convenient to consider a representative cylindrical unit cell. Hence, all the analyses have been performed using axisymmetric idealisation of a cylindrical unit cell consisting of the stone column and the soft soil under the embankment fill. The stone columns are installed in a square orientation which was discussed in chapter 2. Fig. 5-1 shows the schematic of the models employed for these analyses. Half of the model has been used. The vertical and the horizontal displacements in the bottom boundaries were restrained while only the horizontal displacement in the lateral boundaries was restrained. The medium finite element mesh has been used with 15 nodes triangular elements. The Bremerhaven clay has been modelled by the Soft Soil Creep model under undrained conditions while the stone material and the sand fill have been modelled using Mohr Coulomb model under drained conditions. The parameters of the soil are illustrated in Table 5-1.

The embankment fill has been constructed to a height of 5.0 m in two equal layers. Every construction stage has a 2.5 m- layer and takes 21 days. The consolidation analyses are performed during and after each construction stage. A closed consolidation boundary is applied to both sides of the model preventing lateral drainage. The construction sequence is showed in Table 5-2 and Fig. 5-2.

5.3 Discussion of the results

The non-reinforced soft soil and the reinforced soft soil with stone columns have been loaded with the embankment fill in two stages of construction as discussed above. The

used stone column has a diameter (d) of 1.0 m and spacing ratio (S/d) of 3.0. The settlement, the column bulging, the excess pore water pressure and the stress in the soil were calculated. Fig. 5-1 shows the points and sections at which the calculations were carried out. Point A is located at the top of the soil to calculate the settlement and the stress. Point B is located in the soft soil at a depth of 2.0 m to calculate the excess pore water pressure. Point C is located at the top of the stone column at a horizontal distance of d/4 from the column centerline to calculate the settlement and the stress.

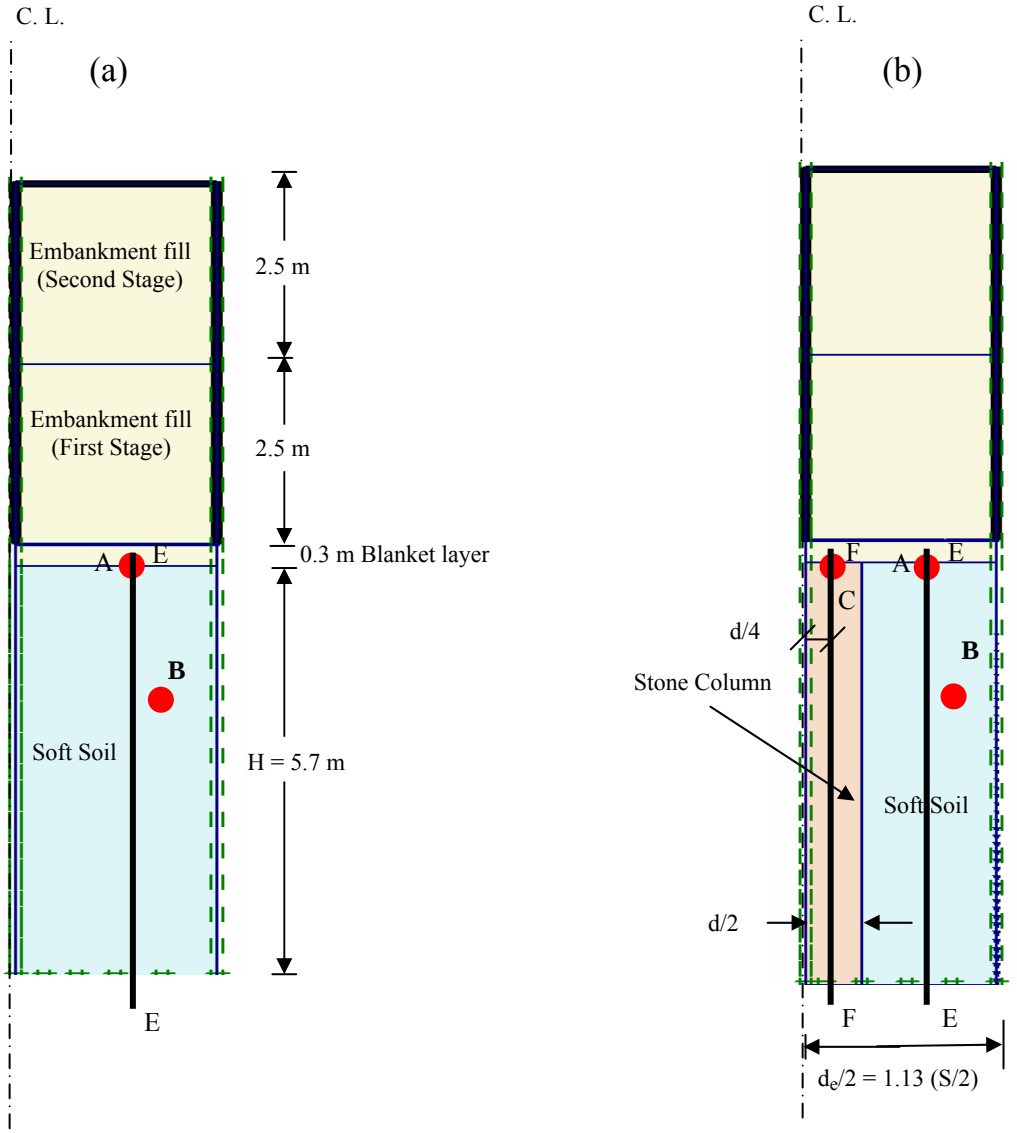

Fig. 5-1 Model parts of the unit cell (a) Non-reinforced soft soil
(b) Stone column reinforced soft soil

5.3.1 Settlement

The settlement (s) was calculated at the surface of the non-reinforced and the reinforced clay at point A, as shown in Fig. 5-1 (a and b). Fig. 5-2 shows the relationships of the time with the construction of the embankment and with the settlement. The first construction stage shows an increase in the settlement with time which is accompanied by dissipating excess pore water pressure. But the rate of the increase in the settlement gradually decreases with increasing time especially in the last period of the consolidation

time. The non-reinforced and the reinforced clay follow the same procedure of the settlement in the second construction stage. But in the second construction stage the settlement is smaller and the consolidation time is faster than in the first construction stage in both cases, as shown in Fig. 5-2, Fig. 5-3 and Fig. 5-4. The consolidation in the first stage enhances the soft soil behavior which leads to an increase of its stiffness and shear strength in the second stage of loading. Hence, the first construction load stage is a preloading for the second construction load.

Table 5-1 Properties and shear strength parameters used for the soils.

Parameter	**Symbol**	**Stone Soil, (Ambily and Gandhi, 2007)**	**Sand, (Ambily and Gandhi, 2007)**	**Bremerhaven clay, (Geduhn, 2005)**[1]
Material model	Type	Mohr-Coulomb	Mohr-Coulomb	Soft Soil Creep
Loading	Condition	Drained	Drained	Undrained and Consolidation
Wet soil unit weight	γ_{wet}, (kN/m^3)	19	18	15
Horizontal permeability	k_h, (m/day)	12	1	$2x10^{-4}$
Vertical permeability	k_v, (m/day)	6	0.5	$1x10^{-4}$
Young's modulus	E, (kN/m^2)	55,000	20,000	-
Poisson's ratio	υ (-)	0.3	0.3	-
Modified compression index	λ* (-)	-	-	0.203
Modified swelling index	κ* (-)	-	-	0.025
Modified secondary compression index	μ*	-	-	0.007
Cohesion	c `, (kN/m^2)	0	0	5
Friction angle	φ ` °	43	30	37.75
Dilatancy angle	ψ°	10	4	0

1) After Richwien, 1981.

Table 5-2 Construction sequences of the embankment fill

Stage	**Phase**	**Fill Height, (m)**	**Time Consumed (day)**
First	1- Construction	0-2.5	21.0
	2- Consolidation	2.5	Time is calculated until the excess pore water pressure is dissipated (1 kPa)
Second	3- Construction	2.5-5.0	21.0
	4- Consolidation	5.0	Time is calculated until the excess pore water pressure is dissipated (1 kPa)

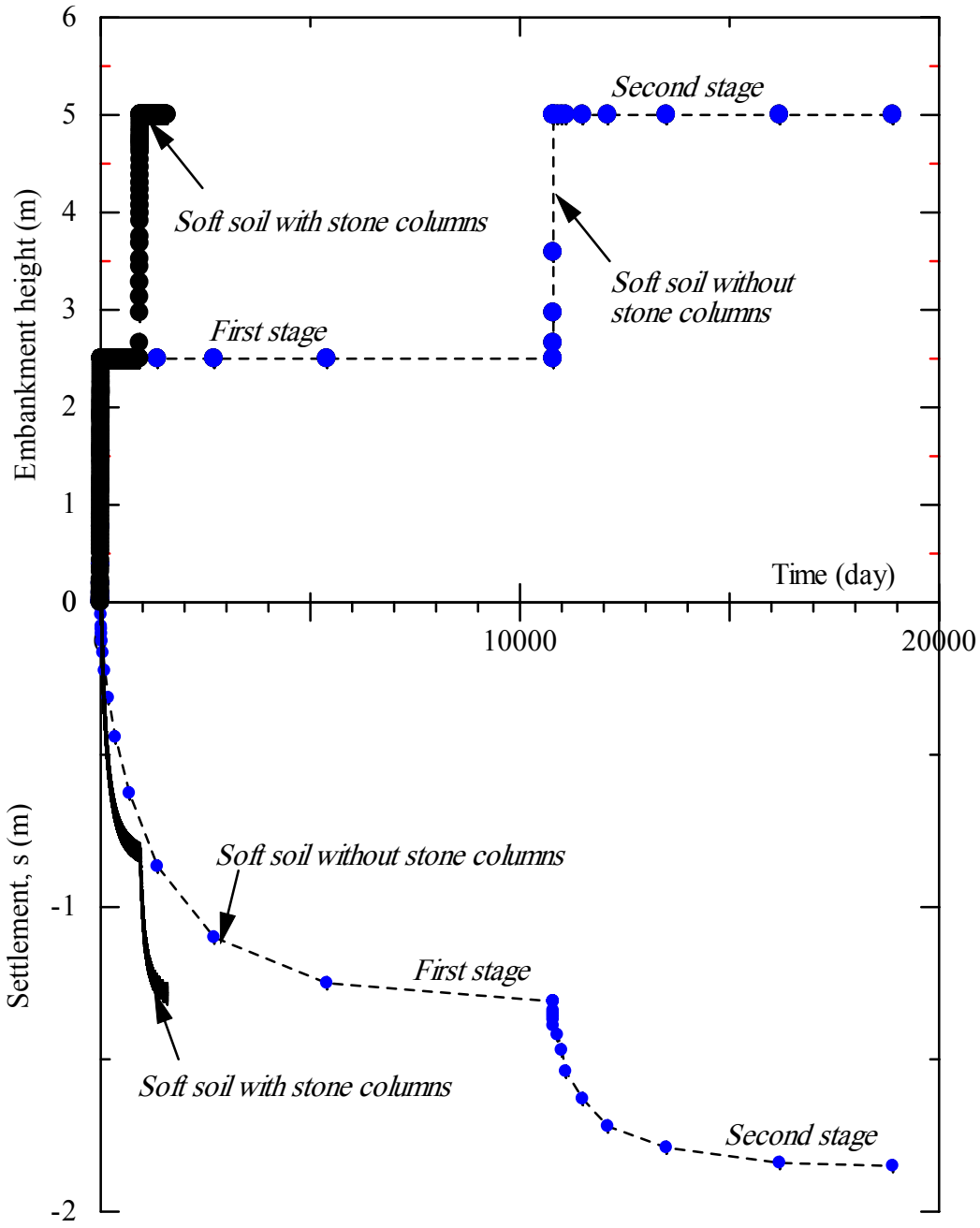

Fig. 5-2 Settlement of the non-reinforced and the reinforced soft soil with ordinary stone columns during the time of the construction at point A

The non-reinforced soft clay needs a very long time to wait until the consolidation is finished which reaches 10,871 days (approximately 30 years). So, the construction on this type of soil is impossible without using any soil improvement methods. When the stone column is used, the settlement is decreased and the consolidation time is accelerated. The time of the construction in the first stage is reduced from 10,781 days (30 years) to 933 days (2.5 years) and the settlement from 1.31 m to 0.82 m. Hence, the construction in the first stage is accelerated too quickly and the settlement is reduced to 0.63 of the non-reinforced clay settlement when using stone columns. At the end of the construction and consolidation, using stone columns in clay reduces the time from 18,872 (51.7 years) to 1,590 (4.36 years) and the settlement also reduced from 1.86 m to 1.29 m.

The settlement distribution at the surface of the non-reinforced and the reinforced clay is also shown in Fig. 5-5 at the consolidation end of both construction stages. The existence of stone columns in soft clay increases the bearing capacity of the soft clay by reducing settlement during the various construction phases. The settlement in the stone column and in the surrounding soft soil is approximately the same (equal vertical strain theory) as illustrated in Fig. 5-5. Castro and Sagaseta (2008) stated that the equal vertical strain condition has been proved to be more realistic under embankments than the other extreme alternative (the so-called 'free vertical strain'). This phenomenon is because of stress transfer from the surrounding clay and stress concentration in the stone column causing yield of the column which will be discussed later.

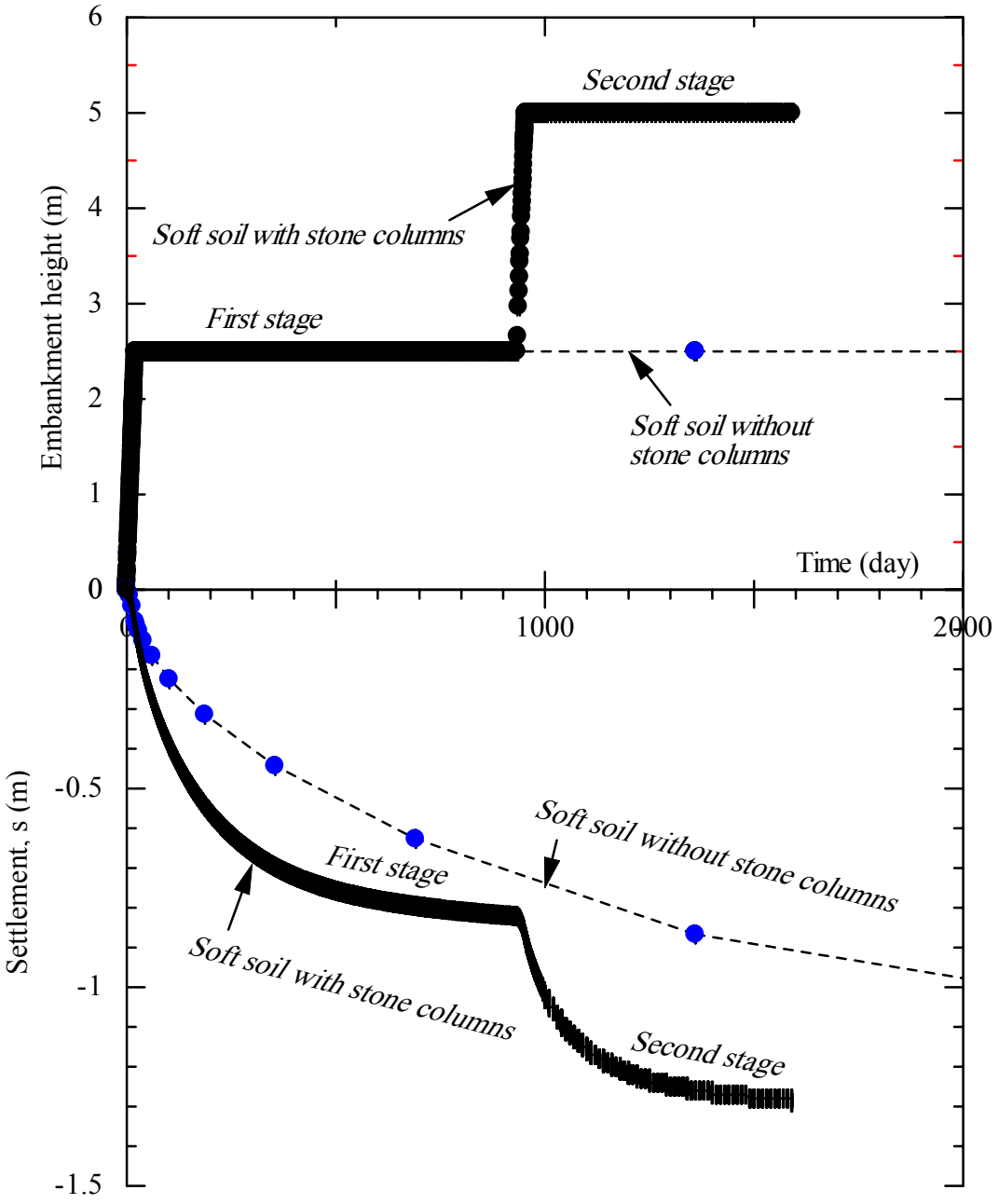

Fig. 5-3 Settlement of the non-reinforced and the reinforced soft soil with ordinary stone columns during the time of the construction at point A

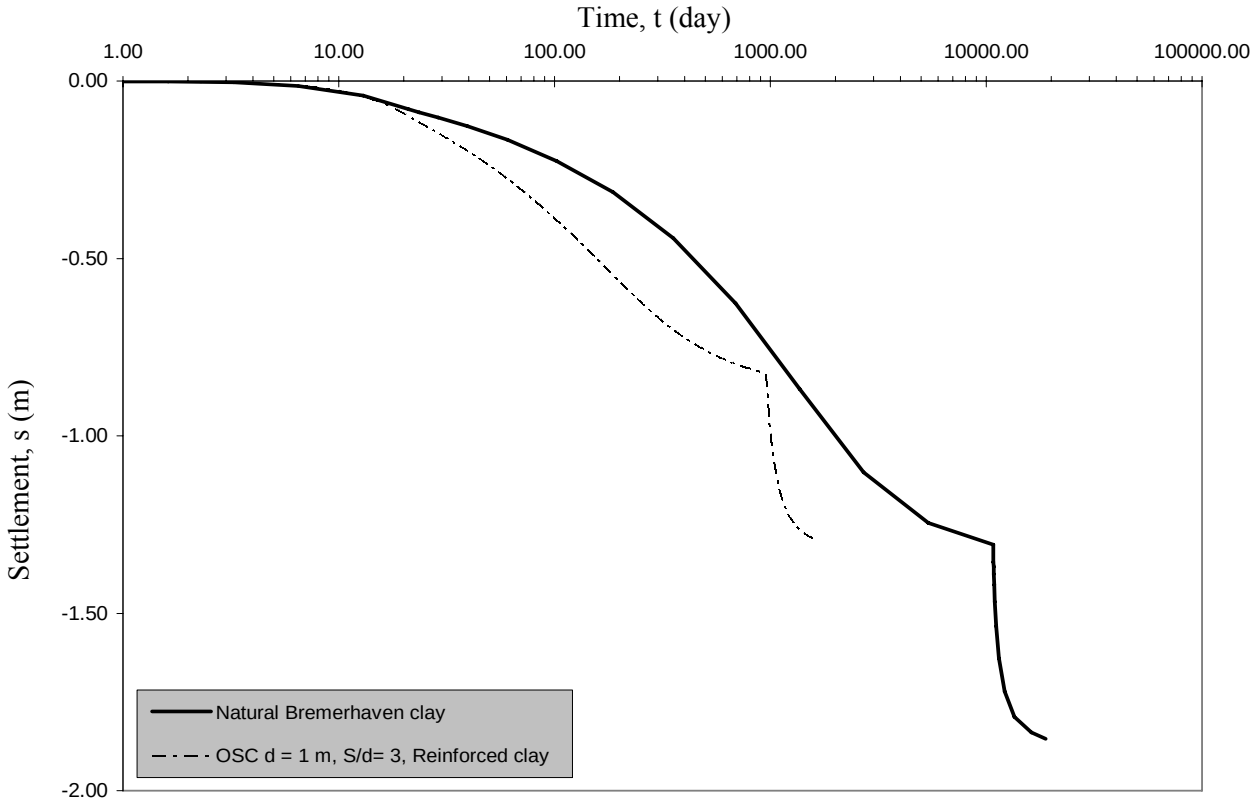

Fig. 5-4 Time-settlement relationship for the nature and the reinforced soft soil with ordinary stone columns (OSC) at point A

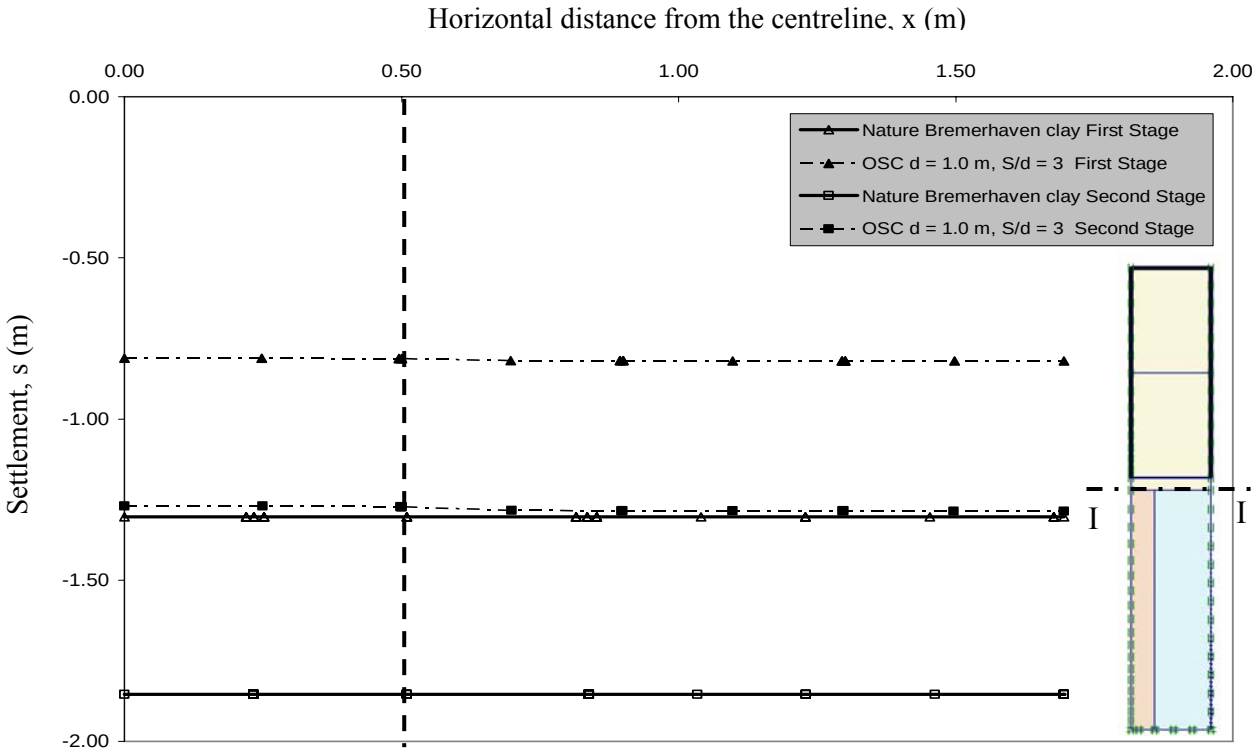

Fig. 5-5 Settlement distribution at the surface of the non-reinforced and the reinforced soft soil with ordinary stone columns (OSC)

5.3.2 Lateral bulging of the stone column

Once the stone column is yielded, its bulging appears due to dilatancy. The lateral bulging of the stone column was calculated after each consolidation phase, as shown in Fig. 5-6. The column displaces laterally into the soft soil with loading especially in the upper part. The lateral displacement of the column starts with zero at the surface and gradually increases with depth until it reaches a maximum value at a depth of 0.9 times of the column diameter (d) in the two construction stages. Then, the lateral displacement decreases gradually along the column to reach zero at the column base. But in the end of consolidation, there is increasing in the lateral bulging in the lower third of the column. This is due to the lateral bulging along the stone column increases with increasing load causing more load transfer to lower depths during the consolidation.

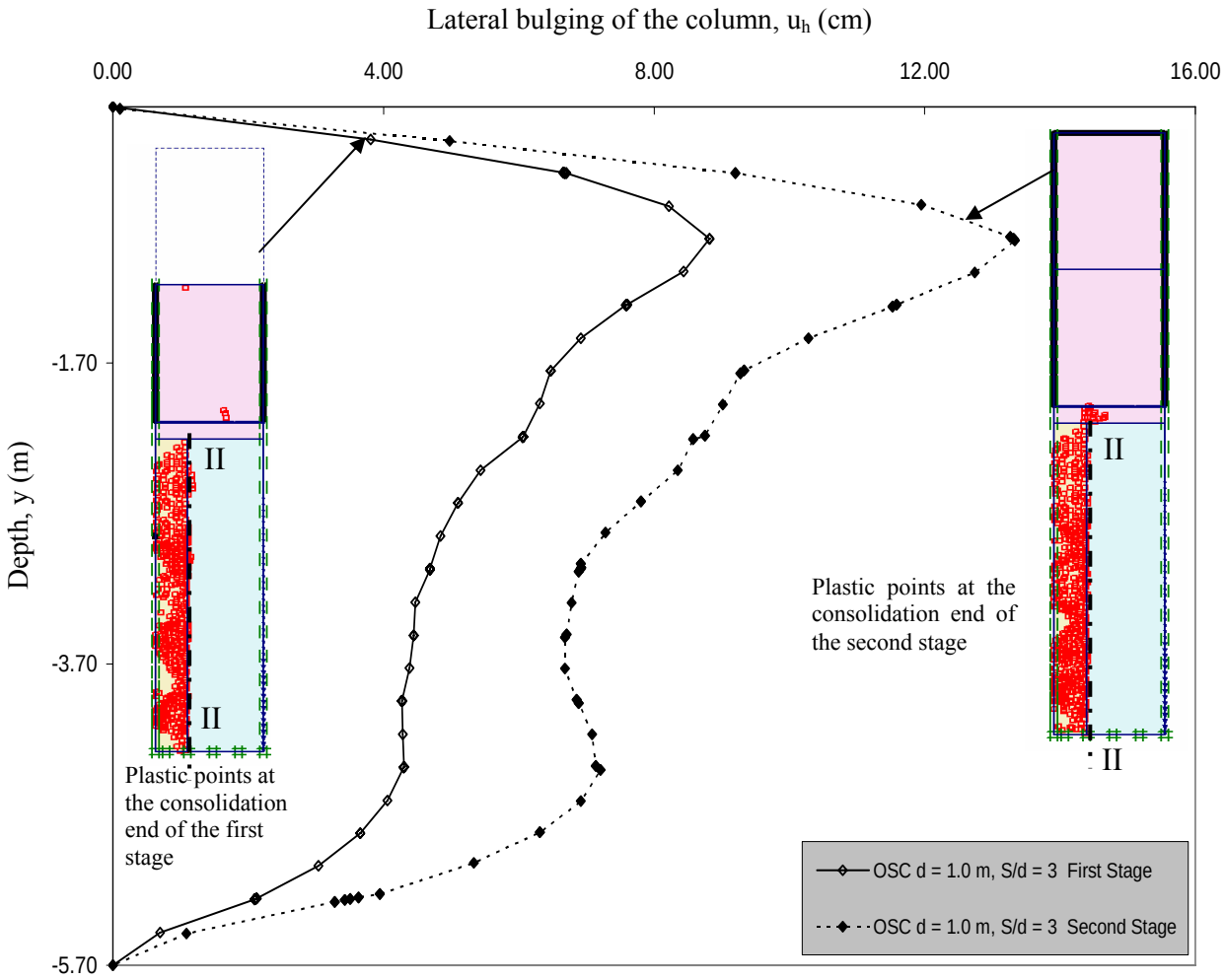

Fig. 5-6 Lateral bulging and yielding distribution of the stone column at the consolidation end of the two construction stages.

5.3.3 Excess pore water pressure

The excess pore water pressure (Δu) in the non-reinforced and the reinforced soft soil was calculated at point B which is located at a depth of 2.0 m, as shown in Fig. 5-1. As soon as the fill load is applied on the saturated soft soil, the excess pore water pressure builds up. The excess pore water pressure increases with time until it reaches maximum values at the end of construction of each stage. After that, the excess pore water pressure decrease gradually during the consolidation directing to the steady state case, as shown in Fig. 5-7. The first and the second stage of construction imply the same behavior of the excess pore water pressure through the consolidation time. But the excess pore water pressure after the second stage of construction is dissipated somewhat more rapidly than that after the first stage of construction, as shown in Fig. 5-8.

The behavior of the excess pore water pressure in the soft soil without stone column and the reinforced soft soil is the same. The excess pore water pressure in the reinforced soft soil has lower values and dissipates more rapidly than that in the non-reinforced soft soil. Hence, using stone columns in clay soil improves the drainage and accelerates the dissipation of excess pore water pressure because the stone columns shorten the drainage paths by adding horizontal drainage paths to the vertical paths as illustrated in Fig. 5-9.

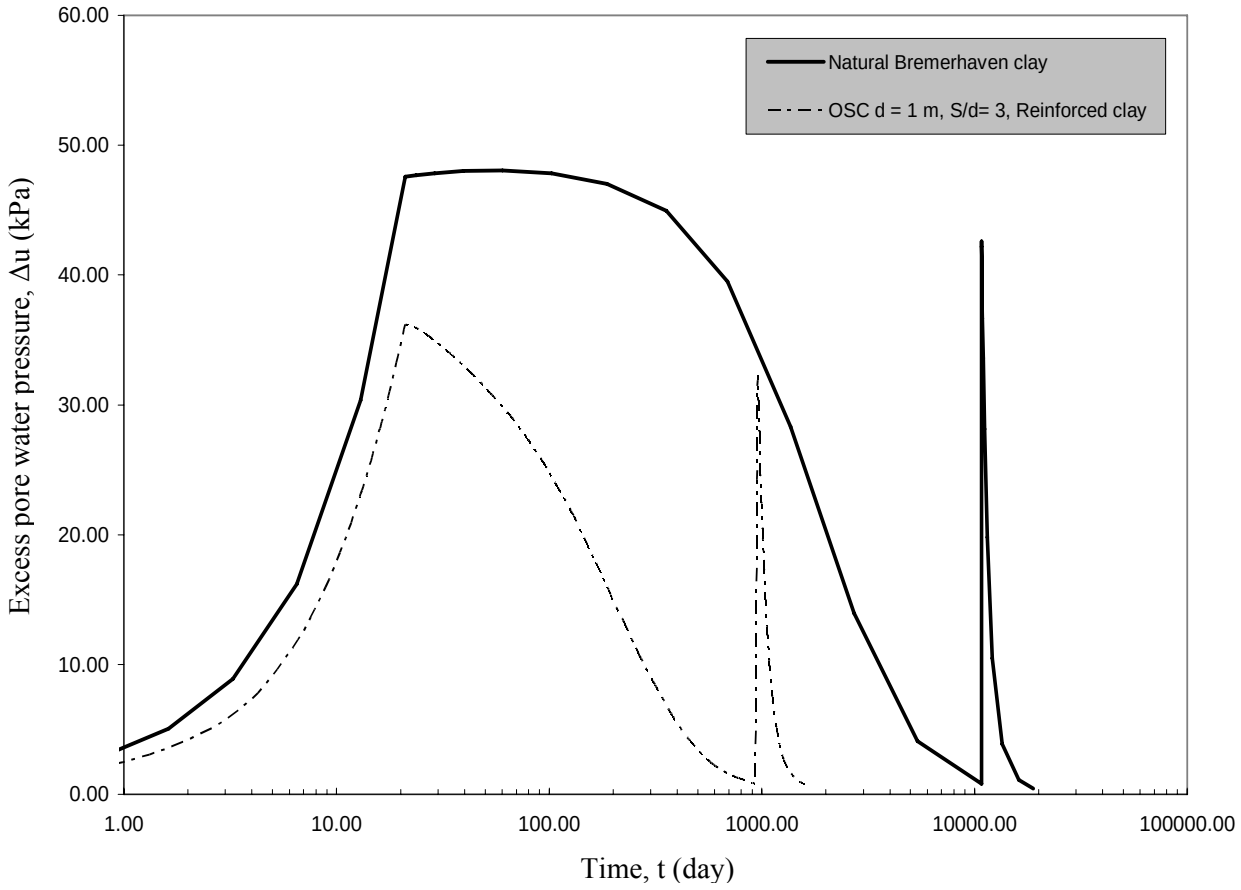

Fig. 5-7 Excess pore water pressure-time relationship at point B for the non-reinforced and the reinforced soft soil with ordinary stone columns (OSC)

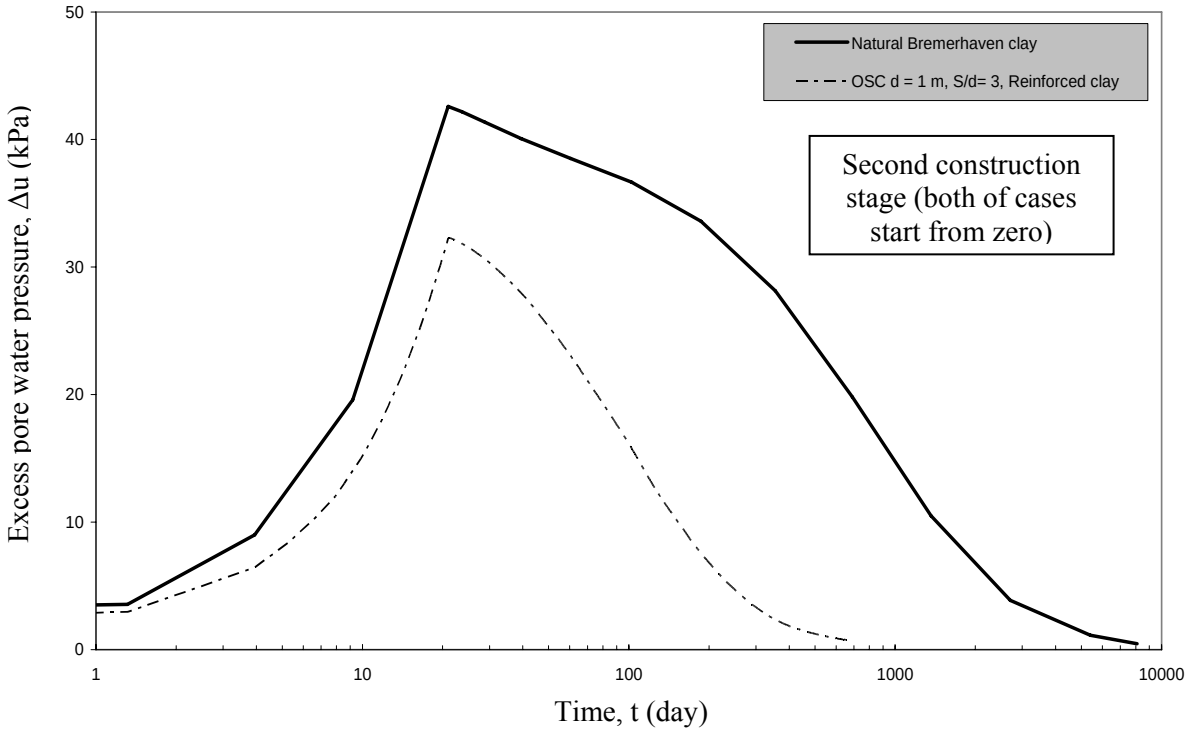

Fig. 5-8 Development of excess pore water pressure during the second loading stage at point B for the non-reinforced and the reinforced soft soil with ordinary stone columns

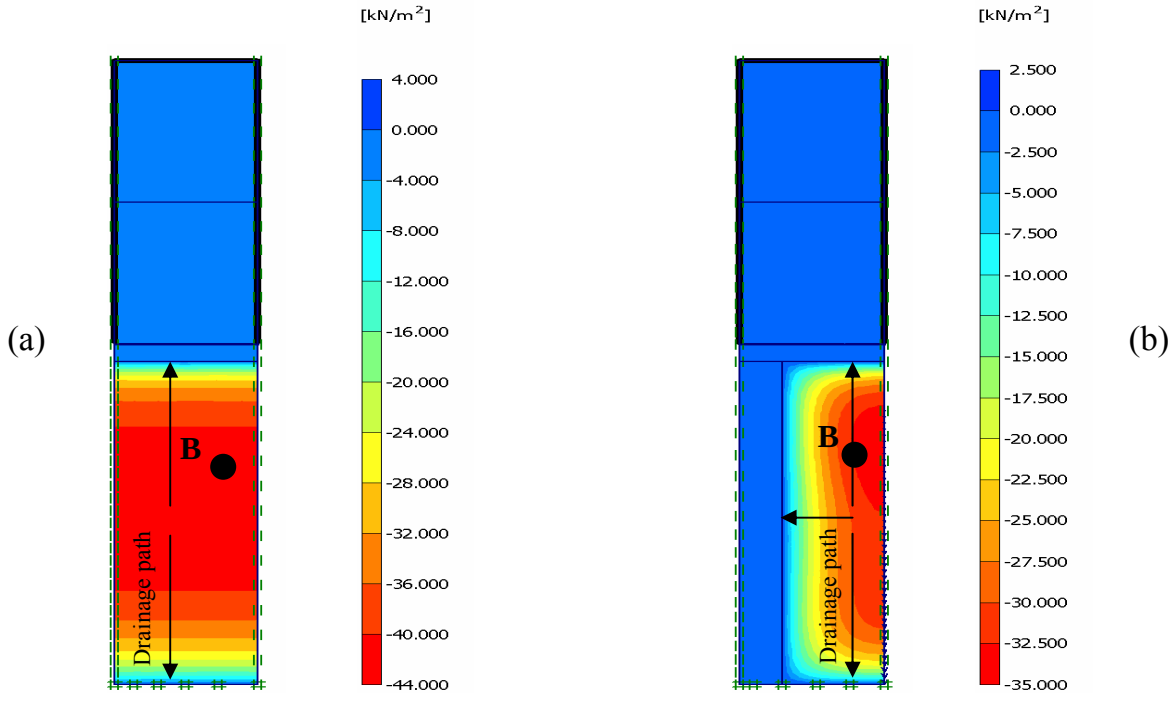

Fig. 5-9 Distribution of the pore water pressure at the end of the second construction stage at (a) Non-reinforced soft soil and (b) Reinforced soft soil with stone columns

5.3.4 Stress in soil

The stress in the non-reinforced soft soil, the reinforced soft soil and the stone column has been studied in the current analyses. The effective vertical stress (σ'_v) was calculated

at the surface in the non-reinforced and the reinforced soft soil at point A, and in the column at point C, as shown in Fig. 5-1 (a and b). The relationship of the effective vertical stress with settlement and with time is shown in Fig. 5-10 and Fig. 5-11, respectively. The effective vertical stress in the non-reinforced and the reinforced soft soil and in the stone column increases with a high rate with increasing settlement and time through increasing embankment fills in both stages of construction. During the consolidation process, directly after the first and the second construction stages have been finished, the vertical effective stress in the non-reinforced and the reinforced soft soil increases with a very small rate. But the rate of the effective vertical stress increase becomes somewhat greater during the consolidation of the second construction stage especially in the reinforced soft soil. Using stone columns reduces the effective vertical stress in the reinforced soil which is smaller than that in the non-reinforced soft soil and high stress values are generated in the stone column, as shown in Fig. 5-10 and Fig. 5-11. Hence, the effective stress in the reinforced soft soil is reduced due to the stress transfer from the soft soil and concentrate in the stone column.

During the consolidation process of the first construction stage, as the settlement and the time increase, the vertical effective stress in the stone column increases with a small rate until it reaches a maximum value. Beyond this value the vertical effective stress decreases with small rate until the second stage of construction starts. During the consolidation process in the second stage, the vertical stress decreases gradually with increasing time and settlement.

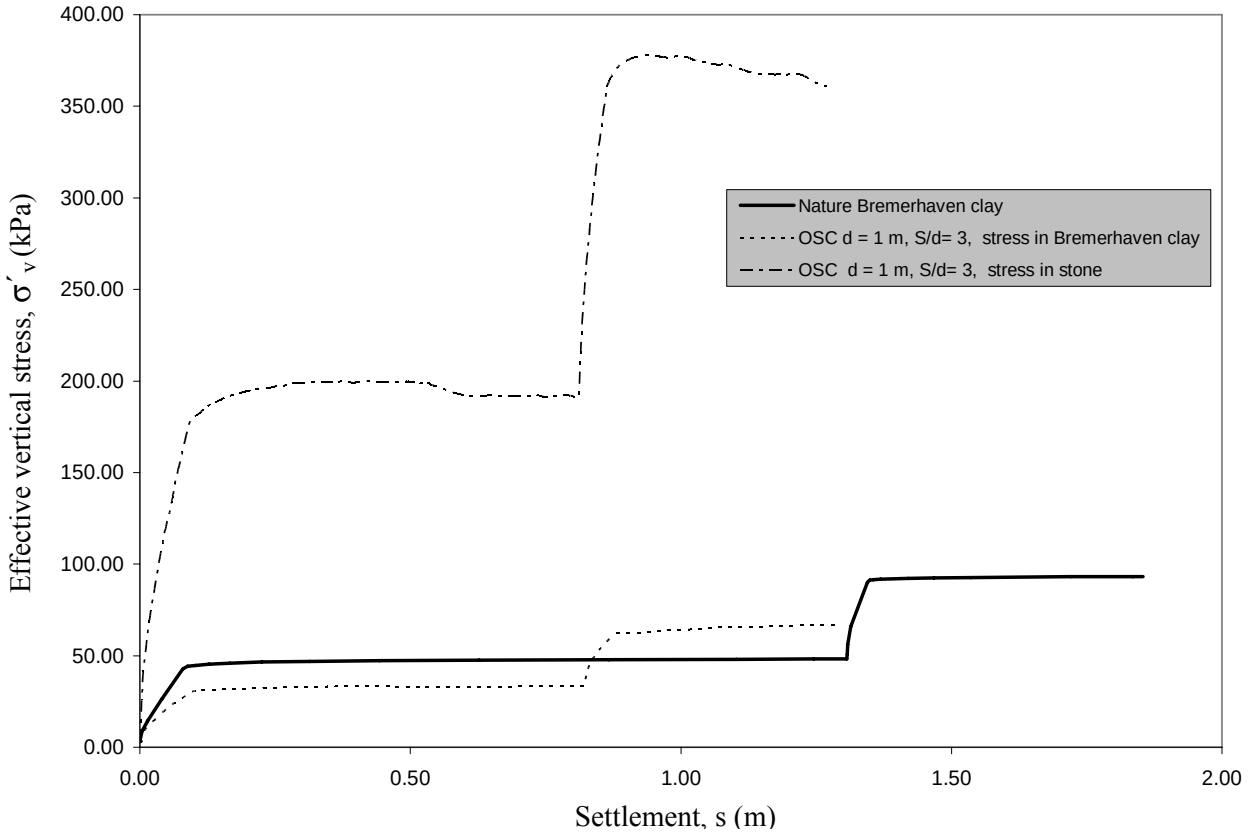

Fig. 5-10 Effective vertical stress-settlement relationship for the nature and the reinforced soft soil at point A and for the stone column at point C

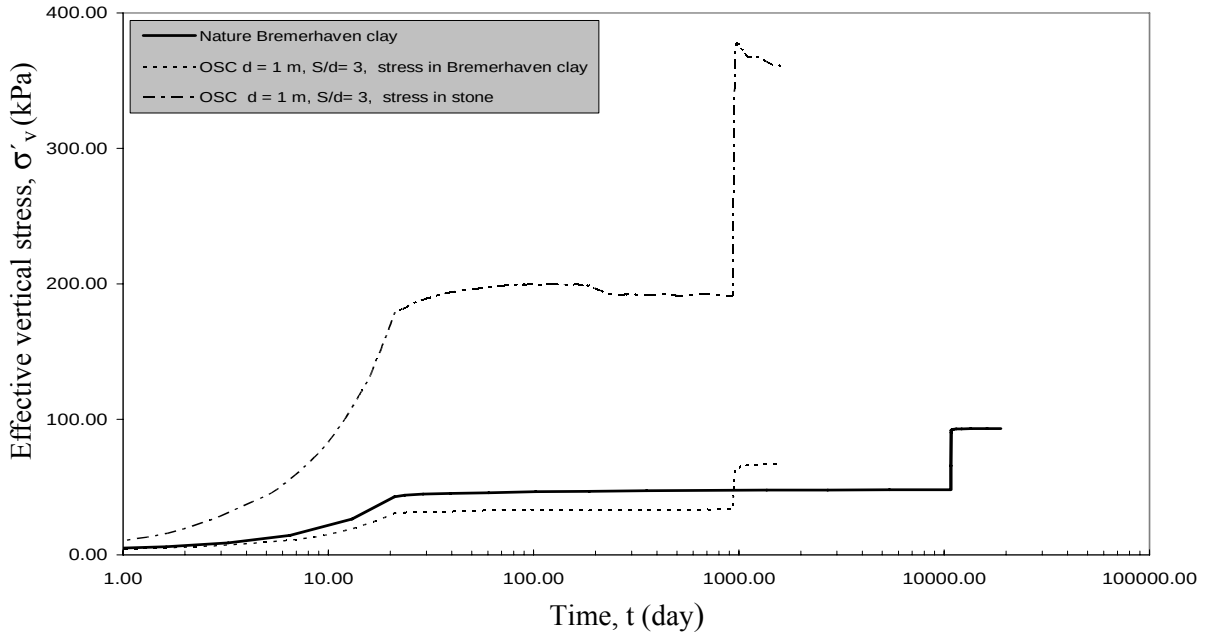

Fig. 5-11 Effective vertical stress-time relationship for the nature and the reinforced soft soil at point A and for the stone column at point C

The decrease in the effective vertical stress in the stone column after the middle of the first stage consolidation and during the second stage consolidation is because of the yielding of the stone column, as shown in Fig. 5-6. Once yielded, the stiffness of the column decreases, and also its radial deformability increases due to dilatancy. Otherwise, the yielding of the column reduces the transfer of vertical load from the soil. The soft soil didn't imply any yielding except the zone which is located very close to the column.

Stress Concentration Factor, (SCF)

The stress concentration factor (SCF) is defined as the ratio of the vertical effective stress in the stone column to the vertical effective stress in the surrounding soft soil, ($SCF = \sigma'_{v(stone\ column)} / \sigma'_{v(clay)}$). The average stress concentration factor was calculated at sections A-A, B-B and C-C which are located at the surface, at a depth of 0.75 m and at a depth of 1.25 m, respectively as shown in Fig. 5-12. The development of the stress concentration factor at the surface is similar to that of the vertical effective stress in the stone column which is discussed above. And the development of the stress concentration factor at sections A-A, B-B and C-C is also approximately similar. The stress concentration factor increases with increasing load during the construction of the first stage until it reaches a maximum value at the construction end. Beyond the maximum stress ratio, it decreases with increasing time until it reaches minimum values at the consolidation end of the first stage. Afterwards, the stress concentration factor increases again with increasing fill load in the second construction stage. After that the stress concentration factor decreases gradually with consolidation time. The stress concentration factor at section C-C is greater than that at section A-A while the stress concentration factor at section B-B is greater than that at both sections A-A and C-C, as shown in Fig. 5-12.

The stress concentration factor at section A-A increases with increasing load until it reaches a higher value of 5.81 after 21 days from the start of the construction. After that,

the stress concentration factor has slightly gradually increases until it reaches a maximum of 6.08 at a time of 200 days. Then, the stress concentration factor decreases gradually with consolidation time and reaches 5.72 at the consolidation end of the first stage. The stress concentration factor increases again with developing load in the second stage which reaches 6.0 at the end of construction. Afterwards, the stress concentration factor decreases gradually with the consolidation time until it reaches 5.4 at the end, as illustrated in Fig. 5-12.

The stress concentration factor at section B-B also increases with increasing load and time until it reaches a maximum of 19.53 after 21 days from the start of the first construction stage. After that, the stress concentration factor decreases gradually with consolidation time and reaches 7.0 at the consolidation end of the first stage. The stress concentration factor increases again with developing load in the second stage which reaches 9.49 at the end of construction. After that the stress concentration factor decreases gradually with the consolidation time until it reaches 6.0 at the end, as shown in Fig. 5-12.

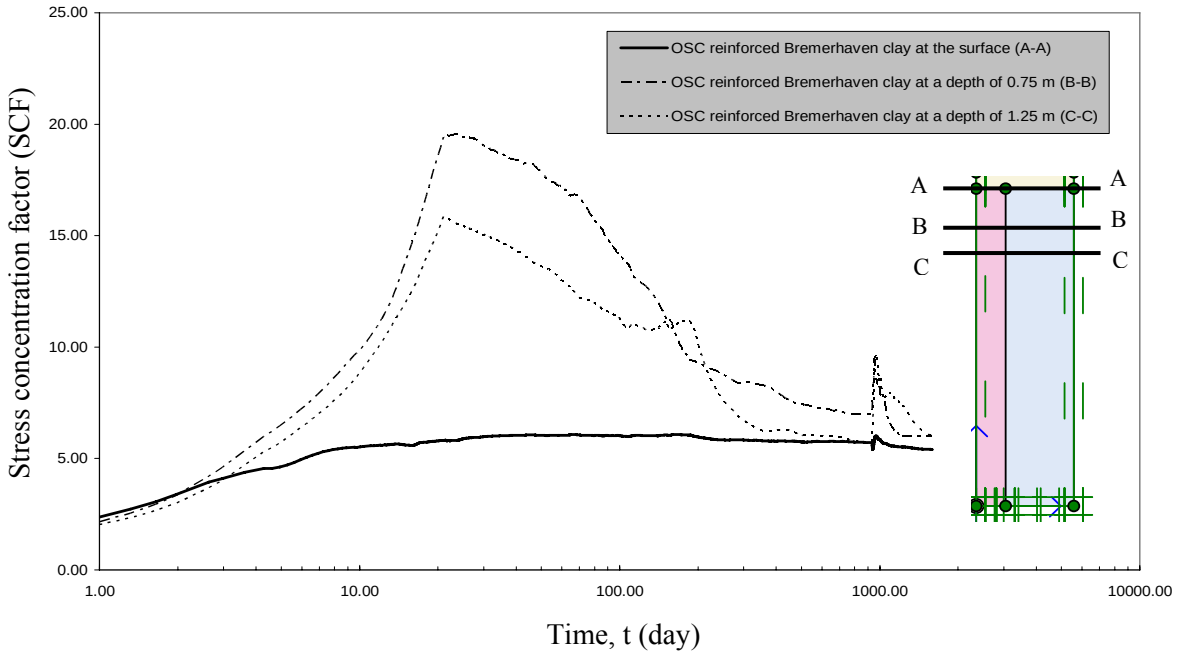

Fig. 5-12 Average stress concentration factor-time relationship for the reinforced soft soil with stone columns at various depths

Finally, the stress concentration factor of section C-C increases with increasing load and time until it reaches a maximum of 15.84 at the construction end which decreases slightly until it reaches 11.15 after a time of 186 days. After that, the stress concentration factor decreases gradually with consolidation time and reaches 5.67 at the consolidation end of the first stage. The decrease in the stress concentration factor is due to the column yielding and the increase in the stiffness and the strength of the surrounding soft soil during the consolidation. Afterwards, the stress concentration factor increases again with developing load in the second stage which reaches 9.30 at the end of construction. After that, the stress concentration factor decreases gradually with the consolidation time until it reaches 6.0 at the end.

The vertical effective stress was calculated in the non-reinforced and the reinforced soft soil at section E-E, and in the stone column at section F-F, as shown in Fig. 5-1, to study the stress concentration through the reinforced clay layer. The vertical effective stress was calculated after the end of consolidation of the first and the second stages of construction. The effective vertical stress in the non-reinforced and the reinforced clay increases gradually with downward direction due to the effect of overburden pressure. The effective vertical stress in the reinforced soft soil is smaller than that in the non-reinforced soft soil across the clay layer because the stress concentration in the column, as shown in Fig. 5-13.

The effective vertical stress in the stone column after the consolidation of the first stage of the construction starts with a value at the surface generating stress concentration factor of 5.72. Then, the effective vertical stress increases with downward direction until it reaches a maximum value at 0.7 m depth of the clay layer. The stress concentration factor at this point is 7.4. Beyond this point, the effective vertical stress decreases with depth until it reaches a minimum value at a depth of 1.7 m generating a stress concentration factor of 4.3. Depths lower than the minimum stress point show a gradual increase in the effective vertical stress and stress concentration which reaches 6.0 at the column base, as shown in Fig. 5-13.

The effective vertical stress in the stone column after the consolidation of the second stage of the construction starts with a value at the surface generating stress concentration factor of 5.4. Then the effective vertical stress increases with downward direction until it reaches a maximum value at 1.3 m depth of clay layer. The stress concentration factor at this point is 6.6. Beyond this point, the effective vertical stress decreases with depth until it reaches a minimum value at a depth of 2.5 m generating a stress concentration factor of 3.3. Depths lower than the minimum stress point show a gradual increase in the effective vertical stress and stress concentration which reaches 6.0 at the column base, as shown in Fig. 5-13.

The stress concentration factors after consolidation along the column are in the range of (3-9) which agree with the field measurements which were discussed in chapter 2. The first construction stage implies stress concentration factors greater than them in the second construction stage. The reason of that is the stone column is yielded during the consolidation and the consolidation in the first construction stage leads to an increase in the shear strength and the stiffness of the soft soil in the second construction stage.

The total and the effective vertical stress, and the excess pore water pressure were calculated in the non-reinforced and the reinforced soft soil at point (B) which is located at a 2.0 m depth, as shown in Fig. 5-9. The total vertical stress (σ_v) and the excess pore water pressure (Δu) in the non-reinforced and the reinforced soft soil increase with increasing load until they reach maximum values at the end of both constructions stages. During the consolidation process after each of construction stage, the effective vertical stress (σ'_v) increases with time while the excess pore water pressure decreases in the non-reinforced and the reinforced soft soil, as shown in Fig. 5-14 and Fig. 5-15, respectively. At the end of the consolidation the excess pore water pressure dissipates and the vertical effective stress reaches maximum values.

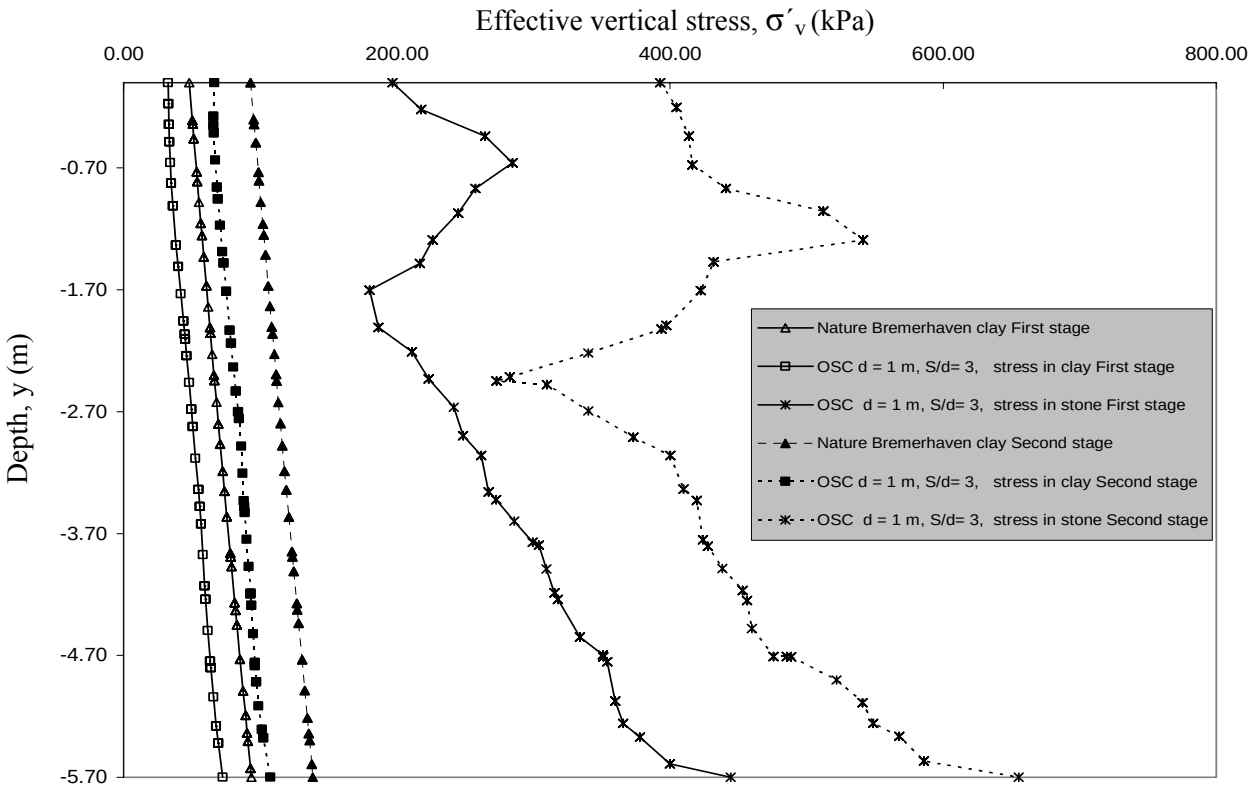

Fig. 5-13 Effective vertical stress distribution for the non-reinforced and the reinforced soft soil at section E-E and for the stone column at section F-F

The total vertical stress in the non-reinforced soft soil is constant during the consolidation process while the total vertical stress in the reinforced soft soil is variable with consolidation time, as shown in Fig. 5-14 and Fig. 5-15. After each construction stage finishes, the total stress in the reinforced clay reaches a maximum value. Beyond the maximum total stress value, the total stress decreases gradually with increasing consolidation time, as illustrated in Fig. 5-15. This phenomenon means that at the construction stage, the load transfer to the columns is less important, and it increases as consolidation proceeds. Inversely, the clayey soil is subjected to a higher total stress at the beginning, implying some degree of "pre-loading" with respect to the final soil total stress. This produces a faster consolidation compared with the case of the non-reinforced clay which has a constant load. Hence, the stress transfer from clay and concentration in stone column participate with a high percentage in the acceleration of the consolidation process and construction time.

The initial pore water pressure dissipates in the reinforced soft soil due to drainage and stress concentration in the stone column. The participation of the stress concentration on the acceleration of consolidation can be computed by calculate the reduction on the total stress in the reinforced soft soil during the consolidation and it is divided by the initial excess pore water pressure, as illustrated in Fig. 5-15 and Eq. (5-1). The rest percentage in the acceleration of consolidation is due to the drainage effect.

$$SC_{accel.} = (\sigma_{v(i)} - \sigma_{v(f)}) / \Delta u_i \qquad [-] \qquad (5\text{-}1)$$

Where $SC_{accel.}$; participation of stress concentration in the consolidation acceleration, $\sigma_{v(i)}$; average initial total vertical stress in the reinforced soft soil (after 21 days in this study),

$\sigma_{v(f)}$; average final total vertical stress in the reinforced soft soil (after consolidation end), Δu_i; average maximum initial excess pore water pressure in the reinforced soft soil (after 21 days in this study).

The stress concentration on the stone column participates in the acceleration of the consolidation process by a percentage of 33.33 % in the first stage and a percentage of 25. 1 % in the second stage.

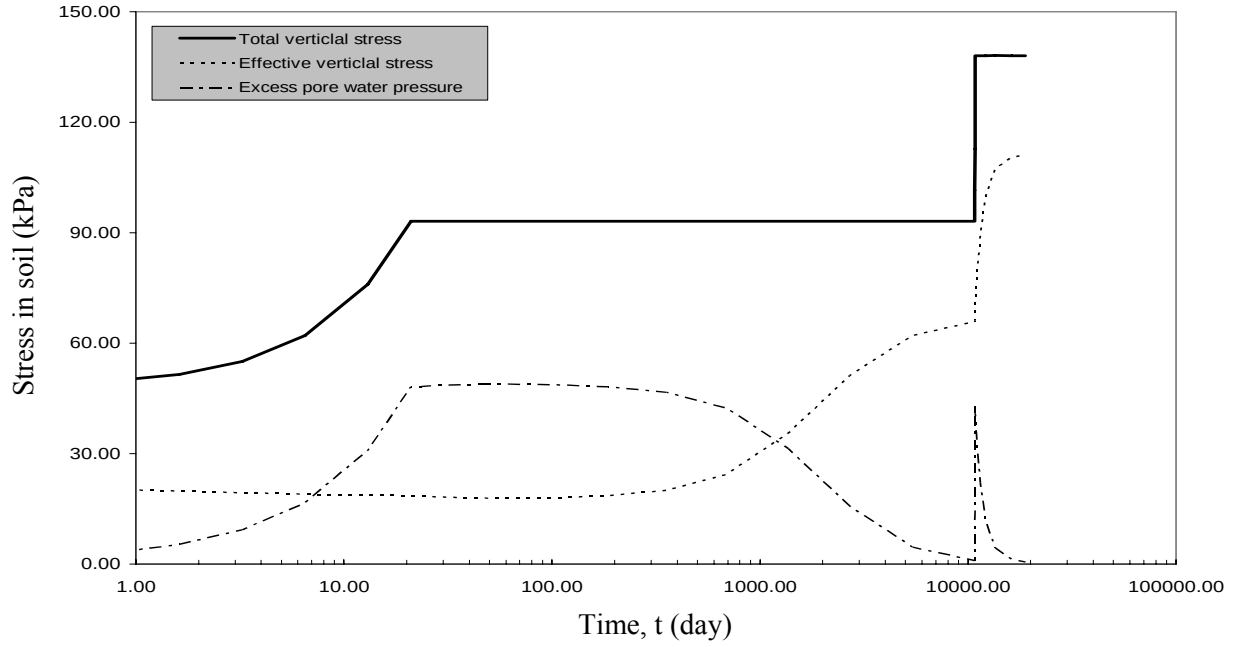

Fig. 5-14 Relationship of the total and effective vertical stress and the excess pore water pressure with time in the non-reinforced soft soil at point B (2.0 m depth)

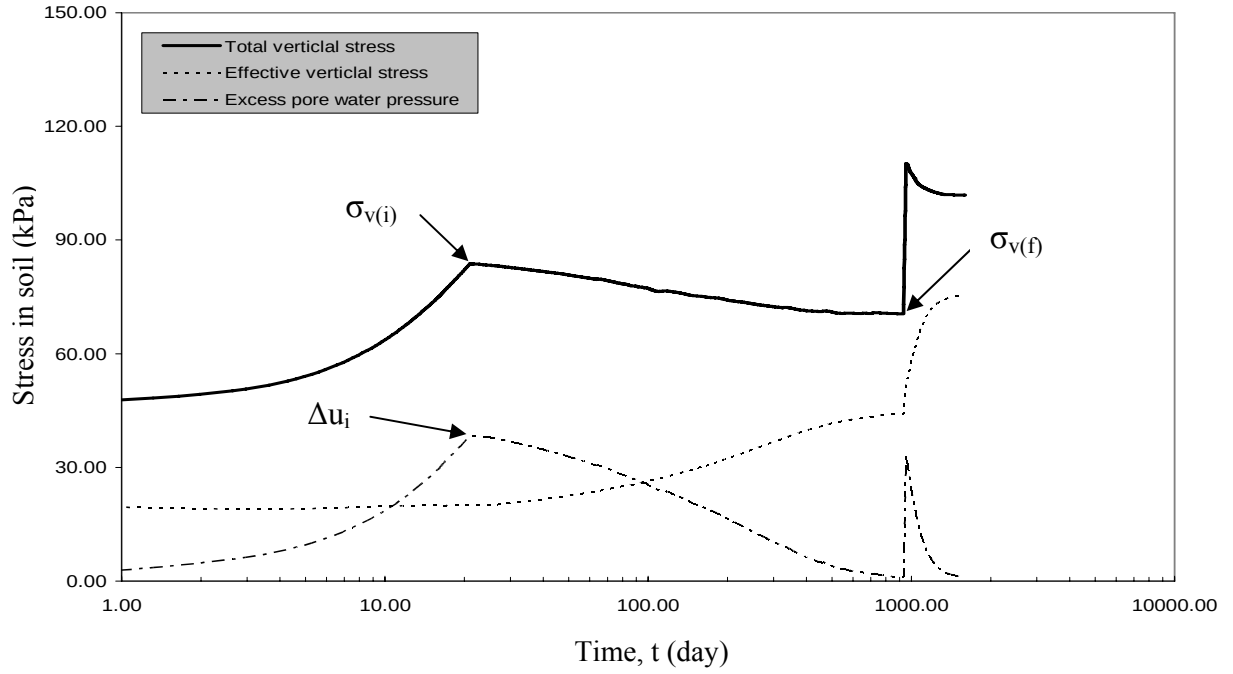

Fig. 5-15 Relationship of the total and effective vertical stress and the excess pore water pressure with time in the reinforced soft soil at point B (2.0 m depth)

6 Behavior of the Reinforced Hamburg Clay with Stone Columns under Embankment Fill

6. 1 Introduction

Related to the previous chapter 5, the Hamburg clay has been studied as a softer soil than Bremerhaven clay to investigate the effect of the stone column reinforcement on the behavior of the very soft soil. The non-reinforced and the reinforced Hamburg clay have been loaded as foundations of a highway embankment. The FEM package of Plaxis 9 program analysis has been used to understand this foundation behavior. The behavior of the system has been investigated through the consolidation process. In the following sections, the modeling of the non-reinforced soft soil and the stone columns surrounded by soft soil, and the discussion of the results of the parametric study are presented. The discussion contains the effect of stone column on soft soil settlement, consolidation time, column bulging, excess pore water pressure and stress in the soil.

6.2 Numerical modeling and selection of parameters

The Hamburg clay layer with 6.0 m depth is used as a soft soil. The same parts and conditions of the unit cell model, which were used in chapter 5, are used in the current analyses. A blanket layer of compacted sand which has 30 cm thickness is also used as a drainage layer. The current analyses consider that the entire area of the non-reinforced and the reinforced Hamburg clay has been loaded with the sand fill as embankment loads. Fig. 6-1 shows the schematic of the models employed for these analyses. Half of the model has been used. The vertical and the horizontal displacements in the bottom boundaries were restrained while only the horizontal displacement in the lateral boundaries was restrained. The medium finite element mesh has been used with 15 nodes triangular elements. The Hamburg clay has been modelled by the Soft Soil Creep model under undrained conditions while stone material and sand fill have been modelled using Mohr Coulomb model under drained conditions. The same parameters of the stone and the sand which were used in chapter 5 have been used in the current analyses. The parameters of the soils are illustrated in Table 6-1.

The embankment fill has been constructed to a height of 5.0 m in two equal layers. Every construction stage has a 2.5 m- layer and takes 21 days. The consolidation analyses are performed during and after each construction stage. A closed consolidation boundary is applied to the both sides of the model preventing lateral drainage. The construction sequence is showed in Table 6-2 and Fig. 6-2

6.3 Discussion of the results

The non-reinforced soft soil and the reinforced soft soil with stone columns have been loaded with the embankment fill in two stages of construction as discussed above. The stone column has a diameter (d) of 1.0 m and spacing ratio (S/d) of 3.0. Settlement, column bulging, excess pore water pressure and stress in the soil were calculated for points A, B, and C. Fig. 6-1 shows the points and the sections at which the calculations were carried out. Point A is located at the top of the soil. Point B is located in soil at a

depth of 2.0 m. Point C is located at the top of the stone column at a horizontal distance of d/4 from the column centerline.

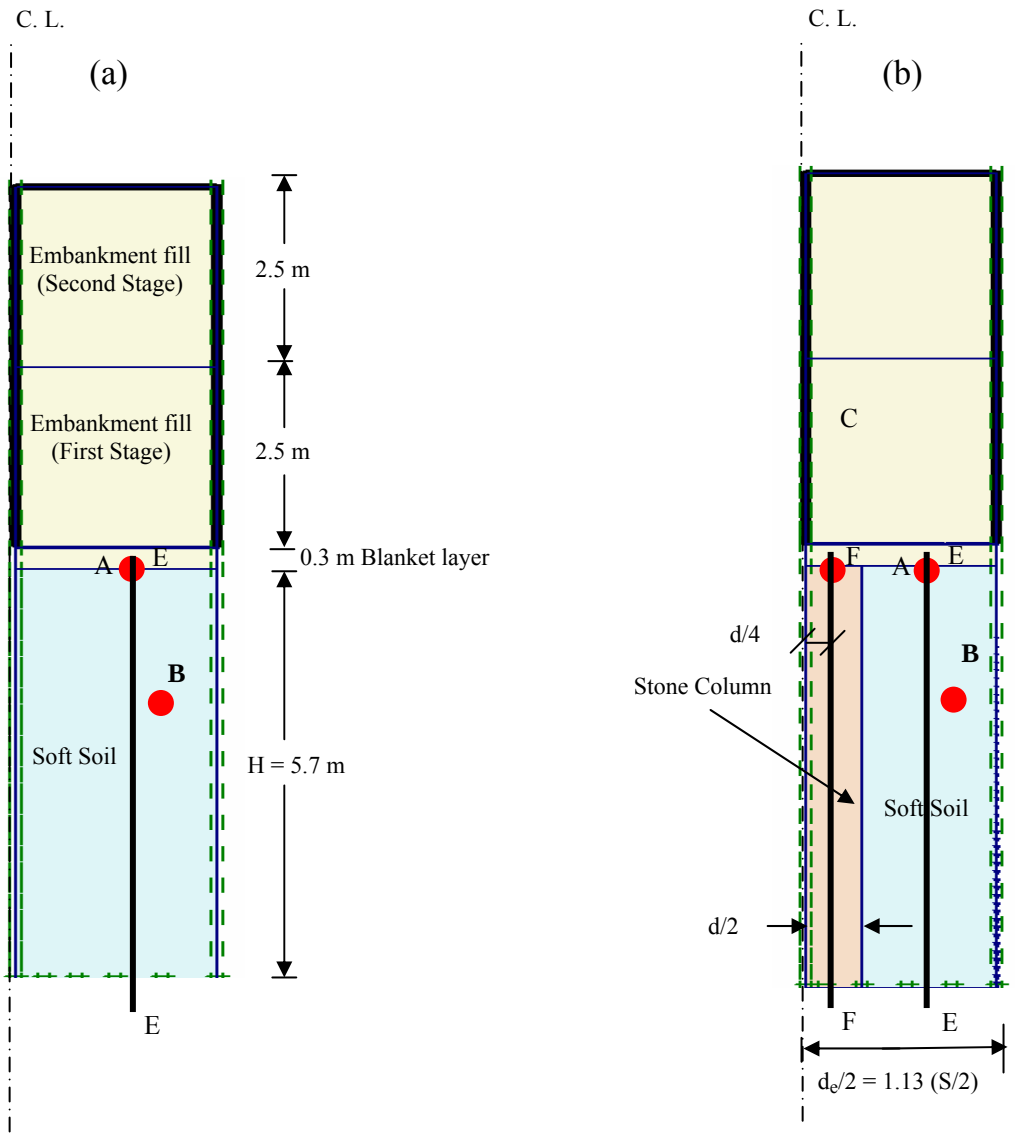

Fig. 6-1 Model parts of the unit cell (a) Non-reinforced Hamburg clay
(b) Stone column reinforced Hamburg clay

6.3.1 Settlement

The settlement, (s) was calculated in the surface of the non-reinforced and the reinforced clay at point A, as shown in Fig. 6-1 (a and b). Fig. 6-2 and Fig. 6-3 show the relationships of the time with the construction of the embankment and with the settlement. The first construction stage shows an increase in the settlement with time which is accompanied by dissipating excess pore water pressure. But the rate of the increase in the settlement gradually decreases with increasing time especially in the last period of the consolidation time. The non-reinforced and the reinforced clay follow the same procedure of the settlement in the second construction stage. But the settlement in the second construction stage is smaller and the consolidation time is faster than in the

first construction stage in both cases, as shown in Fig 6-2, 6-3 and Fig. 6-4. The consolidation in the first stage enhances the soft soil behavior which leads to increase its stiffness and shear strength in the second stage of loading. Therefore, the first construction acts as a preloading for the second construction stage.

Table (6-1), Properties and shear strength parameters used for the soils.

Parameter	**Symbol**	**Stone Soil, (Ambily and Gandhi, 2007)**	**Sand, (Ambily and Gandhi, 2007)**	**Hamburg clay, (Geduhn, 2005)**
Material model	Type	Mohr-Coulomb	Mohr-Coulomb	Soft Soil Creep
Loading	Condition	Drained	Drained	Undrained and Consolidation
Wet soil unit weight	γ_{wet}, (kN/m^3)	19	18	13
Horizontal permeability	k_h, (m/day)	12	1	$3.2x10^{-5}$
Vertical permeability	k_v, (m/day)	6	0.5	$1.6x10^{-5}$
Young's modulus	E, (kN/m^2)	55,000	20,000	-
Poisson's ratio	υ (-)	0.3	0.3	-
Modified compression index	λ* (-)	-	-	0.167
Modified swelling index	κ* (-)	-	-	0.056
Modified secondary compression index	μ*	-	-	0.005
Cohesion	c `,(kN/m^2)	0	0	0
Friction angle	φ ` °	43	30	20
Dilatancy angle	ψ°	10	4	0

Table (6-2) Construction sequence of the embankment fill

Stage	**Phase**	**Fill Height, (m)**	**Time Consumed (day)**
First	1- Construction	0-2.5	21.0
	2- Consolidation	2.5	Time is calculated until the excess pore water pressure is dissipated (1 kPa)
Second	3- Construction	2.5-5.0	21.0
	4- Consolidation	5.0	Time is calculated until the excess pore water pressure is dissipated (1 kPa)

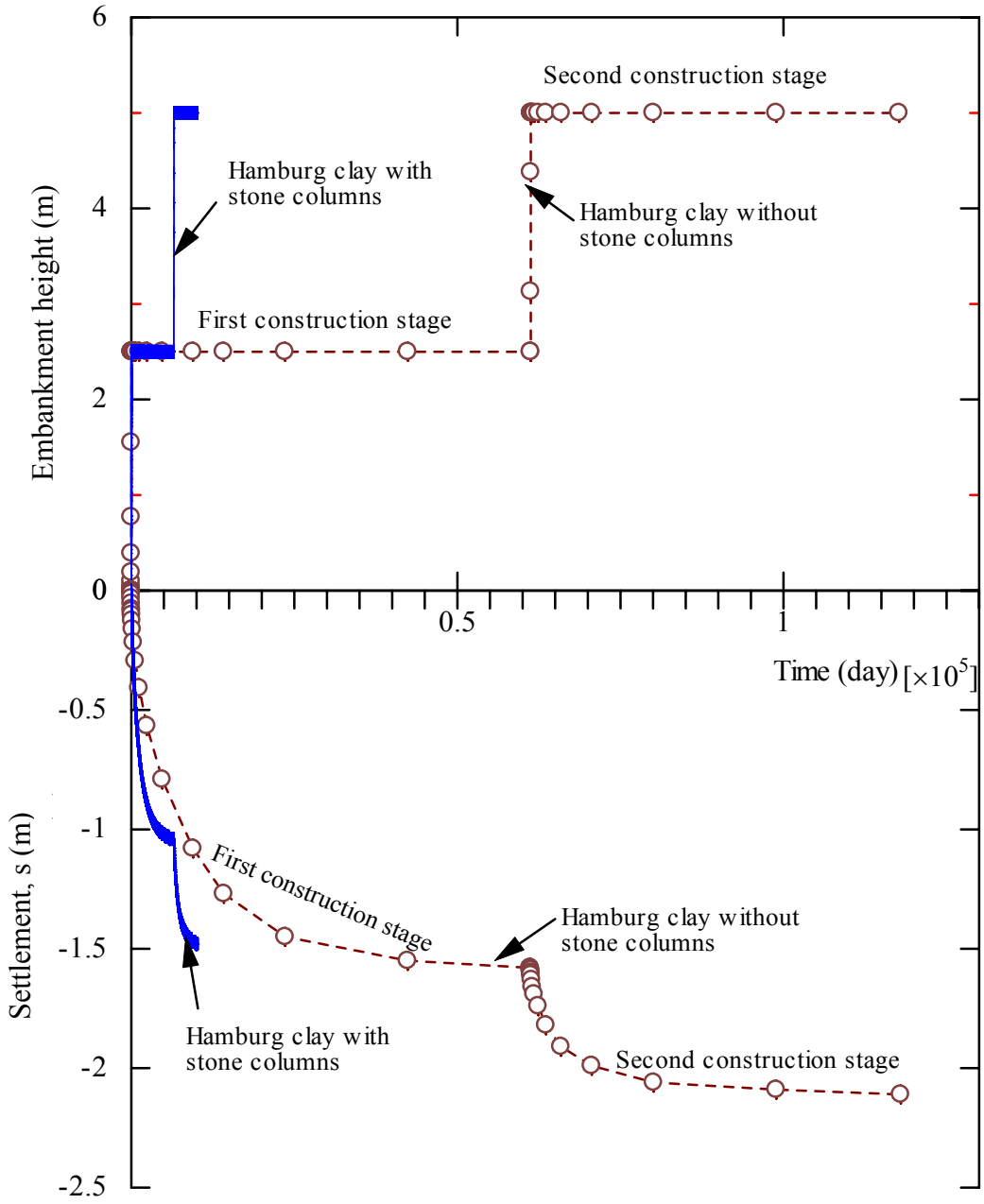

Fig. 6-2 Settlement of the non-reinforced and the reinforced soft soil with stone column along the time of the construction at point A

The non-reinforced soft clay needs a very long time to wait until the consolidation is finished which reaches 61,244 days. The very low permeability and the very high compressibility of this soil lead to such long consolidation time and high settlement. So, the construction on this type of soil is impossible without using any effective soil improvement methods. When the stone column is used, the settlement decreases and the consolidation time is accelerated, as shown in Fig. 6-4. The settlement after the first stage is reduced from 1.58 m to 1.03 m. Hence, the construction in the first stage is accelerated quickly and the settlement is reduced to 0.65 of the non-reinforced clay settlement when using stone columns. The full consolidation of the non-reinforced clay consumes very long time which reaches 117,733 days. Using stone columns in clay reduces the consolidation time to 10,159 days and the settlement also is reduced from 2.11 m to 1.48 m. In spite of the reduction in the consolidation time and the settlement

of the reinforced soft soil, this soft soil type needs more enhancements to keep the construction time and the settlement in applicable procedures and acceptable values, respectively.

The settlement distribution at the surface of the non-reinforced and the reinforced clay at the consolidation end of both construction stages are also shown in Fig. 6-5. The existence of stone columns in soft clay increases the bearing capacity of the soft clay by reducing settlement during the various construction phases. The settlement in the stone column and in the surrounding soft is approximately the same (equal vertical strain theory) as illustrated in Fig. 6-5 and discussed in chapter 5.

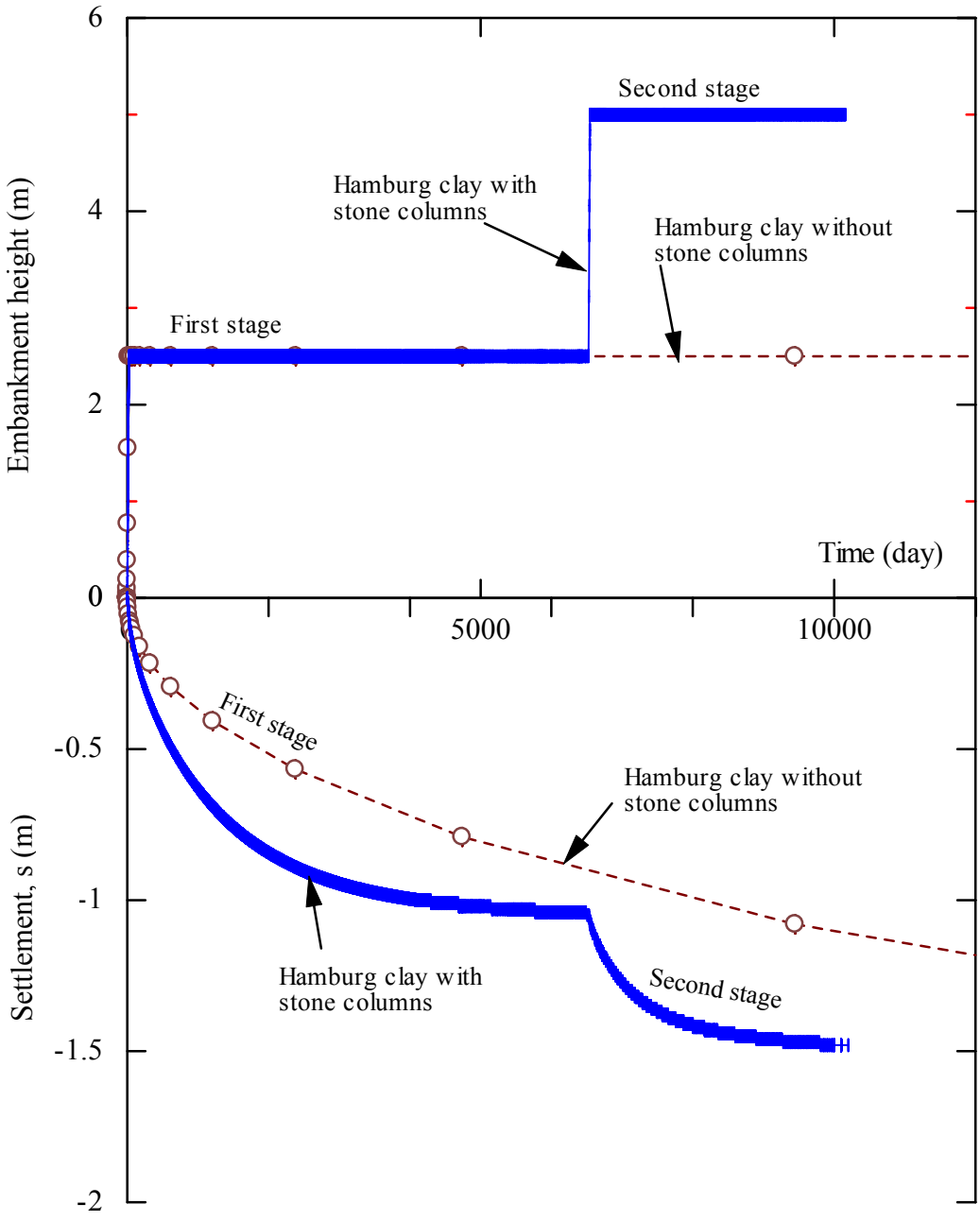

Fig. 6.3 Settlement of the non-reinforced and the reinforced soft soil with stone column along the time of the construction at point A

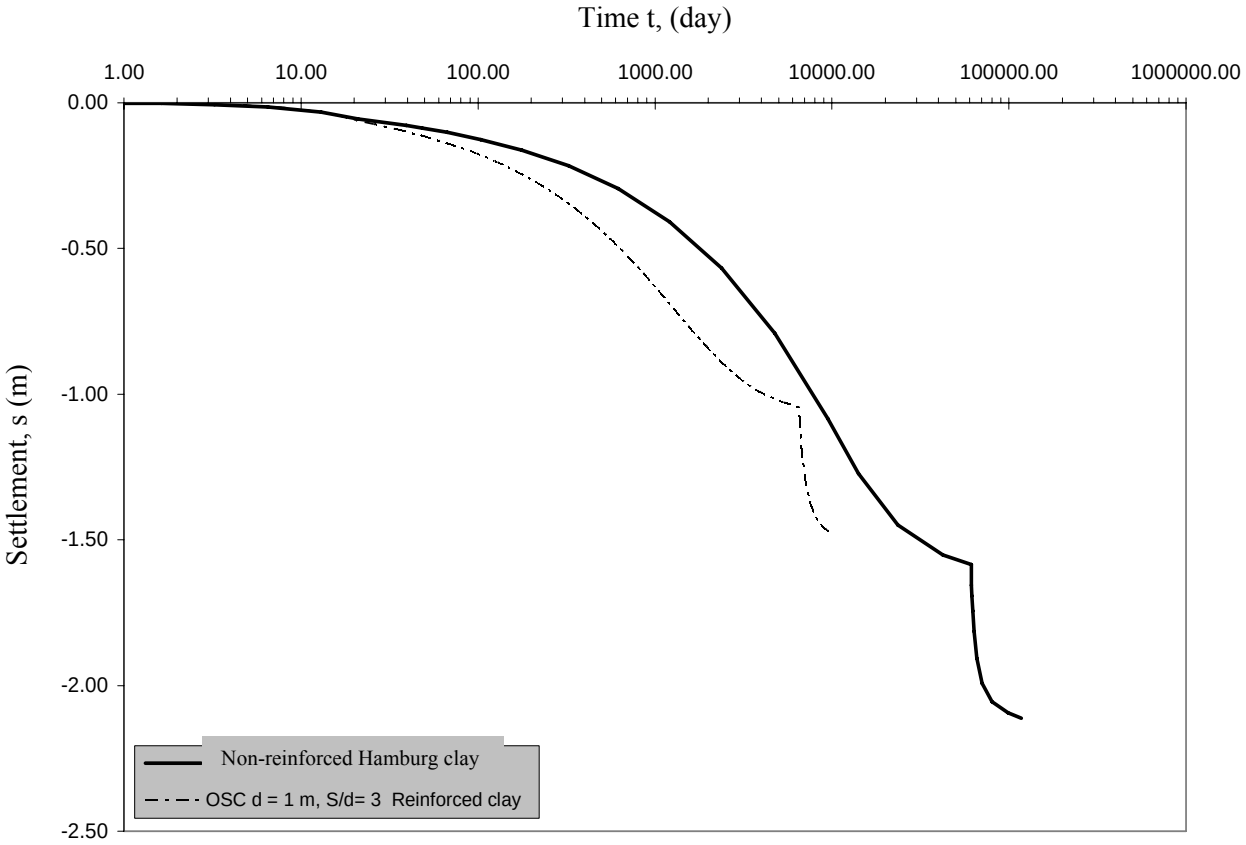

Fig. 6-4 Time-settlement relationship for the non-reinforced and the reinforced Hamburg clay with ordinary stone columns (OSC) at point A

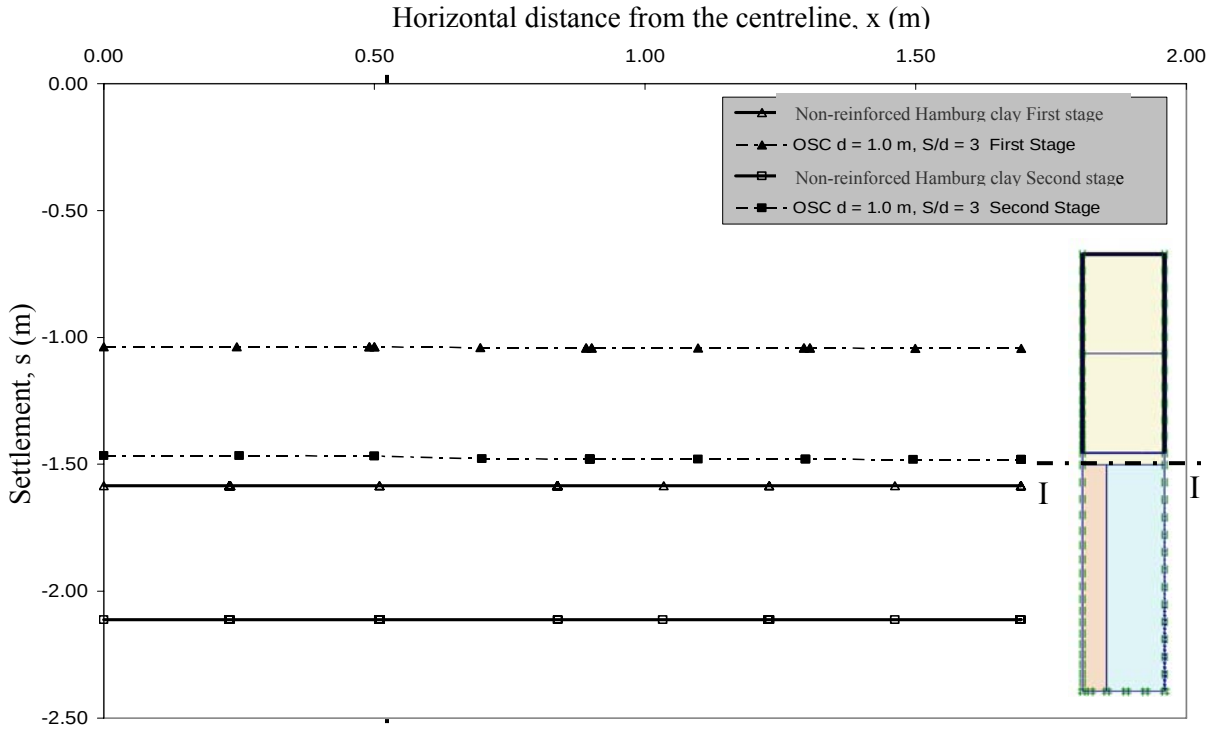

Fig. 6-5 Settlement distribution at the surface of the non-reinforced and the reinforced Hamburg clay with ordinary stone columns (OSC)

6.3.2 Lateral bulging of the stone column

Once the stone column is yielded, its bulging appears due to dilatancy. The lateral bulging of the stone column, (u_h) was calculated after each consolidation phase, as shown in Fig. 6-6. The lateral bulging of the stone column in the two construction stages has the same behavior while the lateral bulging in the second stage is the greater. The column is displaced laterally into the soft soil with loading especially in the upper part. The lateral displacement of the column starts with zero at the surface and gradually increases with depth until it reaches a maximum value at a depth of 0.9 times of the column diameter (d) in the two construction stages. Afterwards, the lateral displacement decreases gradually with depth until it reaches a minimum value at a depth of four times the column diameter (4d). Below this minimum point the lateral bulging increase until it reaches a highest value in the lower third of the column at a depth of 4.5 times the column diameter (d). Then, the lateral bulging decreases gradually to reach zero at the column base. The lateral bulging along the stone column increases with increasing load causing more load transfer to the lower depths during the consolidation.

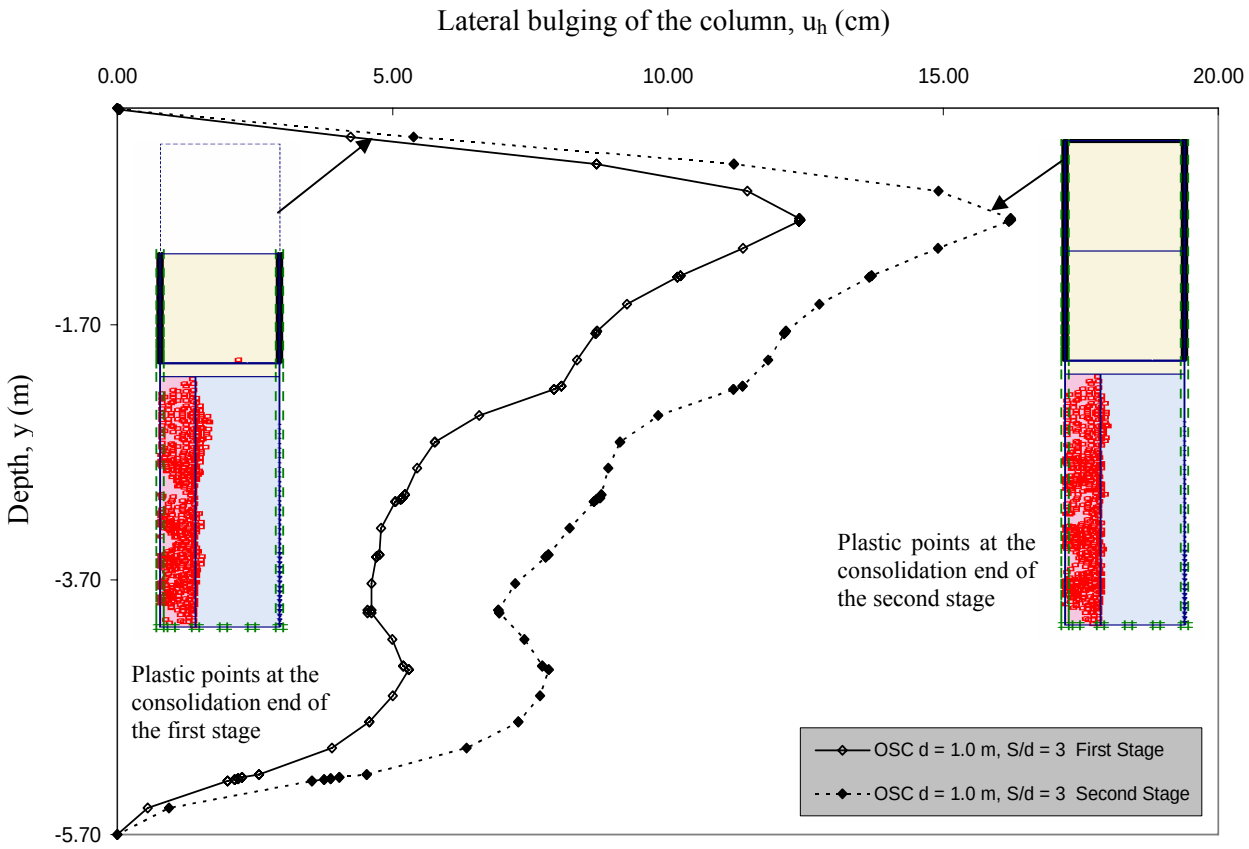

Fig. 6-6 Lateral bulging and yielding distribution of the stone column at the consolidation end of the two construction stages

6.3.3 Excess pore water pressure

The excess pore water pressure (Δu) in the non-reinforced and the reinforced soft soil was calculated at point B which is located at a depth of 2.0 m, as shown in Fig. 6-1. As soon as the fill load is applied on the saturated soft soil, the excess pore water pressure builds up. The excess pore water pressure increases with time until it reaches maximum values at the end of construction of each stage. After that, the excess pore water pressure decrease gradually during the consolidation directing to the steady state case, as shown in Fig. 6-7. The first and the second stage of constructions imply the same behavior of the excess pore water pressure through the consolidation time. But the excess pore water pressure after the second stage of construction is dissipated more rapidly than that after the first stage of construction as shown in Fig. 6-8.

The behavior of the excess pore water pressure in the soft soil without stone column and the reinforced soft soil is the same. The excess pore water pressure in the reinforced soft soil has lower values and dissipates more rapidly than that in the non-reinforced soft soil. Hence, using stone columns in clay soil improves the drainage and accelerates the dissipation of the excess pore water pressure because the stone columns shorten the drainage paths by adding horizontal drainage paths to the vertical paths as illustrated in Fig. 6-9.

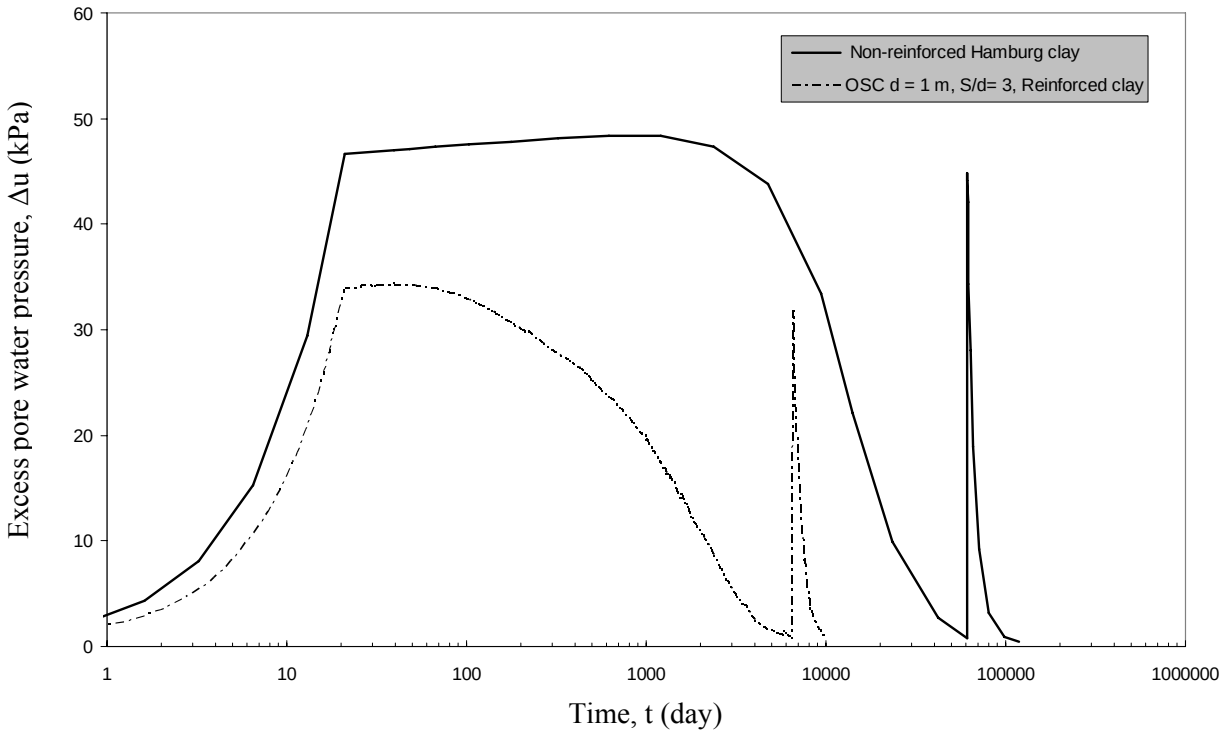

Fig. 6-7 Excess pore water pressure-time relationship at point B for the non-reinforced and the reinforced Hamburg clay with ordinary stone columns (OSC)

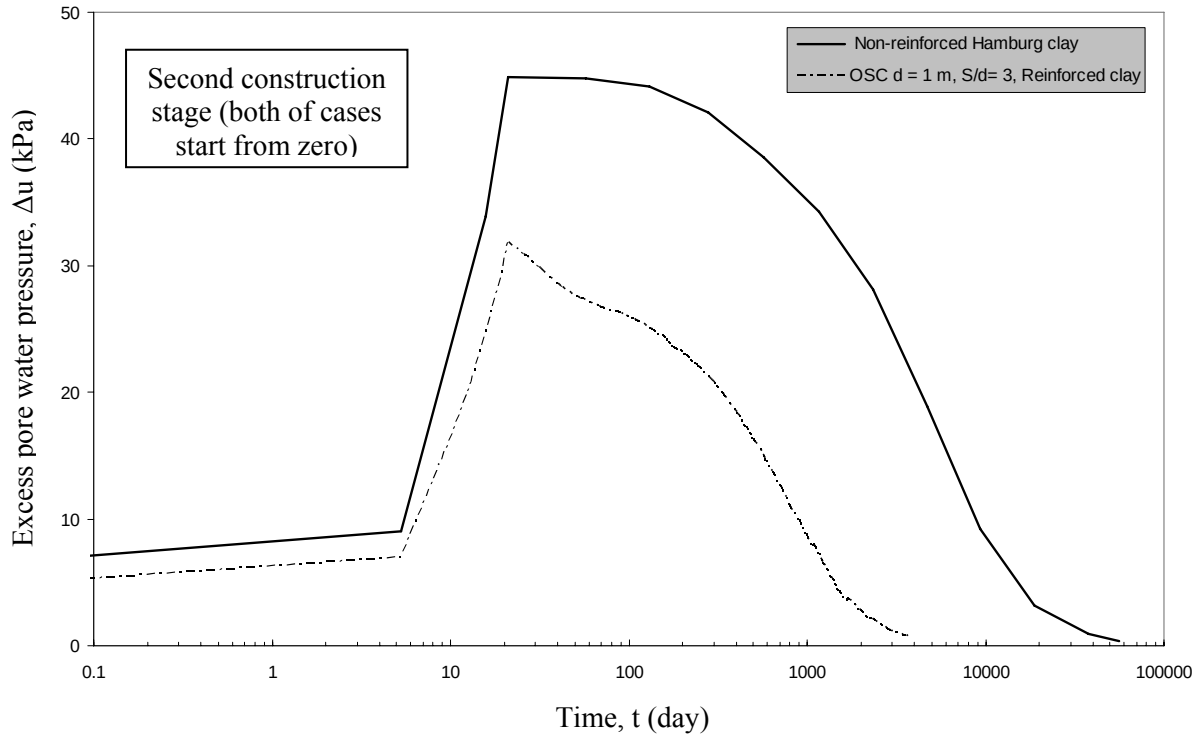

Fig. 6-8 Development of excess pore water pressure during the second loading stage at point B for the non-reinforced and the reinforced soft soil with ordinary stone columns

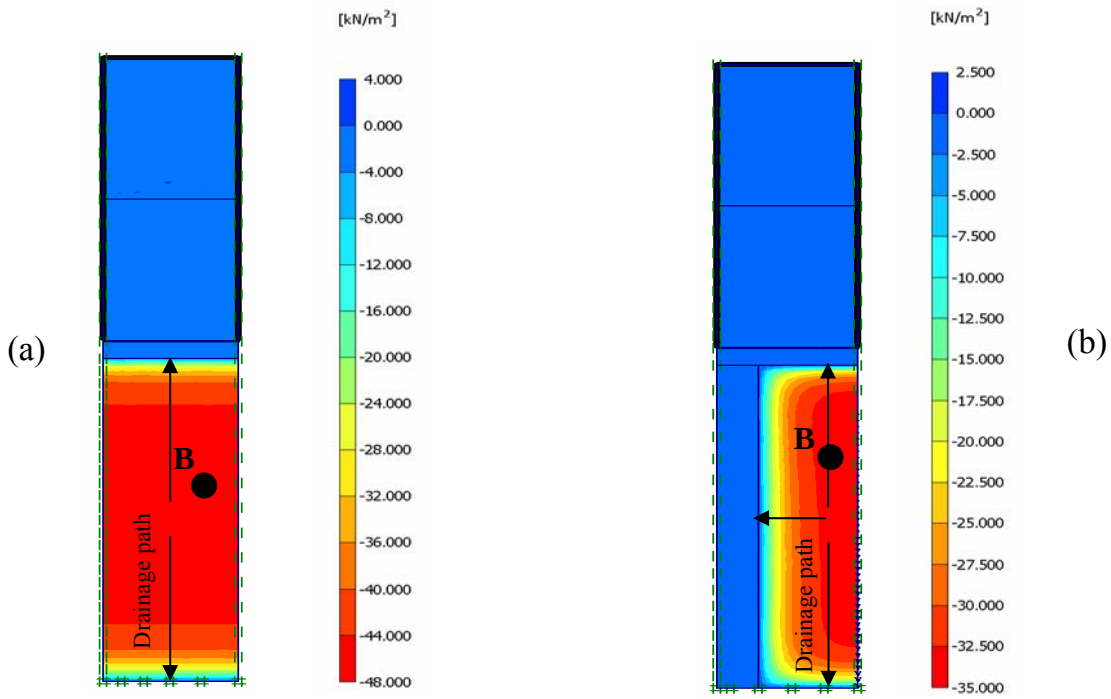

Fig. 6-9 Distribution of the pore water pressure at the end of the second construction stage at (a) Non-reinforced soft soil and (b) Reinforced soft soil with stone columns

6.3.4 Stress in soil

The stress in the non-reinforced soft soil, the reinforced soft soil and the stone column has been studied in the current analyses. The effective vertical stress (σ'_v) was calculated at the surface in the non-reinforced and the reinforced soft soil at point A,

and in the column at point C, as shown in Fig. 6-1 (a and b). The relationship of the effective vertical stress with settlement and with time is shown in Fig. 6-10 and Fig. 6-11, respectively. The effective vertical stress in the non-reinforced and the reinforced soft soil and in the stone column increases with a high rate with increasing settlement and time through increasing embankment fill in both stages of construction. During the consolidation process, directly after the first and the second construction stages have been finished, the vertical effective stress in the non-reinforced and the reinforced soft soil increases with a very small rate. But the rate of the vertical stress increase becomes somewhat greater during the consolidation of the second construction stage especially in the reinforced soft soil. Using stone column reduces the effective vertical stress in the reinforced soil which is smaller than that in the non-reinforced soft soil and generates high stress in the stone column, as shown in Fig. 6-10 and Fig. 6-11. Hence, the effective stress in the reinforced soft soil is reduced due to the stress transfer from the soft soil and concentrate in the stone column.

During the consolidation process of the first construction stage, as settlement and time increase, the vertical effective stress in the stone column increases with a small rate until it reaches a maximum value. Beyond this value the vertical effective stress decreases with a small rate until the second stage of construction starts. While in the consolidation process in the second stage, the vertical stress decreases gradually with increasing time and settlement.

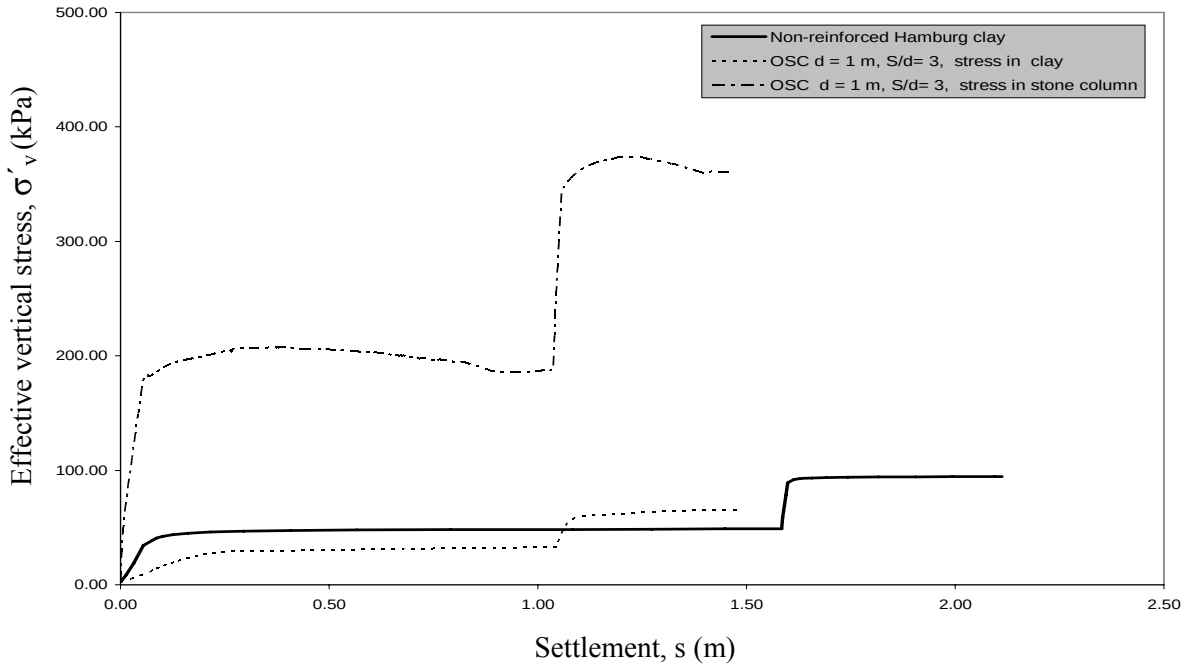

Fig. 6-10 Effective vertical stress-settlement relationship for the non-reinforced and the reinforced soft soil at point A and for the stone column at point C

The decrease in the vertical stress in the stone column after the middle of the first stage consolidation and during the second stage consolidation is because the column yields, as shown in Fig. 6-6. Once yielded, the stiffness of the column decreases, and also its radial deformability increases due to dilatancy. Otherwise, yielding of the column reduces the transfer of vertical load from the soil. The soft soil didn't imply any yielding except the zone which is located very close to the column.

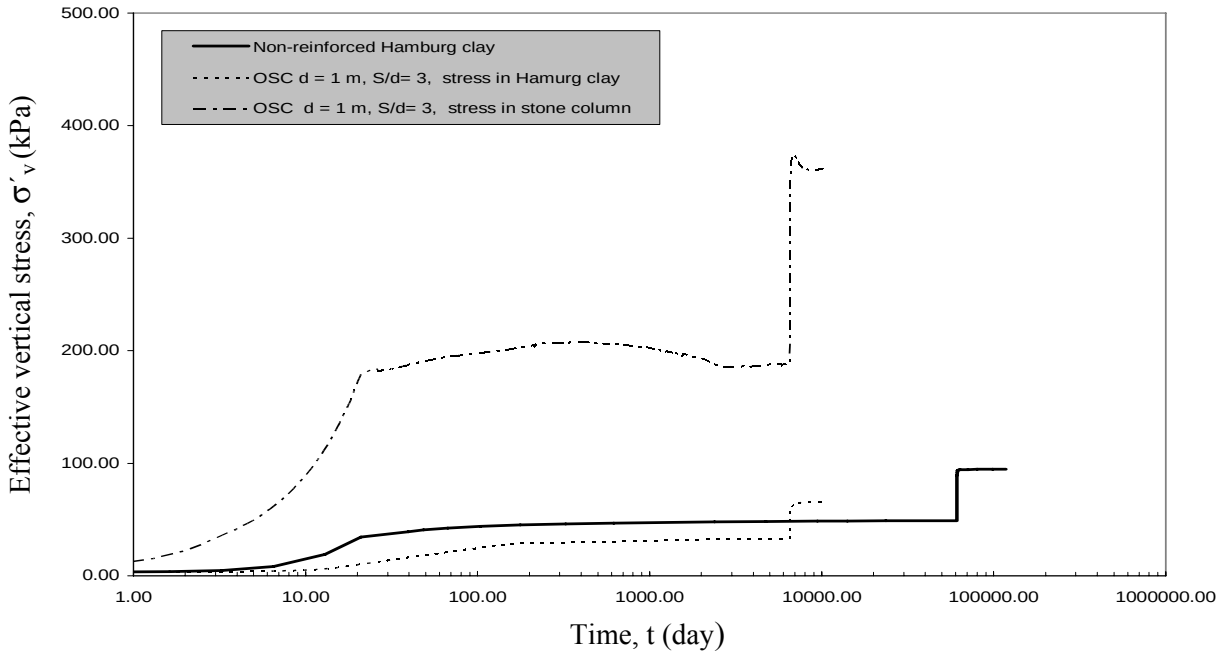

Fig. 6-11 Effective vertical stress-time relationship for the non-reinforced and the reinforced soft soil at point A and for the stone column at point C

Stress concentration Factor, (SCF)

The stress concentration factor (SCF) is defined as the ratio of the vertical effective stress in the stone column to the vertical effective stress in the surrounding soft soil, ($SCF = \sigma'_{v(\text{stone column})} / \sigma'_{v(\text{clay})}$). The average stress concentration factor was calculated at sections A-A, B-B and C-C which are located at the surface, at a depth of 0.75 m and at a depth of 1.25 m, respectively as shown in Fig. 6-12. The development of the stress concentration factor at sections A-A, B-B and C-C is similar. The stress concentration factor increases with increasing load during the construction and also during the consolidation of the first stage until it reaches a maximum value. Beyond the maximum stress ratio, it decreases with increasing construction time until it reaches minimum values at the consolidation end of the first stage. Afterwards, the stress concentration factor increases again with increasing fill load in the second construction stage. After that the stress concentration factor decreases gradually with consolidation time. The stress concentration factor at section C-C is greater than that at section A-A while the stress concentration factor at section B-B is greater than that at both sections A-A and C-C, as shown in Fig. 6-12.

The stress concentration factor of section A-A increases with increasing load until it reaches a maximum of 18.40 after 14 days from the start of the construction. After that the stress concentration factor decreases gradually with consolidation time and reaches 5.72 at the consolidation end of the first stage. The stress concentration factor increases again with developing load in the second stage which reaches 6.37 at the end of construction. Then the stress concentration factor decreases gradually with the consolidation time until it reaches 5.51 at the end, as illustrated in Fig. 6-12.

The stress concentration factor of section B-B increases with increasing load and time until it reaches a maximum of 31.60 after 78 days from the start of the first construction stage. After that the stress concentration factor decreases gradually with consolidation

time and reaches 5.93 at the consolidation end of the first stage. The stress concentration factor increases again with developing load in the second stage which reaches 10.0 at the end of construction. After that the stress concentration factor decreases gradually with the consolidation time until it reaches 5.82 at the end, as shown in Fig. 6-12.

The stress concentration factor of section C-C increases with increasing load and time until it reaches a maximum stress concentration factor around 23.0 which stays for a long time during the consolidation of the first stage. After a time of 480 days the stress concentration factor decreases gradually with consolidation time and reaches 6.23 at the consolidation end of the first stage. The decrease in the stress concentration factor is due to the column yielding and the increase in the stiffness and strength of the surrounding soft soil during the consolidation. The column yielding firstly starts at the top of the column and then it continues in the downward direction, as shown in Fig. 6-12. Afterwards, the stress concentration factor increases again with developing load in the second stage which reaches 10.02 at the end of construction. After that the stress concentration factor decreases gradually with the consolidation time until it reaches 6.03 at the end.

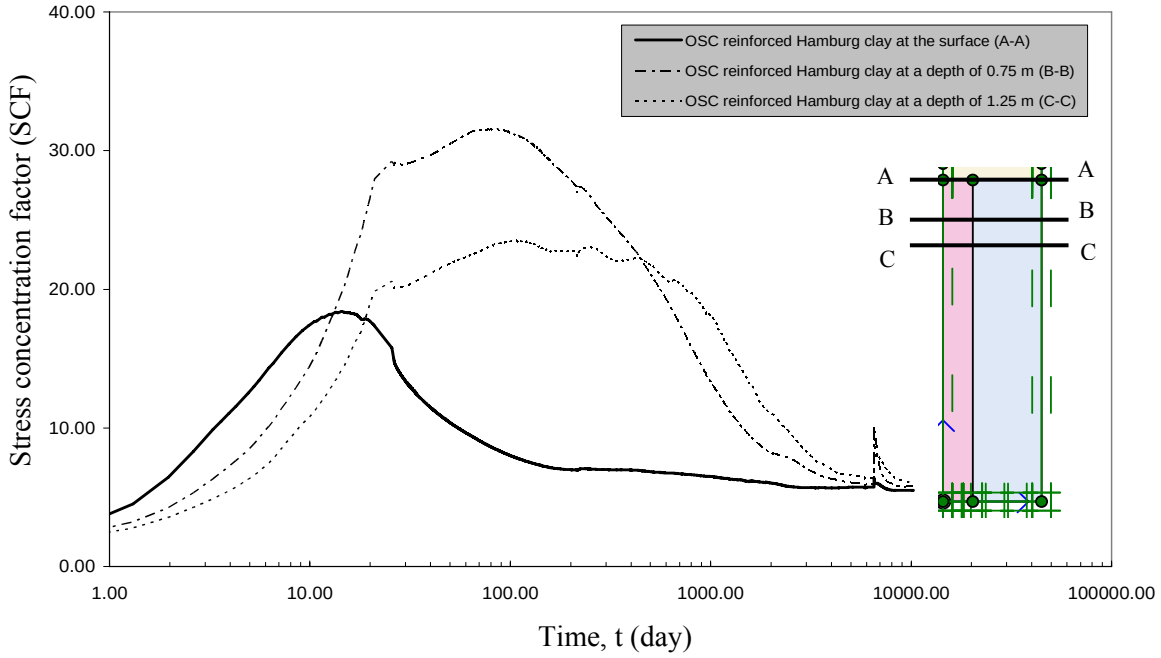

Fig. 6-12 Average stress concentration factor-time relationship for the reinforced soft soil with stone columns at various depths

The vertical effective stress was calculated in the non-reinforced and the reinforced soft soil at section E-E, and in the stone column at section F-F, as shown in Fig. 6-1, to study the stress concentration through the reinforced clay layer. The vertical effective stress was calculated after the end of consolidation in the first and the second stages of construction. The effective vertical stress in the non-reinforced and the reinforced clay increases gradually with downward direction due to the effect of overburden pressure. The effective vertical stress in the reinforced soft soil is smaller than that in the non-reinforced soft soil across the clay layer because of the stress concentration in the column, as shown in Fig. 6-13.

The effective vertical stress in the stone column after the consolidation of the first stage of the construction starts with a value at the surface generating stress concentration factor of 5.72. Then the effective vertical stress increases with downward direction until it reaches a maximum value at 1.1 m depth of the clay layer. The stress concentration factor at this point is 6.30. Beyond this point, the effective vertical stress decreases with depth until it reaches a minimum value at a depth of 2.2 m generating stress concentration factor of 3.4. Depths lower than the minimum stress point show a gradual increase in the effective vertical stress and stress concentration which reaches 6.0 at the column base, as shown in Fig. 6-13.

The effective vertical stress in the stone column after the consolidation end starts with a value at the surface generating stress concentration factor of 5.51.Then the effective vertical stress increases with downward direction until it reaches a maximum value at 2.22 m depth of clay layer. The stress concentration factor at this point is 6.1. Beyond this point, the effective vertical stress decreases with depth until it reaches a minimum value at a depth of 3.0 m generating stress concentration factor of 4.27. Depths lower than the minimum stress point show gradual increase in the effective vertical stress and stress concentration which reaches 5.6 at the column base, as shown in Fig. 6-13.

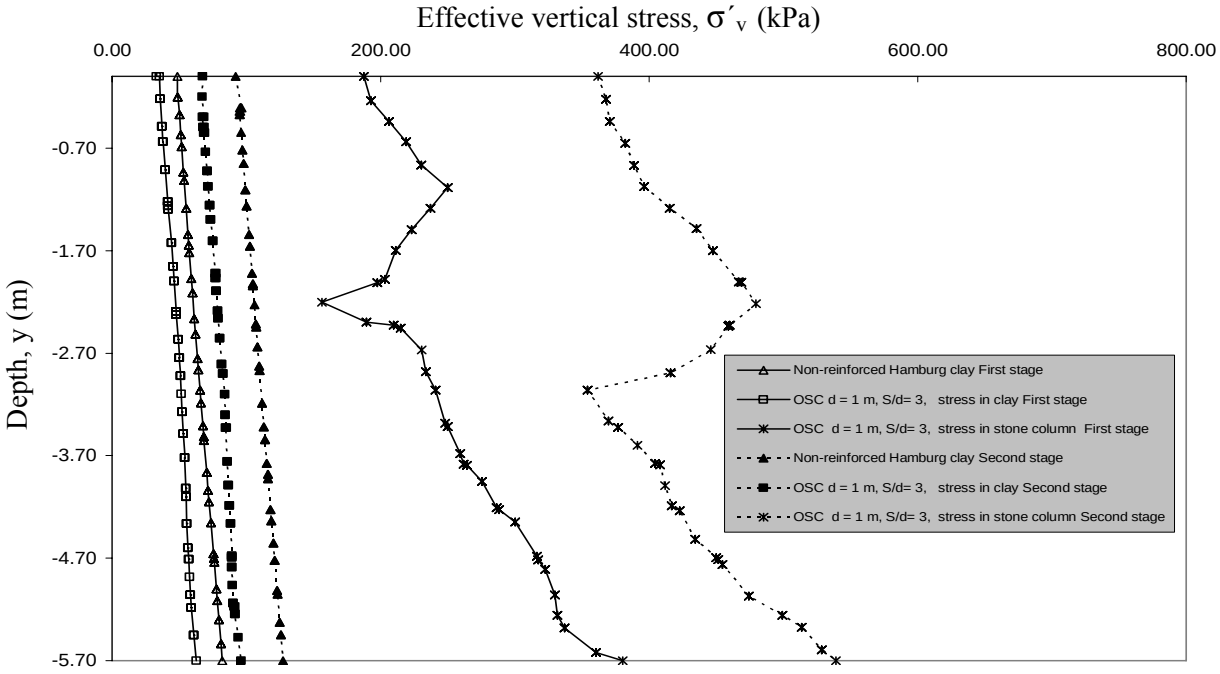

Fig. 6-13 Effective vertical stress distribution for the non-reinforced and the reinforced soft soil at section E-E and for the stone column at section F-F

The steady state stress concentration factors along the stone column are in the range of (3-9) which agree with the field measurements. In general, the first construction stage implies stress concentration factors greater than them in the second construction stage. The reason of that is the consolidation in the first construction stage leads to an increase in the shear strength and the stiffness of the soft soil in the second stage and also because the column became in the plastic stage.

The total and the effective vertical stress, and the excess pore water pressure were calculated in the non-reinforced and the reinforced soft soil at point (B) which is located at a depth of 2.0 m, as shown in Fig. 6-9. The total vertical stress (σ_v) and the excess pore water pressure (Δu) in the non-reinforced and the reinforced soft soil increase with increasing load until they reach maximum values at the end of both constructions stages. During the consolidation process after each of construction stage, the effective vertical stress (σ'_v) increases with time while the excess pore water pressure decreases in the non-reinforced and the reinforced soft soil, as shown in Fig. 6-14 and Fig. 6-15, respectively. At the end of the consolidation the excess pore water pressure is dissipated and the vertical effective stress reaches maximum values.

The total vertical stress in the non-reinforced soft soil is constant during the consolidation process while the total vertical stress in the reinforced soft soil is variable with consolidation time, as shown in Fig. 6-14 and Fig. 6-15, respectively. Once each construction stage finishes, the total stress in the reinforced clay reaches a maximum value. Beyond the maximum total stress value, the total stress decreases gradually with increasing consolidation time, as illustrated in Fig. 6-15. This phenomenon means that at the construction stage, the load transfer to the columns is less important, and it increases as consolidation proceeds. Inversely, the clayey soil is subjected to a higher total stress at the beginning, implying some degree of "pre-loading" with respect to the final soil total stress. This produces a faster consolidation compared with the case of non-reinforced clay which has a constant load. Hence, the stress transfer from clay and concentration in stone column participate with a significant percentage in the acceleration of the consolidation process and construction time.

The participation percentage of the stress concentration on the acceleration of consolidation can be computed by equation (5-1). The stress concentration on the stone column participates in the acceleration of the consolidation process by a percentage of 20.6 % in the first stage and a percentage of 15.06 % in the second stage.

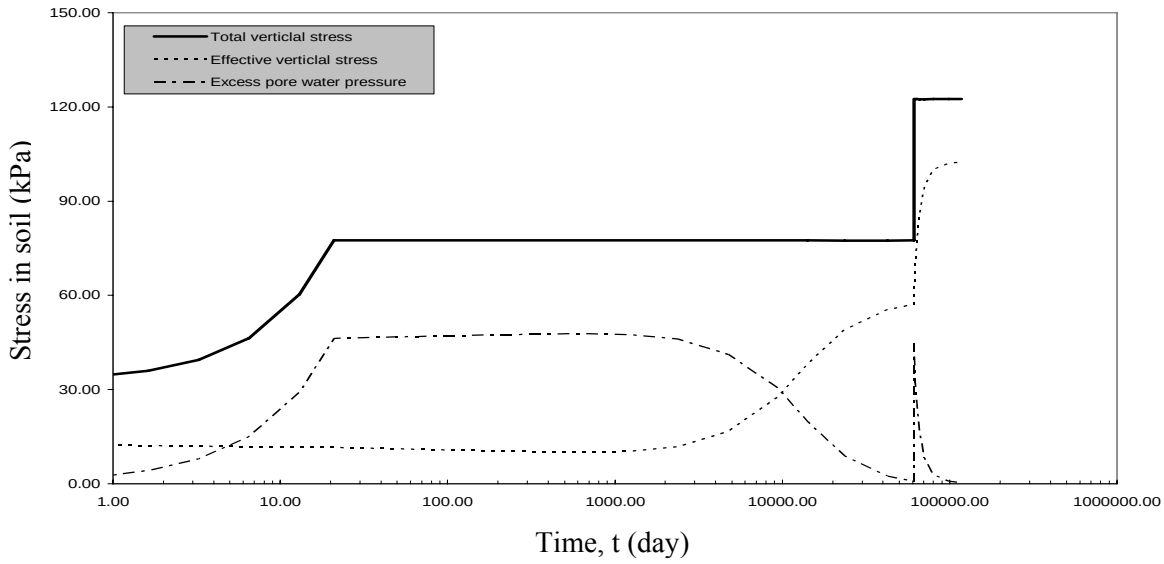

Fig. 6-14 Relationship of the total and effective vertical stress and the excess pore water pressure with time in the non-reinforced soft soil at point B (2.0 m depth)

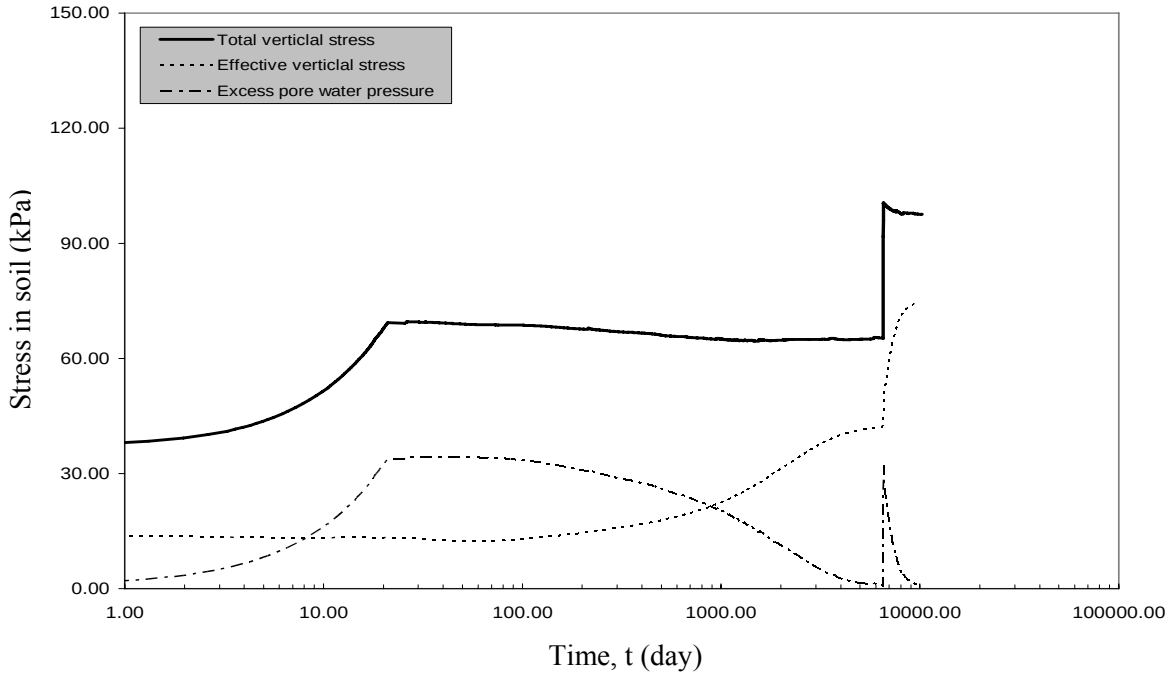

Fig. 6-15 Relationship of the total and effective vertical stress and the excess pore water pressure with time in the reinforced soft soil at point B (2.0 m depth)

6.4 Discussion

The Hamburg clay has a smaller bearing capacity when compared with the Bremerhaven clay. The consolidation settlement is also larger and the consolidation time is longer in Hamburg clay. The reason of that is the Hamburg clay has smaller shear strength, lower permeability and higher compressibility than the Bremerhaven clay.

Therefore, using stone columns in the Bremerhaven clay is more effective than in the Hamburg clay. The stone columns-Bremerhaven clay foundation system has a higher bearing capacity, smaller settlement and column bulging, faster consolidation time and lower excess pore water pressure than the stone columns-Hamburg clay foundation system. As stated before, the stress transfer and stress concentration in column participate in the acceleration of clay consolidation. The participation of the column stress concentration in the acceleration of the Bremerhaven clay consolidation is higher than that in the Hamburg clay.

7 Behavior of the Reinforced Soft Clay with Ordinary Stone Columns under Embankment Fill

7. 1 Introduction

The reinforced Bremerhaven clay and Hamburg clay with stone columns were studied in chapters 5 and 6, respectively. In the current chapter the Bremerhaven clay and the Hamburg clay are reinforced with the ordinary stone columns with different spacings and diameters. The reinforced soft soils have been loaded as foundations of a highway embankment. The behavior of the reinforced soft soil has been investigated through the consolidation process. In the following sections, the modeling of the stone columns and the surrounding soft soil, and the discussion of the results of the parametric study are presented. The discussion contains the influence of varying spacing distance between the columns and diameter of the stone column on the reinforced soft soil settlement, consolidation time, column bulging, excess pore water pressure and stress in the soil.

7.2 Numerical modeling and selection of parameters

The Bremerhaven clay and the Hamburg clay layers which have a thickness of 6.0 m are reinforced by stone columns. The same parts and conditions of the unit cell model, which were used in chapter 5 and chapter 6, are used in the current analyses. The stone columns are installed in a square orientation which was discussed in chapter 2. A blanket layer of compacted sand which has 30 cm thickness is also used as a drainage layer. The current analyses consider that the entire area of the reinforced Bremerhaven clay and Hamburg clay has been loaded with the sand fill as embankment loads. Fig. 7-1 shows the schematic of the models employed for these analyses. Half of the model has been used. The vertical and the horizontal displacements in the bottom boundaries were restrained while only the horizontal displacement in the lateral boundaries was restrained. The automatic finite element mesh has been used with 15 nodes triangular elements. The Bremerhaven clay and the Hamburg clay have been modeled by the Soft Soil Creep model under undrained conditions while stone material and sand fill have been modeled using Mohr Coulomb model under drained conditions. The same parameters of the soft soils, the stone and the sand which were used in chapter 5 and chapter 6 have been used in the current analyses. The parameters of the soils are illustrated in Table 7-1.

The same construction sequence which was used in chapter 5 and chapter 6 has been used in the current chapter. The embankment fill has been constructed to a height of 5.0 m in two equal layers. Every construction stage has a 2.5 m- layer and takes 21 days. The consolidation analyses are performed during and after each construction stage. A closed consolidation boundary is applied to both sides of the model preventing lateral drainage. The construction sequence is showed in Table 7-2 and Fig. 7-2

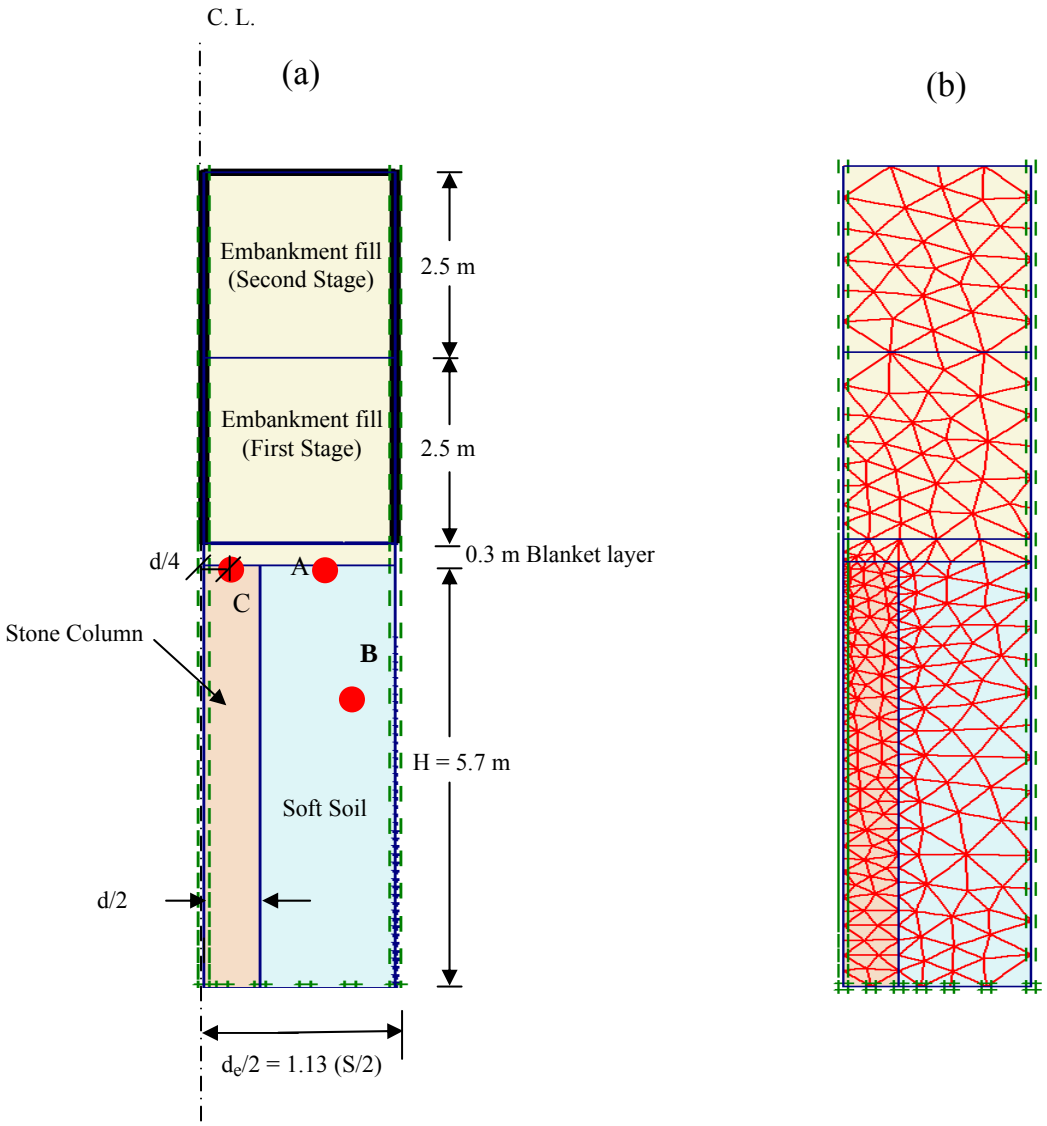

Fig. 7-1 Unit cell of the stone column reinforced soft clay (a) Model parts
(b) Finite element mesh

7.3 Discussion of the results

This part of the current research contains that the reinforced soft soils with stone columns have been loaded with the embankment fill in two stages of construction to study the effect of spacing between the columns and column diameter on the behavior of the reinforced soft soils during and after the consolidation.

Table 7-3 presents all cases which have been analyzed here. This table contains two groups which will be discussed in the following paragraphs. Group A contains stone columns with a diameter of 1.0 m and various spacing ratios which are S/d = 2, 3 and 4. While Group B includes stone columns with a spacing ratio S/d = 2 and various diameters which are d = 0.6 m, 1.0 m and 1.4 m. Settlement, column bulging, excess pore water pressure and stress in the soil were calculated for each group.

Table 7-1 Properties and shear strength parameters used for the soils

Parameter	Symbol	Stone, (Ambily and Gandhi, 2007)	Sand, (Ambily and Gandhi, 2007)	Bremer-haven clay, (Geduhn, 2005)	Hamburg clay, (Geduhn, 2005)
Material model	Type	Mohr-Coulomb	Mohr-Coulomb	Soft Soil Creep	Soft Soil Creep
Loading	Condition	Drained	Drained	Undrained	Undrained
Wet soil unit weight	γ_{wet}, (kN/m^3)	19	18	15	13
Horizontal permeability	k_h, (m/day)	12	1	$2x10^{-4}$	$3.2x10^{-5}$
Vertical permeability	k_v, (m/day)	6	0.5	$1x10^{-4}$	$1.6x10^{-5}$
Young's modulus	E, (kN/m^2)	55,000	20,000	-	-
Poisson's ratio	υ (-)	0.3	0.3	-	-
Modified compression index	λ^* (-)	-	-	0.203	0.167
Modified swelling index	κ^* (-)	-	-	0.025	0.056
Modified secondary compression index	μ^*	-	-	0.007	0.005
Cohesion	c$'$, (kN/m^2)	0	0	5	0
Friction angle	φ' °	43	30	37.75	20
Dilatancy angle	ψ°	10	4	0	0

Table 7-2 Construction sequences of the embankment fill

Stage	Phase	Fill Height, (m)	Time Consumed (day)
First	1- Construction	0-2.5	21.0
	2- Consolidation	2.5	Time is calculated until the excess pore water pressure is dissipated (1 kPa)
Second	3- Construction	2.5-5.0	21.0
	4- Consolidation	5.0	Time is calculated until the excess pore water pressure is dissipated (1 kPa)

Fig. 7-1 shows the points and sections at which the calculations were carried out. Point A is located at the top of the soil. Point B is located in the soil at a depth of 2.0 m. Point C is located at the top of the stone column at a horizontal distance of d/4 from the column centerline.

Table 7-3 Parametric study

Group No.	Column Diameter, d (m)	Spacing ratio between the Columns, (S/d)	Surrounding Soft Soil Conditions
A	1.0	2 3 4	Undrained and consolidation
B	0.6 1.0 1.4	2	

7.3.1 Group (A): Effect of spacing between the columns (S)

The Bremerhaven clay and the Hamburg clay are reinforced by ordinary stone columns which have a diameter of 1.0 and various spacing distance to diameter ratios S/d of 2, 3 and 4, as shown in Table 7-3.

Settlement

The settlement, (s) was calculated in the surface of the reinforced clays at point A, as shown in Fig. 7-1. Fig. 7-2 shows the relationship between the settlement and the embankment height with the construction time specified to the two stages for various volumes of the reinforced Bremerhaven clay around the stone columns. The development of the settlement with consolidation time is the same for all the spacing distances. The construction time and the consolidation settlement of the reinforced clays increase with increasing spacing distance between the columns, as shown in Fig. 7-3. When the spacing distance between the columns is small in a significant area, the number of columns in that area is large and the drainage paths are short. This leads to more acceleration in the consolidation and construction time. More columns also lead to a decrease of the settlement and an increase of the bearing capacity, as illustrated in Fig. 7-2, Fig. 7-3 and Table 7-4. Hence, the reinforced Bremerhaven clay with stone columns of spacing ratio S/d = 2 has the smallest settlement and the shortest consolidation time in both construction stages of the studied cases.

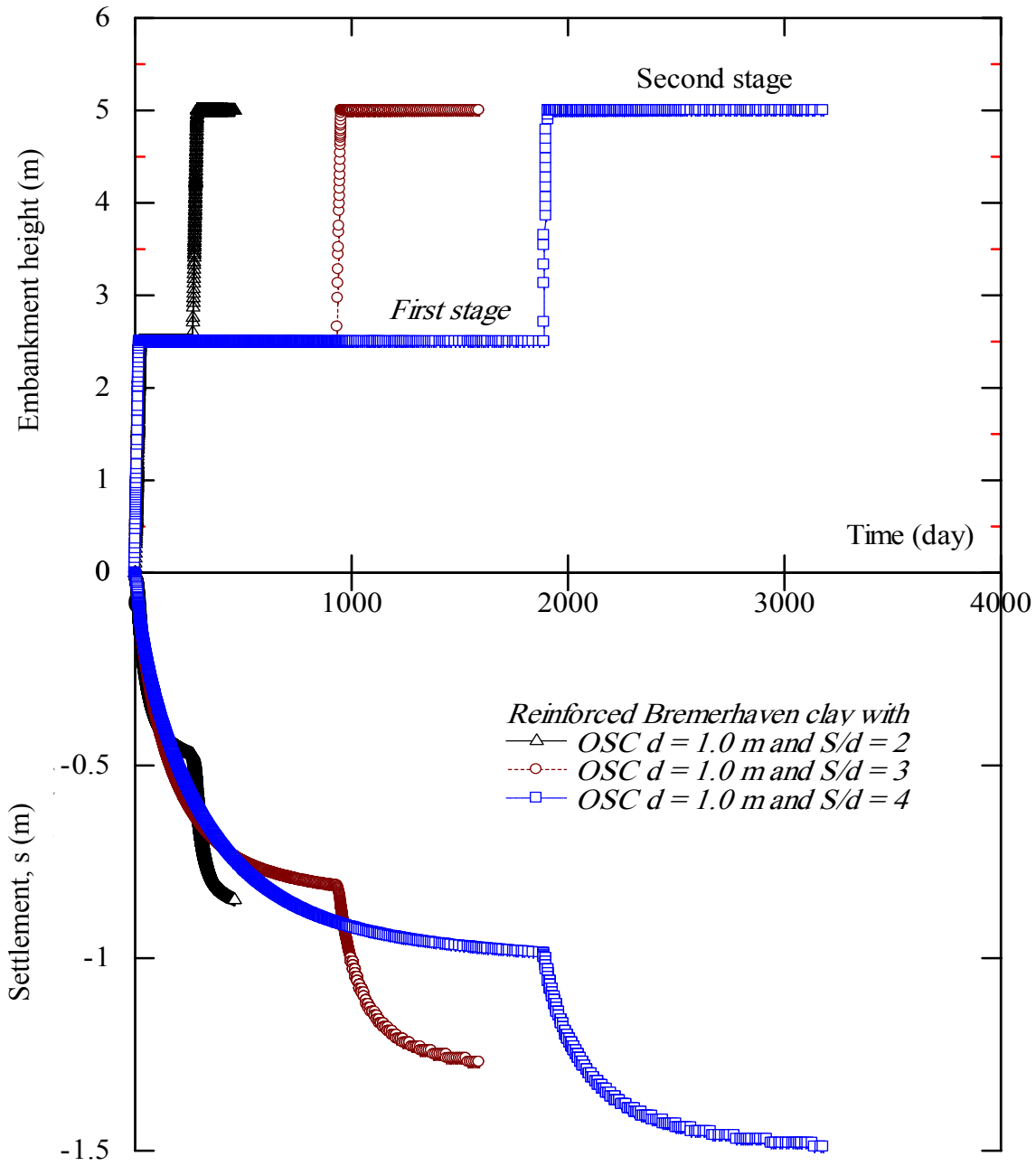

Fig. 7.2 Settlement of the reinforced Bremerhaven soft soil with stone columns along the time of the construction

The settlement distribution at the surface of the reinforced Bremerhaven clay after the consolidation end of both construction stages is also shown in Fig. 7-4. The existence of stone columns in soft clay increases the bearing capacity of the soft clay by reducing settlement during the various construction phases. The settlement in the stone column and in the surrounding soft soil is constant and approximately the same (equal vertical strain theory) as illustrated in Fig. 7-4 and discussed in chapter 5.

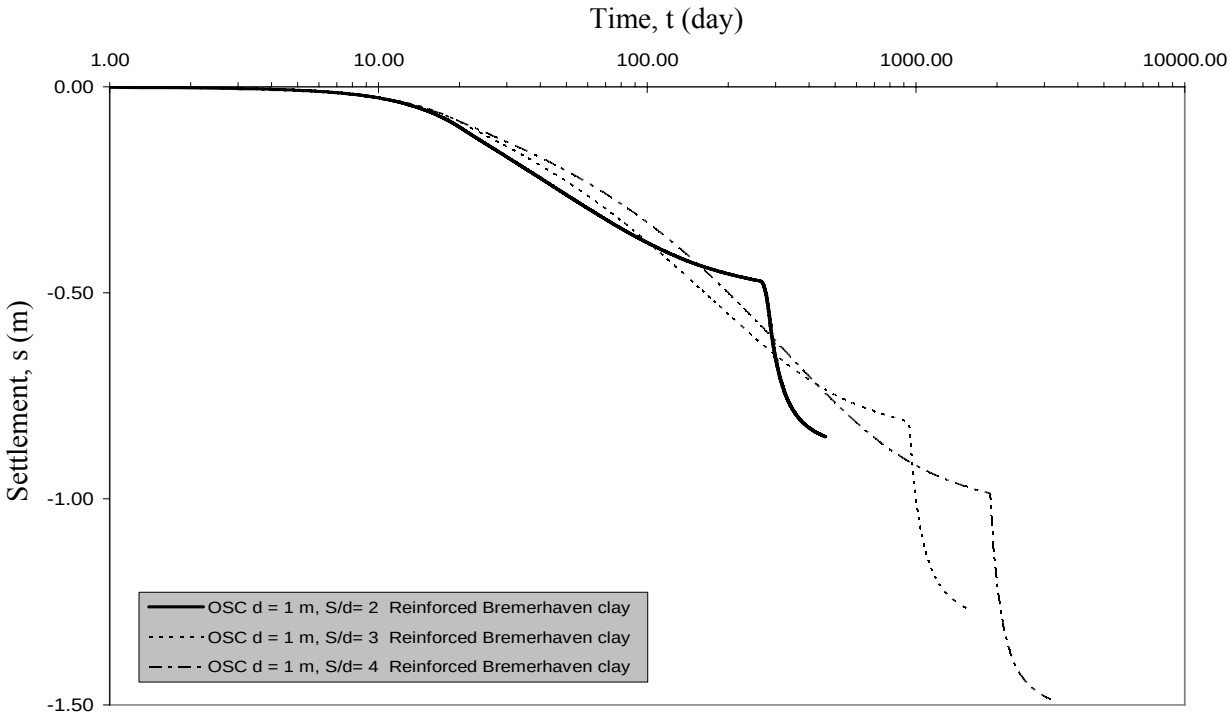

Fig. 7-3 Time-settlement relationship for the reinforced Bremerhaven clay with ordinary stone columns (OSC)

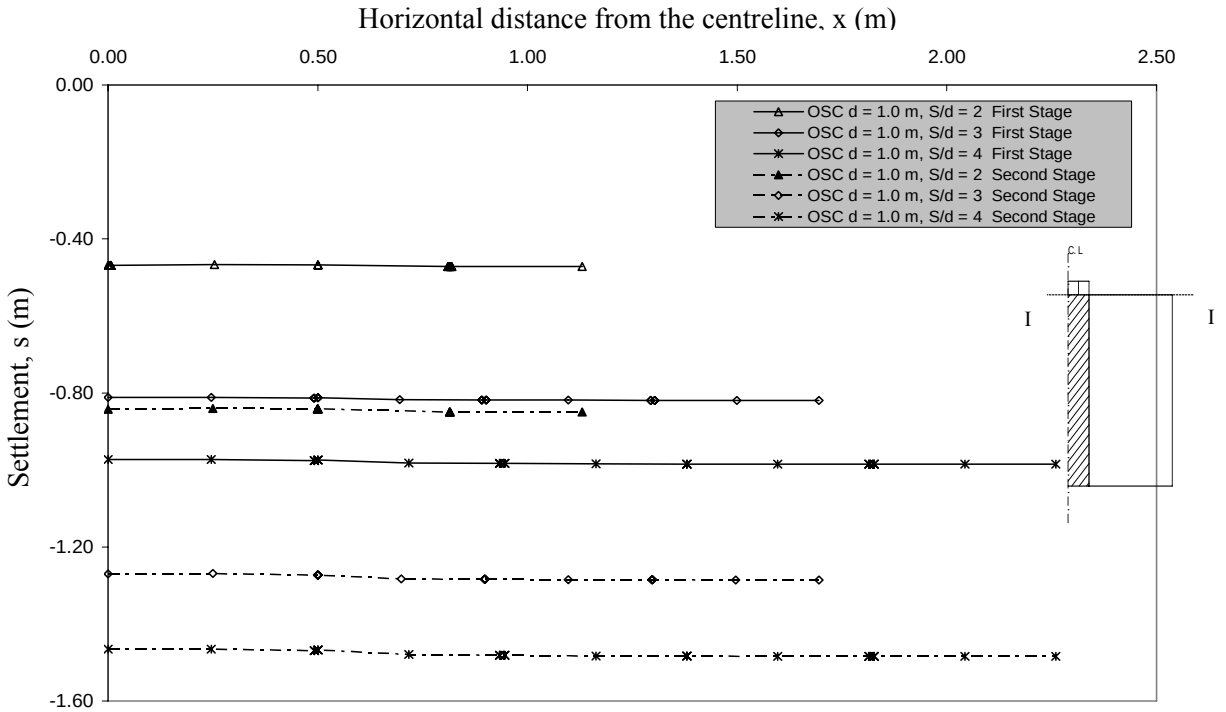

Fig. 7-4 Settlement distribution at the surface of the reinforced Bremerhaven clay with ordinary stone columns (OSC)

The settlement increases after each construction stage with increasing spacing distance between the columns. The reduction in the settlement when the spacing ratio is reduced from S/d = 3 to S/d = 2 is greater than that when the spacing ratio is reduced from S/d = 4 to S/d = 3, as shown in Table 7-4.

Table 7-4 Reductions in the time and the settlement of the reinforced Bremerhaven clay

Case of the soft Soil	Consolidation end of the first construction stage				Consolidation end of the second construction stage (time started from the beginning of loading)			
	Time, t (day)	R_t (%)	Settlement, s (m)	R_s (%)	Time, t (day)	R_t (%)	Settlement, s (m)	R_s (%)
Non-reinforced Bremerhaven clay	10781	-	1.31	-	18872	-	1.86	-
Reinforced clay with d = 1.0 m and S/d = 4	1885	17.5	1.0 m	76	3182	16.9	1.49	80
Reinforced clay with d = 1.0 m and S/d = 3	933	8.7	0.82	63	1590	8.4	1.29	69
Reinforced clay with d = 1.0 m and S/d = 2	265	2.5	0.47	36	459	2.4	0.86	46

R_t is the ratio between the consolidation time of the reinforced clay with ordinary stone columns and the consolidation time of the non-reinforced clay. R_s is the ratio between the total settlement of the reinforced clay with ordinary stone columns and the total settlement of the non-reinforced clay.

Fig. 7-5 shows the relationship of the time versus the construction of the embankment and versus the settlement for various volumes of the reinforced Hamburg clay around the stone columns. The development of the settlement along consolidation time also is the same for all the spacing ratios. The construction time and the consolidation settlement of the reinforced clay increase with increasing spacing distance between the columns. The smaller the spacing distance between the columns is, the faster the consolidation is and the smaller also the settlement is, as shown in Fig. 7-6 and Table 7-5.

The reinforced Hamburg clay has longer consolidation time and greater settlement than the reinforced Bremerhaven clay for all the spacing ratios. Using stone columns with spacing ratio of S/d = 2 in Hamburg clay has the best reduction of the settlement and the best acceleration of the consolidation among the other spacing ratios. Hence, using stone columns with spacing ratios greater than S/d = 2 is not effective and doesn't lead to applicable construction procedures on the reinforced Hamburg clay.

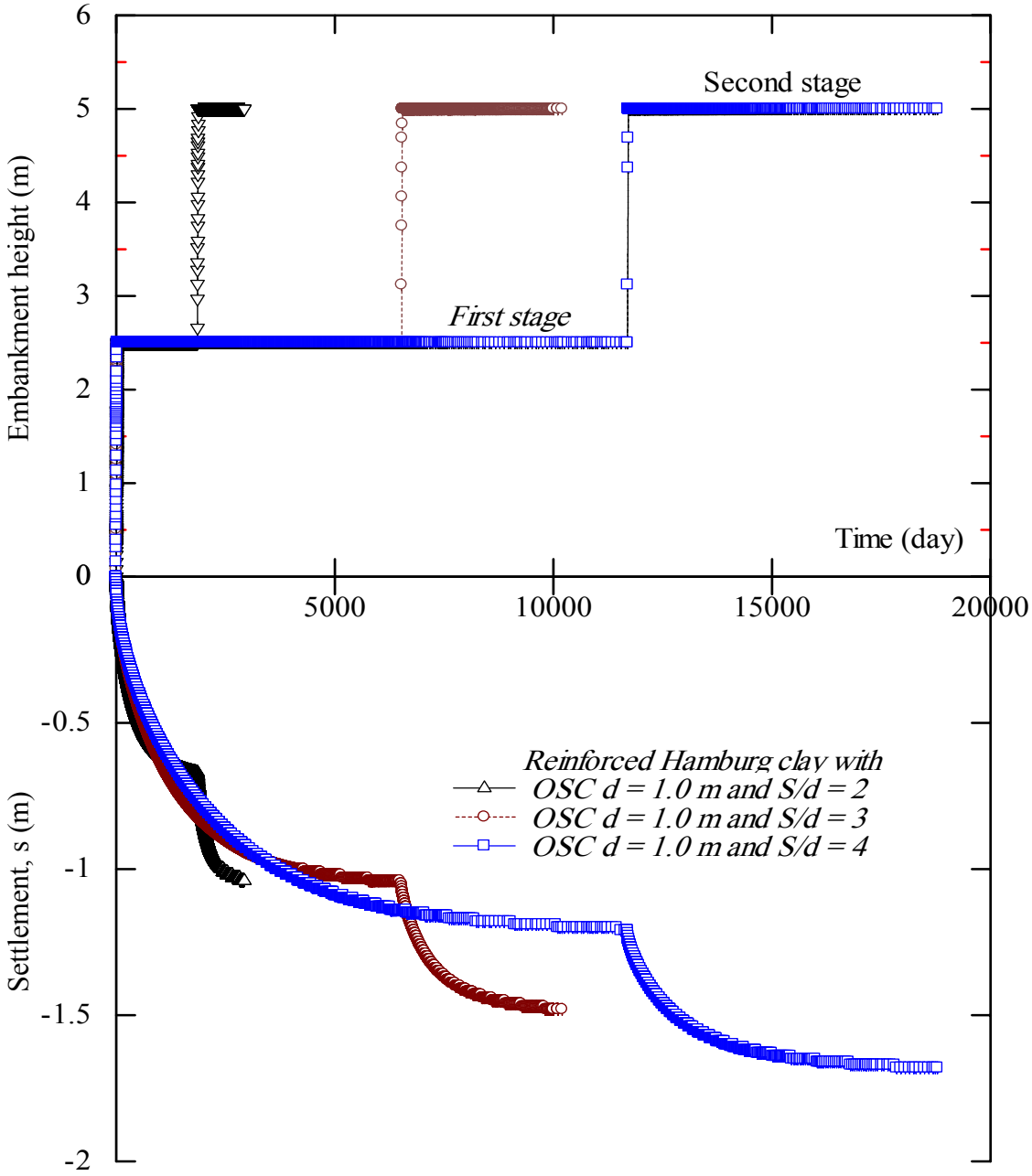

Fig. 7.5 Settlement of the reinforced Hamburg soft soil with stone column along the time of the construction

The settlement distribution at the surface of the reinforced Hamburg clay after the consolidation end of both construction stages is also shown in Fig. 7-7. The existence of stone columns in soft clay also increases the bearing capacity of the soft clay by reducing settlement during the various construction phases. The settlement in the stone column and in the surrounding soft soil is constant and approximately the same. The settlement increases with increasing spacing distance. The reinforced Hamburg clay induces a settlement and a consolidation time greater than those of the Bremerhaven clay. The reason is that the Hamburg clay has a high compressibility and a smaller permeability than the Bremerhaven clay.

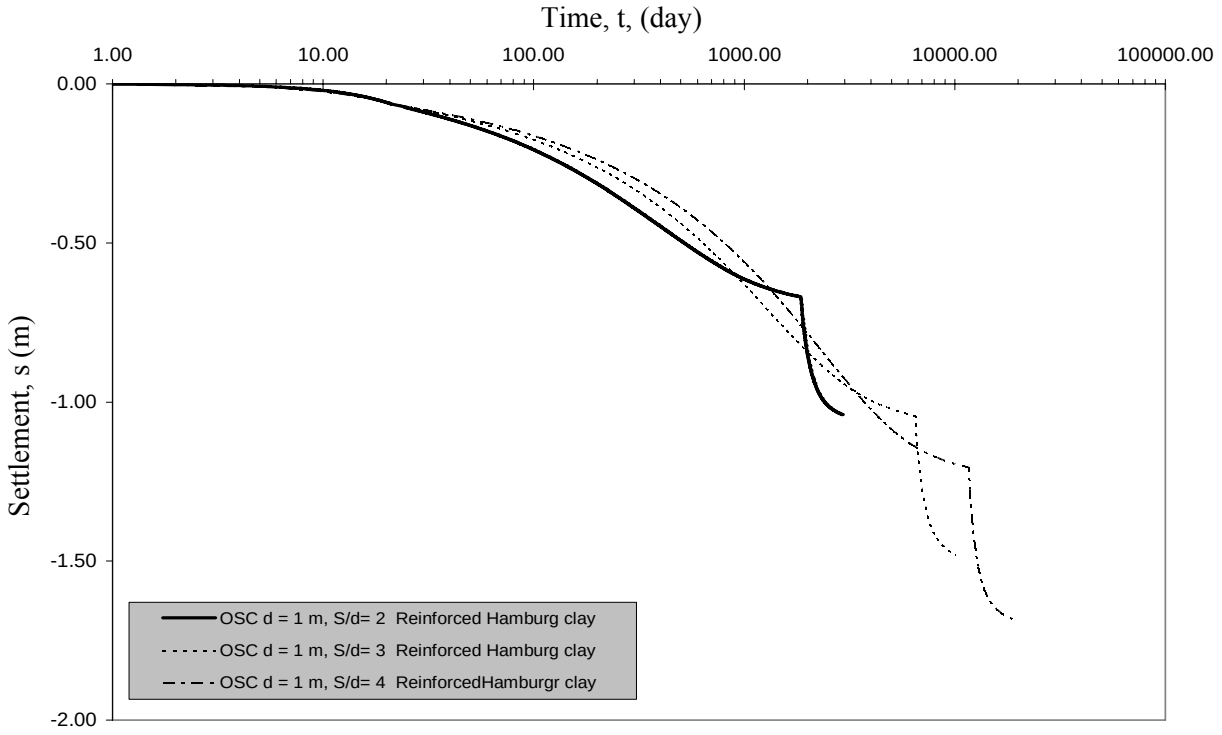

Fig. 7-6 Time-settlement relationship for the reinforced Hamburg clay with ordinary stone columns (OSC)

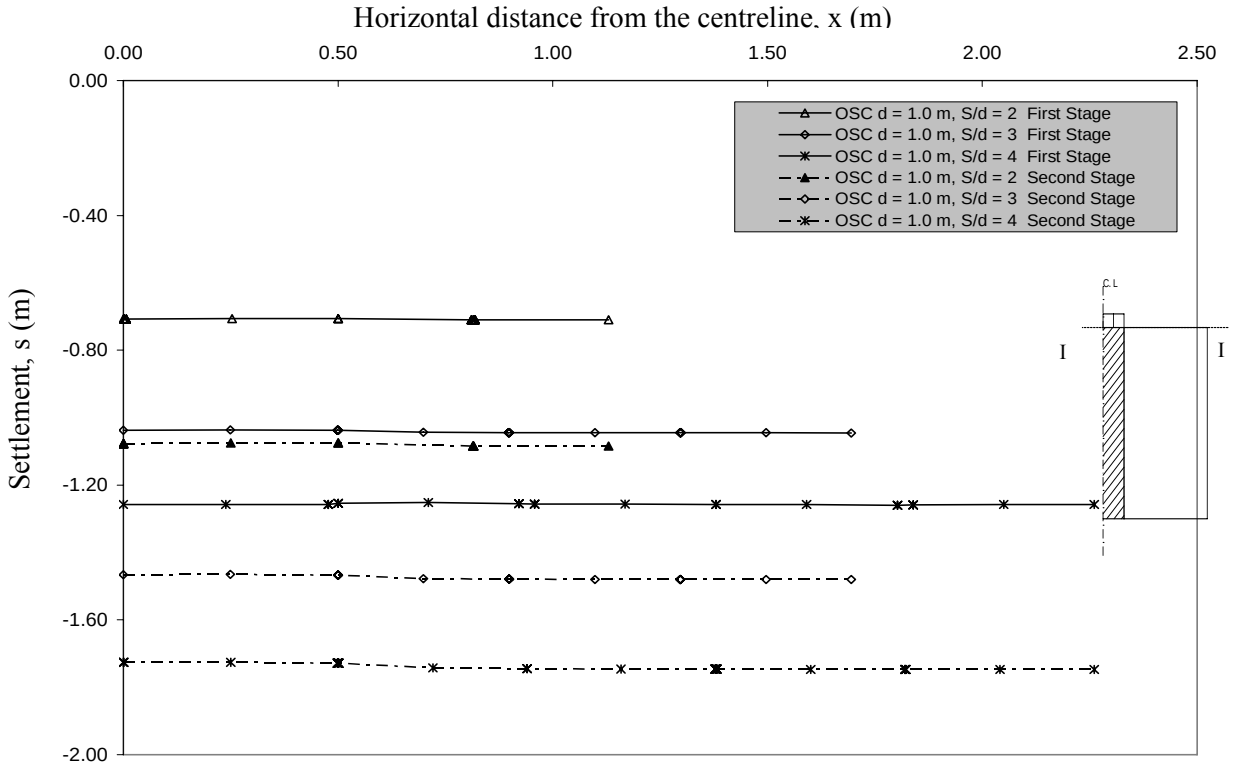

Fig. 7-7 Settlement distribution at the surface of the reinforced Hamburg clay with ordinary stone columns (OSC)

Table 7-5 Reductions in the time and the settlement of the reinforced Hamburg clay

Case of the soft Soil	Consolidation end of the first construction stage				Consolidation end of the second construction stage (time started from the beginning of loading)			
	Time, t (day)	R_t (%)	Settlement, s (m)	R_s (%)	Time, t (day)	R_t (%)	Settlement, s (m)	R_s (%)
Non-reinforced Hamburg clay	61244	-	1.58	-	117733	-	2.11	-
Reinforced clay with d = 1.0 m and S/d = 4	11694	19.	1.21	77	18784	16	1.69	80.
Reinforced clay with d = 1.0 m and S/d = 3	6526	10.7	1.03	65	10159	8.6	1.48	70.
Reinforced clay with d = 1.0 m and S/d = 2	1856	3.	0.67	42	2923	2.5	1.05	50.

Lateral bulging of the stone column

The lateral bulging of the stone column, (u_h) was calculated after each consolidation phase in the reinforced Bremerhaven clay and Hamburg clay, as shown in Fig. 7-8 and Fig. 7-9, respectively. Once the stone column is yielded, its bulging appears due to dilatancy. The lateral bulging of the stone columns in the Bremerhaven and the Hamburg clays shows a similar distribution for all spacing ratios. The lateral bulging along the stone column increases with increasing load causing more load transfer to the lower depths during the consolidation. The lateral bulging values in the Hamburg clay are generally greater than those in Bremerhaven clay for the all spacing ratios as shown in Fig. 7-8 and Fig. 7-9. The lateral bulging of the stone column increases with increasing spacing distance between the columns.

Excess pore water pressure

The excess pore water pressure (Δu) in the reinforced Bremerhaven clay and in the reinforced Hamburg clay was calculated at point B which is located at a depth of 2.0 m, as shown in Fig. 7-1. As soon as the fill load is applied on the saturated soft soil, the excess pore water pressure builds up. The excess pore water pressure increases with time until it reaches maximum values at the end of construction of each stage of the reinforced Bremerhaven and Hamburg clay. After that, the excess pore water pressure decrease gradually during the consolidation directing to the steady state case, as shown in Fig. 7-10 and Fig. 7-12. The first and the second stage of constructions imply the same behavior of the excess pore water pressure through the consolidation time. But the excess pore water pressure after the second stage of construction is dissipated more rapidly than that after the first stage of construction, as shown in Fig. 7-11 and 7-13.

The excess pore water pressure in the reinforced Bremerhaven clay increases and its dissipation consumes long time with increasing spacing distance between the columns. Compared to the other spacing ratios, the excess pore water pressure values of the reinforced Bremerhaven clay with stone columns spacing ratio S/d of 2 are much smaller and they dissipate more rapidly, as illustrated in Fig. 7-10.

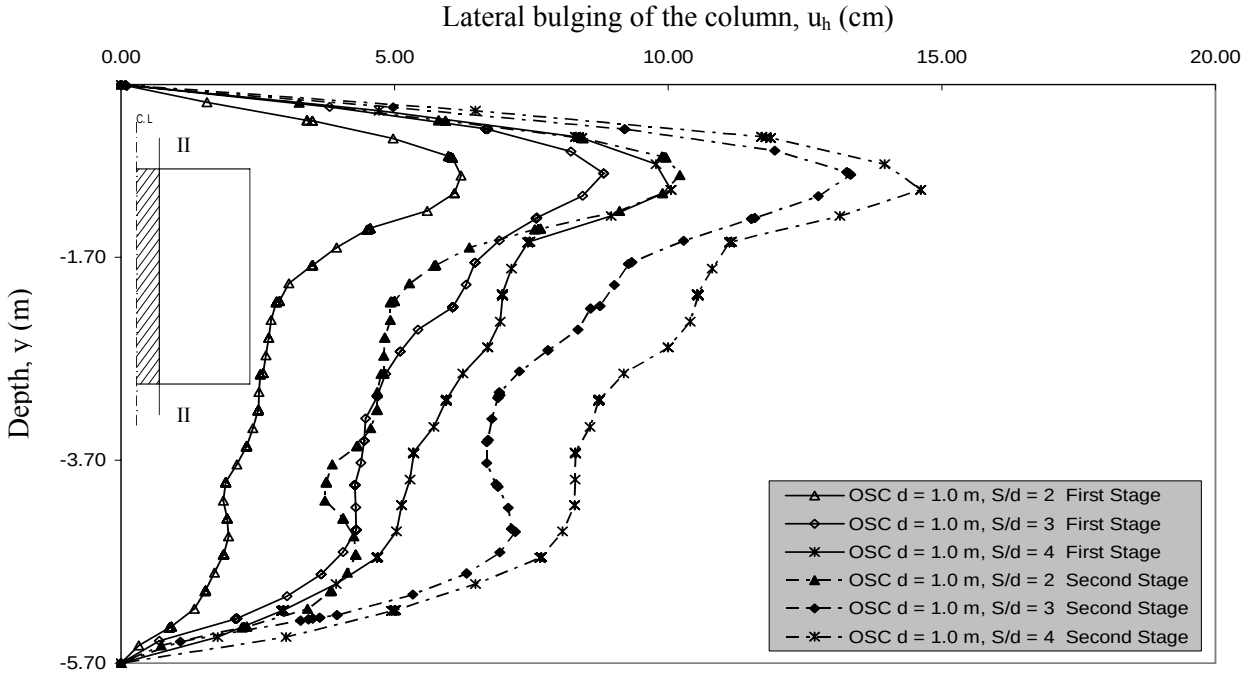

Fig. 7-8 Lateral bulging distribution of the stone columns surrounded by the Bremerhaven clay with d = 1.0 m and various spacing ratios

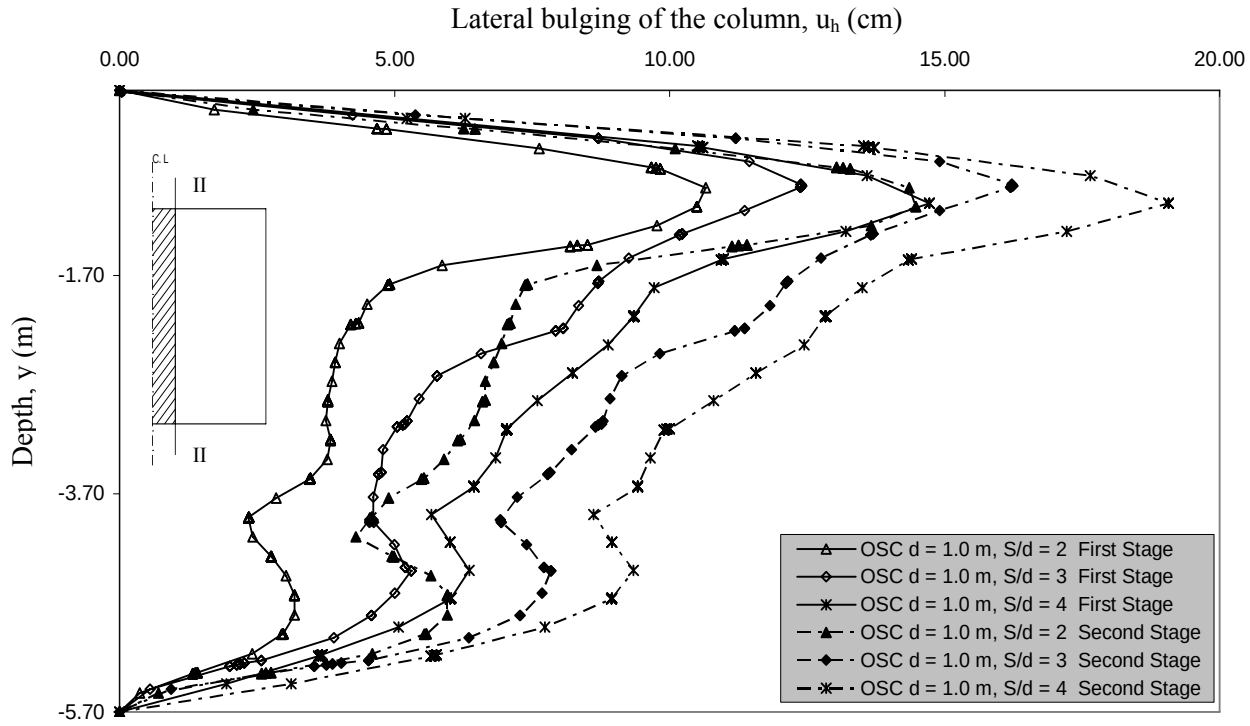

Fig. 7-9 Lateral bulging distribution of the stone columns surrounded by the Hamburg clay with d = 1.0 m and various spacing ratios

The excess pore water pressure in the reinforced Hamburg clay increases along the consolidation and its dissipation consumes also a long time with increasing spacing distance between the columns. Beyond a spacing ratio of S/d = 3, there is no considerable improvement in the dissipation acceleration of the excess pore water pressure, as shown in Fig. 7-12. Therefore, when the Bremerhaven and the Hamburg clay are reinforced by stone columns with spacing ratio S/d = 2, the smallest the pore water pressure along the consolidation is and the shortest the time of dissipation the pore water pressure is.

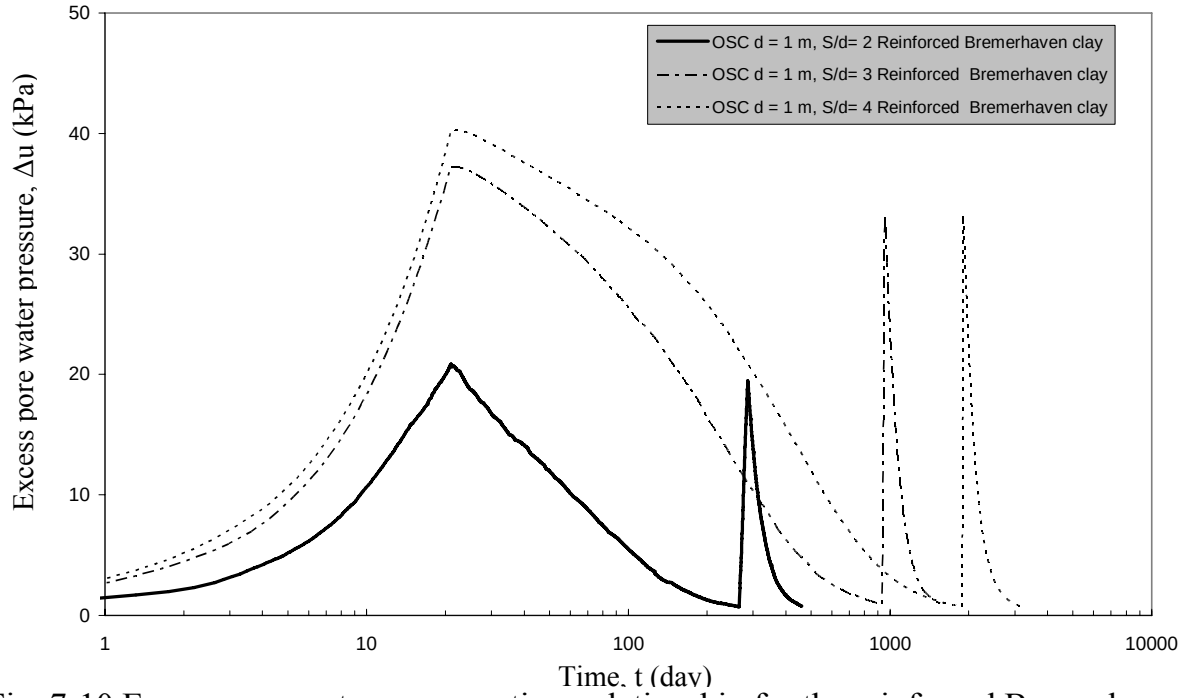

Fig. 7-10 Excess pore water pressure-time relationship for the reinforced Bremerhaven clay using stone columns with d = 1.0 m and various spacing ratios

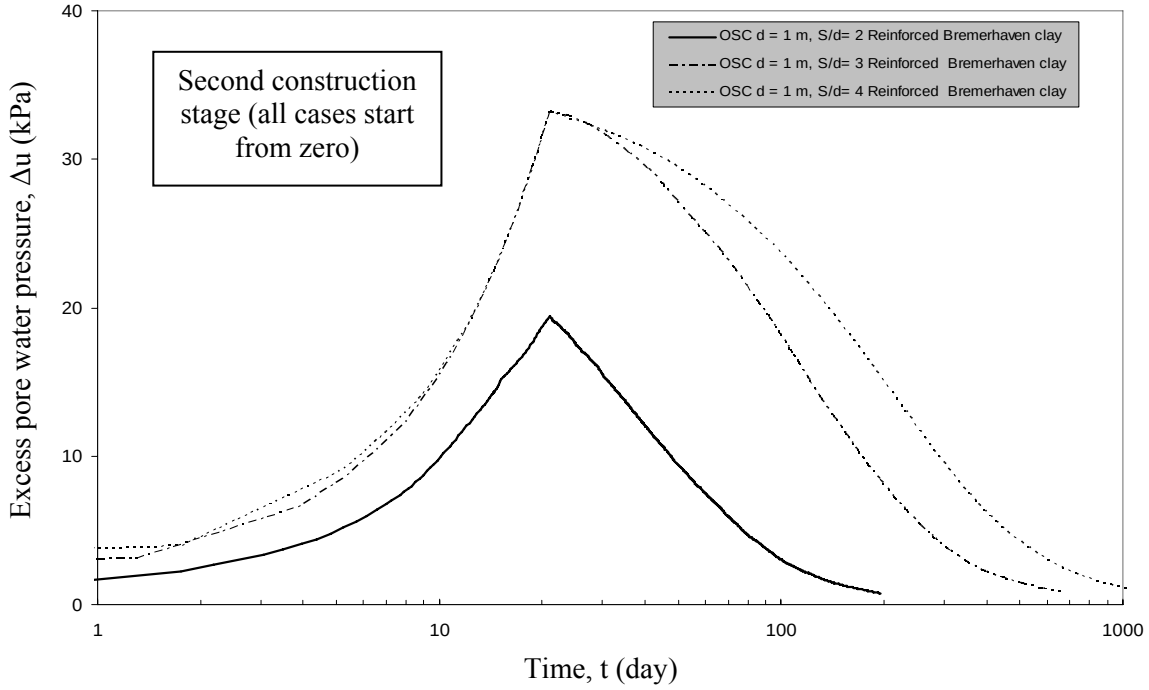

Fig. 7-11 Development of excess pore water pressure during the second construction stage for the reinforced Bremerhaven clay using stone columns with d = 1.0 m and various spacing ratios

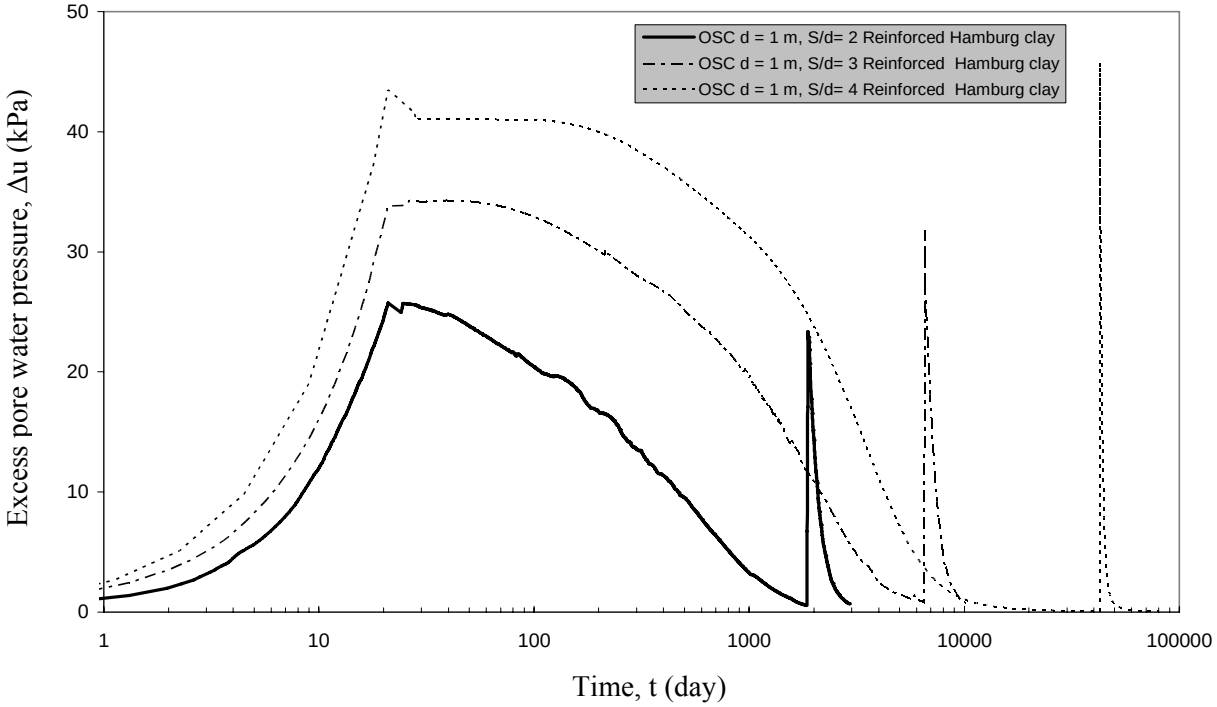

Fig. 7-12 Excess pore water pressure-time relationship for the reinforced Hamburg clay using stone columns with d = 1.0 m and various spacing ratios

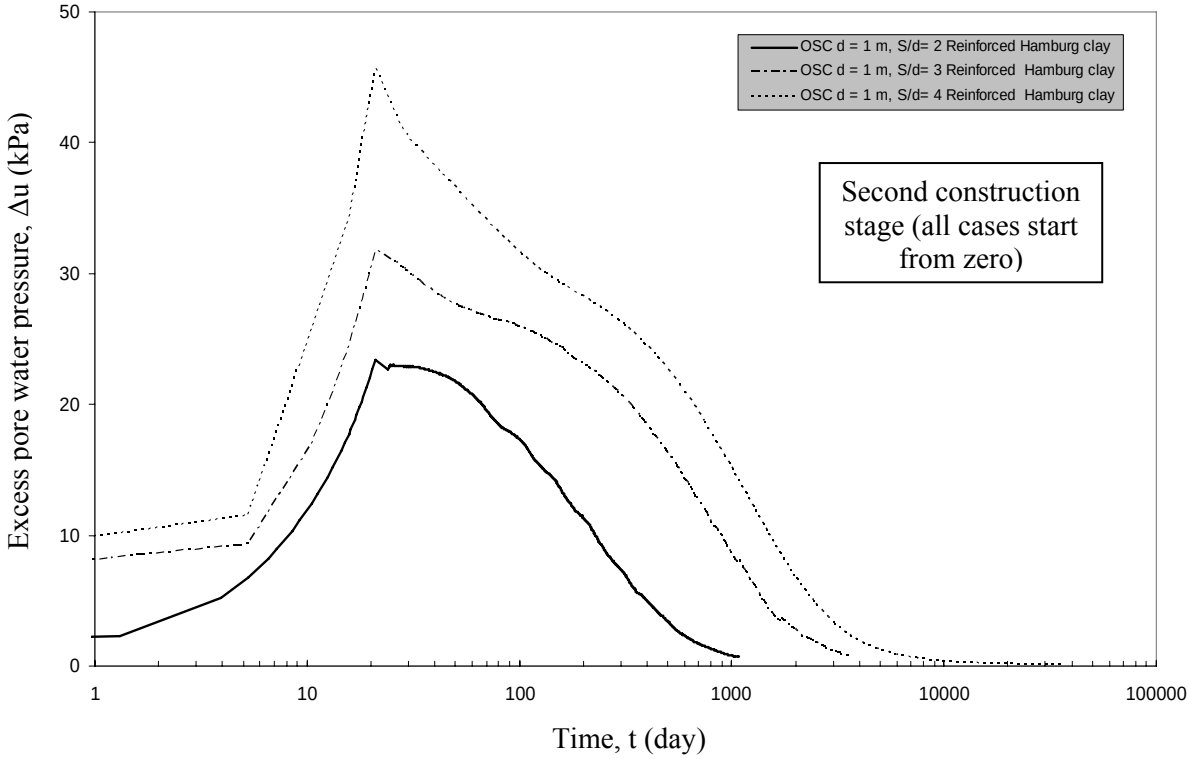

Fig. 7-13 Development of excess pore water pressure during the second stage for the reinforced Hamburg clay using stone columns with d = 1.0 m and various spacing ratios

Stress in soil

The effective vertical stress (σ'_v) was calculated at the surface in the reinforced soft soil at point A, and in the column at point C, as shown in Fig. 7-1-a. The relationship of the effective vertical stress with settlement for the reinforced Bremerhaven clay and the reinforced Hamburg clay is shown in Fig. 7-14 and Fig. 7-15, respectively. The effective vertical stress in the reinforced soft soil and in the stone column increases with a high

rate with increasing settlement through increasing embankment fill in both stages of construction. During the consolidation process, directly after the first and the second construction stages have been finished, the vertical effective stress in the reinforced soft soil increases with a very small rate. However, the rate of the vertical stress increase becomes greater during the consolidation of the second construction stage. During the consolidation process of the first construction stage, as settlement increases, the vertical effective stress in the stone column increases with a small rate until it reaches a maximum value. Beyond this value the vertical effective stress decreases with a small rate until the second stage of construction starts. While in the consolidation of the second stage, the vertical stress decreases gradually with increasing settlement. This phenomenon is due to the column yielding as discussed in chapters 5 and 6.

The effective vertical stress in the stone columns increases with increasing spacing distance between the columns. The effective stress in the reinforced Bremerhaven clay and Hamburg clay also increases with increasing spacing distance between the columns. The greater the spacing distance between the columns is, the higher the vertical stress in the stone columns, the higher the vertical stress in the surrounding soft soil and the greater the settlement are, as shown in Fig. 7-14 and 7-15.

When the spacing distance between the columns is greater, more stress is gathered from the surrounding soft soil and transfers to the stone columns which lead to an increase of the vertical stress in the columns. Additionally, the smaller spacing columns cause more reduction in the stress of the surrounding soft soil than the wider spacing columns, as illustrated in Fig. 7-14 and Fig. 7-15. In general, the stone columns in the Hamburg clay have vertical effective stress slightly larger than those in the Bremerhaven clay through all the construction phases. The reason of that is the Hamburg clay has a smaller shear strength which leads to an increase of the stress transfer to the stone columns.

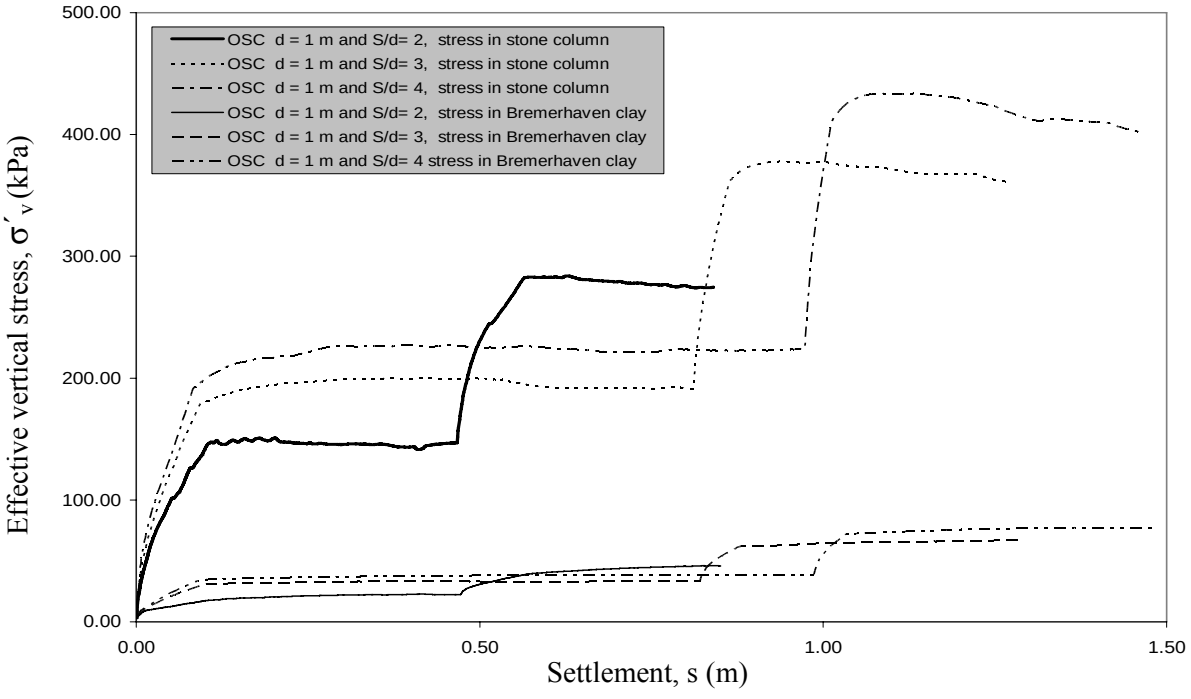

Fig. 7-14 Effective vertical stress-settlement relationship for the reinforced Bremerhaven clay at point A and for the stone column at point C

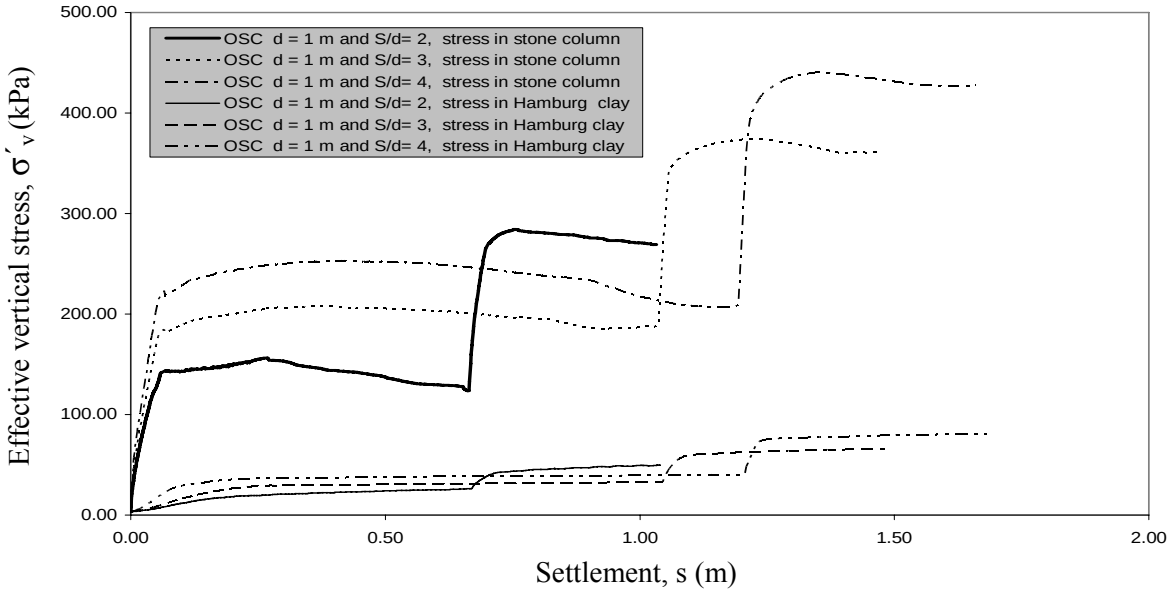

Fig. 7-15 Effective vertical stress-settlement relationship for the reinforced Hamburg clay at point A and for the stone column at point C

The total vertical stress was calculated in the reinforced Bremerhaven clay and in the reinforced Hamburg clay at point (B) which is located at a depth of 2.0 m, as shown in Fig. 7-1-a. The results are shown in Fig. 7-16 and 7-17. The total vertical stress (σ_v) in the reinforced soft soil increases with increasing load until it reaches maximum values at the end of both construction stages. During each consolidation process, the total stress decreases with increasing time but the reduction of the total stress in the consolidation of the first construction stage is greater than that in the consolidation of the second construction stage, as shown in Fig. 7-16 and Fig. 7-17. This phenomenon is due to the stress concentration which is in the first construction stage greater than that in the second construction stage, as discussed in Chapters 5 and 6.

The total vertical stress in the reinforced Bremerhaven and Hamburg clays increases with increasing spacing distance between the columns through the all construction phases. Hence, the smaller the spacing distance between the columns is, the more the decrease in the total stress of the surrounding soft soil is which leads to more improvements in the behavior of the reinforced soft soil. The rate of the reduction in the total stress during each consolidation phase of the soft soil increases with decreasing spacing distance between the columns. The greater the rate of the reduction of the total stress during a consolidation phase is, the higher the participation percentage of the stress transfer and concentration in the acceleration of the consolidation time. The role of the stress concentration in the acceleration of the consolidation process can be calculated by equation (5-1) which is;

$$SC_{accel.} = (\sigma_{v(i)} - \sigma_{v(f)}) / \Delta u_i \qquad [-]$$

Where $SC_{accel.}$; participation of stress concentration in the consolidation acceleration, $\sigma_{v(i)}$; average initial total vertical stress in the reinforced soft soil (after 21 days in this study), $\sigma_{v(f)}$; average final total vertical stress in the reinforced soft soil (after consolidation end), Δu_i; average maximum initial excess pore water pressure in the reinforced soft soil (after 21 days in this study).

Table 7-6 Stress concentration participation on the acceleration of the consolidation

Stone column stress concentration effect on	% ($SC_{accel.}$) of Bremerhaven clay, d = 1.0 m			% ($SC_{accel.}$) of Hamburg clay, d = 1.0 m		
	S/d = 2	S/d = 3	S/d = 4	S/d = 2	S/d = 3	S/d = 4
First construction stage	36.34	33.33	20.18	28.50	20. 60	19.70
Second construction stage	31.70	25.10	13.13	25.89	15.06	12.60

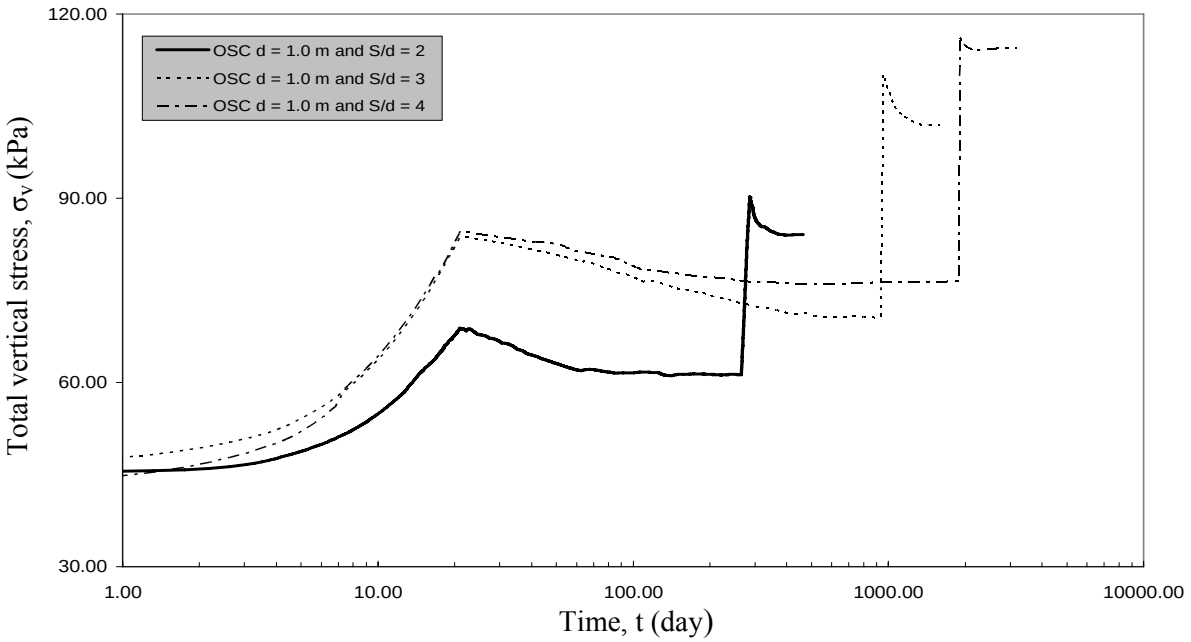

Fig. 7-16 Total vertical stress-settlement relationship for the reinforced Bremerhaven clay at point B at a depth of 2.0 m

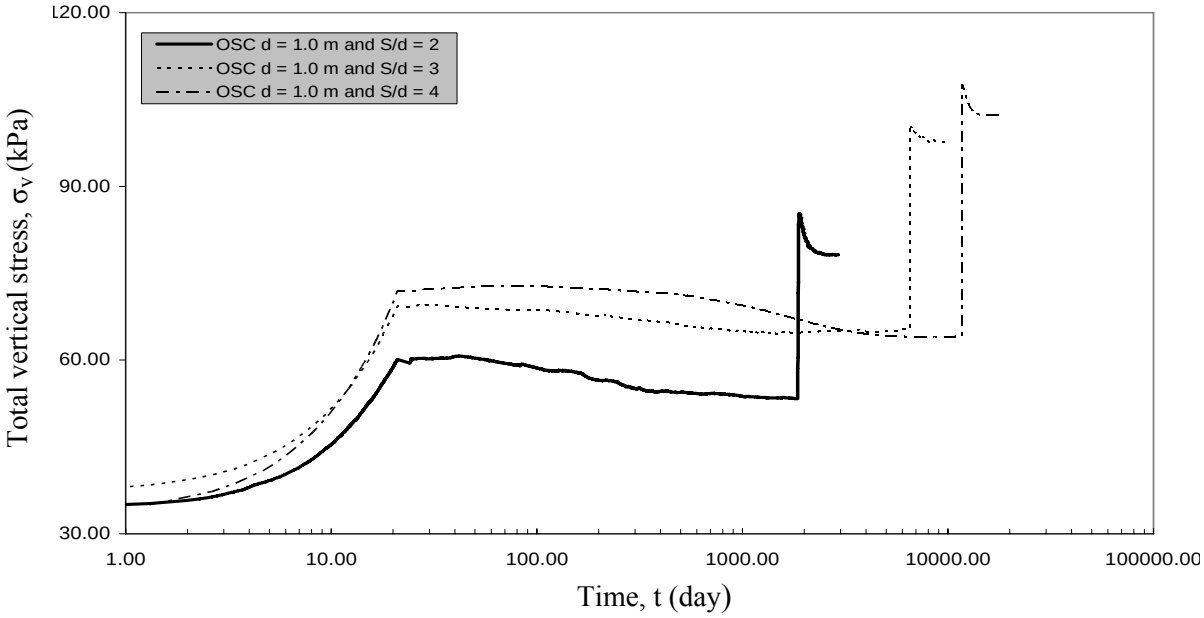

Fig. 7-17 Total vertical stress-settlement relationship for the reinforced Hamburg clay at point B at a depth of 2.0 m

The reinforced Bremerhaven clay has greater rate of reductions in the total stress and greater percentages of the consolidation acceleration than the reinforced Hamburg clay as shown in Table 7-6. Therefore as stated before, the ordinary stone columns are more effective in the Bremerhaven clay than in the Hamburg clay.

7.3.2 Group (B): Effect of the diameter of the stone column (d)

The above discussion indicated that the reinforced soft soil by stone columns with the smallest spacing ratio S/d of 2 provides the best bearing capacity among the investigated cases. Now, various diameters of 0.6 m, 1.0 m and 1.4 m have been used maintaining the spacing ratio S/d = 2 to investigate the effect of the diameter on the reinforcement of the Bremerhaven clay and the Hamburg clay.

Settlement

Fig. 7-18 shows the relationship of the time with the construction of the embankment from a side and with the settlement from the other side for the reinforced Bremerhaven clay. The development of the settlement with consolidation time is the same for all the used diameters. The consolidation time of the reinforced clay increases with increasing diameter of the column as shown also in Fig. 7-19. But the settlement has a small increase with increasing diameter of the stone column because the spacing ratio is constant for the different used diameters. When the diameter of the columns is small in a significant area of the reinforced clay under the embankment, the number of columns in this area is high which leads to a decrease of the drainage path. The short drainage paths accelerate the consolidation and construction time as illustrated in Fig. 7-18, Fig. 7-19 and Table 7-7. Hence, at the same spacing ratio of S/d = 2 the reinforced Bremerhaven clay with a stone column of diameter d = 0.6 m has the smallest settlement and the shortest consolidation time in both construction stages of the studied cases. That stone column reduces the final consolidation time of the Bremerhaven clay from 18872 days (51.7 years) to 192 days (6 months) and the consolidation settlement from 1.86 m to 0.838 m.

Table 7-7 Reductions in the time and the settlement of the reinforced Bremerhaven clay

Case of the soft Soil	Consolidation end of the first construction stage				Consolidation end of the second construction stage (time started from the beginning of loading)			
	Time, t (day)	R_t (%)	Settlement, s (m)	R_s (%)	Time, t (day)	R_t (%)	Settlement, s (m)	R_s (%)
Non-reinforced Bremerhaven clay	10781	-	1.31	-	18872	-	1.86	-
Reinforced clay with S/d = 2 and d = 1.4 m	483	4.5	0.49	37	838	4.4	0.87	46.8
Reinforced clay with S/d = 2 and d = 1.0 m	265.2	2.5	0.47	36	459	2.4	0.857	46
Reinforced clay with S/d = 2 and d = 0.6 m	111	1.0	0.457	35	192	1.0	0.838	45

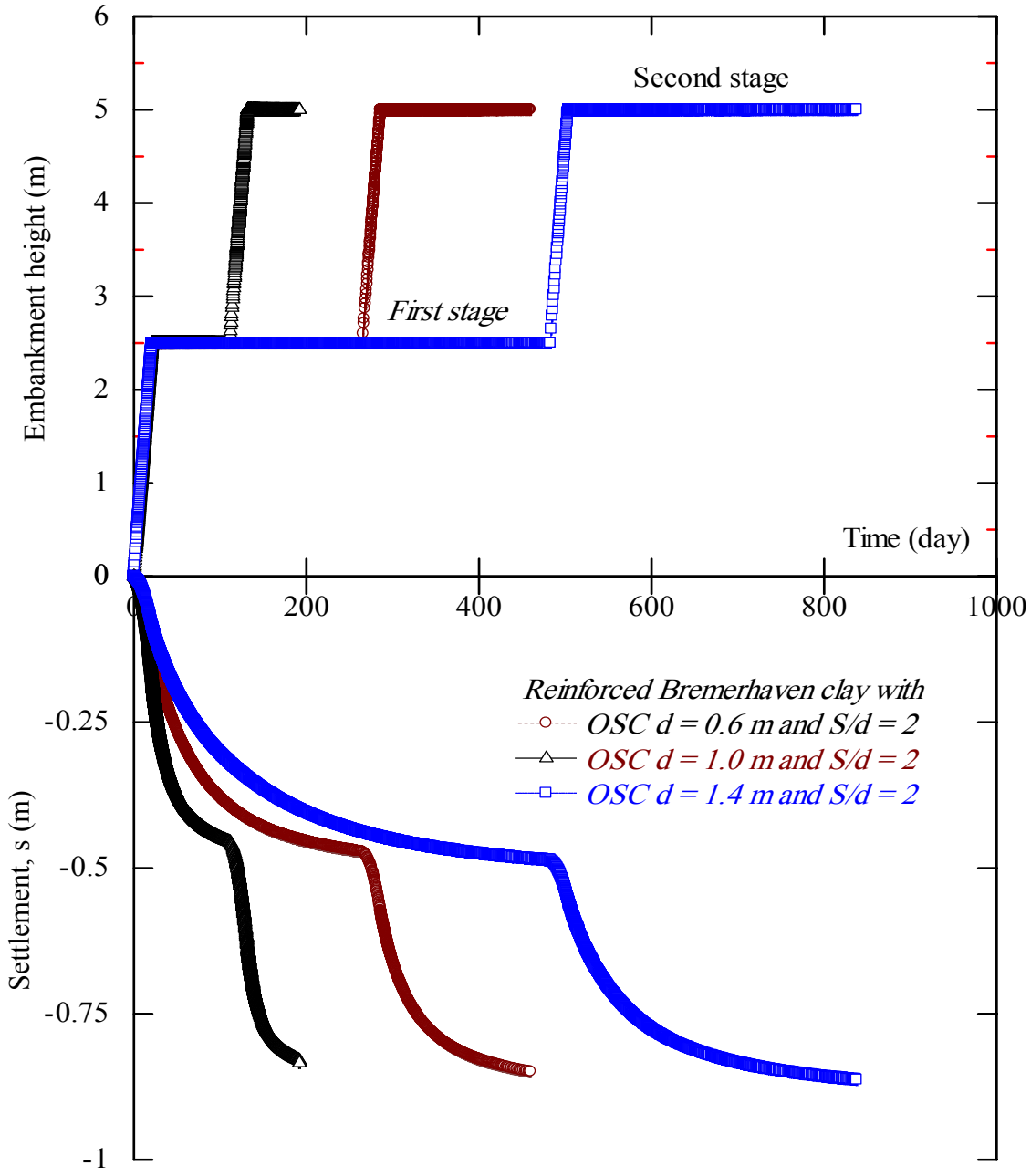

Fig. 7.18 Settlement of the reinforced Bremerhaven soft soil with stone column along the time of the construction

The settlement distribution at the surface of the reinforced Bremerhaven clay after the consolidation end of each construction stages is also shown in Fig. 7-20. The settlement in the stone column and in the surrounding soft soil is constant and approximately the same. The increase of the settlement is insignificant with increasing column diameter after each construction stage, as illustrated in Fig. 7-20 and Table 7-7. This is because the areas with different diameters under the load have the same area ratio of the stone column to the surrounding soil due to the constant spacing ratio, S/d. Therefore the effect of the column diameter on the consolidation time is greater than that on the consolidation settlement.

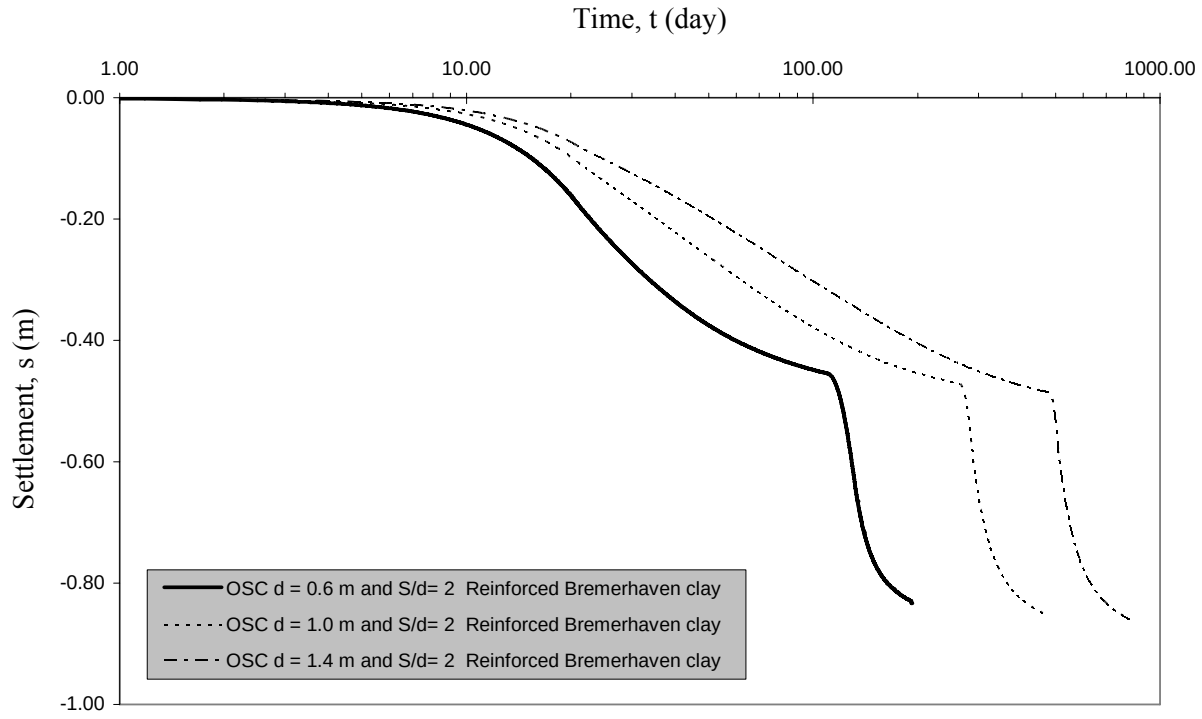

Fig. 7-19 Time-settlement relationship for the reinforced Bremerhaven clay with ordinary stone columns (OSC)

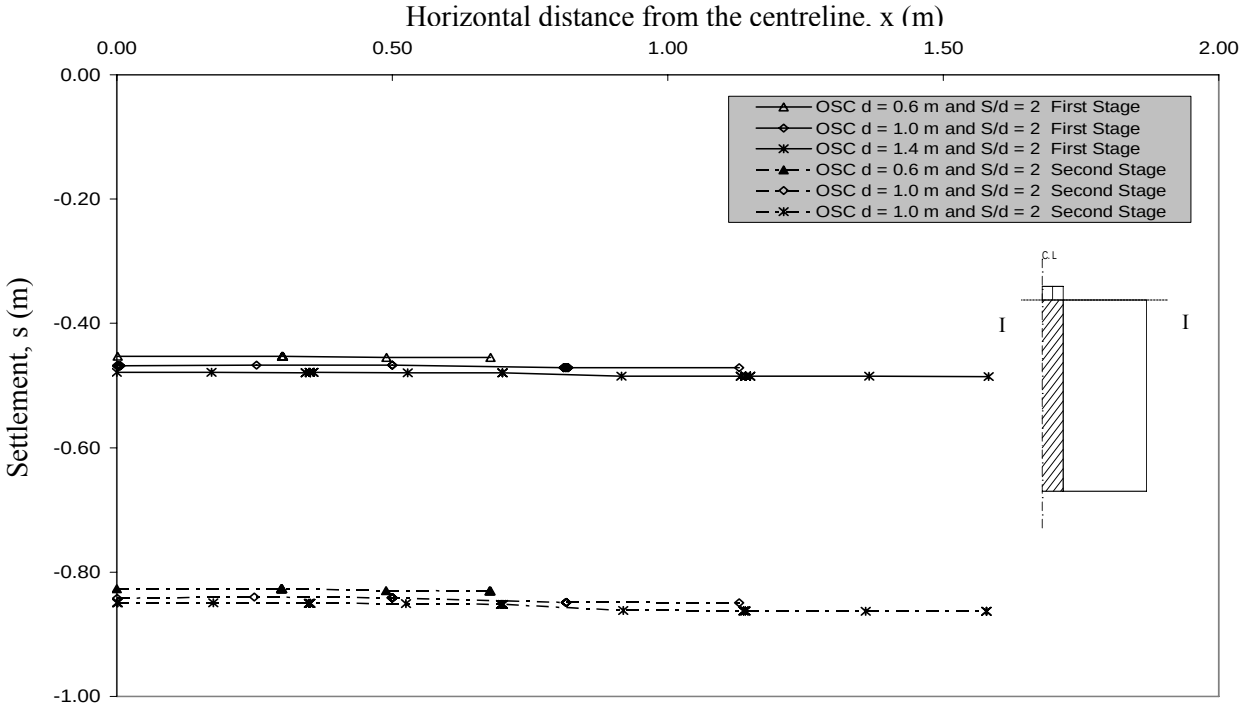

Fig. 7-20 Settlement distribution at the surface of the reinforced Bremerhaven clay with ordinary stone columns (OSC)

Fig. 7-21 shows the relationship of time and the construction of the embankment as well as the settlement for various diameters of the stone columns in the Hamburg clay. The development of the settlement with consolidation time is the same for all the diameters. The consolidation time of the reinforced clay increases with increasing diameter of the

columns while the settlement has an insignificant increase. The smaller the diameter of the columns is, the faster the consolidation is, as shown in Fig. 7-22 and Table 7-8. Using stone columns with spacing ratio of S/d = 2 and diameter of d = 0.6 m in Hamburg clay leads to the best acceleration of the consolidation and the best reduction of the settlement in the studied cases. When the Hamburg clay is reinforced by such stone columns, the final consolidation time is reduced from 117733 days (321.7 years) to 1168 days (3.19 years) and the consolidation settlement is reduced from 2.11 m to 1.03 m. Generally, the reinforced Hamburg clay has longer consolidation time and greater settlement than the reinforced Bremerhaven clay for all the diameters.

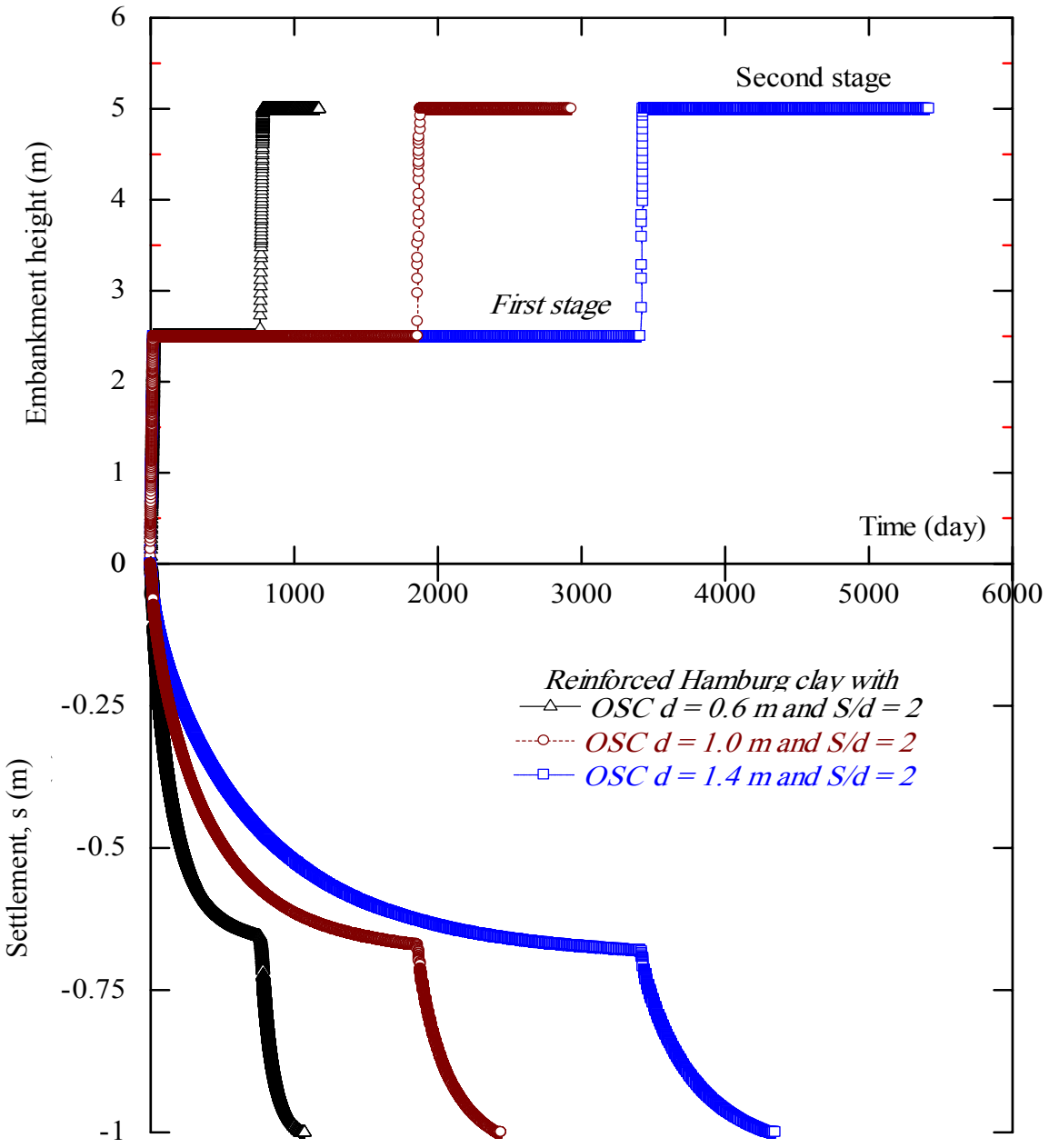

Fig. 7.21 Settlement of the reinforced Hamburg soft soil with stone column along the time of the construction

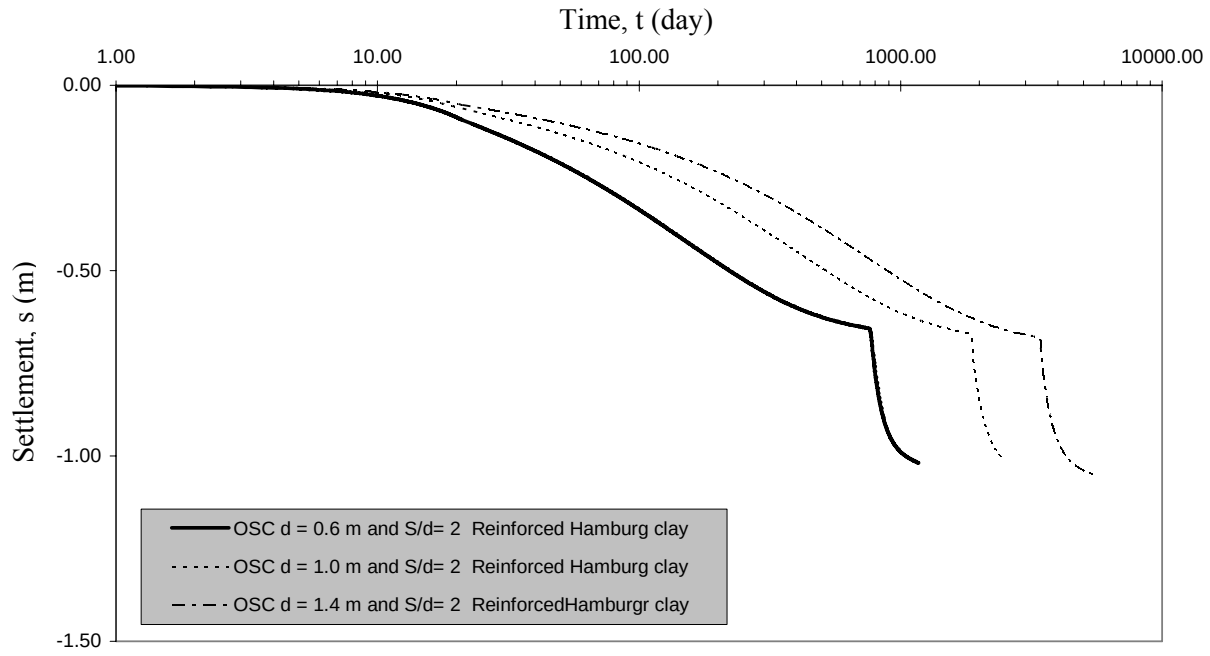

Fig. 7-22 Time-settlement relationship for the reinforced Hamburg clay with ordinary stone columns (OSC)

Table 7-8 Reductions in the time and the settlement of the reinforced Hamburg clay

Case of the soft Soil	**Consolidation end of the first construction stage**				**Consolidation end of the second construction stage (time started from the beginning of loading)**			
	Time, t (day)	**R_t (%)**	**Settlement, s (m)**	**R_s (%)**	**Time, t (day)**	**R_t (%)**	**Settlement, s (m)**	**R_s (%)**
Non-reinforced Hamburg clay	61244	-	1.58	-	117733	-	2.11	-
Reinforced clay with S/d = 2 and d = 1.4 m	3414	5.6	0.68	43	5411	4.6	1.06	50.2
Reinforced clay with S/d = 2 and d = 1.0 m	1856	3.0	0.67	42.4	2923	2.5	1.05	49.8
Reinforced clay with S/d = 2 and d = 0.6 m	760	1.24	0.658	41.6	1168	1.0	1.03	48.8

The settlement distribution at the surface of the reinforced Hamburg clay at the consolidation end of both construction stages is also shown in Fig. 7-23. The settlement in the stone column and in the surrounding soft soil is constant and approximately the same. The settlement has an insignificant increase with increasing column diameter after each consolidation phase, as illustrated in Fig. 7-23 and Table 7-8. Hence, the effect of the column diameter on the consolidation time is greater than the consolidation settlement.

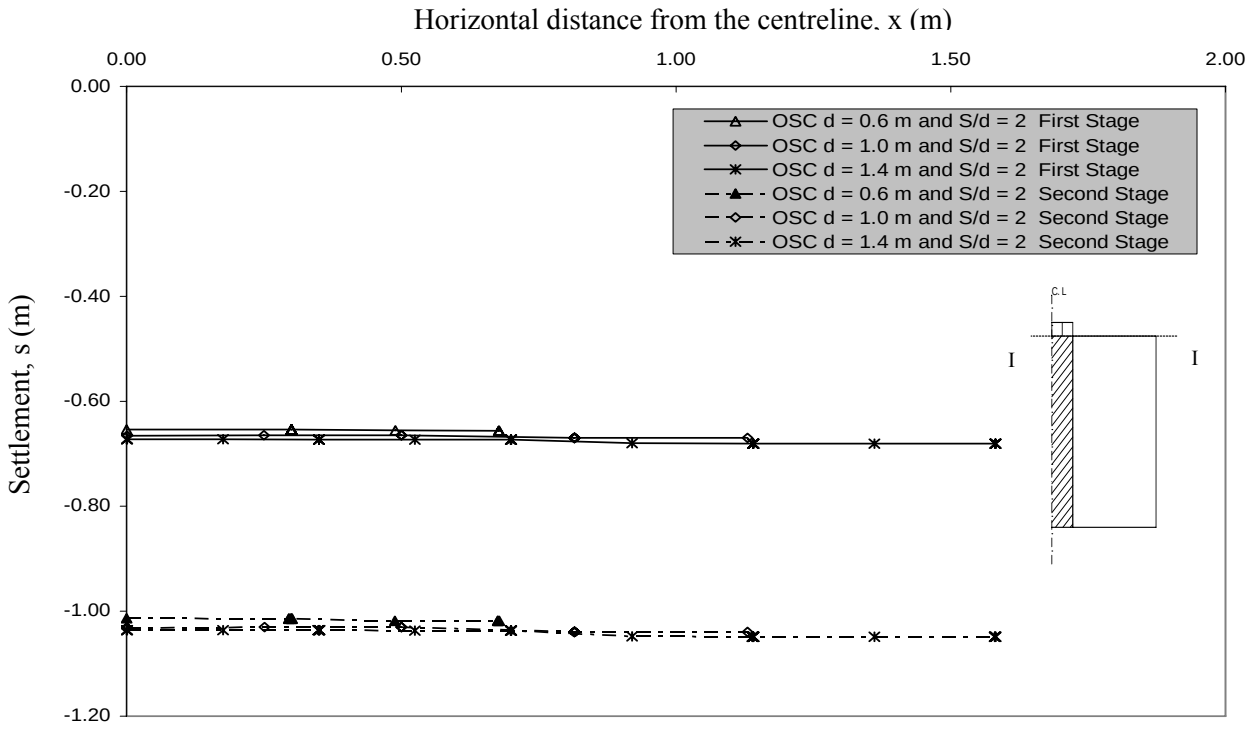

Fig. 7-23 Settlement distribution at the surface of the reinforced Hamburg clay with ordinary stone columns (OSC)

Lateral bulging of the stone column

The lateral bulging of the stone column, (u_h) was calculated after each consolidation phase in the reinforced Bremerhaven clay and Hamburg clay, as shown in Fig. 7-24 and Fig. 7-25, respectively. The lateral bulging of the stone columns after the consolidation of the first and the second construction stages shows a similar development for the same diameter. The lateral bulging along the stone column increases with increasing load causing more load transfer to the lower depths during the consolidation. The lateral bulging values in the Hamburg clay are greater than those in the Bremerhaven clay for all the diameters, as shown in Fig. 7-24 and Fig. 7-25.

The lateral bulging of the stone column increases with increasing diameter of the columns. This is because at the constant spacing ratio the smaller stone column diameters are more confined and they have smaller absolute spacing distances than the larger diameters. The increase rate of the lateral bulging after the consolidation of the first stage is smaller than that after the end of the consolidation.

Excess pore water pressure

The excess pore water pressure (Δu) in the reinforced Bremerhaven clay and in the reinforced Hamburg clay was calculated at the point B which is located at a depth of 2.0 m, as shown in Fig. 7-1-a. The development of the excess pore water pressure of the reinforced Bremerhaven clay and the reinforced Hamburg clay is approximately similar along all the construction phases for the various used diameters. The excess pore water pressure in the reinforced Bremerhaven clay increases and its dissipation consumes a longer time with increasing diameter of the column. The excess pore water pressure values of the reinforced Bremerhaven clay with stone columns diameter, d of 0.6 m are

lower and they dissipate more rapidly than those with greater diameters, as illustrated in Fig. 7-26 and Fig. 7-27. In general, the excess pore water pressure implies lower values along the consolidation and they dissipate more rapidly in the reinforced Bremerhaven clay than those in the reinforced Hamburg clay for all the used diameters.

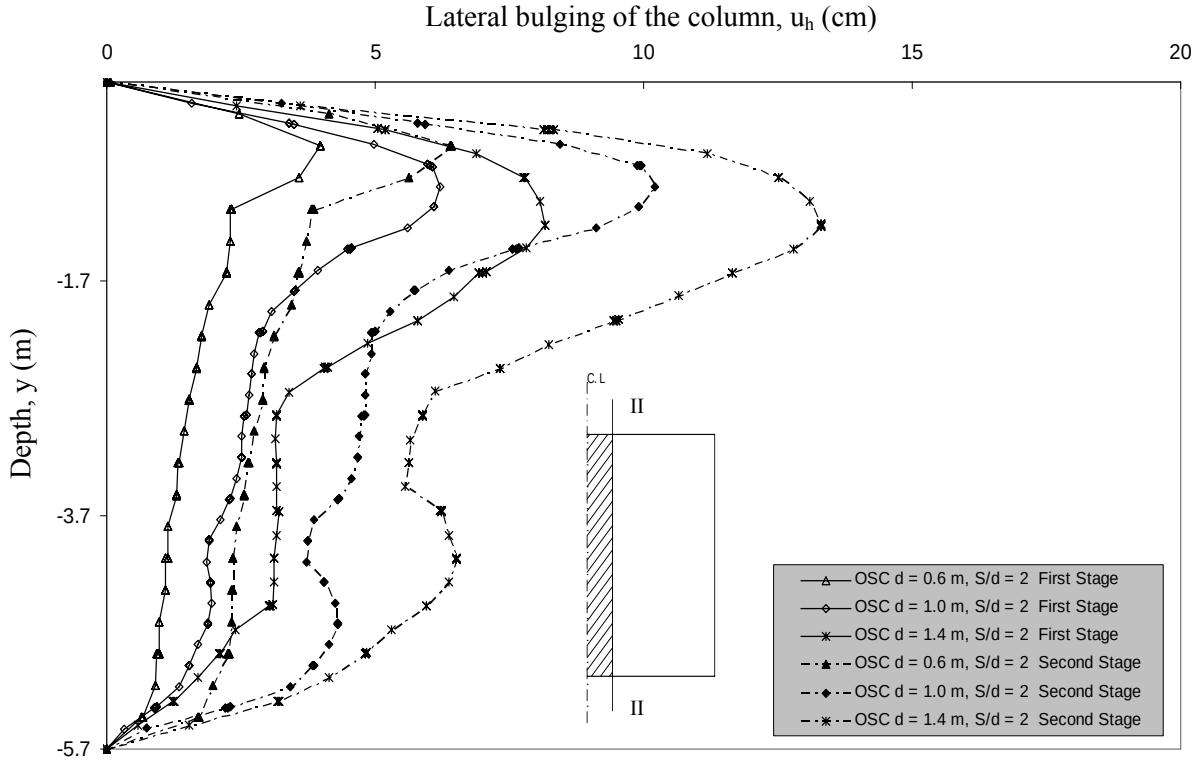

Fig. 7-24 Lateral bulging distribution of the reinforced Bremerhaven clay using stone columns with S/d = 2 and various diameters

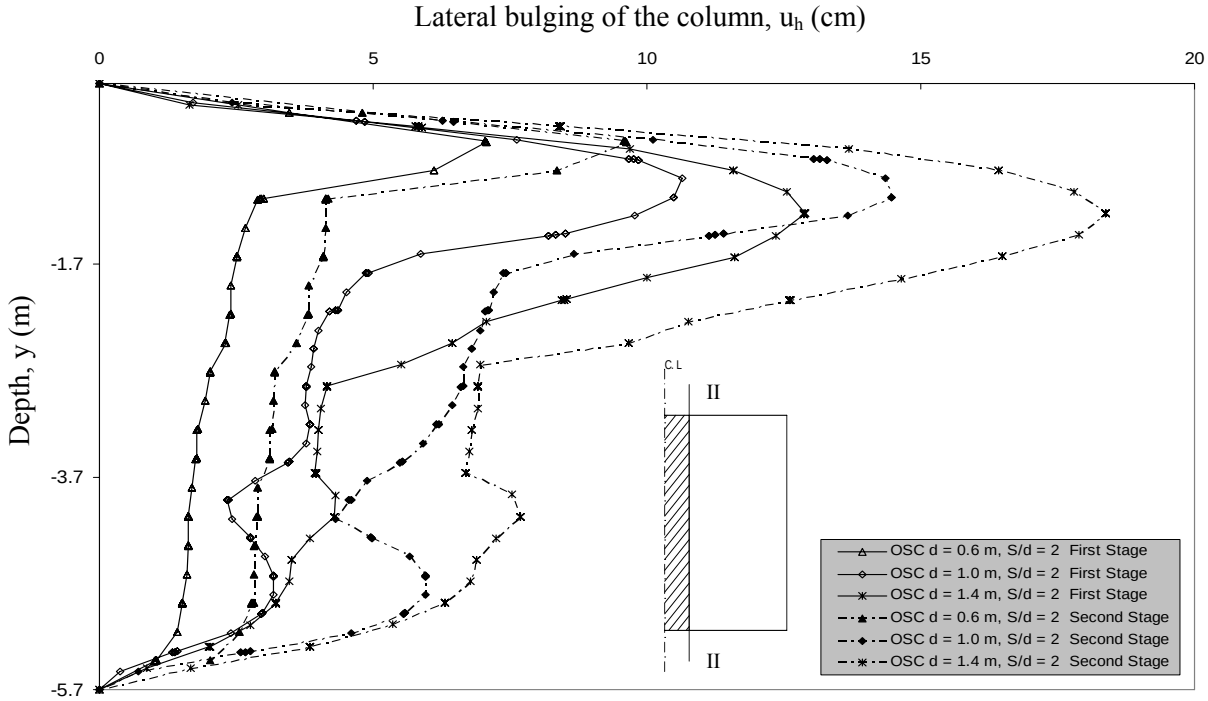

Fig. 7-25 Lateral bulging distribution of the reinforced Hamburg clay using stone columns with S/d = 2 and various diameters

The excess pore water pressure in the reinforced Hamburg clay increases during the consolidation and its dissipation consumes also a longer time with increasing diameter of the columns, as shown in Fig. 7-28 and Fig. 7-29. The smaller the column diameter is, the lower the values of the pore water pressure are and the more the excess pore water pressure dissipation is. Hence, when the Bremerhaven and the Hamburg clay are reinforced by stone columns with spacing ratio S/d = 2 and diameter of d = 0.6 m, the smallest the excess pore water pressure values along the consolidation are and the shortest the time of the pore water pressure dissipation is.

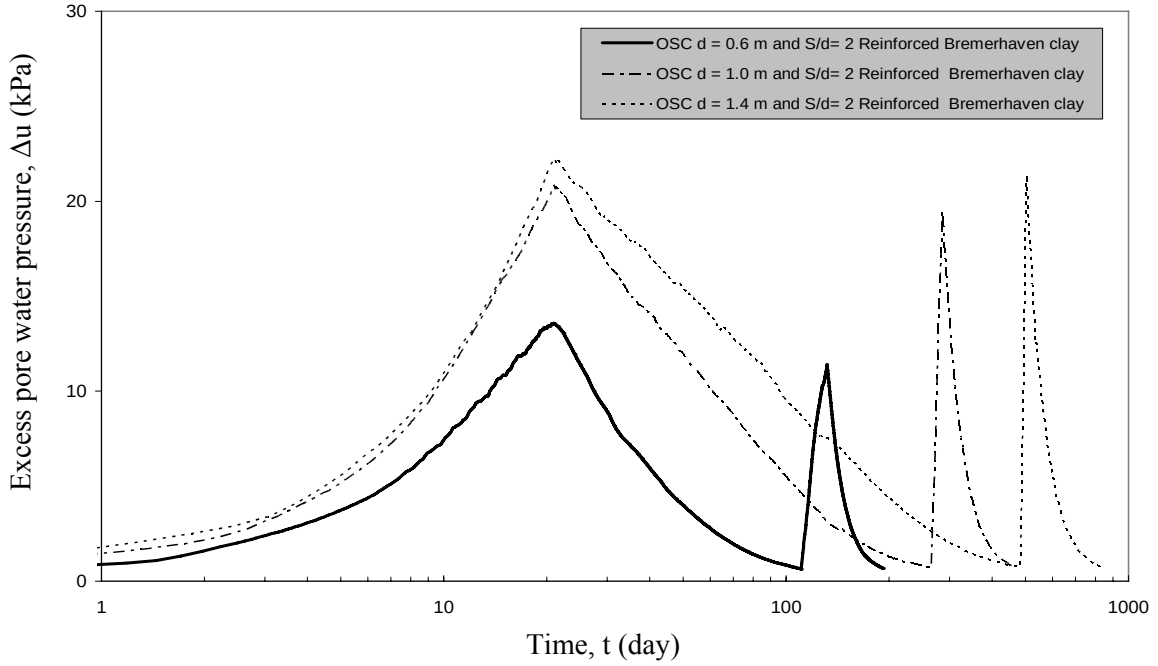

Fig. 7-26 Excess pore water pressure-time relationship for the reinforced Bremerhaven clay using stone columns with S/d = 2 and various diameters

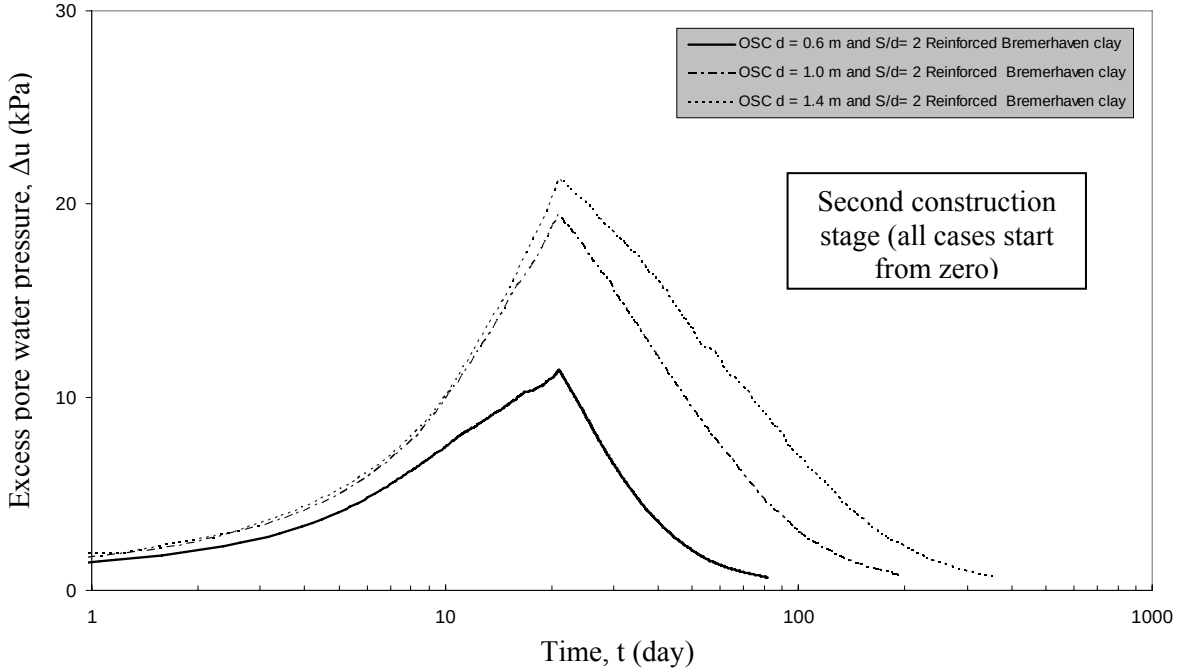

Fig. 7-27 Development of the excess pore water pressure during the second stage for the reinforced Bremerhaven clay using stone columns with various diameters

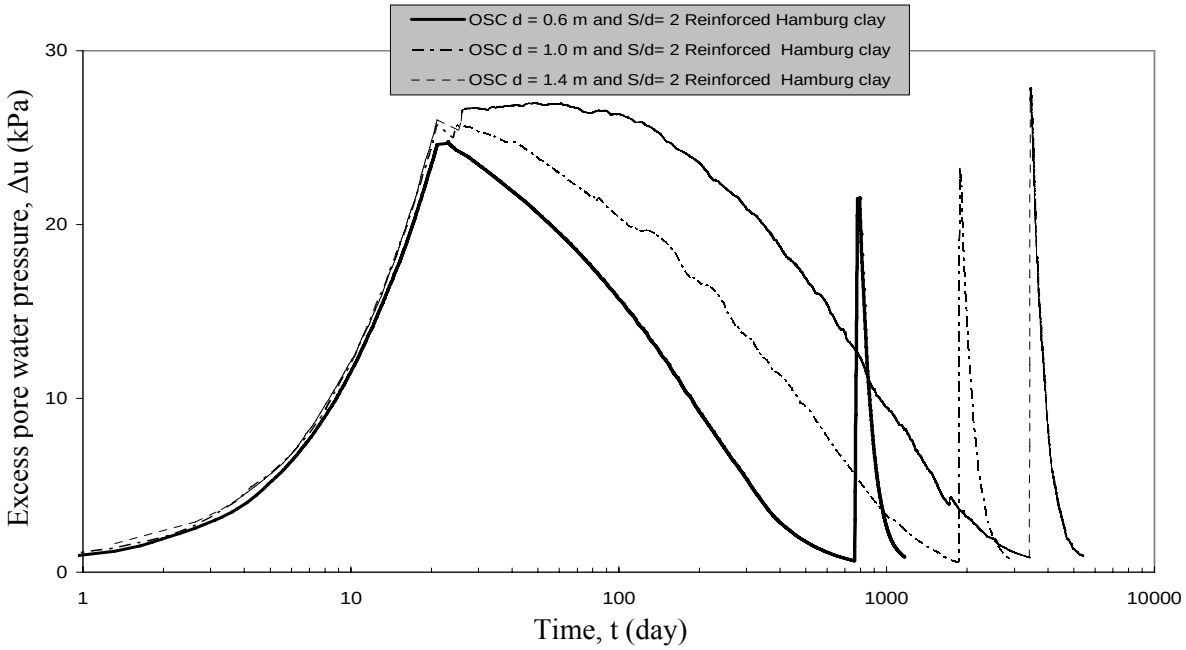

Fig. 7-28 Excess pore water pressure-time relationship for the reinforced Hamburg clay using stone columns with S/d = 2 and various diameters

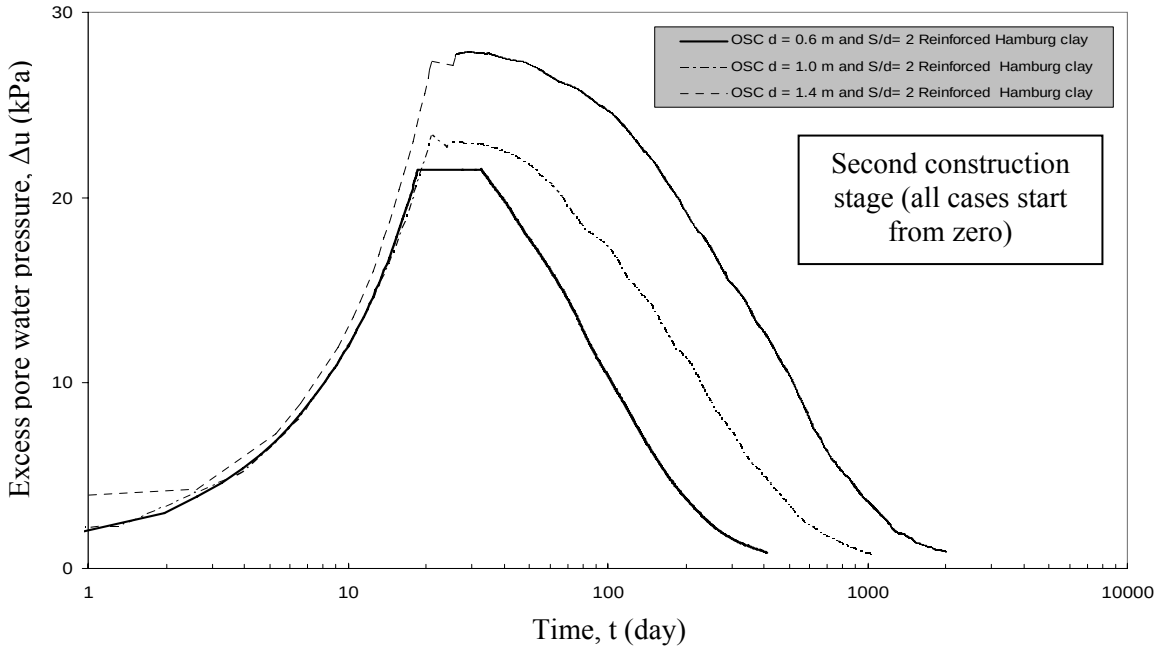

Fig. 7-29 Development of the excess pore water pressure during the second stage for the reinforced Hamburg clay using stone columns with various diameters

Stress in soil

The effective vertical stress (σ'_v) was calculated at the surface of the reinforced Bremerhaven clay and the reinforced Hamburg clay at point A, and in the column at point C, as shown in Fig. 7-1-a. The relationship of the effective vertical stress with settlement for the reinforced Bremerhaven clay and the reinforced Hamburg clay is shown in Fig. 7-30 and Fig. 7-31, respectively. The development of the effective vertical stress in both reinforced soft soils is approximately similar and also its development in the stone columns is approximately the same for the various used diameters.

The effective vertical stress in the stone column increases with increasing diameter of the columns while the vertical effective stress in the reinforced soft soil has an insignificant decrease with increasing diameter of the columns. At the same spacing ratio S/d of 2, the greater the diameter of the stone columns is, the greater the absolute spacing distance between the columns is and the higher the vertical stress in the stone columns is generated, as shown in Fig. 7-30 and 7-31. When the diameter of the columns is greater, the more stress transfers form the soft soil to and concentrates in the stone columns which leads to a reduction in the stress of the surrounding soil.

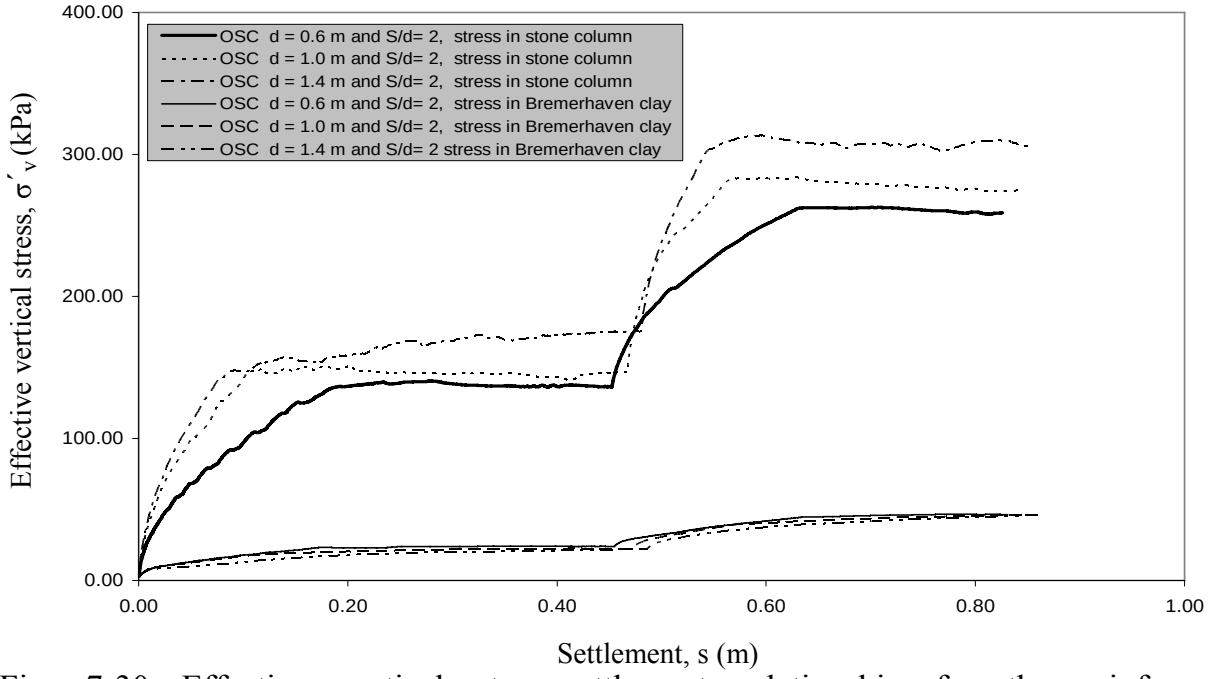

Fig. 7-30 Effective vertical stress-settlement relationship for the reinforced Bremerhaven clay at point A and for the stone column at point C

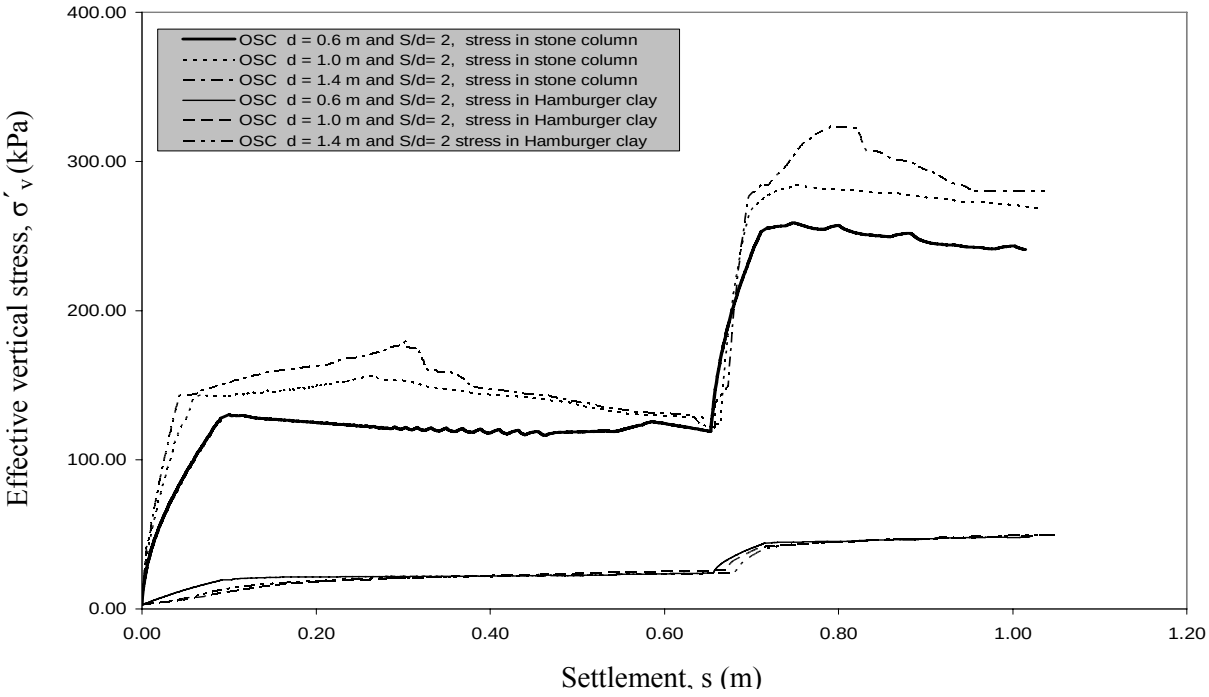

Fig. 7-31 Effective vertical stress-settlement relationship for the reinforced Hamburg clay at point A and for the stone column at point C

The total vertical stress (σ_V) was calculated in the reinforced Bremerhaven clay and in the reinforced Hamburg clay at the point (B) which is located at a depth of 2.0 m, as shown in Fig. 7-1-a. The development of the total vertical stress in both reinforced Bremerhaven clay and Hamburg clay is approximately the same for the used diameters, as shown in Fig. 7-32 and Fig. 7-33.

The total vertical stress in the reinforced Bremerhaven clay and Hamburg clay decreases with decreasing diameter of the columns through all construction phases. Hence, the smaller the diameter of the columns is, the more the reduction in the total stress of the surrounding soft soil is which leads to more improvements in the behavior of the reinforced soft soil. This is more pronounced in the reinforced Bremerhaven clay.

The rate of the reduction in the total stress during each consolidation phase of the soft soil increases with decreasing diameter of the columns. The greater the rate of the reduction of the total stress during a consolidation phase leads to a higher participation percentage of the stress transfer in the acceleration of the consolidation. Generally, the rate of the reductions of the total stress and also the participation of the stress concentration during the consolidation of the first construction stage are greater than those during the consolidation of the second construction stage. The reinforced Bremerhaven clay has greater rate of reductions in the total stress than the reinforced Hamburg clay as shown in Table 7-9. Therefore, these results emphasized that the ordinary stone columns are more effective in the Bremerhaven clay because the Hamburg clay has a lower shear strength and permeability than the Bremerhaven clay.

Table 7-9 Stress concentration participation on the acceleration of the consolidation

Stone column stress concentration effect on	% ($SC_{accel.}$) of Bremerhaven clay, (S/d = 2)			% ($SC_{accel.}$) of Hamburg clay (S/d = 2)		
	d = 0.6 m	d = 1.0 m	d = 1.4 m	d = 0.6 m	d = 1.0 m	d = 1.4 m
First construction stage	52.32	36.34	35.31	30.21	28.50	26.67
Second construction stage	41.15	31.70	17.95	26.61	25.89	24.36

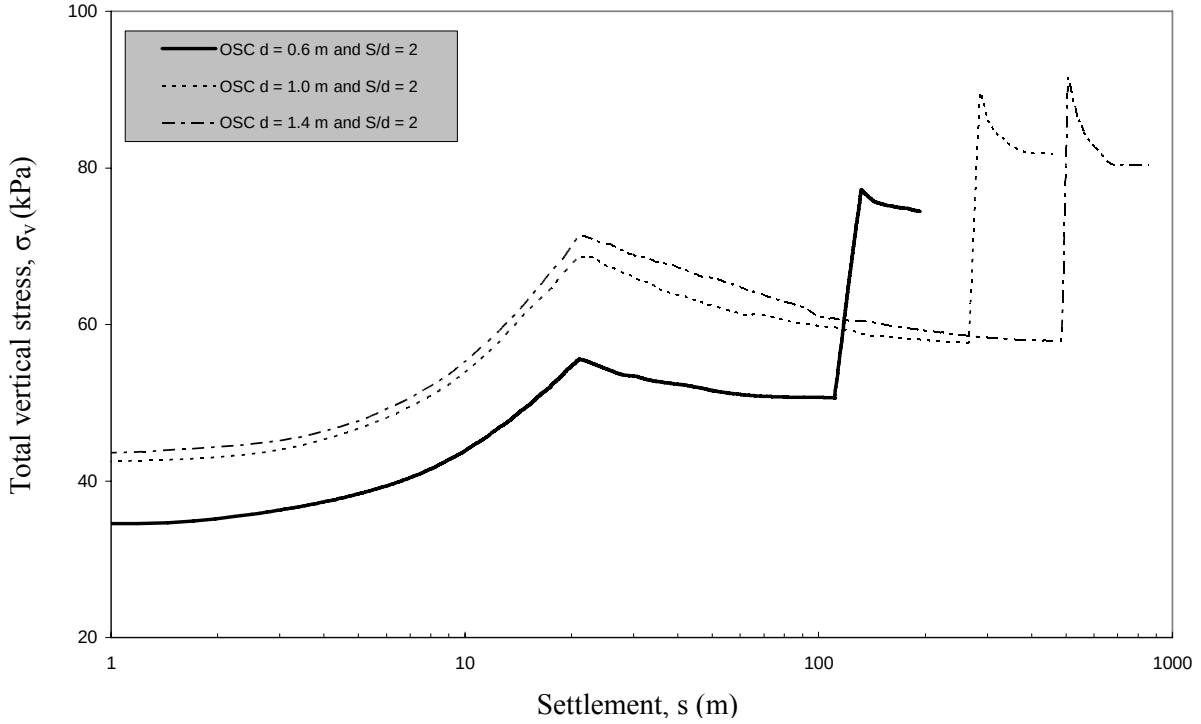

Fig. 7-32 Total vertical stress-settlement relationship of the reinforced Bremerhaven clay at point B at a depth of 2.0 m

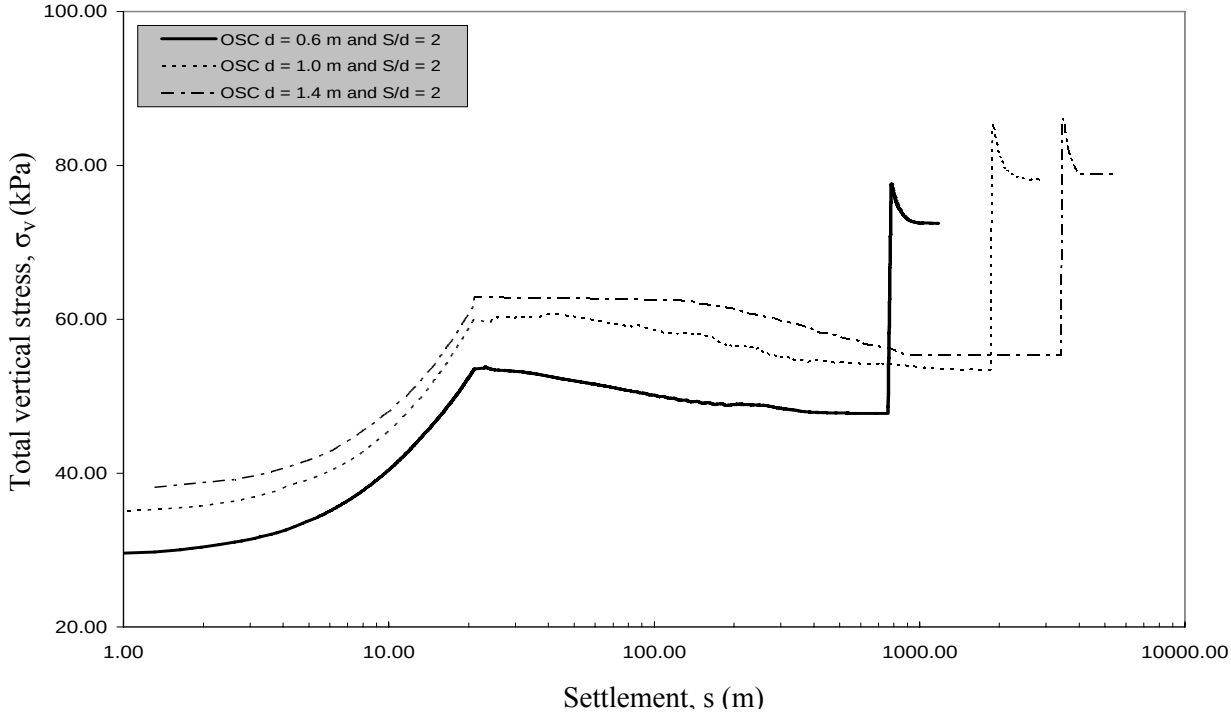

Fig. 7-33 Total vertical stress-settlement relationship of the reinforced Hamburg clay at point B at a depth of 2.0 m

8 Behavior of the Reinforced Soft Clay with Encased Stone Columns under Embankment Fill

8. 1 Introduction

The reinforced Bremerhaven and Hamburg clays with ordinary stone columns were studied in chapter 7. In the current chapter the Bremerhaven clay and the Hamburg clay are reinforced with the ordinary and the encased stone columns to study the effect of varying stiffness and depth of the encasement on the behavior of the reinforced soft soil. The reinforced soft soil has been loaded as a foundation of a highway embankment. The behavior of the reinforced soft soil has been investigated through the consolidation process. In the following sections, the modeling of the stone columns, soft soil and encasement, and the discussion of the results of the parametric study are presented. The discussion contains the effect of varying stiffness of the geogrid encasement and depth of the encasement on the reinforced soft soil settlement, consolidation time, column bulging, pore water pressure and stress in the soil.

8.2 Numerical modeling and selection of parameters

The Bremerhaven clay and the Hamburg clay layers which have a thickness of 6.0 m are reinforced by ordinary and encased stone columns. The stone columns are installed in a square orientation which was discussed in chapter 2. A blanket layer of compacted sand which has 30 cm thickness is also used. The current analyses consider that the entire area of the reinforced Bremerhaven clay and the reinforced Hamburg clay has been loaded with the sand fill as embankment loads. Fig. 8-1 shows the schematic of the models employed for these analyses. The Bremerhaven clay and the Hamburg clay have been modelled by the Soft Soil Creep model under undrained conditions while stone materials and sand fills have been modelled using Mohr Coulomb model under drained conditions. The same parameters of the soft soils, the stone and the sand which were used in chapter 7 have been used in the current analyses. The parameters of the soils are illustrated in Table 8-1.

The three types of geogrid which were used in chapter 4 have been used in the current analyses. The stone columns have been encased by Secugrid 20/20 Q1, Secugrid 30/30 Q1 and Combigrid 40/40 Q1 which have stiffness values, J of 400 kN/m, 600 kN/m and 800 kN/m, respectively as depicted in Table 8-2.

The embankment fill has been constructed to a height of 5.0 m in two equal layers. Every construction stage has a 2.5 m- layer and takes 21 days. The consolidation analyses are performed during and after each construction stage. A closed consolidation boundary is applied to both sides of the model preventing lateral drainage. The construction sequence is shown in Table 8-3 and Fig. 8-2

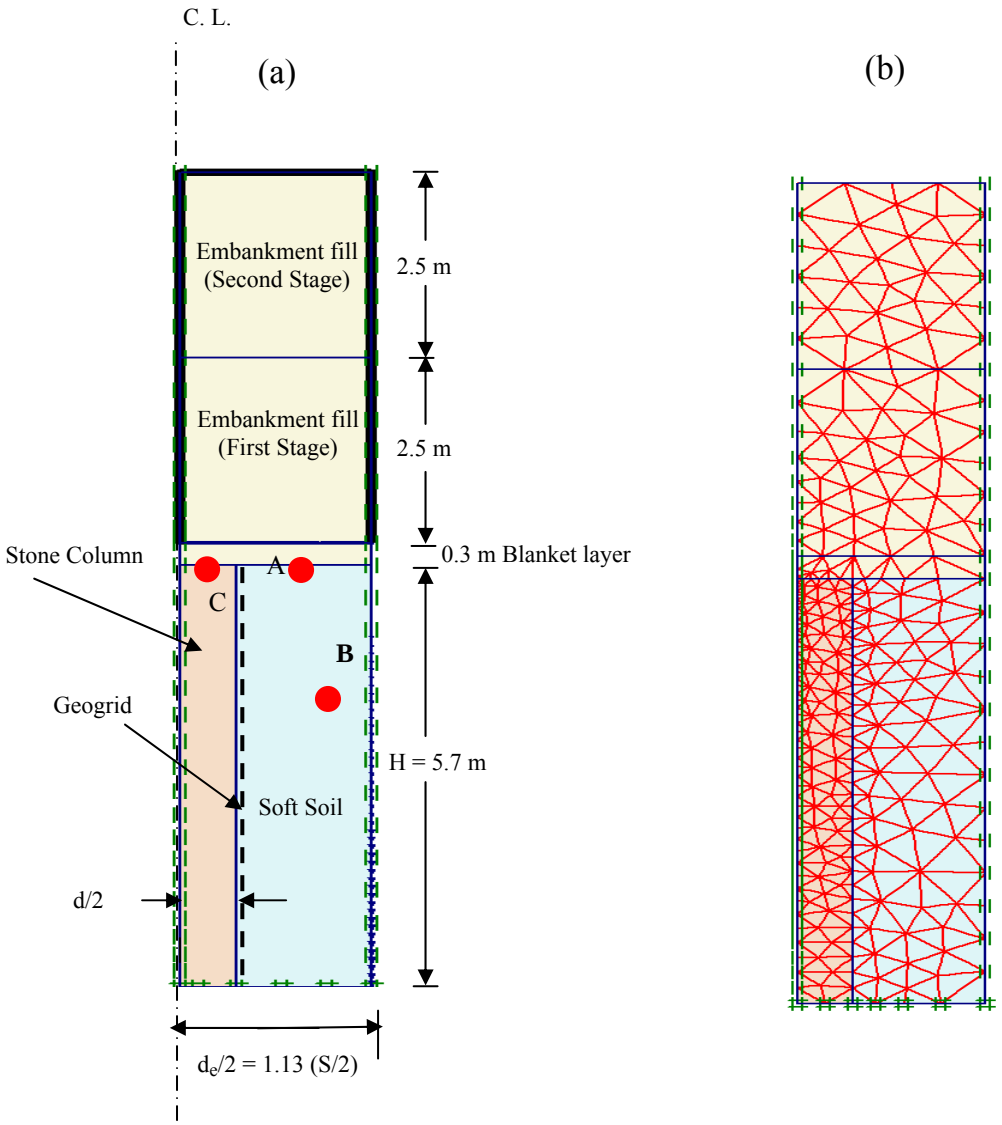

Fig. 8-1 Unit cell of the stone column reinforced soft clay (a) Model parts
(b) Finite element mesh

8.3 Discussion of the results

This part of the current research contains the analyses of the reinforced soft soil with encased stone columns. The reinforced soft soil has been loaded with the embankment fill in two stages of construction to study the effect of the encasement stiffness and the encasement depth on the behavior of the reinforced soft soil during and after the consolidation.

Table 8-4 presents the cases which have been analyzed here. This table contains two groups which will be discussed in the following paragraphs. In group A the stone column with a spacing ratio S/d of 2 and a diameter d of 0.6 m is encased with different geogrid stiffness values (J) which are 400 kN/m, 600 kN/m and 800 kN/m. In the group B the partially encased stone columns with a spacing ratio S/d of 2, a diameter d of 0.6 m and geogrid stiffness, J of 800 kN/m are used. The partial encased columns with ratios of encasement depth to column diameter h/d of 1, 2, 3, 5, 7 and

9.5 (full depth) are used to reinforce the Bremerhaven clay. Settlement, column bulging, excess pore water pressure and stress in the soil were calculated in each case.

Table 8-1 Properties and shear strength parameters used for the soils

Parameter	**Symbol**	**Stone, (Ambily and Gandhi, 2007)**	**Sand, (Ambily and Gandhi, 2007)**	**Bremer-haven clay, (Geduhn, 2005)**	**Hambu-rg clay, (Geduhn, 2005)**
Material model	Type	Mohr-Coulomb	Mohr-Coulomb	Soft Soil Creep	Soft Soil Creep
Loading	Condition	Drained	Drained	Undrained	Undrained
Wet soil unit weight	γ_{wet}, (kN/m^3)	19	18	15	13
Horizontal permeability	k_h, (m/day)	12	1	$2x10^{-4}$	$3.2x10^{-5}$
Vertical permeability	k_v, (m/day)	6	0.5	$1x10^{-4}$	$1.6x10^{-5}$
Young's modulus	E, (kN/m^2)	55,000	20,000	-	-
Poisson's ratio	υ (-)	0.3	0.3	-	-
Modified compression index	λ* (-)	-	-	0.203	0.168
Modified swelling index	κ* (-)	-	-	0.025	0.056
Modified secondary compression index	μ*	-	-	0.007	0.005
Cohesion	c$'$, (kN/m^2)	0	0	5	0
Friction angle	φ$'$ °	43	30	37.75	20
Dilatancy angle	ψ°	10	4	0	0

Table 8-2 Properties of the geogrid materials

Property	**Unit**	**Secugrid 20/20 Q1**	**Secugrid 30/30 Q1**	**Combigrid 40/40 Q1**
Raw material	-	Polypropylene (PP), white		
Mass per unit area	g/m^2	155	200	240
Max. tensile strength, md / cmd*	kN/m	20 /20	30 /30	40 /40
Elongation at nominal strength, md / cmd*	%	8 / 8		
Tensile strength at 2% elongation, md / cmd*	kN/m	8 / 8	12 / 12	16 / 16
Axial stiffness at 2% elongation, J	kN/m	400	600	800
Aperture size, md x cmd*	mm x mm	33 x 33	32 x 32	31 x 31

* Based on md = machine direction and cmd = cross machine direction

Fig. 8-1 shows the points at which the calculations were carried out. Point A is located at the top of the soil at which the maximum settlement occurs. Point B is located in the soil at a depth of 2.0 m to calculate the excess pore water pressure. Point C is located at the top of the stone column at a horizontal distance of d/4 from the column centerline in order to calculate the maximum settlement in the column.

Table 8-3 Construction sequences of the embankment fill

Stage	Phase	Fill Height, (m)	Time Consumed (day)
First	1- Construction	0-2.5	21.0
	2- Consolidation	2.5	Time is calculated until the excess pore water pressure is dissipated (1 kPa)
Second	3- Construction	2.5-5.0	21.0
	4- Consolidation	5.0	Time is calculated until the excess pore water pressure is dissipated (1 kPa)

Table 8-4 Parametric study

Group No.	Column Diameter, d (m)	Spacing ratio between Columns (S/d)	Geogrid Encasement			Surround-ing Soft Soil Conditions
			Name	Stiffness, J (kN/m)	Depth ratio (h/d)	
A	0.6	2	Secugrid 20 Secugrid 30 Combigrid 40	400 600 800	Full depth	Undrained and consolidation
B	0.6	2	Combigrid 40	800	1 2 3 5 7 9.5 (Full depth)	

8.3.1 Group (A): Effect of the encasement stiffness (J)

The Bremerhaven clay and the Hamburg clay are reinforced by encased stone columns which have a diameter of 0.6 and a spacing ratio of S/d = 2 with different encasement stiffness values, as shown in Table 8-4.

Settlement

The settlement, (s) was calculated in the surface of the reinforced Bremerhaven clay at point A, as shown in Fig. 8-1. Fig. 8-2 shows the relationship of the settlement and the embankment height along the construction time specified to the two construction stages for various encasement stiffness values. Generally, the development of the settlement with consolidation time is similar for all encasement types. Once the stone columns are encased with geogrid, the construction time and the consolidation settlement of the reinforced Bremerhaven clay are reduced with a high degree. Therefore, the encasement causes a huge increase in the bearing capacity of the reinforced clay. The consolidation settlement also decreases with increasing stiffness of the geogrid encasement, as shown in Fig. 8-2, Fig. 8-3 and Table 8-5. The reason of that is the higher the encasement stiffness is, the more the confinement and the stiffness of the overall stone column are. It is illustrated from Fig. 8-2 and Fig. 8-3

that, the consolidation time is approximately constant with increasing stiffness of the encasement. Therefore, the encasement stiffness has no significant effect on the consolidation time.

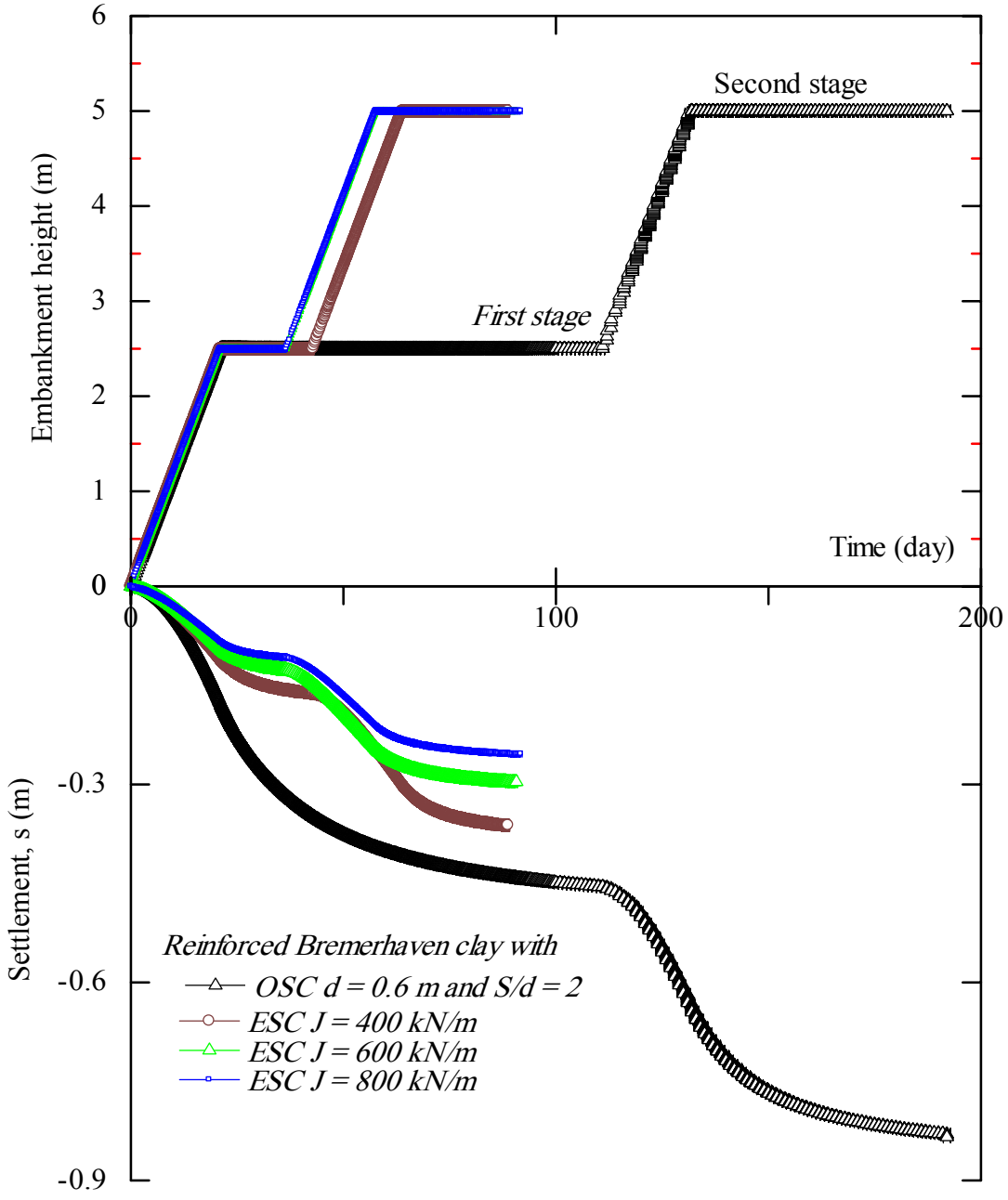

Fig. 8.2 Settlement of the reinforced Bremerhaven clay with ordinary and encased stone columns along the time of the construction

The settlement distribution at the surface of the reinforced Bremerhaven clay after the consolidation end of both construction stages is also shown in Fig. 8-4. The encasement of stone columns in the soft clay increases the bearing capacity of the soft clay by reducing settlement during the various construction phases. The greater the stiffness of the geogrid encasement is, the more the reduction of the settlement is. The settlement in the ordinary stone column and in the surrounding soft soil is constant

and approximately the same while there is a differential settlement between the encased stone columns and the surrounding soft soil, as shown in Fig. 8-4. The differential settlement is generated because of the increase in the stiffness ratio between the encased stone columns and the surrounding soft soil.

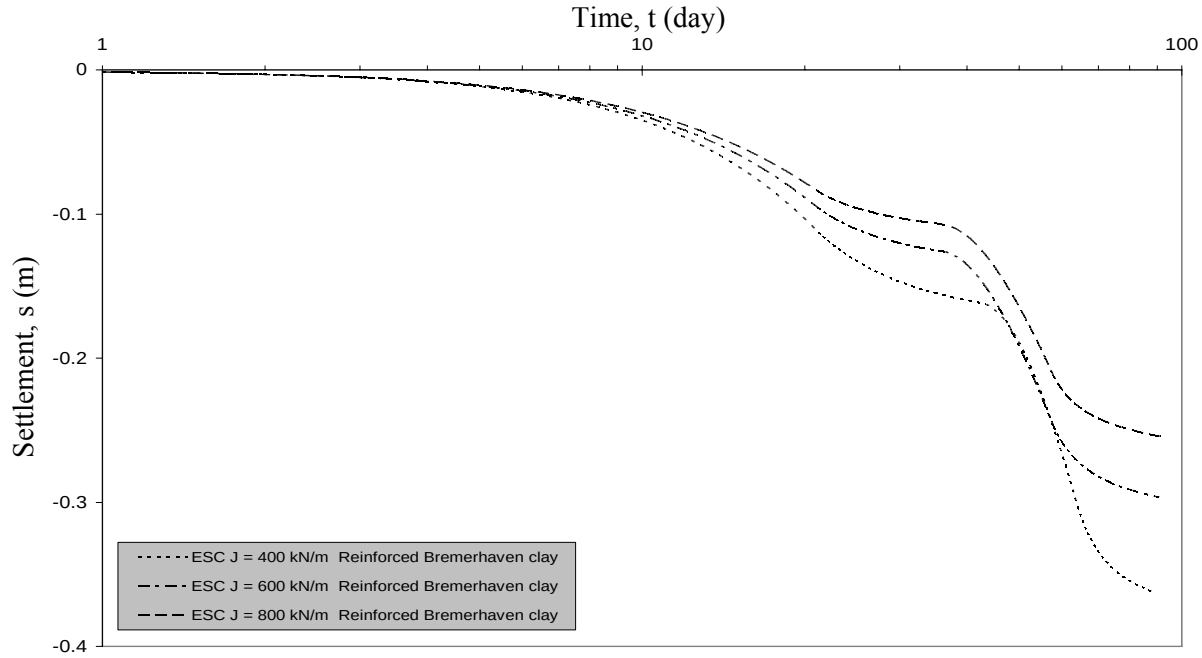

Fig. 8-3 Time-settlement relationship for the reinforced Bremerhaven clay with encased stone columns using different encasement stiffness values

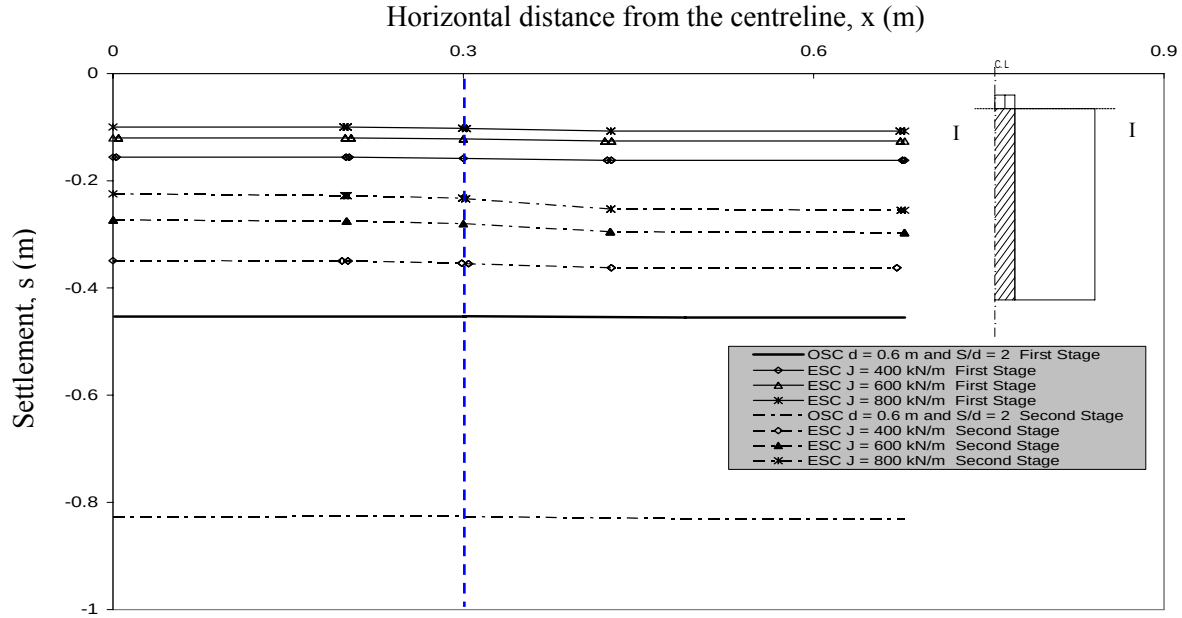

Fig. 8-4 Settlement distributions at the surface of the reinforced Bremerhaven clay with encased stone columns using different encasement stiffness values

Therefore, the settlement decreases after each construction stage with increasing geogrid stiffness. The reduction in the settlement when the geogrid stiffness rises from J = 400 kN/m to J = 600 kN/m is greater than that when the geogrid stiffness rises from J = 600 kN/m to J = 800 kN/m, as shown in Table 8-5. The encased stone

columns with geogrid stiffness of J = 800 kN/m in Bremerhaven clay reduces the settlement to 12.9 % of the non-reinforced clay settlement and to 28.6 % of the ordinary column-reinforced clay settlement.

Table 8-5 Reductions in the settlement of the reinforced Bremerhaven clay

Case of the soft Soil	Consolidation end of the first construction stage			Consolidation end of the second construction stage		
	Settlement, s (m)	$R_{s(NR)}$ (%)	$R_{s(R)}$ (%)	Settlement, s (m)	$R_{s(NR)}$ (%)	$R_{s(R)}$ (%)
Non-reinforced Bremerhaven clay	1.31	-	-	1.86	-	-
Reinforced clay with OSC d = 0.6 m and S/d = 2	0.46	35.1	-	0.84	45.2	-
Reinforced clay with ESC, J = 400 kN/m	0.16	12.2	35.1	0.36	19.4	42.9
Reinforced clay with ESC, J = 600 kN/m	0.12	9.2	26.1	0.29	15.6	34.5
Reinforced clay with ESC, J = 800 kN/m	0.1	7.6	21.7	0.24	12.9	28.6

$R_{s(NR)}$ is the ratio between the total settlement of the reinforced soft soil with encased columns and the total settlement of the non-reinforced clay. $R_{s(R)}$ is the ratio between the total settlement of the reinforced clay with encased stone columns and the total settlement of the reinforced clay with ordinary stone columns.

Fig. 8-5 shows the relationship of the time versus the construction of the embankment and versus the settlement for the reinforced Hamburg clay with ordinary and encased stone columns. In general, the development of the settlement along consolidation time also is approximately similar for all the encasement stiffness values. The encasement of the stone column causes a great reduction in the consolidation settlement which leads to a huge increase in the bearing capacity of the reinforced soil. The consolidation settlement also decreases with increasing stiffness of the geogrid encasement, as shown in Fig. 8-5 and Fig. 8-6. The reason of that is the increase of the encasement stiffness leads to increase the confinement and the stiffness of the overall stone column. It is also illustrated from Fig. 8-5 and Fig. 8-6 that, the consolidation time of the reinforced Hamburg clay isn't dependable on the encasement stiffness. Therefore, the encasement stiffness has no significant effect on the consolidation time when it is used to encase the stone column in the Hamburg clay.

The reinforced Hamburg clay has longer consolidation time and greater settlement than the reinforced Bremerhaven clay for all the encasement stiffness values. Using encased stone columns in Hamburg clay causes only a reduction of the settlement while the encased stone column in the Bremerhaven clay causes a reduction in the settlement and an acceleration of the consolidation time.

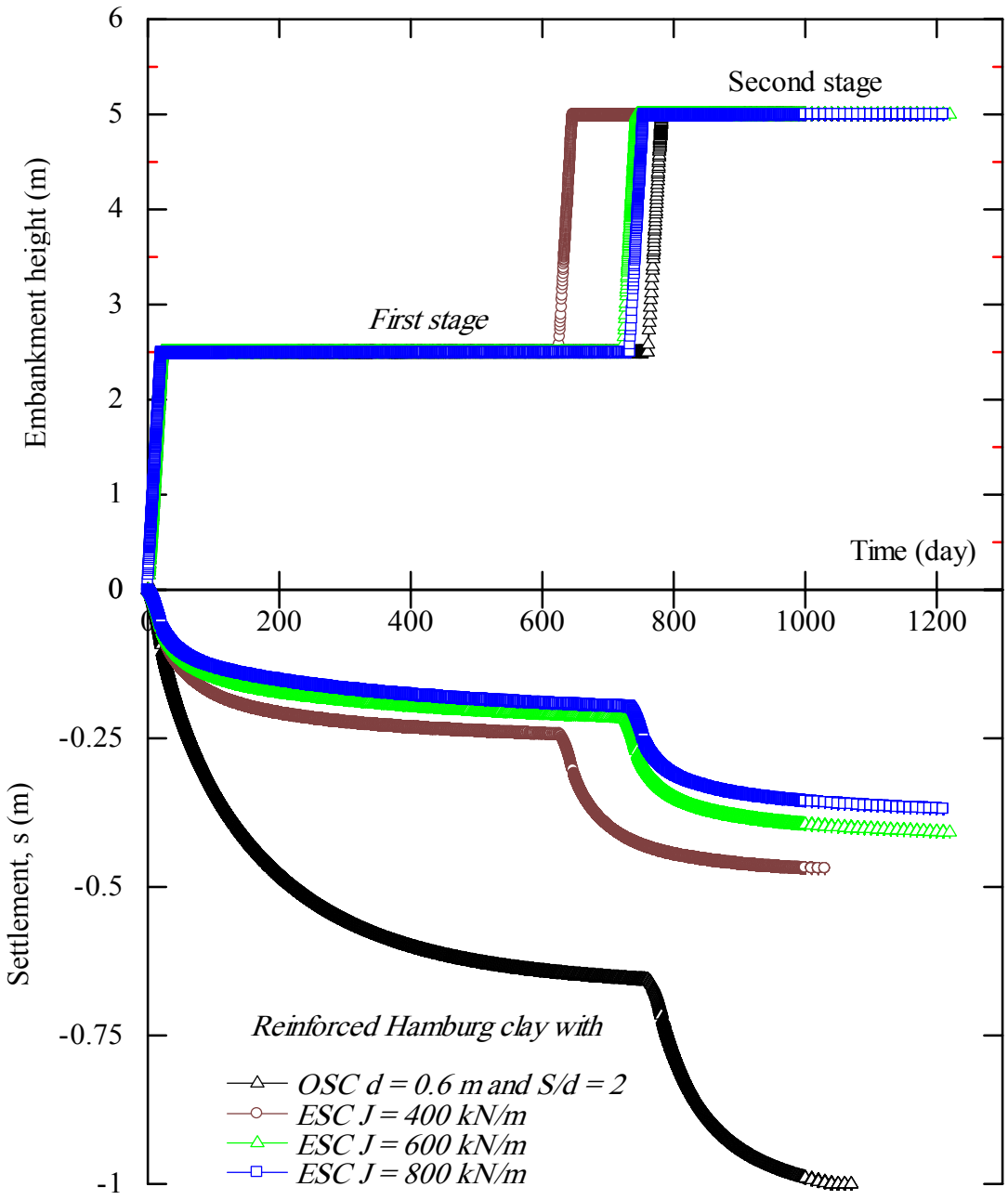

Fig. 8.5 Settlement of the reinforced Hamburg clay with encased stone columns along the time of the construction

The settlement distribution at the surface of the reinforced Hamburg clay after the consolidation end of both construction stages is also shown in Fig. 8-7. The encasement of stone columns in Hamburg clay increases the bearing capacity of the soft clay by reducing settlement during the various construction phases. The settlement of the reinforced Hamburg clay decreases with increasing stiffness of the encasement, as illustrated also in Table 8-6. The higher the stiffness of the geogrid encasement is, the more the reduction of the settlement is. The encased stone columns with geogrid stiffness of J = 800 kN/m in Hamburg clay reduces the settlement to 17.1 % of the non-reinforced clay settlement and to 35.0 % of the ordinary columns-reinforced clay settlement. The settlement in the ordinary stone column and in the surrounding soft soil is constant and approximately the same while there is a

differential settlement between the encased stone columns and the surrounding Hamburg clay, as shown in Fig. 8-7. The differential settlement increases with increasing encasement stiffness which is clearer in the Hamburg clay than the Bremerhaven clay.

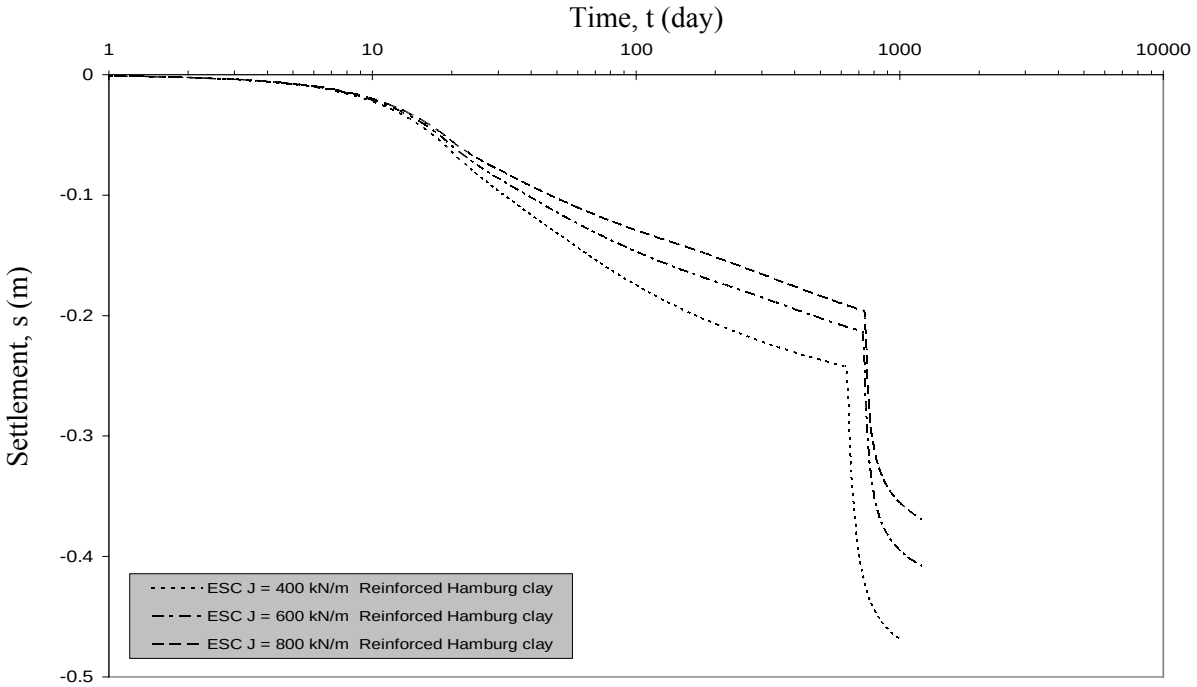

Fig. 8-6 Time-settlement relationship for the reinforced Hamburg clay with encased stone columns using different encasement stiffness values

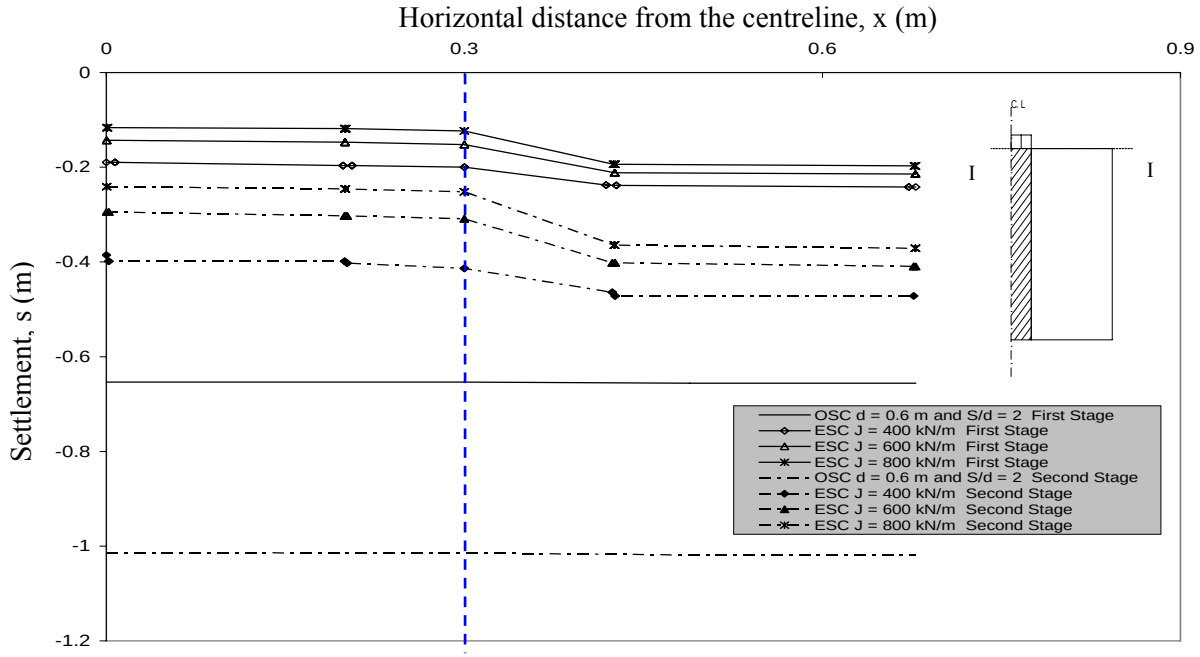

Fig. 8-7 Settlement distributions at the surface of the reinforced Hamburg clay with encased stone columns using different encasement stiffness values

The reinforced Hamburg clay induces a settlement and consolidation time greater than those of the reinforced Bremerhaven clay. The reason is that the Hamburg clay has smaller shear strength and permeability than the Bremerhaven clay.

Table 8-6 Reductions in the settlement of the reinforced Hamburg clay

Case of the soft Soil	Consolidation end of the first construction stage			Consolidation end of the second construction stage		
	Settlement, s (m)	$R_{s(NR)}$ (%)	$R_{s(R)}$ (%)	Settlement, s (m)	$R_{s(NR)}$ (%)	$R_{s(R)}$ (%)
Non-reinforced Hamburg clay	1.58	-	-	2.11	-	-
Reinforced clay with OSC d = 0.6 m and S/d = 2	0.66	41.6	-	1.03	48.3	-
Reinforced clay with ESC, J = 400 kN/m	0.24	15.2	36.3	0.47	22.3	45.3
Reinforced clay with ESC, J = 600 kN/m	0.21	13.3	31.8	0.40	19.0	38.8
Reinforced clay with ESC, J = 800 kN/m	0.19	12.0	28.8	0.36	17.1	35.0

Lateral bulging of the stone column

The lateral bulging of the stone column, (u_h) was calculated after each consolidation phase in the reinforced Bremerhaven clay and Hamburg clay, as shown in Fig. 8-8 and Fig. 8-9, respectively. Once the stone column is encased, its bulging decreases largely and becomes organized along the stone column. The lateral bulging of the encased stone columns in the Bremerhaven and the Hamburg clays shows a similar distribution for all encasement stiffness values. The lateral bulging of the encased stone columns decreases and becomes more organized with increasing geogrid stiffness. The higher the encasement stiffness is, the more the confinement and the stiffness of the overall encased stone column are which leads to increase the bearing capacity of the reinforced soft soil. The lateral bulging along the encased stone column increases with increasing load causing more load transfer to the lower depths during the consolidation. The ordinary and the encased stone columns in Hamburg clay implies greater lateral bulging than those in Bremerhaven clay. The reason of that is thus surrounding clay provides with a weaker lateral support and it has lower shear strength than the surrounding Bremerhaven clay

Radial hoop tension forces

Fig. 8-10 and Fig. 8-11 show the radial hoop tension forces in geogrid materials distributed along the stone column in Bremerhaven and Hamburg clays after the first and the second consolidation stage, respectively. Generally, the development of the hoop tension forces of the encased stone columns in Bremerhaven clay and Hamburg clay is approximately similar. The hoop tension forces start with a value at the top. Below that, the hoop tension forces increase downwards until they reach a maximum value at a depth of approximately 1.1 times the diameter of the column in Bremerhaven clay and 2.5 times the diameter of the column in Hamburg clay. Beyond that, the hoop tension force values decrease gradually to reach zero at the column base. The hoop tension force distribution is similar to that for the lateral bulging of the stone column.

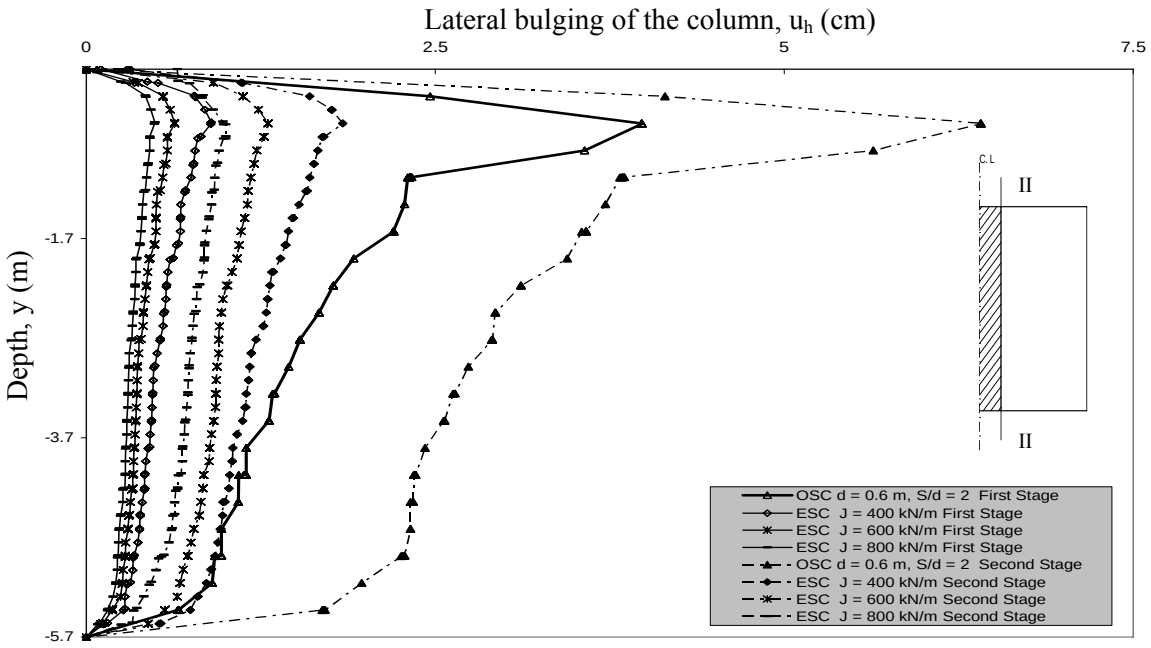

Fig. 8-8 Lateral bulging distribution of the ordinary and the encased stone columns surrounded by the Bremerhaven clay using different encasement stiffness values

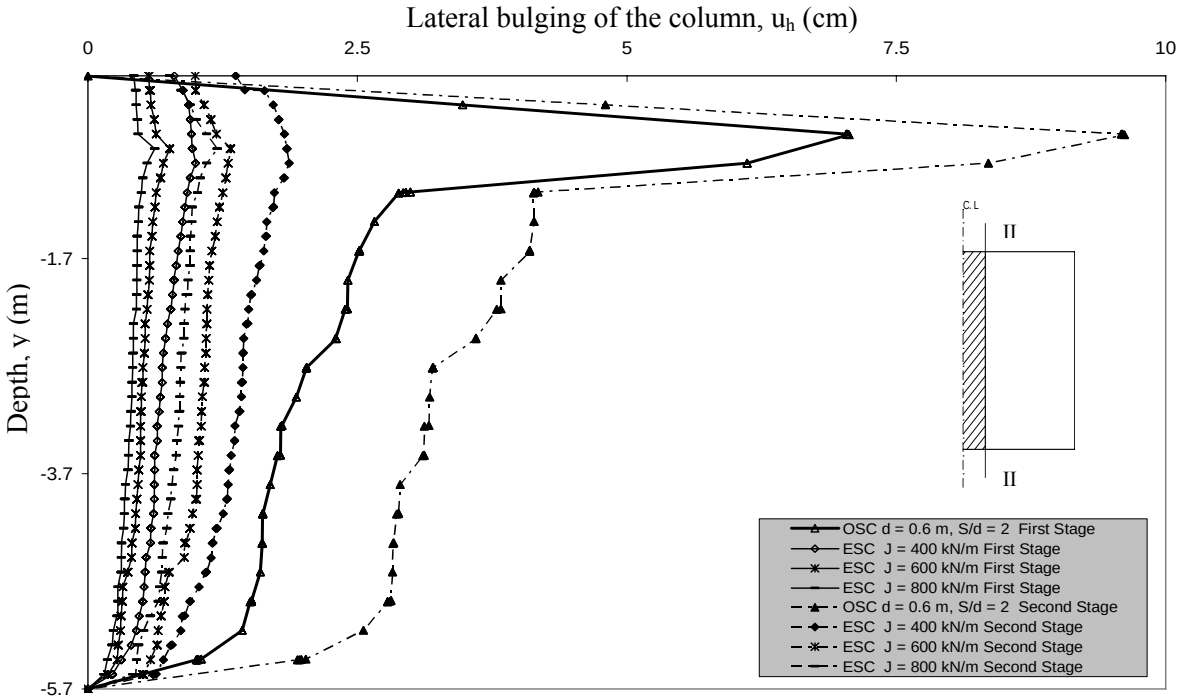

Fig. 8-9 Lateral bulging distribution of the ordinary and the encased stone columns surrounded by the Hamburg clay using different encasement stiffness values

The hoop tension forces increase with increasing geogrid encasement stiffness. The degree of improvement in encased stone column-soft soil foundation behavior increases with increasing hoop tension forces in the encasement material. Hence, the higher the stiffness of the geogrid encasement is, the more the generated radial forces in the encasement and the more the enhancement in the reinforced soil behavior are.

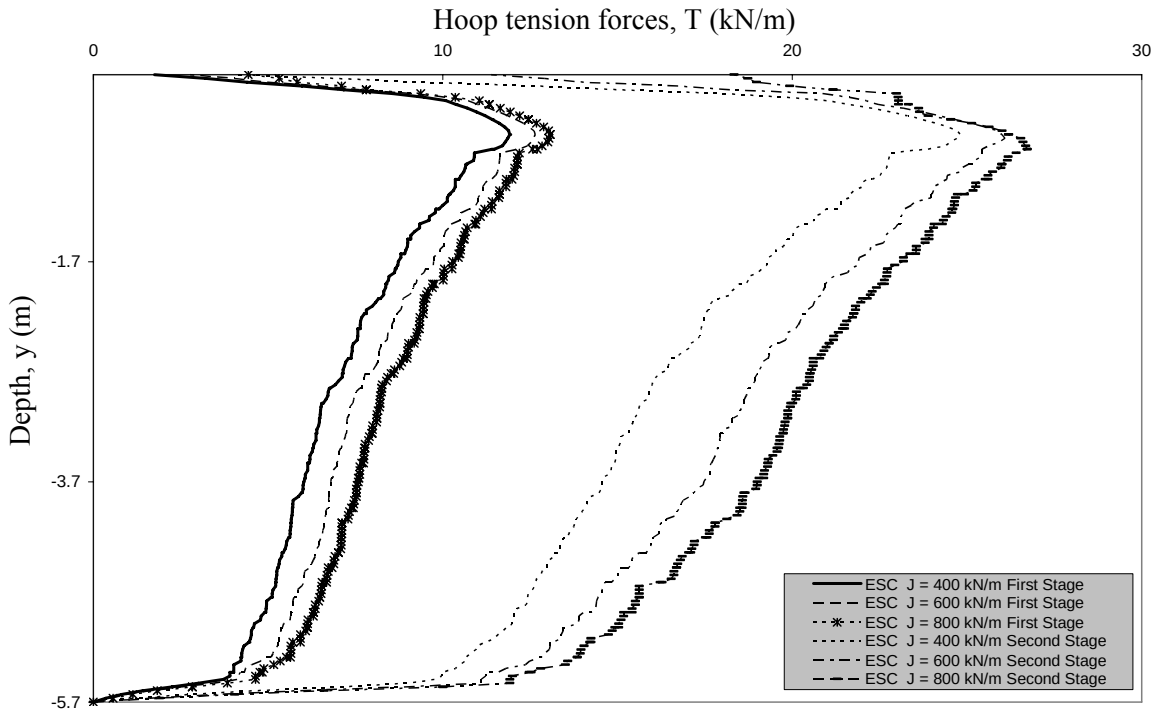

Fig. 8-10 Hoop tension force distribution of the reinforced Bremerhaven clay with encased stone columns using different encasement stiffness values

In the other side, the encasement in the reinforced Hamburg clay induces tension forces somewhat greater than that in the reinforced Hamburg clay for various geogrid stiffness values. This is due to the surrounding Hamburg clay has a weaker lateral support than the surrounding Bremerhaven clay. Hence, the lower the lateral support from the surrounding soft soil to the encased stone columns is, the higher the generated hoop tension forces in the encasement are.

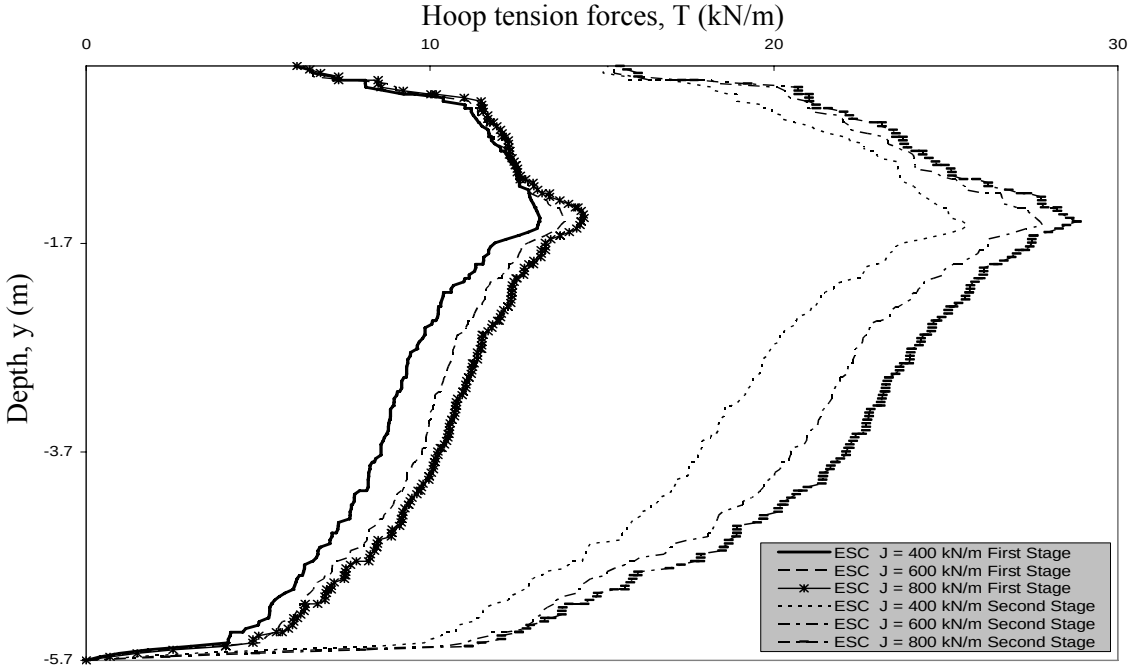

Fig. 8-11 Hoop tension force distribution of the reinforced Hamburg clay with encased stone columns using different encasement stiffness values

Excess pore water pressure

The excess pore water pressure (Δu) in the reinforced Bremerhaven clay and in the reinforced Hamburg clay was calculated at point B which is located at a depth of 2.0 m, as shown in Fig. 8-1. As soon as the fill load is applied on the saturated soft soil, the excess pore water pressure builds up. The excess pore water pressure increases with time until it reaches maximum values at the end of the construction of each stage of the reinforced Bremerhaven and Hamburg clay. After that, the excess pore water pressure decreases gradually during the consolidation directing to the steady state case, as shown in Fig. 8-12 and Fig. 8-14. The first and the second stage of constructions imply the same behavior of the excess pore water pressure through the consolidation time.

The excess pore water pressure in the reinforced Bremerhaven clay with encased stone column decreases and its dissipation consumes shorter time in comparison with the reinforced Bremerhaven clay with ordinary stone columns. The excess pore water pressure in the reinforced Bremerhaven clay with encased stone columns decreases with increasing stiffness of the encasement, as illustrated in Fig. 8-12 and Fig. 8-13.

The excess pore water pressure in the reinforced Hamburg clay with encased stone columns induces lower values in comparison with the reinforced Hamburg clay with ordinary stone columns. The greater the stiffness of the geogrid encasement is, the lower the excess pore water pressure values during all the construction phases are, as shown in Fig. 8-14 and Fig. 8-15. Therefore, when the Bremerhaven and the Hamburg clay are reinforced by encased stone columns with encasement stiffness of J = 800 kN/m, the smallest the pore water pressure values along the consolidation are in the reinforced soil compared to the other cases.

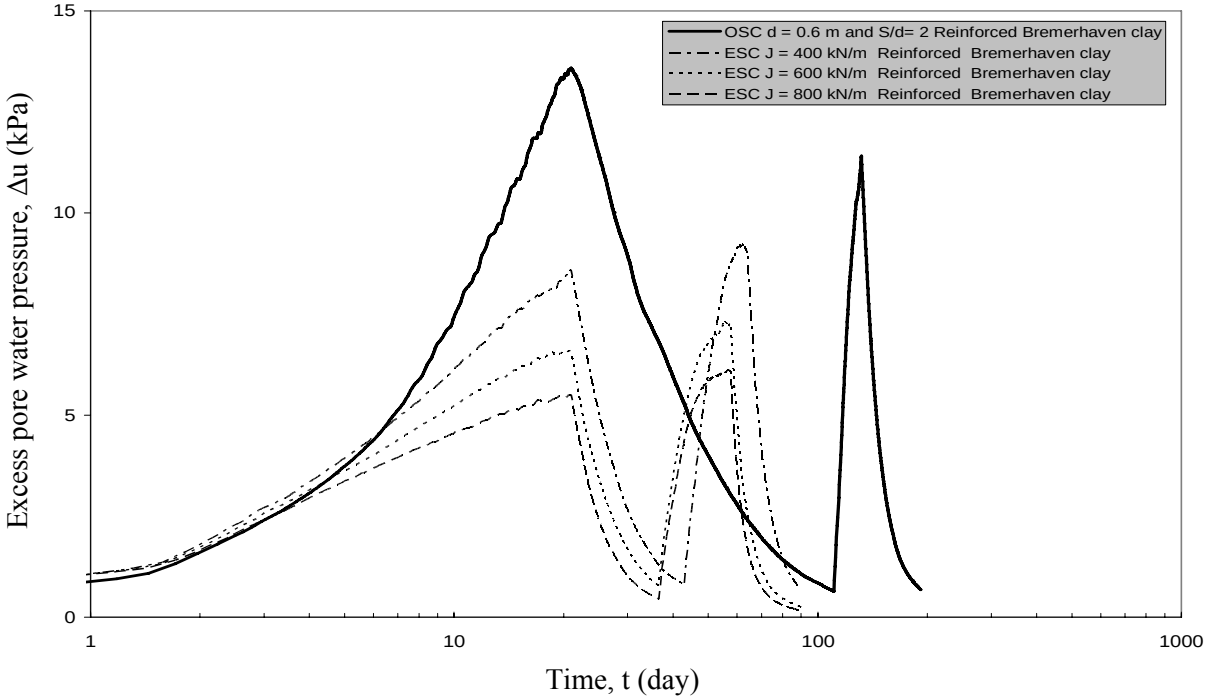

Fig. 8-12 Excess pore water pressure-time relationship for the reinforced Bremerhaven clay with ordinary and encased stone columns (ESC)

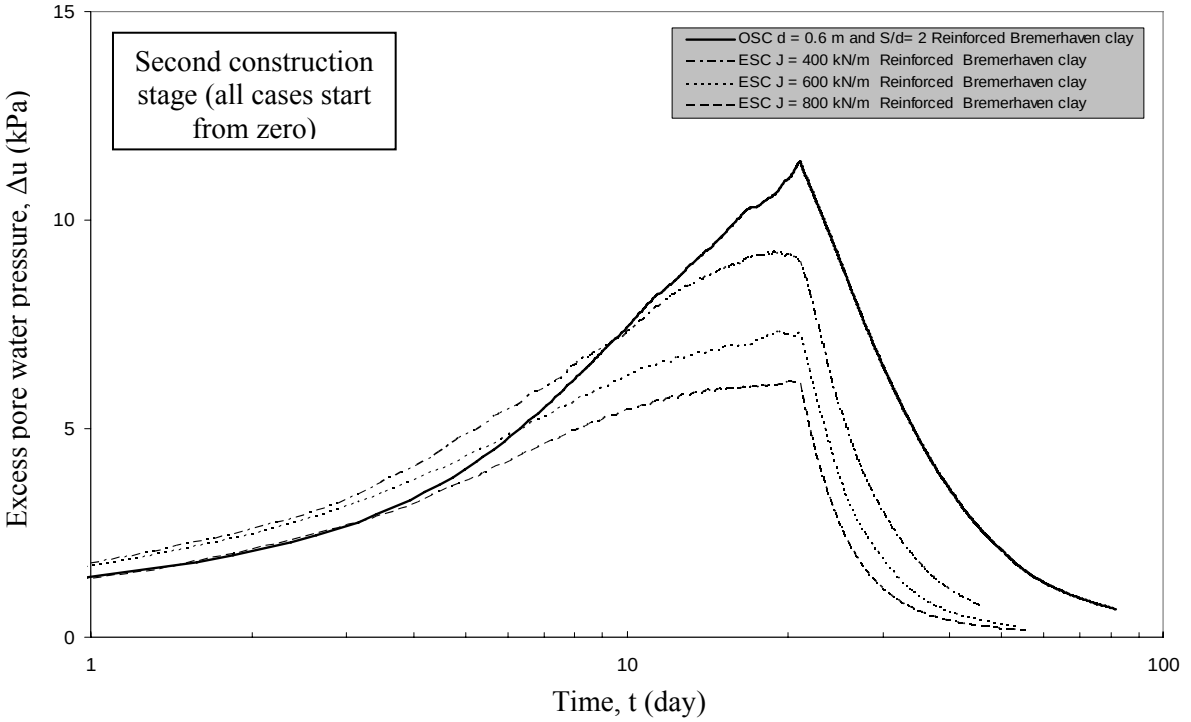

Fig. 8-13 Development of excess pore water pressure during the second loading stage for the reinforced Bremerhaven clay with ordinary and encased stone columns (ESC)

In general, the excess pore water pressure implies higher values along the consolidation and consumes longer consolidation time in the Hamburg clay than in the Bremerhaven clay. This is due to that the Hamburg clay has lower permeability than the Bremerhaven clay.

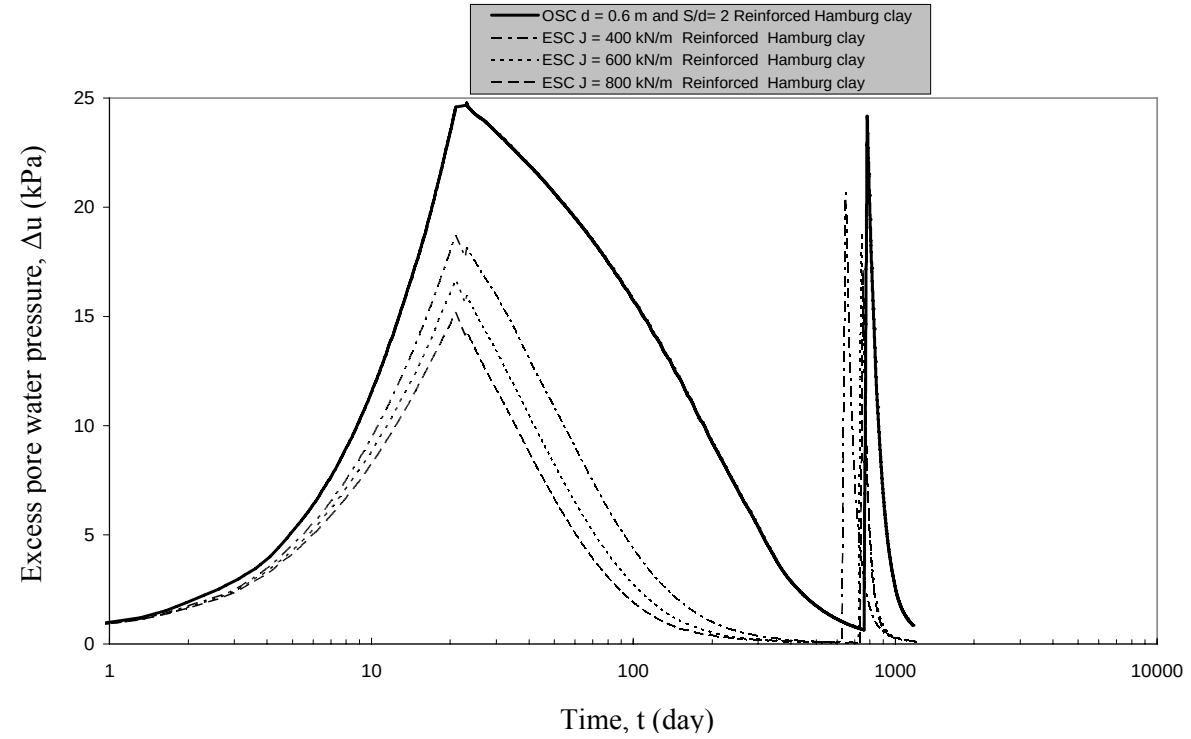

Fig. 8-14 Excess pore water pressure-time relationship for the reinforced Hamburg clay with ordinary and encased stone columns (ESC)

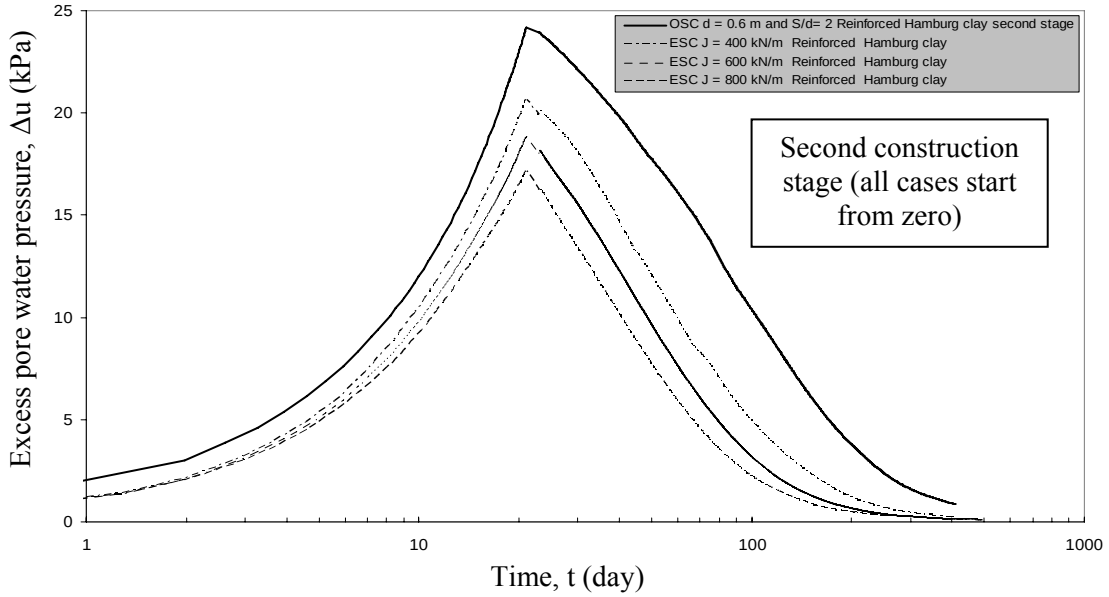

Fig. 8-15 Development of excess pore water pressure during the second loading stage for the reinforced Hamburg clay with ordinary and encased stone columns (ESC)

Stress in soil

The effective vertical stress (σ'_v) was calculated at the surface of the reinforced soft soil at point A, and at the top of the column at point C, as shown in Fig. 8-1-a. The relationships of the effective vertical stress with settlement for the stone columns and the reinforced Bremerhaven clay are shown in Fig. 8-16 and Fig. 8-17, respectively. The relationships of the effective vertical stress with settlement for the stone columns and the reinforced Hamburg clay are shown in Fig. 8-18 and Fig. 8-19, respectively. The trends of the effective stress of the stone columns in the Bremerhaven clay and in the Hamburg clay are approximately similar. The development of the effective stress with settlement in the reinforced Bremerhaven clay and the Hamburg clay is also approximately similar.

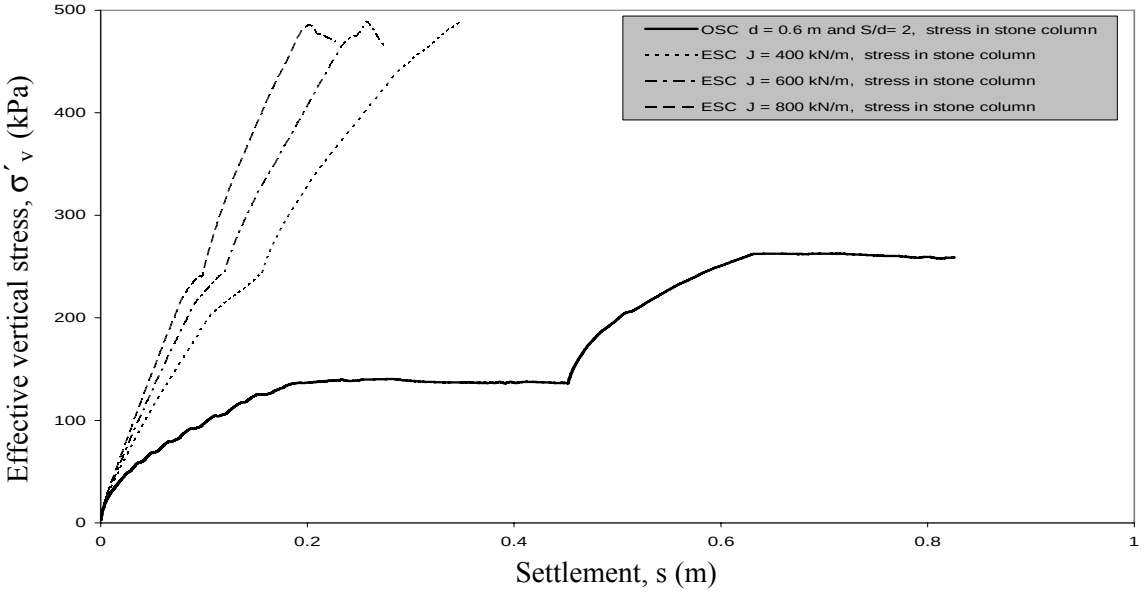

Fig. 8-16 Effective vertical stress-settlement relationship for the ordinary and encased stone columns in Bremerhaven clay at point C

The effective vertical stress in the encased stone columns is higher than that in the ordinary stone columns. This is because the encasement increases the stiffness of the overall stone columns which leads to increase the stress concentration in and the stress transfer to the encased stone columns. The effective vertical stress in the encased stone columns increases and the settlement decreases with increasing stiffness of the geogrid encasement, as illustrated in Fig. 8-16 and Fig. 8-18. At the last period of the second stage of consolidation, the encased stone columns imply maximum values of effective stress which increase with decreasing encasement stiffness.

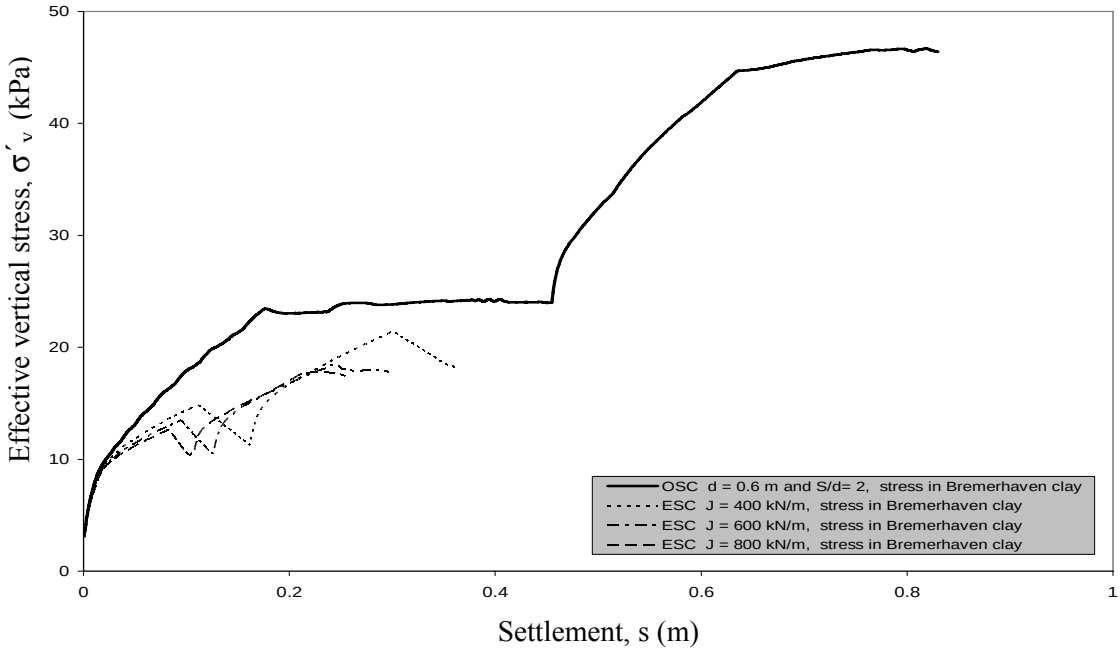

Fig. 8-17 Effective vertical stress-settlement relationship for the reinforced Bremerhaven clay at point A

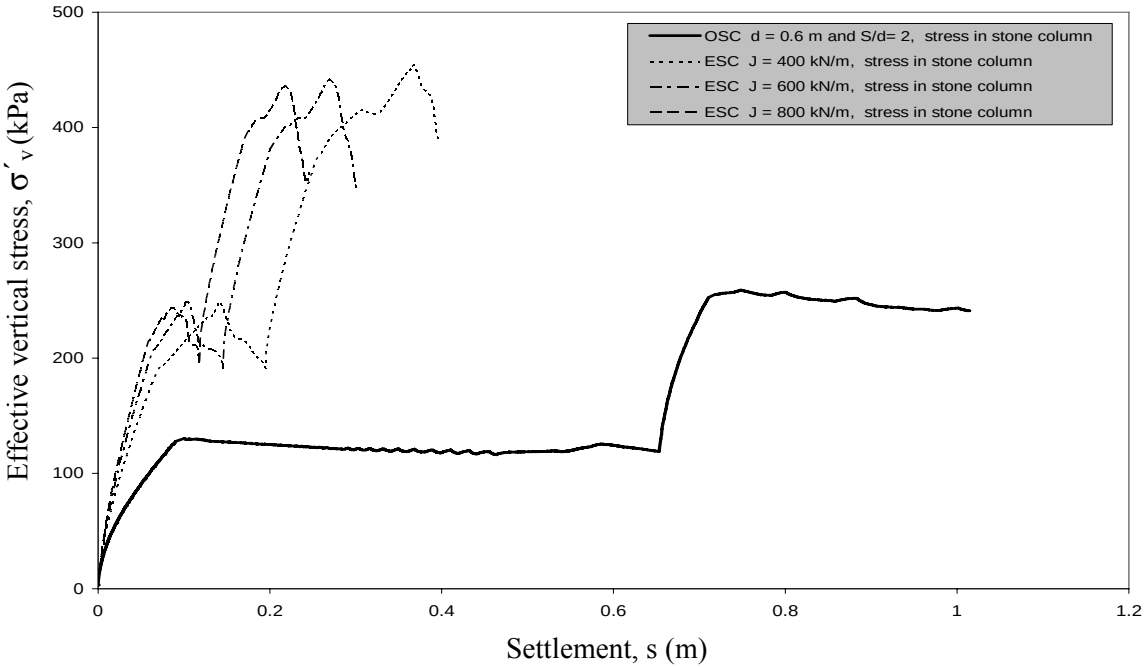

Fig. 8-18 Effective vertical stress-settlement relationship for the ordinary and the encased stone columns in Hamburg clay at point C

In contrast, the encasement of the stone column causes reduction of the effective stress in the surround soft soil, as shown in Fig. 8-17 and Fig. 8-19. The effective stress in the surrounding soil decreases with increasing stiffness of the geogrid encasement which also causes reduction in the settlement of the soft soil. This phenomenon is due to the stress transfer from the surrounding soft soil to the encased stone column which increases with increasing encasement stiffness. Therefore, the higher the encasement stiffness is, the more the stiffness of the overall encased column is. The increase in the stiffness of the overall encased stone column leads to increase the stress concentration in the column and to increase also the stress transfer from the surrounding soil. The stress concentration phenomenon has an important role in reducing settlement and increasing bearing capacity of the reinforced soil.

In general, the encased stone columns in the Hamburg clay have vertical effective stress slightly lower than that in the Bremerhaven clay through all the construction phases. This is due to the stress transfer from the Bremerhaven clay is greater than the stress transfer from the Hamburg clay. Hence, the settlement in the reinforced Bremerhaven clay is smaller than that in the Hamburg clay. It can be concluded that the encased stone columns are more effective in the Bremerhaven clay than in the Hamburg clay.

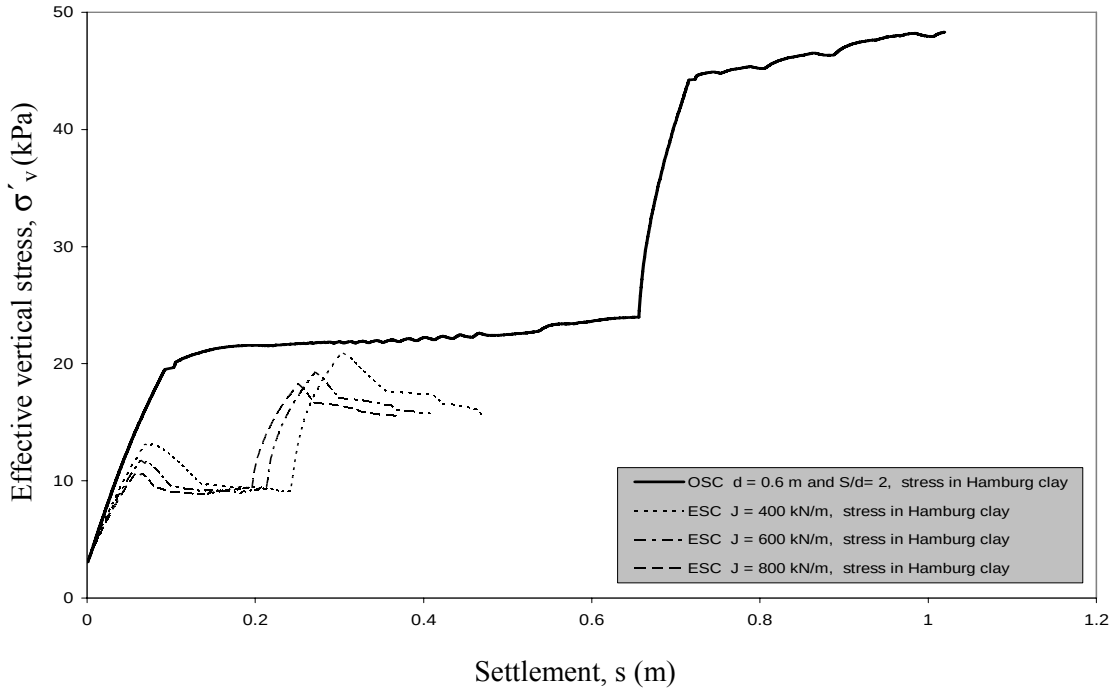

Fig. 8-19 Effective vertical stress-settlement relationship for the reinforced Hamburg clay at point A

The total vertical stress, (σ_v) was calculated in the reinforced Bremerhaven clay and in the reinforced Hamburg clay at point B which is located at a depth of 2.0 m, as shown in Fig. 8-1-a. The results are shown in Fig. 8-20 and Fig. 8-21. Each figure includes the total stress in the reinforced soft soil with ordinary and encased stone columns. Generally, the total vertical stress (σ_v) in the reinforced soft soil increases with increasing load until it reaches maximum values at the end of each construction

stage. During each consolidation process, the total stress decreases with increasing time but the reduction of the total stress in the consolidation of the first construction stage is greater than that in the consolidation of the second construction stage. This phenomenon is due to the stress concentration which is in the first construction stage is greater than that in the second construction stage.

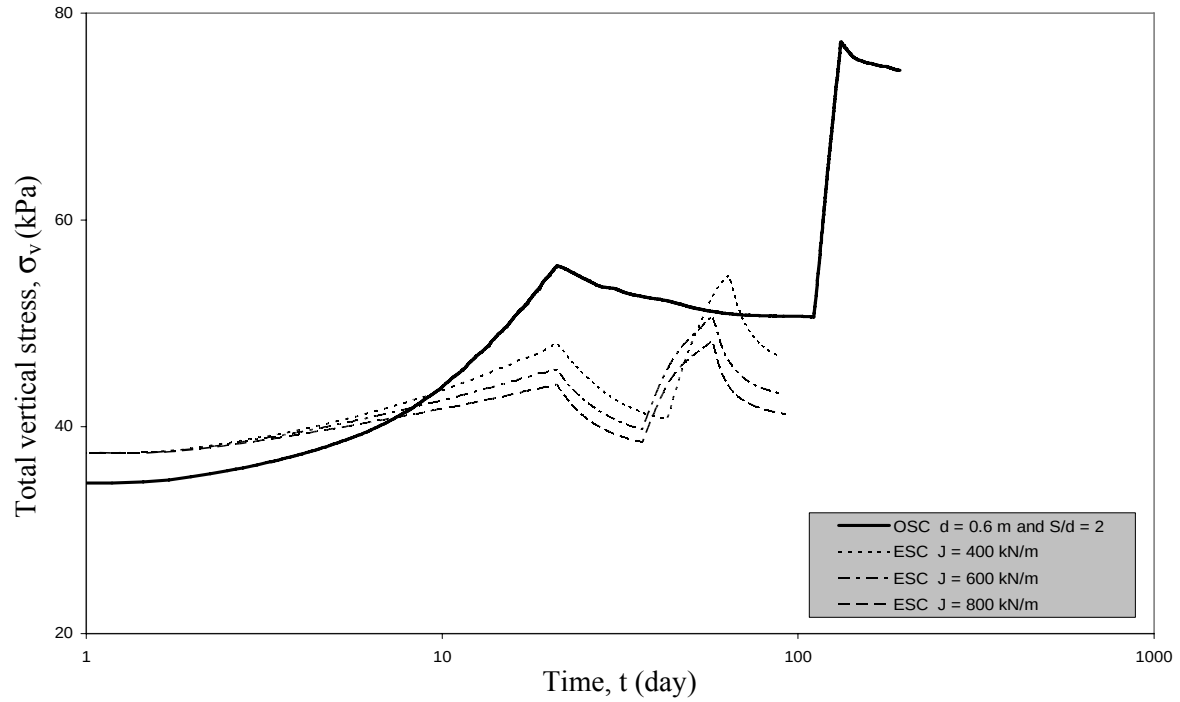

Fig. 8-20 Total vertical stress-settlement relationship for the reinforced Bremerhaven clay at point B at a depth of 2.0 m

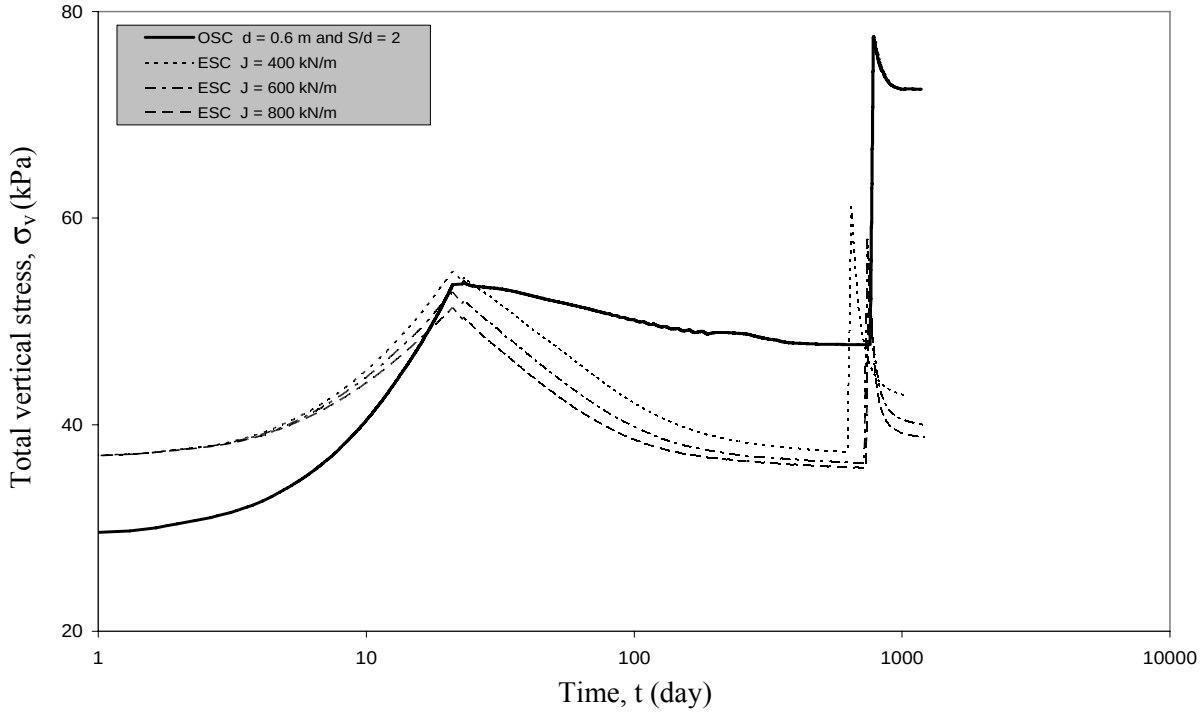

Fig. 8-21 Total vertical stress-settlement relationship for the reinforced Hamburg clay at point B at a depth of 2.0 m

The reinforced soft soil with encased stone columns implies total vertical stress values lower than the reinforced soft soil with ordinary stone columns through the all construction phases. The total stress values in the reinforced soft soil decrease with increasing stiffness of the geogrid encasement. Hence, the higher the encasement stiffness is, the more the decrease in the total stress of the surrounding soft soil is which leads to more improvements in the behavior of the reinforced soft soil.

8.3.2 Group (B): Effect of the encasement depth (h)

The above discussion indicates that the reinforced soft soil by encased stone columns with the highest stiffness (J = 800 kN/m) of the encasement provides the best bearing capacity among the investigated cases. Now, various ratios of the encasement depth to the column diameter h/d of 1, 2, 3, 5, 7 and 9.5 (full depth) have been investigated maintaining spacing ratio of S/d = 2, diameter of d = 0.6 m and encasement stiffness of J = 800 kN/m. The Bremerhaven clay has been reinforced by partial encased stone columns to study the effect of the encasement depth on the reinforced soft soil.

Settlement

Fig. 8-22 shows the relationship of the time with the construction of the embankment as well as with the settlement for the reinforced Bremerhaven clay. The development of the settlement with the consolidation time is approximately the same for all the used encasement depths. In general, the consolidation time and the settlement of the reinforced clay decrease gradually with increasing depth of the encasement as shown in Fig. 8-22 and Fig. 8-23. Therefore, the increase of the encasement depth leads to increase the stiffness of the overall encased stone columns which causes the increase of the bearing capacity and the decrease of the consolidation time. The full encased stone columns have the smallest settlement and the shortest consolidation time in comparison with the partially encased stone columns, as illustrated in Fig. 8-22 and Fig. 8-23.

Table 8-7 Reductions in the settlement of the reinforced Bremerhaven clay

Case of the Bremerhaven clay	Consolidation end of the first construction stage			Consolidation end of the second construction stage		
	Settlement, s (m)	$R_{s(NR)}$ (%)	$R_{s(R)}$ (%)	Settlement, s (m)	$R_{s(NR)}$ (%)	$R_{s(R)}$ (%)
Non-reinforced	1.31	-	-	1.86	-	-
OSC d = 0.6 m and S/d = 2	0.46	35.1	-	0.84	45.2	-
ESC, h/d = 1	0.43	32.8	93.5	0.80	43.0	95.2
ESC, h/d = 2	0.35	26.7	76.1	0.70	37.6	83.3
ESC, h/d = 3	0.30	22.9	65.2	0.61	32.8	72.6
ESC, h/d = 5	0.21	16.0	45.7	0.47	25.3	56.0
ESC, h/d = 7	0.15	11.5	32.6	0.36	19.4	42.9
ESC, h/d = 9.5 Full depth	0.1	7.6	21.7	0.24	12.9	28.6

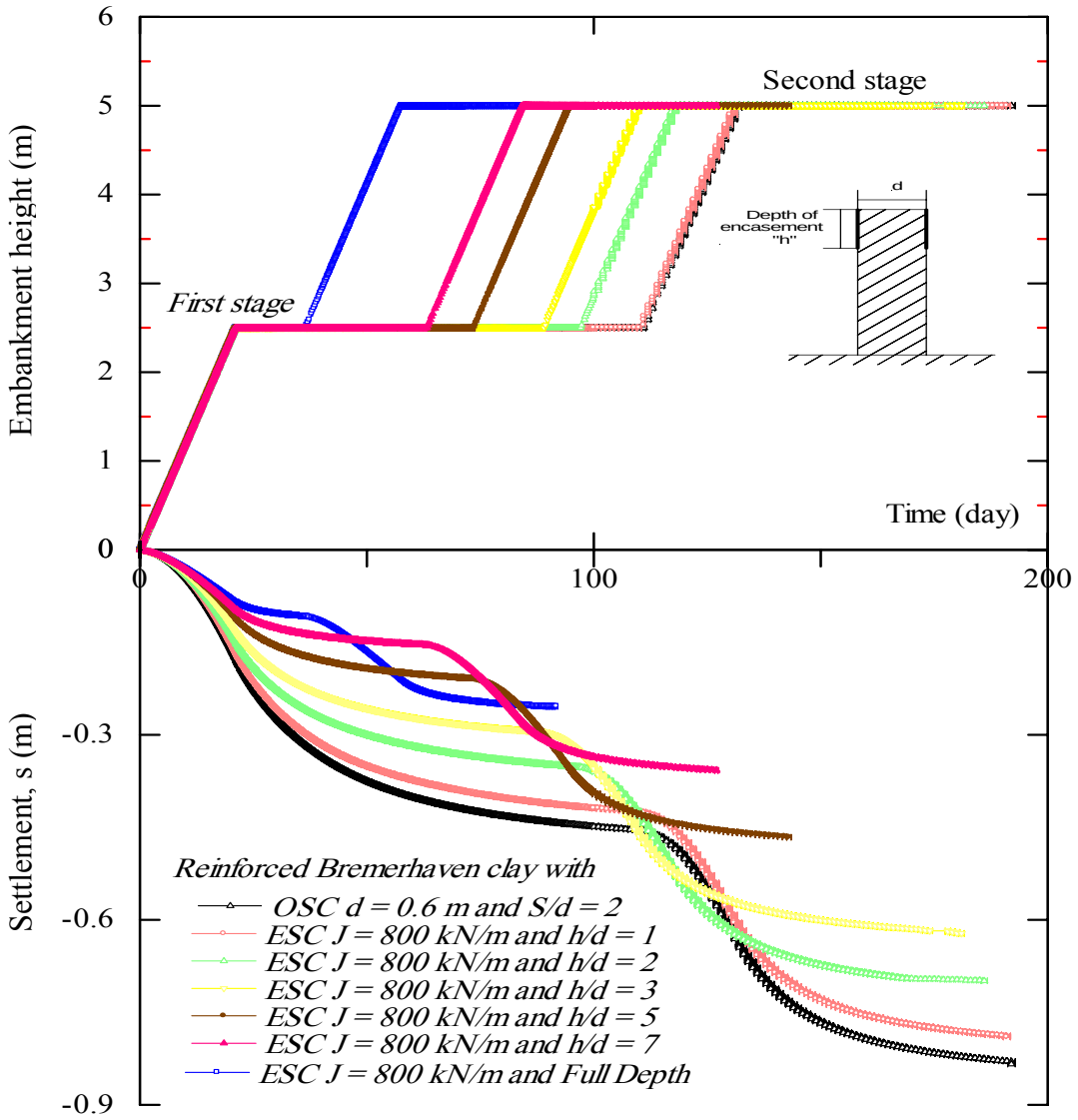

Fig. 8.22 Settlement of the reinforced Bremerhaven clay with stone column along the time of the construction for various encasement depths

The settlement distribution at the surface of the reinforced Bremerhaven clay after the consolidation end is also shown in Fig. 8-24. The settlement in both stone columns and surrounding soil decreases gradually with increasing encasement depth unit it reaches minimum values at the full encased stone column, as illustrated in Table 8-7. The settlement in the ordinary stone column and in the surrounding soft soil is constant.

The differential settlement between the encased stone column and the surrounding soil appears and increases gradually with increasing encasement depth. The differential settlement reaches maximum values when using full encased stone columns, as shown in Fig. 8-24. The stiffness of the overall encased stone column increases with increasing encasement depth which leads to increase the differential stiffness between the encased stone column and the surrounding soil. Hence, the deeper the encasement depth is, the greater the differential stiffness and the differential settlement between the encased stone column and the surrounding soil are.

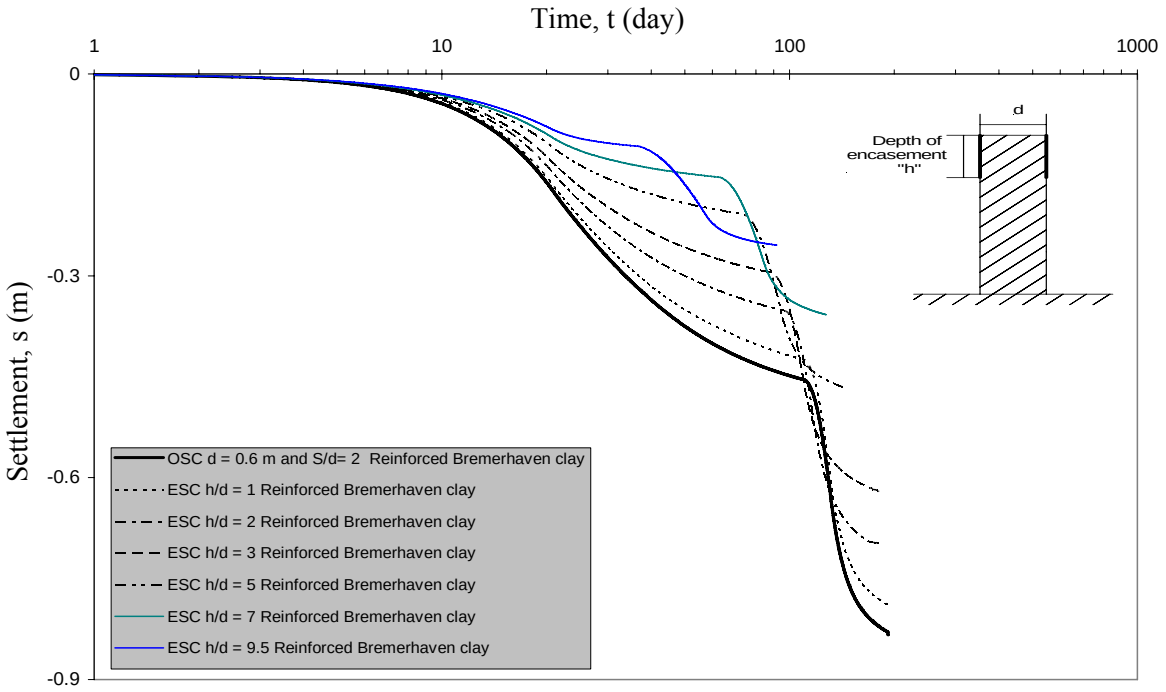

Fig. 8-23 Time-settlement relationship for the reinforced Bremerhaven clay with encased stone columns using different encasement depths

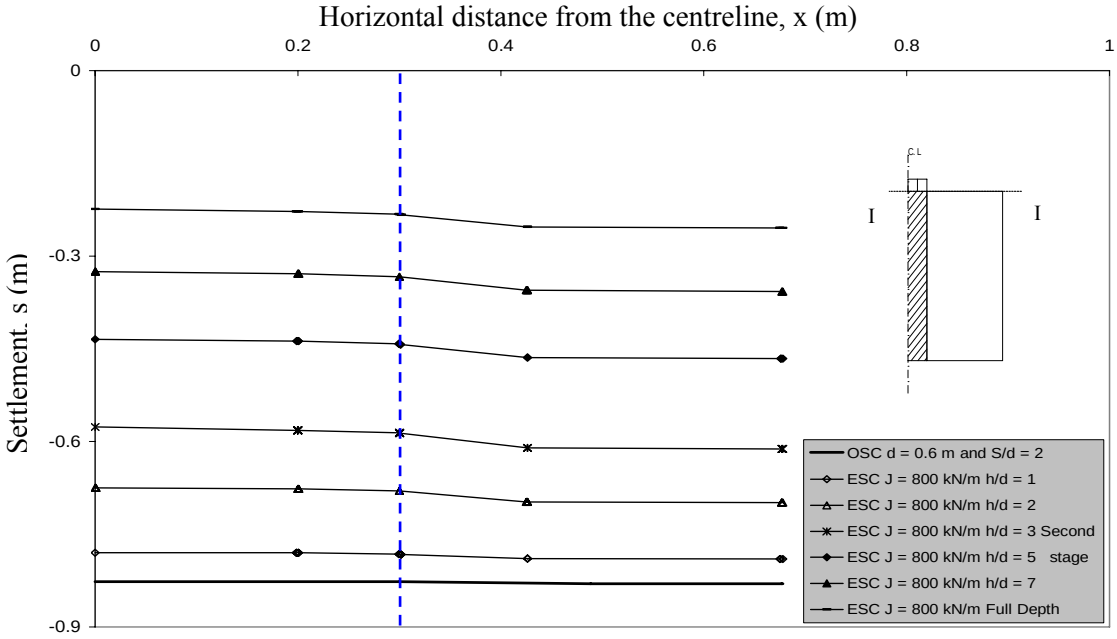

Fig. 8-24 Settlement distribution at the surface of the reinforced Bremerhaven clay with encased stone columns using different encasement depths

Lateral bulging of the stone column

The lateral bulging of the stone column, (u_h) was calculated after the end of the consolidation in the reinforced Bremerhaven clay with ordinary and partially encased stone columns, as shown in Fig. 8-25. It was well established from the ordinary stone columns that the lateral bulging is distributed along the stone column after the consolidation end. Fig. 8.25 shows the distribution of the lateral bulging of the

encased stone column through its depth using various encasement depths. The bulging of the column reduces to minimum values in all depth of the column when the column is encased completely, h/d = 9.5. When the stone column is partially encased, its bulging in the encased zone is slightly smaller than that of the full encased column case. But the non-encased zone has higher values of the column bulging. The non-encased zone in the column starts with a maximum value which generates a largely differentially lateral bulging at the end point of the encasement. Below that, the lateral bulging values decrease gradually with depth until it reaches zero at the column base, as shown in Fig. 8.25. The shallower the encasement depth is, the higher the lateral bulging values in the non-encased zone of the stone column are. Hence, the encasement is required to a depth that equals the depth of the stone column.

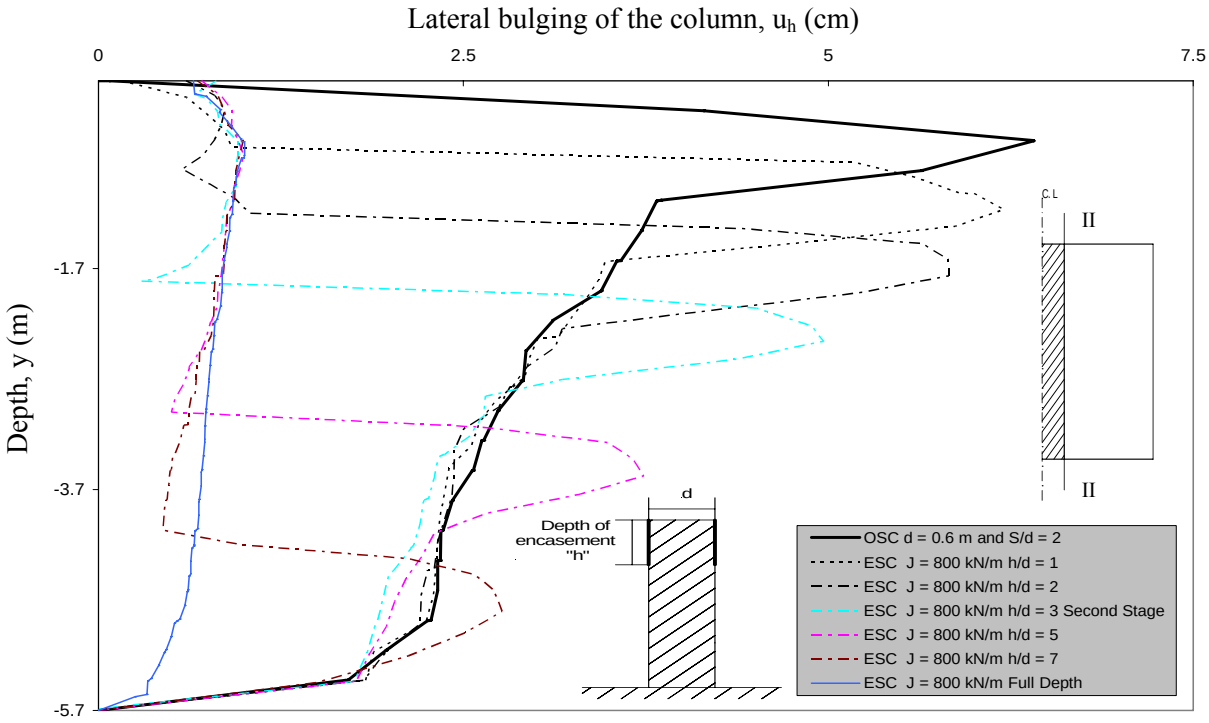

Fig. 8-25 Lateral bulging distribution of the reinforced Bremerhaven clay with encased stone columns using various encasement depths

Hoop tension force in the encasement

The distribution of the hoop tension force, (T) of the geogrid as a partial encasement of the stone column in Bremerhaven clay is shown in Fig. 8-26 after the end of the consolidation. The full encasement induces a value of hoop tension force at the top. Then the tension force values increase with depth until they reach a maximum value at a depth of 1.1 times the column diameter. Below this depth, the tension forces decrease gradually until they reach zero at the base of the column.

The distribution of the hoop tension forces is similar to that of the lateral bulging of the stone column. When the stone column is reinforced by partial encasement, the tension forces are implied in the encased part of the column. The tension force values in the partial encasement of the stone column are smaller than those of the full

encasement. While the end points of the partial encasements greater than encasement depth h/d = 1 have peak values of tension force which are larger than that of the full encasement at the same location. Because the end point of the partial encasement is free and is subjected to lateral stress from the stone column where there is a largely differentially lateral bulging of the column. Below the encasement depth of h/d = 1, the shallower the encasement is, the higher the peak value of the tension force at the end point of the encasement is, as illustrated in Fig. 8.26. The partial encasement depth which equals twice the column diameter experiences the highest peak value of the tension forces at the end point of the encasement.

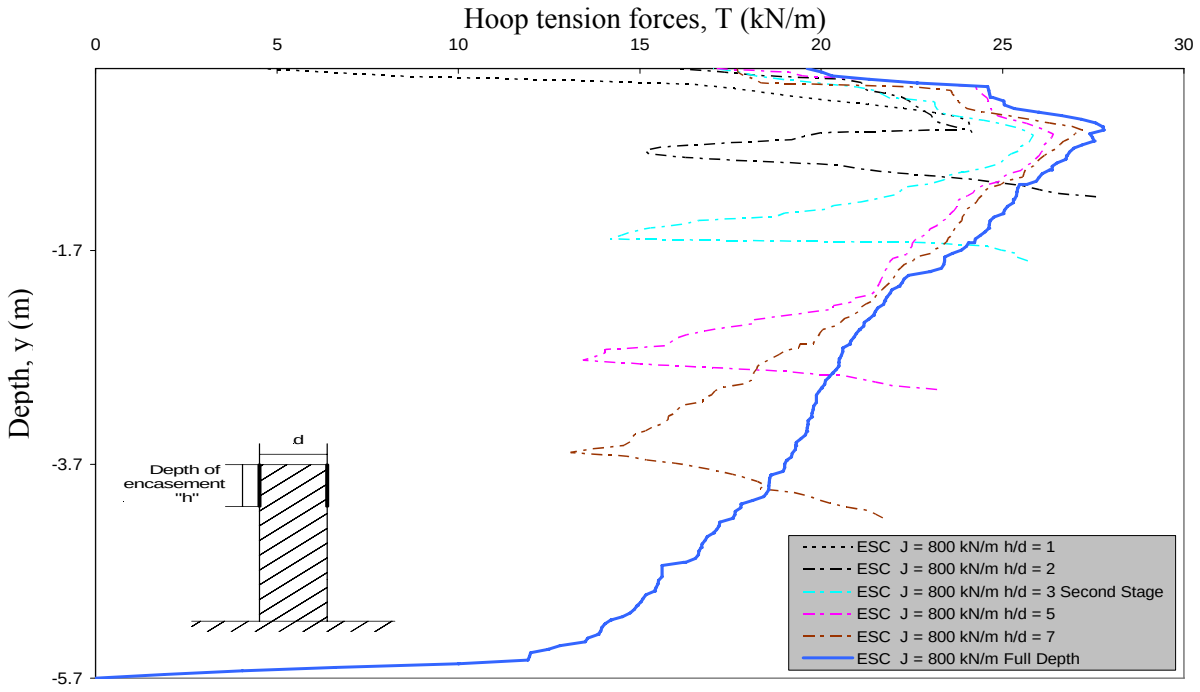

Fig. 8-26 Hoop tension force distribution of the reinforced Bremerhaven clay with encased stone columns using various encasement depths

Excess pore water pressure

The excess pore water pressure (Δu) in the reinforced Bremerhaven clay with partially encased stone columns was calculated at the point B which is located at a depth of 2.0 m, as shown in Fig. 8-1-a. The developments of the excess pore water pressure of the reinforced Bremerhaven clay with ordinary and partially encased stone columns are approximately similar along all the construction phases, as illustrated in Fig. 8-27 and Fig. 8-28. The reinforced Bremerhaven clay with partially encased stone columns of h/d = 1 and h/d = 2 imply excess pore water pressure values slightly lower than the reinforced clay with ordinary stone columns in the consolidation of the first stage. During the second consolidation stage, the partially encased stone columns of h/d = 1 and 2 cause no significant reduction in the pore water pressure and its dissipation time. More reduction in the excess pore water pressure and its dissipation time occurs when encasement of the stone column has a depth ratio of h/d = 3.

The partially encased stone columns deeper than h/d = 3 cause a huge reduction in the pore water pressure of the surrounding soil and accelerate the time of pore water pressure dissipation. The encased stone column with the depth of h/d = 7, and full depth induce approximately similar excess pore water pressure values in the surrounding soft soil. In the other hand, the dissipation time of the excess pore water pressure decreases with increasing depth of the geogrid encasement, as shown in Fig. 8-27. It can be concluded that, the reinforced Bremerhaven clay with full depth-encased stone column has the smallest pore water pressure values and shortest consolidation time in comparison with the shallower encasement depths.

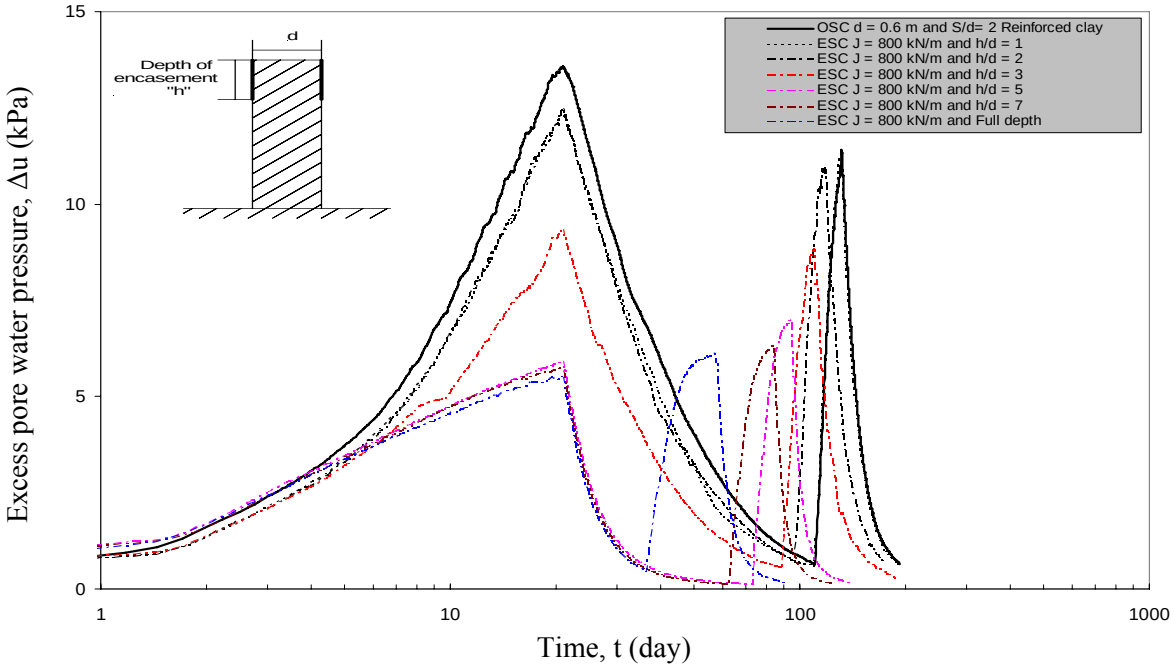

Fig. 8-27 Excess pore water pressure-time relationship for the reinforced Bremerhaven clay with encased stone columns using various encasement depths

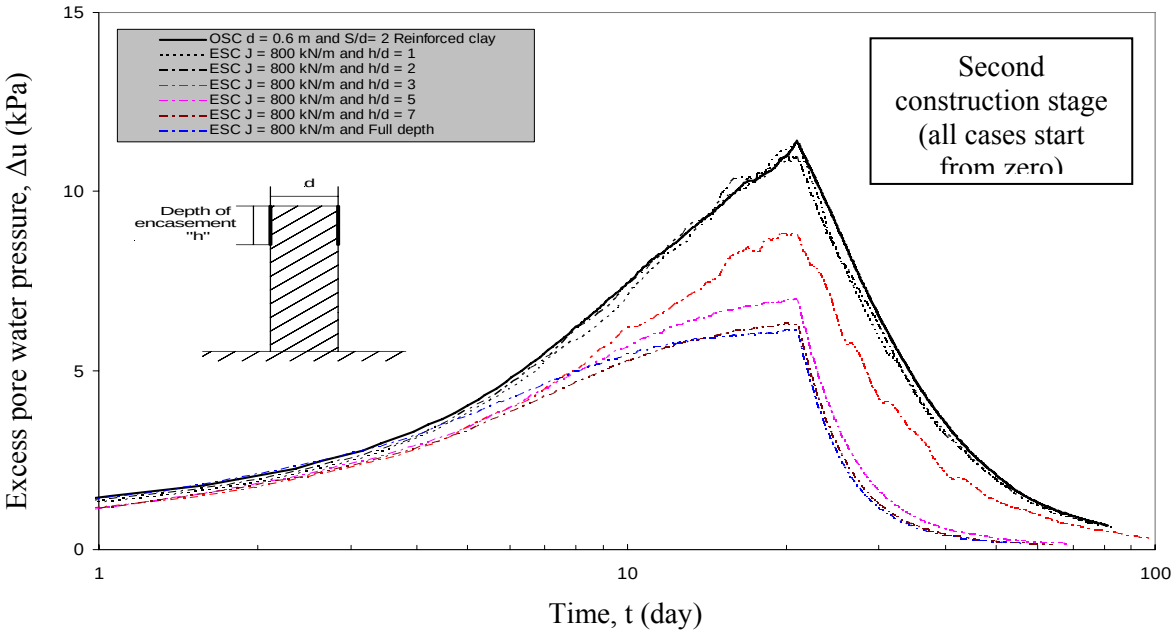

Fig. 8-28 Development of Excess pore water pressure during the second loading stage for the reinforced Bremerhaven clay with partially encased stone columns

Stress in soil

The effective vertical stress (σ'_v) was calculated at the surface of the reinforced Bremerhaven clay at point A, and in the column at point C, as shown in Fig. 8-1-a. The relationship of the effective vertical stress with settlement for the reinforced Bremerhaven clay with ordinary and partially encased stone columns was carried out. The effective vertical stress and settlement relationship in the stone column and in the reinforced clay are shown in Fig. 8-29 and Fig. 8-30, respectively. The development of the effective vertical stress in the ordinary and the partially encased stone columns are approximately similar. When the stone column is partially encased with encasement depth of h/d = 1, its effective stress increases and its settlement decrease, as shown in Fig. 8-29. Additional increase in the effective stress and more reduction in the settlement of the encased stone column occur with increasing depth of the geogrid encasement. The vertical effective stress in the surrounding soil also decreases with increasing depth of the encasement, as illustrated in Fig. 8-30.

As stated before, the increase in the encasement depth leads to increase the stiffness of the overall encased stone column. The higher the overall stiffness of the partially encased stone column is, the more the stress transfer from the surrounding soil to the column is. The increase of the stress concentration leads to increase the effective stress in the column and to reduce it in the surrounding soil. Hence, the more the stress concentration in the encased stone columns is, the lower the effective stress in the surrounding soil and the smaller the settlement are. The full encased stone column implies the highest effective stress in it and the smallest effective stress and settlement in the surrounding soft soil in comparison with the shallower encasement depths.

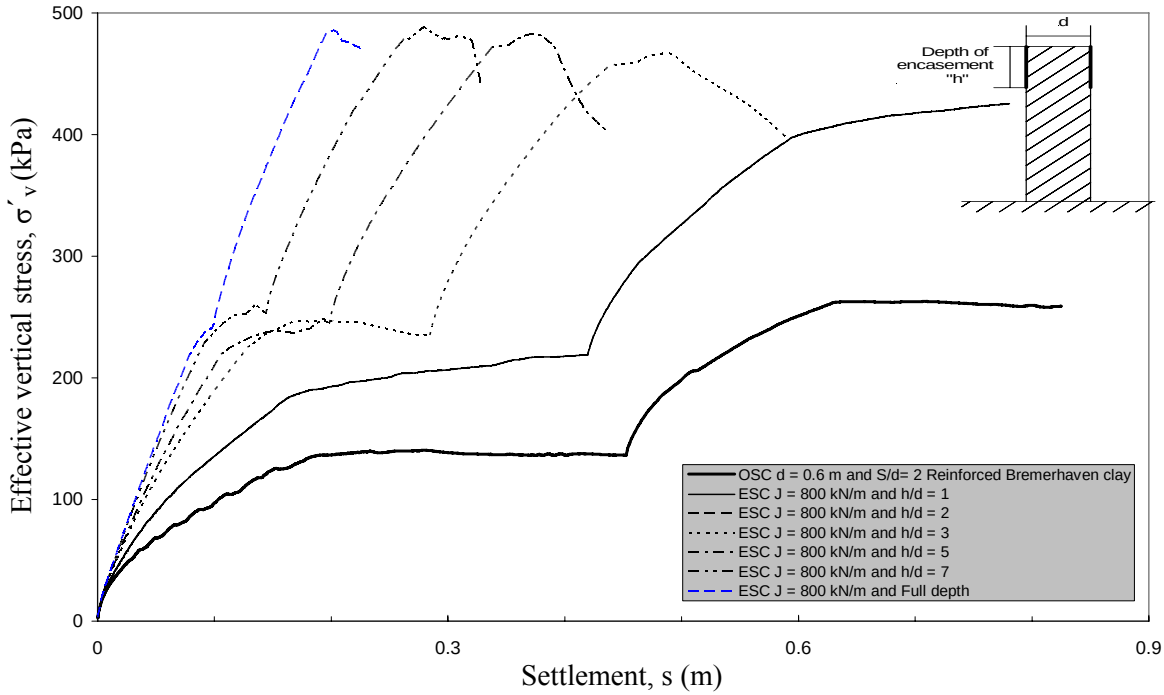

Fig. 8-29 Effective vertical stress-settlement relationship for the encased stone column in Bremerhaven clay at point C using various encasement depths

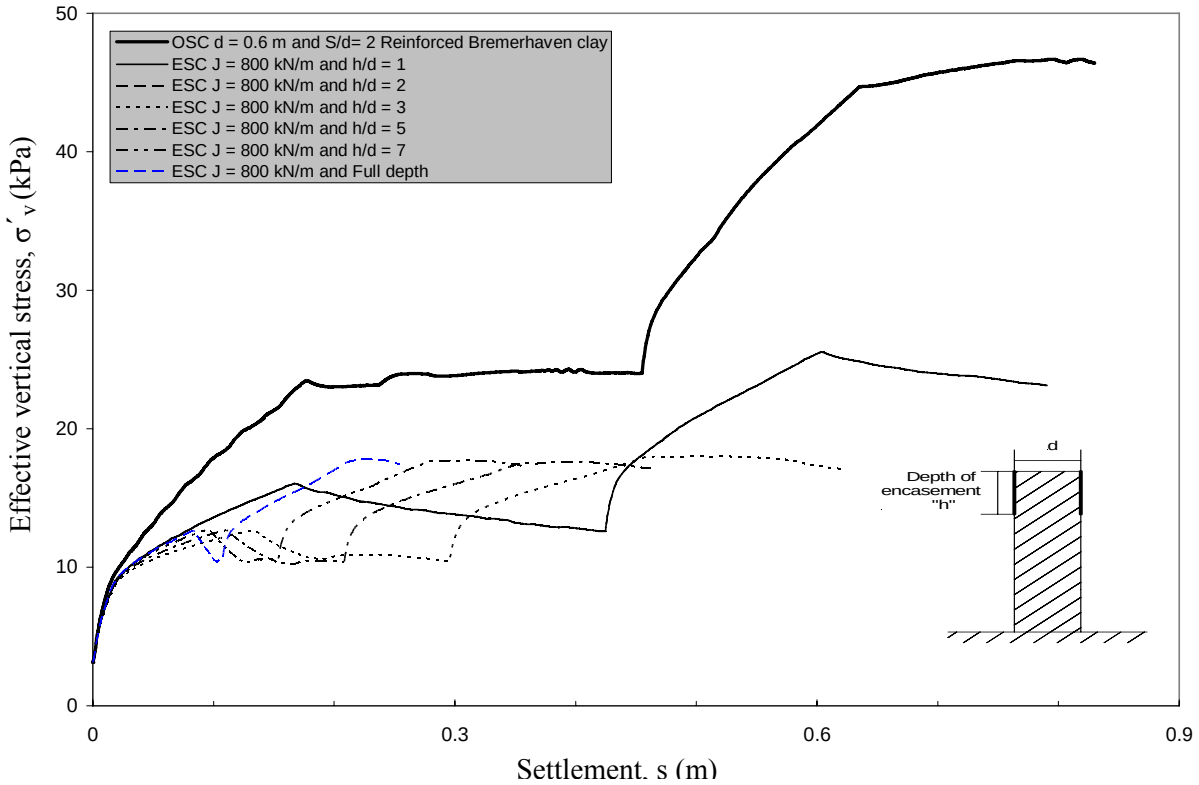

Fig. 8-30 Effective vertical stress-settlement relationship for the reinforced Bremerhaven clay at point A using various encasement depths

The total vertical stress (σ_v) was calculated in the non-reinforced and the reinforced Bremerhaven clay with partially encased stone columns at point (B) which is located at a depth of 2.0 m, as shown in Fig. 8-1-a. The development of the total vertical stress in the reinforced Bremerhaven clay is approximately similar for all encasement depths, as shown in Fig. 8-31.

The total vertical stress in the reinforced Bremerhaven clay decreases with increasing depth of the geogrid encasement through all construction phases. Hence, the deeper the encasement reaches, the more the decrease in the total stress of the surrounding soft soil is which leads to more improvement in the behavior of the reinforced soft soil. This is more pronounced in the Bremerhaven clay with partially encased stone columns which have encasement depths deeper than the depth of h/d = 3.

The rate of the reduction in the total stress during each consolidation phase of the soft soil increases with increasing encasement depth. The greater the rate of the reduction of the total stress during a consolidation phase leads to a higher participation percentage of the stress transfer from the soil to the column in the acceleration of the consolidation. Generally, the rate of the reductions of the total stress and also the participation of the stress concentration during the consolidation of the first stage are greater than those during the consolidation of the second stage.

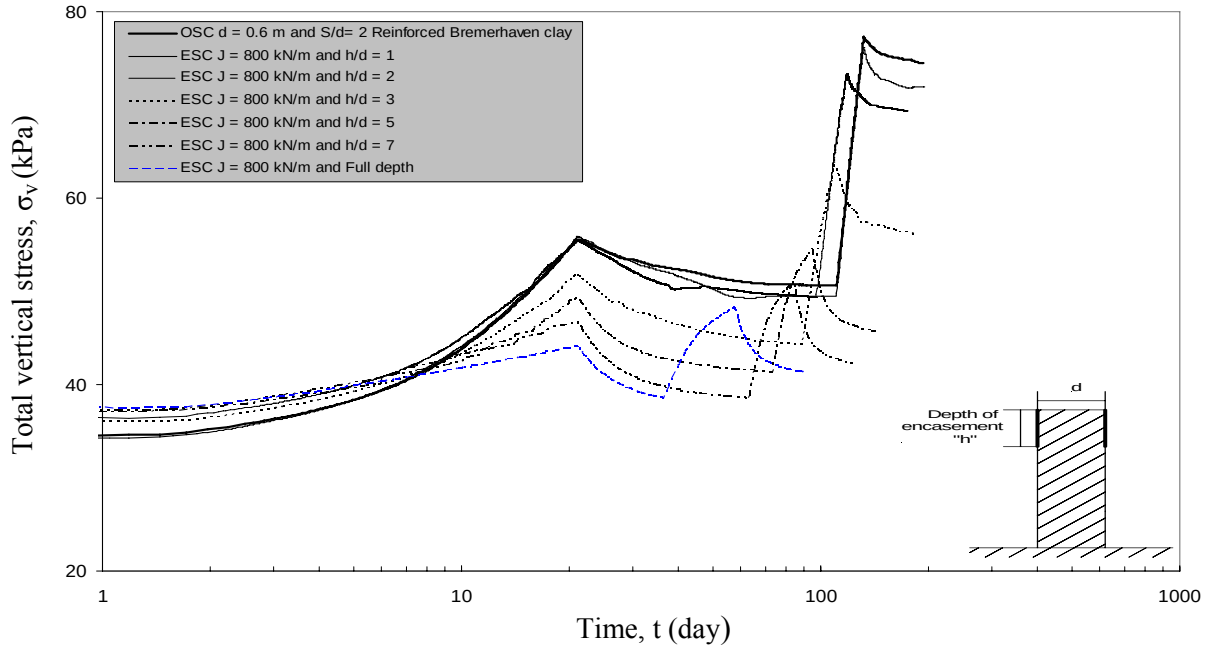

Fig. 8-31 Total vertical stress-settlement relationship of the reinforced Bremerhaven clay at point B at a depth of 2.0 m

8.4 Discussion

The encasement of the stone column leads to enhance its performance in the soft soil. The geogrid encasement provides the stone column with the required lateral support to prevent the excessive lateral bulging and settlement. The encasement also prevents the mixing of the fine grains soil with the stone material to keep the drainage performance of the stone column.

The encasement increases the overall stiffness of the encased stone columns which increases with increasing encasement stiffness. Using encased stone column in reinforcing soft soil leads to increase the bearing capacity and to decrease the consolidation time, the column bulging, the pore water pressure and stress in the surrounding soil. More reductions occur in the settlement, the lateral bulging of the column, pore water pressure and stress in the reinforced soil with increasing stiffness of the geogrid encasement. The encased stone columns in reinforcing Bremerhaven clay are more effective than those in reinforcing Hamburg clay. The reason of that is the Bremerhaven clay has greater shear strength and permeability than the Hamburg clay.

The reinforced soft soil using partial encased stone columns has been investigated to determine the suitable encasement depth. The consolidation time and settlement of the reinforced soft soil decrease with increasing depth of the encasement which leads to increase the bearing capacity. As well as the lateral bulging of the encased column decrease with increasing encasement depth. The deeper the encasement depth is, the more the overall stiffness and the stress concentration of the encased stone columns are. The pore water pressure and the stress in the surrounding soft soil decrease with increasing encasement depth. Hence, using full encased stone columns provides the best behavior of the reinforced soft soil in comparison with using partial encased stone columns.

9. A Case Study of an Embankment Constructed on Reinforced Soft Soil with Stone Columns

9. 1 Introduction

As known in the past chapters, using stone columns in soft soil increases the bearing capacity and accelerates consolidation and construction time of the embankment. In this chapter, a case history of an embankment constructed on the reinforced soft soil with ordinary stone columns has been chosen to be simulated. Plane strain and axisymetric techniques are used to simulate the embankment parts. The embankment rested on a layer of soft soil with a thickness of 6.0 m. The soft soil layer is located over a stiff clay layer. The field measurements and the FEM results have been compared. The encased stone columns have been also used to reinforce the soft soil in the FEM analyses to induce the influence of the encasement on the behavior the stone columns-soft soil foundation.

In the following sections, the modeling of the embankment, the soft and stiff soil and stone columns, and the discussion of the results are presented. The discussion contains comparison between the field measurements and the FEM results of the embankment on the reinforced soft soil with ordinary stone columns. The comparison of the unit cell results for the ordinary and the encased stone columns reinforcing soft soil is also discussed.

9.2 Case history description

The FEM simulation has been applied for the modeling of an embankment construction for Penchala Toll Plaza project at New Pantai Expressway, Malaysia. A brief description of the project was given by Tan et al. (2008). The embankment geometry with the stone column reinforced soft profile is shown in Fig. 1 having a line of symmetry on the left boundary. The 20 m wide and 1.8 m high embankment is filled by sandy material. The stone columns have a diameter of 0.8 m and a spacing distance between columns of 2.4 m. The stone columns, arranged in a square grid, extend through the soft soil for a depth of 6 m above the layer of the stiff clay. The upper crust layer is 1 m thick fill of hard soil, which was provided as a replacement of soft-clay surface to improve the ground for a stable construction platform as well as drainage of water during consolidation. The groundwater level is one meter below the ground surface. Two settlement plates (SP1 and SP2), as shown in Fig. 1, were installed in situ to measure the settlement at the center of the embankment and at 8 m from its edge.

9.3 Numerical modeling and selection of parameters

The case history of the embankment was adopted from the study of Tan et al. (2008). Tan et al (2008) also simulated the embankment parts by the Plaxis 3D Tunnel Version 2 using 15-node wedge elements. Owing to the software limitations, the stone columns in three dimensional model were given as equivalent geometry with square cross-sectional area in place of the actual circular geometry.

The plane-strain modeling is possible as the embankment extended to a distance of more than 200 m with approximately uniform cross-sectional geometry. Hence, in the current study the plane-strain modeling has been done. In this the stone columns are modelled as walls using a width of 0.21 m and a spacing distance of 2.4 m. The plane-strain column width is given by the following relationship based on the equivalence area of the replacement ratio according to Tan et al. (2008):

$$b_c = B\,(r_c^{\,2} / r_e^{\,2}) \qquad (9\text{-}1)$$

Where b_c is the half width of the wall, B = (S/2) is the half of the spacing distance between columns, r_c = (d/2) is the radius of the stone column and r_e = (d_e/2) is the radius of the drainage zone or the unit cell which is equivalent to the plane strain width. Where is in square orientation r_e = 1.13 B, as shown in Fig. 9-3-a.

The unit cell technique has been also used in this study to simulate the embankment using 15-node wedge elements axisymetric model in Plaxis version 9. The unit cell consists of a stone column and the surrounding soft soil over the stiff clay, as shown in Fig. 9-3. The geogrid material has been used to encase the stone columns which has a stiffness of J = 800 kN/m. This type of geogrid was proved to be the best among the others in reinforcing stone columns, as stated in chapters 4 and 8. All the soils and stone columns material have been modelled with Mohr-Coulomb model, which is considered realistic approximations of the soils. The parameters of the soils are shown in Table 9-1.

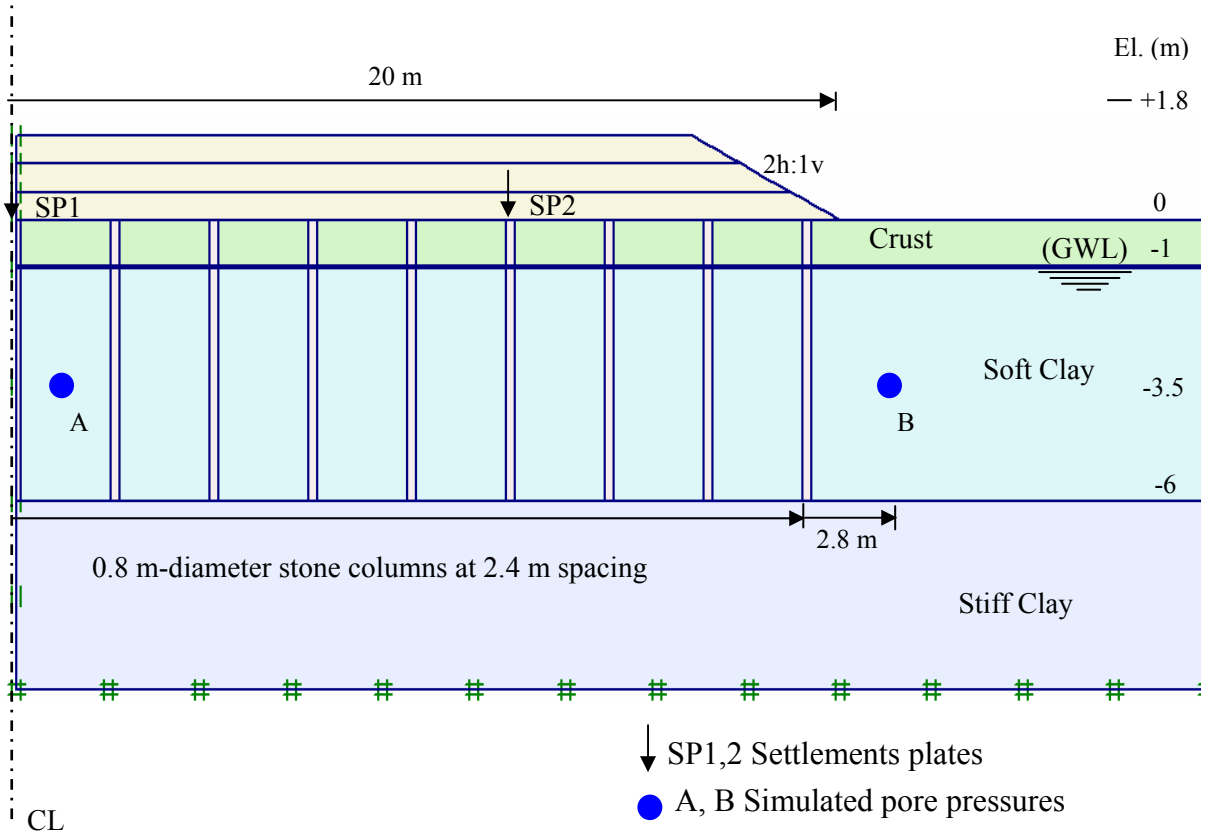

Fig. 9-1 Cross section of embankment case history through centreline of stone columns

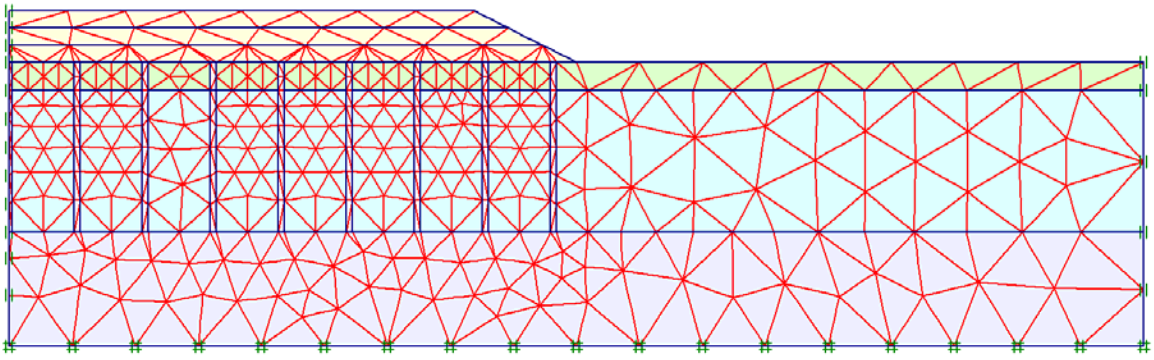

Fig. 9-2 Finite element mesh of the embankment case history through centreline of stone columns

9.4 Simulation procedures and results

The project involved rapid embankment construction. The stone columns have been first installed by partial soil replacement. Then, the construction of the embankment has been done in 1.8 m height consisting of three equal layers (0.6 m increment in embankment height in each layer). Each layer of embankment construction has been simulated with 3 days, giving altogether 9 days for the construction. The consolidation process has been applied during and after the construction. The consolidation has been continued after construction with no change in loading condition until the remaining excess pore water pressure fell below a specified near zero value (1 kPa), which reach the end of the simulation.

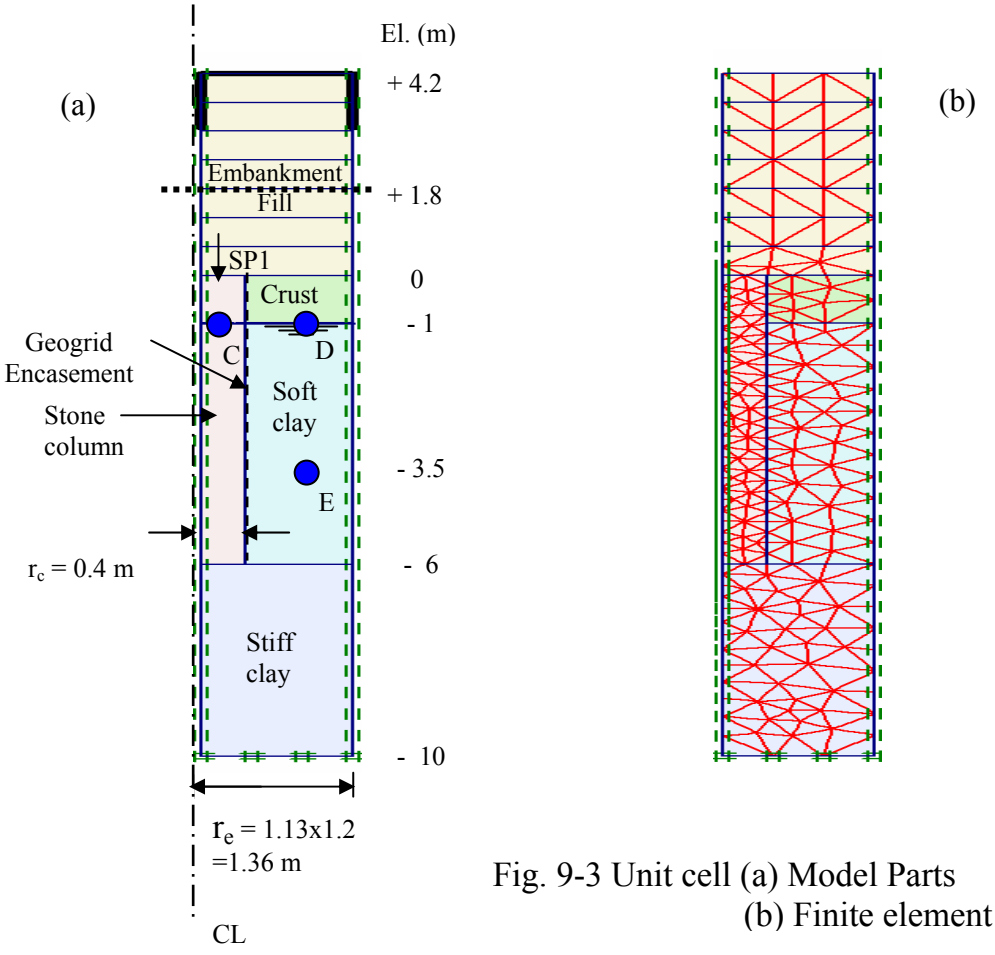

Fig. 9-3 Unit cell (a) Model Parts
(b) Finite element mesh

Table 9-1 Material parameters for embankment models

Material	Unsaturated γ (kN/m^3)	Saturated γ (kN/m^3)	ν	E (kPa)	k_h (m/s)	k_v (m/s)	ć (kPa)	φ́ (deg)
Embankment Fill	18	20	0.3	15,000	1.16×10^{-5}	1.16×10^{-5}	3	33
Crust	17	18	0.3	15,000	3.47×10^{-7}	1.16×10^{-7}	3	28
Soft clay	15	15	0.3	1,100	3.47×10^{-9}	1.16×10^{-9}	1	20
Stiff clay	18	20	0.3	40,000	3.47×10^{-9}	1.16×10^{-9}	3	30
Stone column	19	20	0.3	30,000	1.16×10^{-4}	1.16×10^{-4}	5	40

9.4.1 Comparison with data from the case history (1.8 m embankment height)

Settlement

The settlement was calculated at SP1 in the plane strain model and in the unit cell models to compare the results with the field measurements. Fig. 9-4 shows the relationship of the settlement with time for the field data and the models of the embankment at SP1. The settlement increases with time with rapid rate until the time reaches approximately 35 days. After that, the settlement increases with time with a very small rate. The settlement hasn't approximately any increase after the time of 90 days. That means that the consolidation is finished.

There is a good agreement between the FEM results and the field measurements. The plane strain model induces settlement somewhat more than the field measurement. In the other hand, the unit cell model for the ordinary stone columns implies settlement very close to the field settlement as shown in Fig. 9-4. Hence, the axisymetric model induces better agreement with field measurements than that of the plane strain model.

The stone column has been encased with geogrid material which has a Stiffness of J = 800 kN/m. The embankment over the reinforced soil with encased stone columns is also modelled by the axisymetric model, as the unit cell model is shown in Fig. 9-3-a. The reinforced soft soil with encased stone column has a settlement smaller than that of the reinforced soft soil with ordinary stone column, as shown in Fig. 9-4. Fig. 9-4 shows also the consolidation settlement is accelerated when encasing the stone columns.

Fig. 9-5 and 9-6 show the settlement along the horizontal distance from the embankment centreline after 20 days and 90 days since the embankment has been constructed. The field measurements are compared with the FEM models which are the plane strain and the axisymetric models. The measured settlement at SP1 and SP2 is approximately the same which leads to that the settlement under the embankment is constant. The constant settlement is agreed by the plane strain modelling after both times of 20 days and 90 days. The plane strain model induces a good agreement for

the field settlement after 90 days while it implies an overestimation for the field settlement after 20 days. The plane strain model also predicts the settlement distribution under and beyond the embankment. Beyond the embankment toe, the settlement converts to heave which decreases with increasing consolidation time.

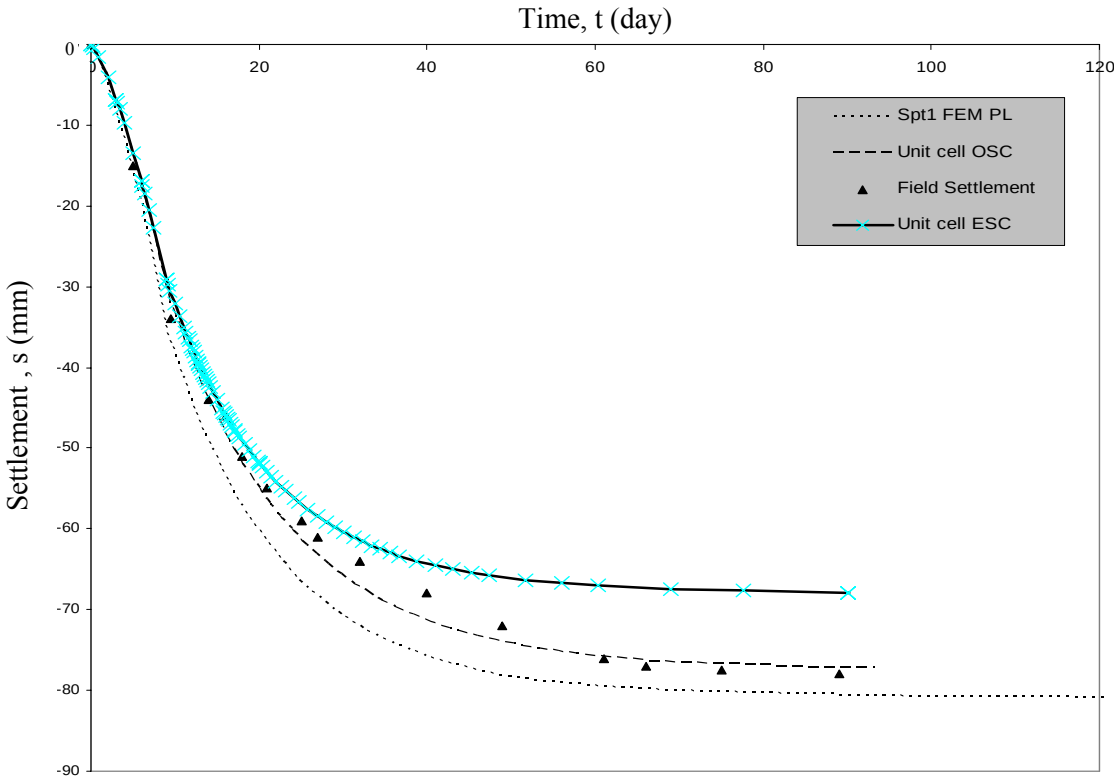

Fig. 9-4 Comparison between simulated and field settlement at SP1

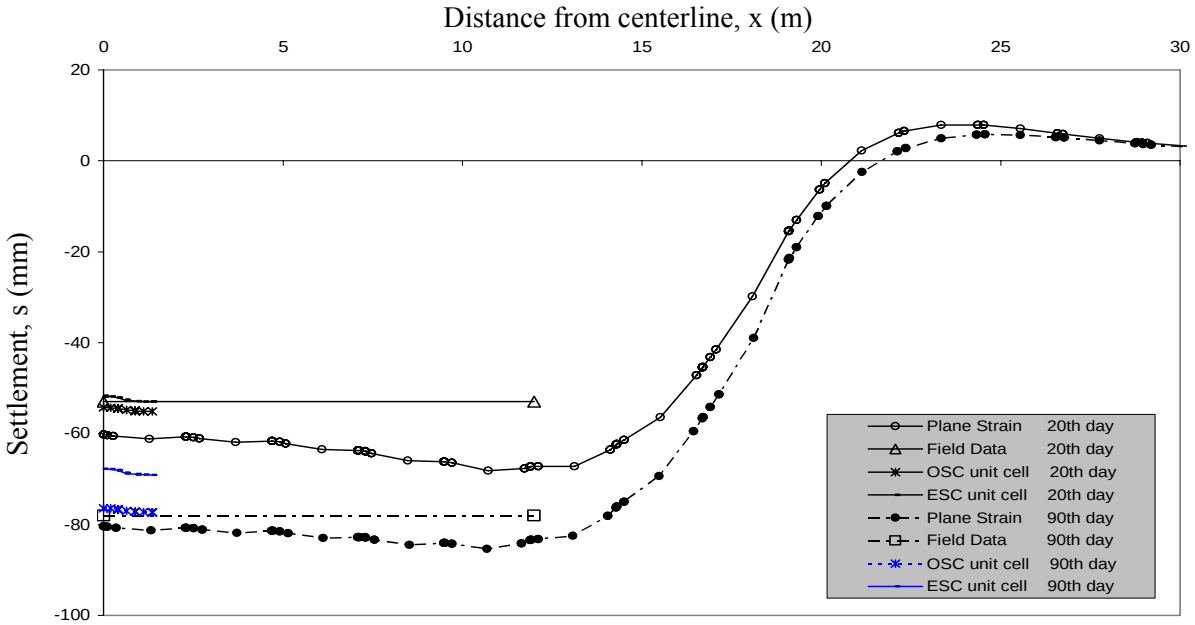

Fig. 9-5 Comparison between simulated and field settlement of embankment profiles

Fig. 9-6 is a part from Fig. 9-5 which shows the settlement distribution along the unit cell. The unit cell has also a constant settlement. The axisymetric FEM model for the unit cell shows a good agreement with the field settlement especially after 90 days. The axisymetric model induces better agreement with the field settlement than that of plane strain model, as illustrated in Fig. 9-6.

When the stone column is encased by geogrid material, a reduction in the settlement occurs after 90 days from the construction. In the other hand, there is no significant reduction in the settlement after 20 days from construction. Hence, the encasement has a greater influence on the settlement after the consolidation in comparison with the period directly after the construction. This phenomenon is due to the encasement increases the column stiffness which leads to increase the stress transfer and stress concentration during the consolidation, as discussed in chapter 8. The encasement of the stone column also causes more improvements in the settlement when the applied load increases.

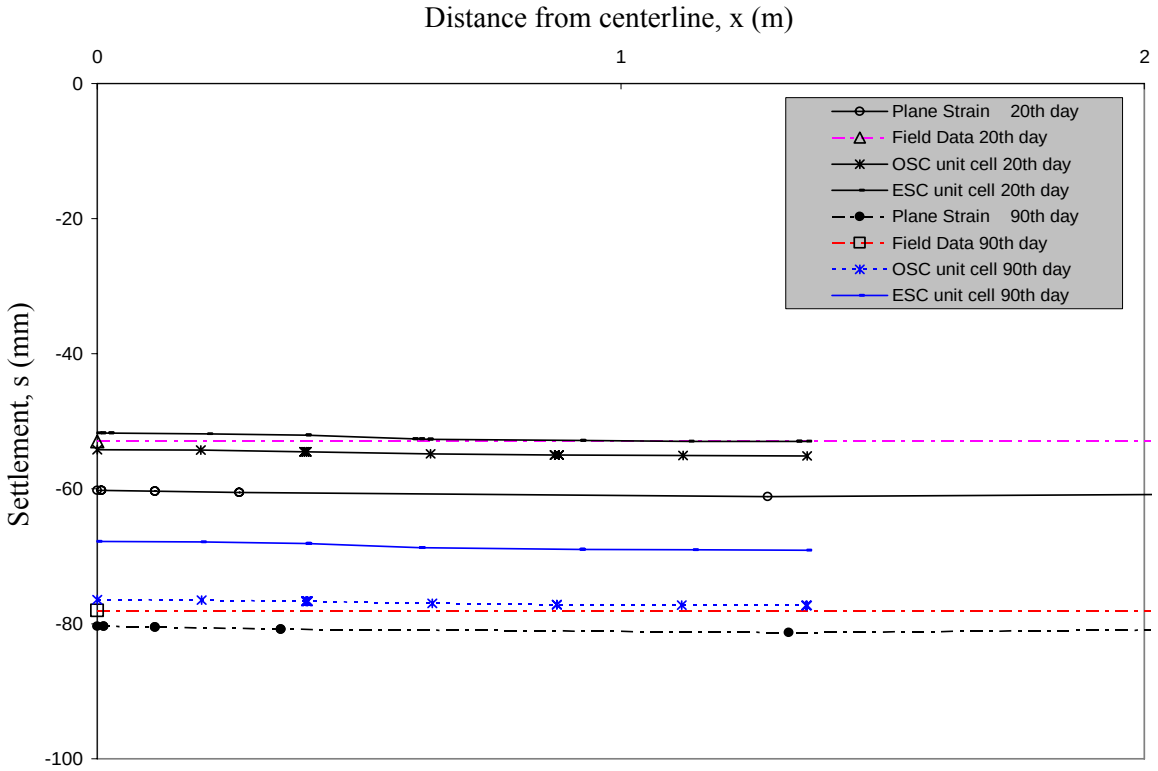

Fig. 9-6 Comparison between simulated and field settlement through the unit cell

Excess pore water pressure

The excess pore water pressure was calculated from the plane strain model at locations A and B which is compared with the 3D simulation from the study of Tan et al. (2008). The excess pore water pressure was calculated from the axisymetric model at point E which is compared with the pore water pressure at location A in the other models. Fig. 9-7 and Fig. 9-8 show the simulated excess pore water pressure with time at locations A and B, respectively. The excess pore water pressure at A in the models has an initial peak value of approximately 17 kPa due to the embankment construction and then dissipates with different rates to nearly zero after 90 days. The plane strain

model and the unit cell model induce a good agreement with 3D model. The excess pore water pressure of the plane strain model and the unit cell model has also a very good agreement at location A. In the other hand, the excess pore water pressure in the reinforced soft soil with encased stone columns has a minor lower peak value than that in the reinforced soft soil with ordinary stone columns, as shown in Fig. 9-7.

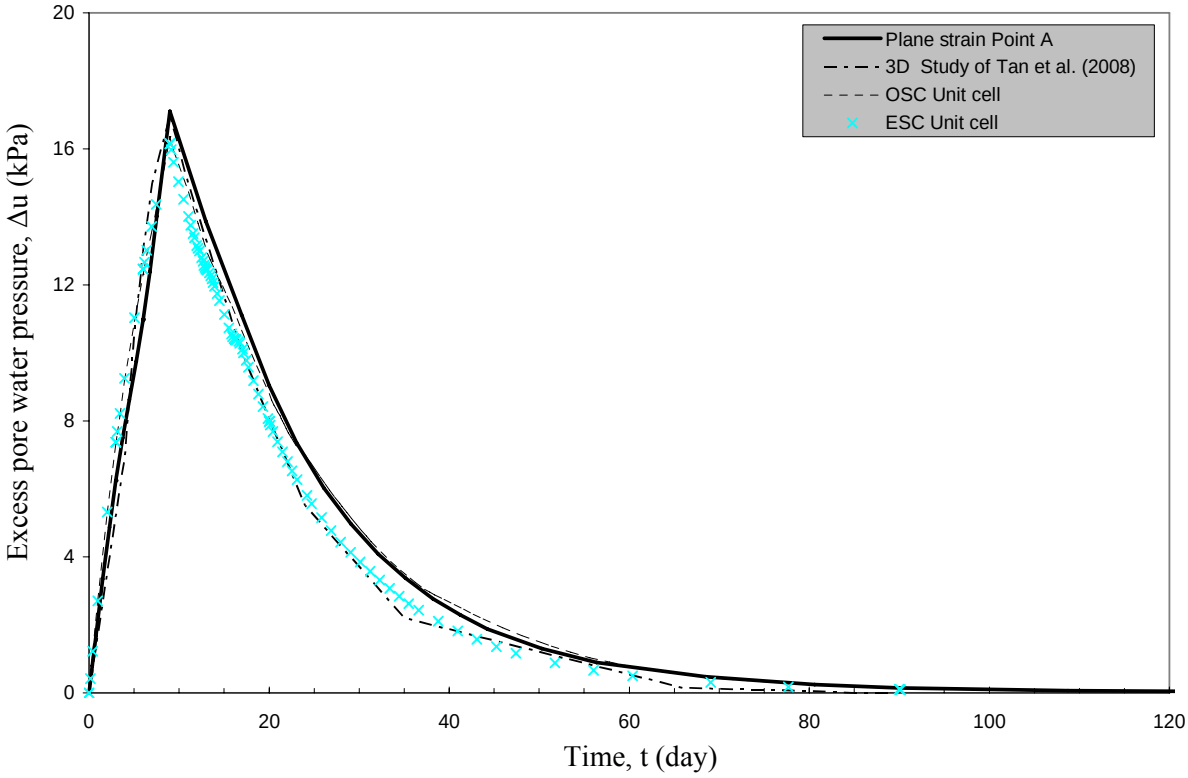

Fig. 9-7 Simulated excess pore water pressure in embankment models at point A

On the other side, at point B (Fig. 9-8), 2 m away from the embankment edge, the excess pore water pressure was calculated by the plane strain model and has been compared with the results of 3D simulation, (Tan et al. 2008). The two models show a good agreement for the distribution of the excess pore water pressure along the consolidation time. The excess pore water pressure at point B has significantly lower peak value than under directly the embankment loads at point A (Fig. 9-7 and Fig. 9-8), which means that the excess pore water pressure discrepancies are only confined within a distance of several meters from the stone columns. The excess pore water pressure here takes much longer than 120 days to dissipate and hence the acceleration of consolidation by the stone columns is hardly evident at this location.

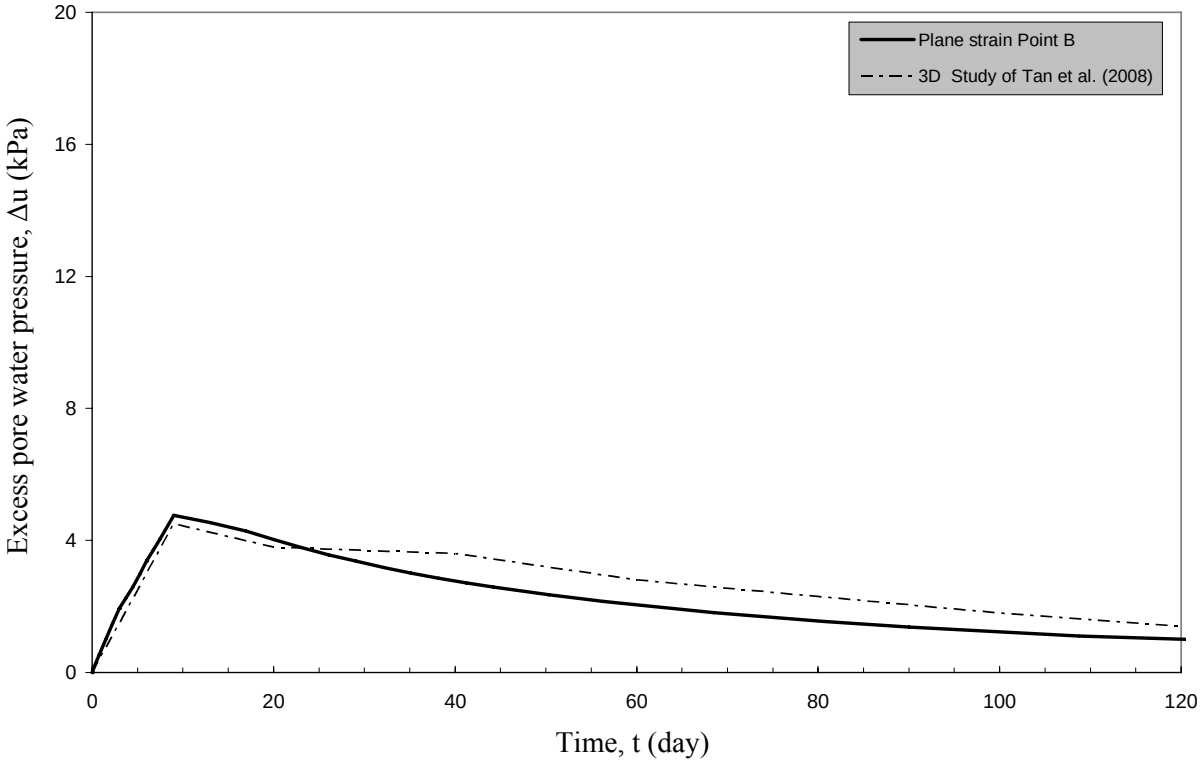

Fig. 9-8 Simulated excess pore water pressure in embankment models at point B

9.4.2 Effect of geogrid encasement under a higher embankment (4.2 m)

The above discussion proved that, the results of the FEM axisymetric model are in a good agreement with the field measurements. The encasement increases the stone column stiffness and also increases the stress transfer and the stress concentration as discussed in chapter 8. Additionally, the improvement in the behavior of the reinforced soft soil-encased stone column foundation increases with developing consolidation time and with increasing applied load. From this fact, the unit cell technique has been used to study the effect of the encased stone column under a higher embankment on the behavior of the reinforced soft soil.

Simulation procedures

As in the last simulation, the embankment has been rapidly constructed in three equal layers in the first construction stage. Each layer has 0.6 m height and consumes 3 days. After the construction of 9 days, the consolidation has been applied under constant loading until the excess pore water pressure dissipates. Then the second stage of construction is simulated in 2.4 m height consisting of four equal layers. Each layer has also 0.6 m height and consumes 3 days which results an embankment with height of 4.2 m, as illustrated in Fig. 9-3. Finally, the consolidation process is also applied during and after construction until the excess pore water pressure diminishes and reaches values lower than 1 kPa.

The axisymetric FEM analyses have been performed to simulate the embankment on the reinforced soft soil with ordinary and encased stone columns. In addition to the geogrid material with stiffness of J = 800 kN/m, another geogrid material with a higher stiffness value which is J = 2000 kN/m is used to study the effect of the high geogrid stiffness on the behavior of the reinforced soft soil.

Fig. 9-3 shows the model parts of the higher embankment and the points at which the calculations were carried out. Location SP1 is on the top of the stone column to calculate the settlement. Point C is located at 1 m depth in the stone column to calculate the stress. Point D is located at 1 m depth in the soft soil to calculate the stress. And Point E is located also at 3.5 m depth in the soft soil to calculate the excess pore water pressure and the stress.

Settlement

Fig. 9-9 shows the relationship between the consolidation settlement and the consolidation time at location SP1 for the reinforced soft soil with the ordinary and the encased stone columns. The consolidation settlement decreases to lower values and the consolidation time accelerates when the stone columns are encased with geogrid material. An additional reduction in the settlement and acceleration in the consolidation time occurs when the encasement stiffness increases from 800 kN/m to 2000 kN/m. Therefore, the encasement of stone columns in the soft clay increases the bearing capacity of the soft clay by reducing settlement during the various construction phases.

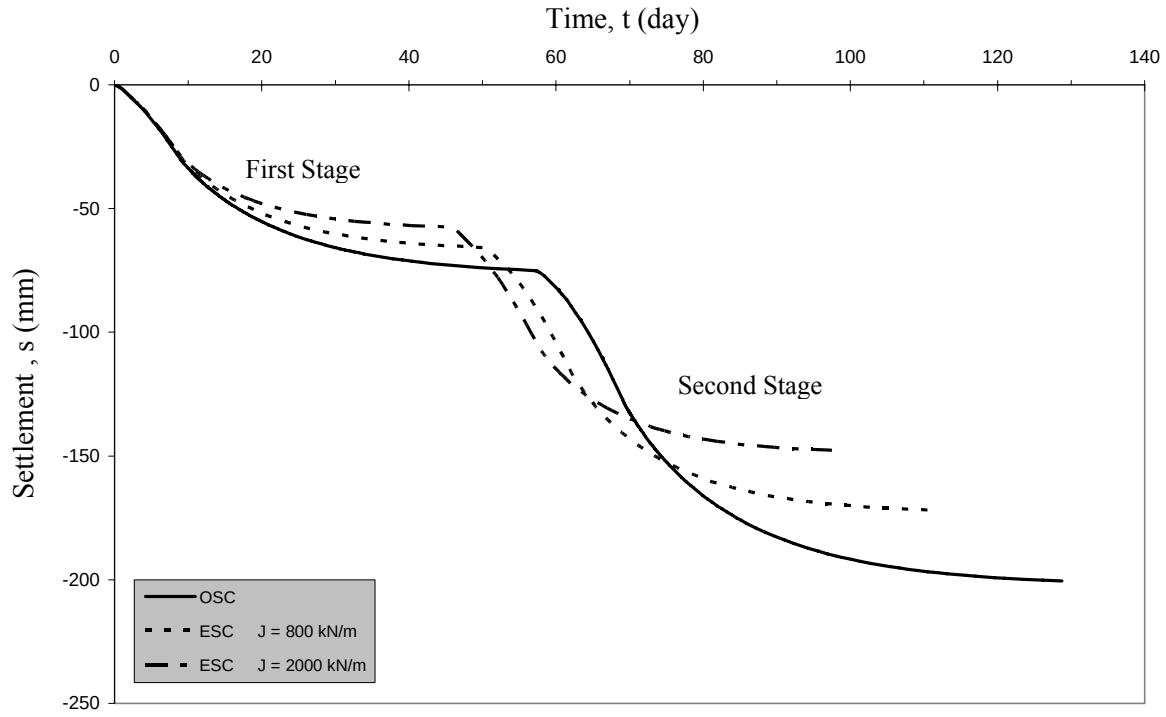

Fig. 9-9 Settlement-time relationship at SP1

Fig. 9-10 also shows the distribution of the settlement at the surface for the reinforced soft soil with the ordinary and the encased stone columns at the end of the consolidation. The final settlement also decreases when the stone columns are encased. An additional reduction in the final settlement occurs with increasing stiffness of the encasement. Hence, the greater the stiffness of the geogrid encasement is, the more the reduction of the settlement is. The settlement in the ordinary stone column and in the surrounding soft soil is constant and approximately the same while there is a differential settlement between the encased stone columns and the

surrounding soft soil, as shown in Fig. 9-10. The differential settlement is generated because the increases in the stiffness ratio between the encased stone columns and the surrounding soft soil.

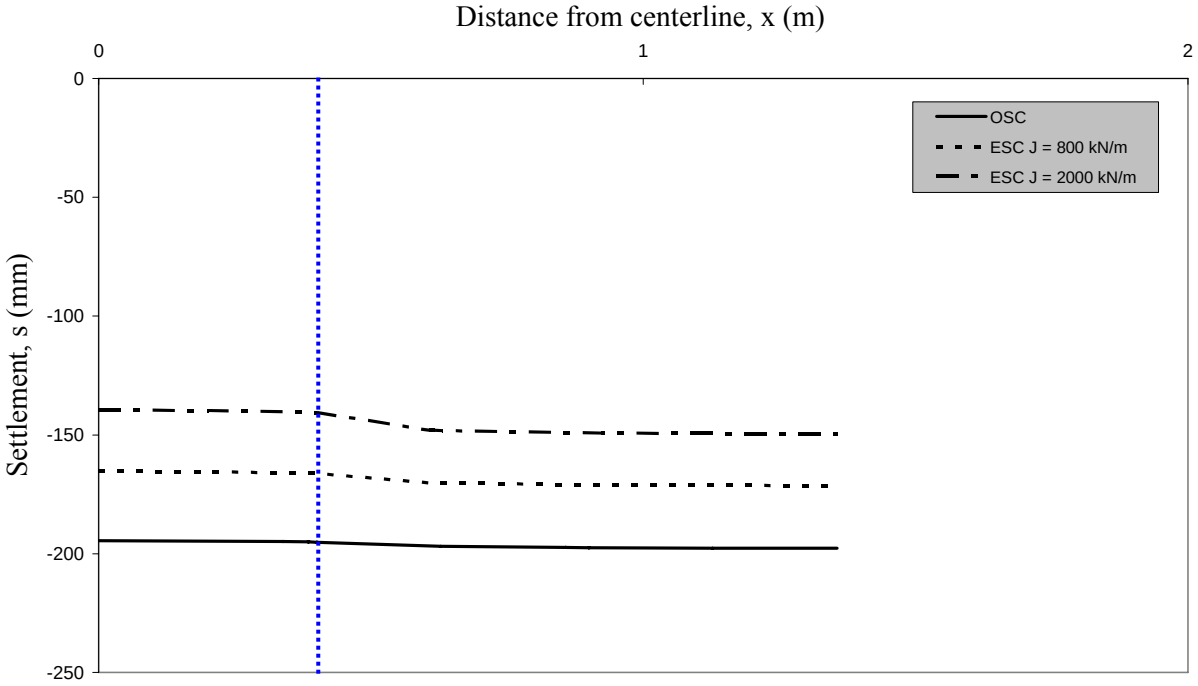

Fig. 9-10 Settlement distribution at the surface through the unit cell

Excess pore water pressure

The excess pore water pressure was calculated at point E which located at a depth of 3.5 m for the reinforced soft soil with the ordinary and the encased stone columns. As soon as the fill load is applied on the saturated soft soil, the excess pore water pressure builds up. The excess pore water pressure increases with time until it reaches peak values at the end of the construction of each stage. The peak value in the second stage is the greater because the applied load in the second stage is also the greater. After each peak value, the excess pore water pressure decreases gradually during the consolidation directing to the steady state case, as shown in Fig. 9-11.

The excess pore water pressure in the reinforced clay with encased stone column decreases and its dissipation consumes shorter time in comparison with the reinforced clay with ordinary stone columns. This is more pronounced in the second stage than in the first stage of consolidation. The excess pore water pressure and its dissipation time in the reinforced clay with encased stone columns decrease with increasing stiffness of the encasement, as illustrated in Fig. 9-11.

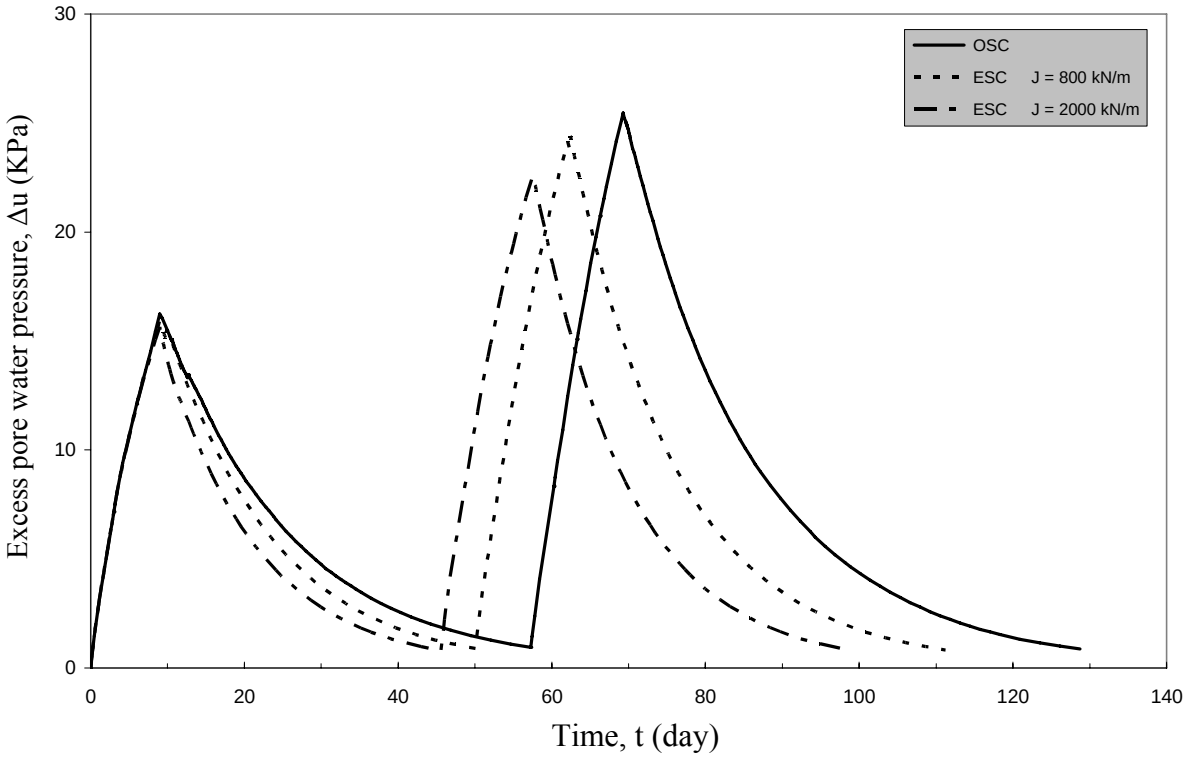

Fig. 9-11 Excess pore water pressure-time relationship for point E at depth of 3.5 m

Stress

The vertical effective stress was calculated in the stone column at Point C and in the surrounding soft soil at point D, as illustrated in Fig. 9-3. Fig. 9-12 shows the effective vertical stress along the consolidation time in the ordinary and the encased stone columns, and in the surrounding soil. The trends of the effective stress of the ordinary and the encased stone columns in the clay are approximately similar. The developments of the effective stress with time in the reinforced clay are also approximately similar.

The effective vertical stress in the encased stone columns is higher than that in the ordinary stone columns. This is because the encasement increases the stiffness of the overall stone columns which leads to increase the stress concentration in and the stress transfer to the encased stone columns. The effective vertical stress in the encased stone columns increases and the consolidation time decreases with increasing stiffness of the geogrid encasement, as illustrated in Fig. 9-12. In contrast, the encasement of the stone column causes reduction in the effective stress in the surrounding soft soil. The effective stress in the surrounding soil has a small decrease with increasing stiffness of the geogrid encasement which also causes a reduction in the consolidation time of the soft soil.

This phenomenon is due to the stress transfer from the surrounding soft soil to the encased stone column which increases with increasing encasement stiffness. Therefore, the higher the encasement stiffness is, the more the stiffness of the overall encased column is. The increase in the stiffness of the overall encased stone column leads to increase the stress concentration in the column and to increase also the stress transfer from the surrounding soil, as depicted in Fig. 9-13. The stress concentration

phenomenon has an important role in reducing consolidation settlement, accelerating consolidation time and increasing bearing capacity of the reinforced soil.

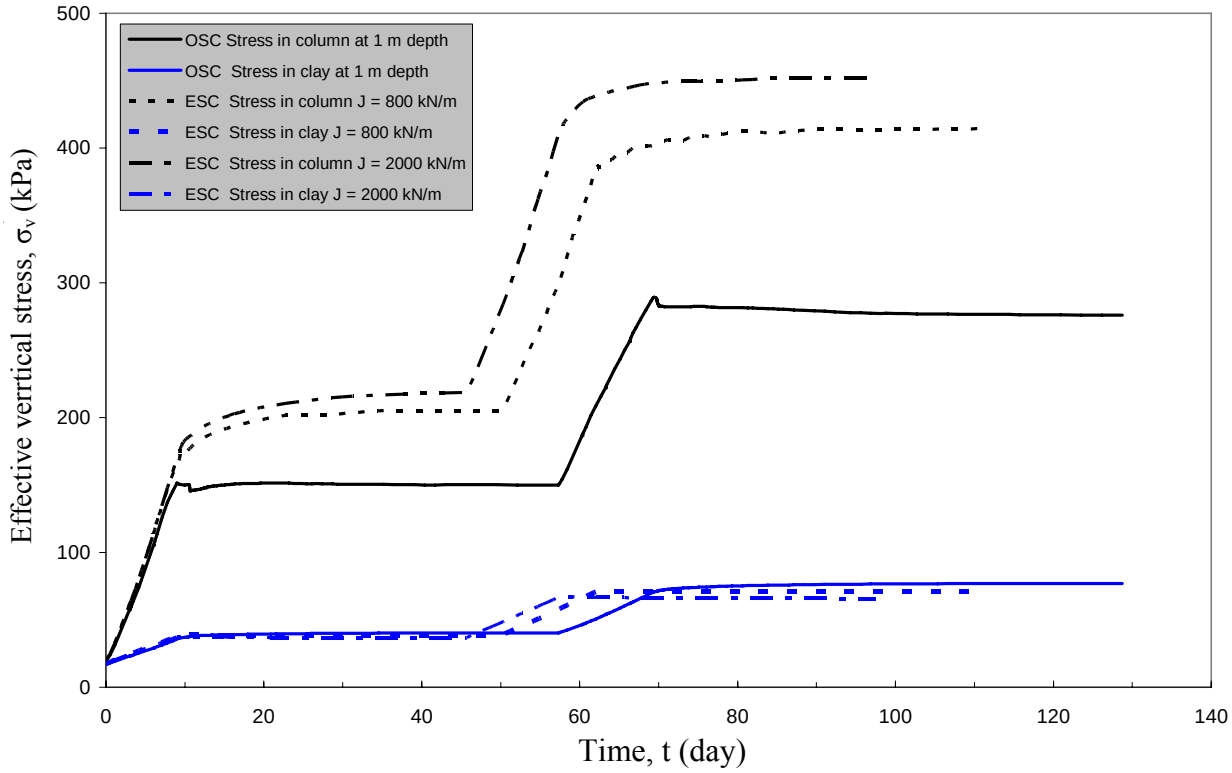

Fig. 9-12 Vertical stress-time relationship at depth of 1.0 m

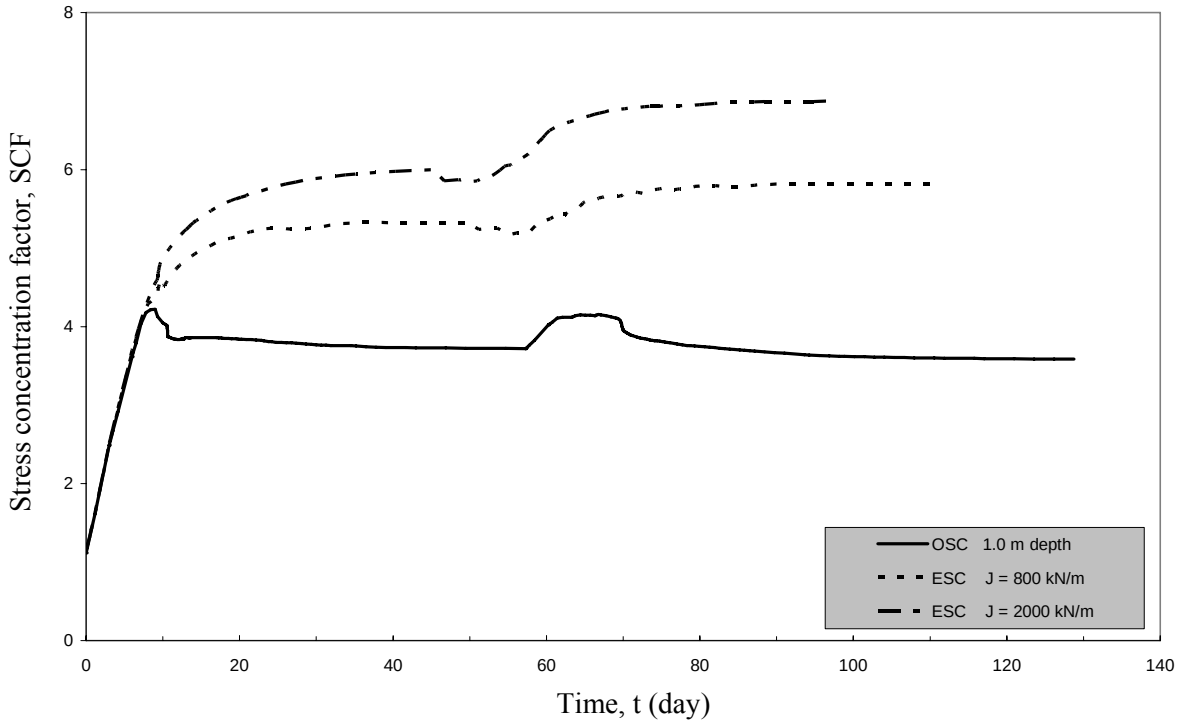

Fig. 9-13 Stress concentration factor-time relationship at depth of 1.0 m

The total stress in the reinforced soft soil with the ordinary and the encased stone columns was calculated at point E which is located at a depth of 3.5 m. The relationship of the total vertical stress with consolidation time is shown in Fig. 9-14. The reinforced soft soil with encased stone columns implies total vertical stress values lower than that of the reinforced soft soil with ordinary stone columns through all construction phases. The total stress values in the reinforced soft soil decrease with increasing stiffness of the geogrid encasement during the consolidation. As discussed in the last chapters, the reduction in the total stress of the reinforced soft soil with encased stone column is a result for the stress transfer and stress concentration which increases with increasing encasement stiffness. Hence, the higher the encasement stiffness is, the higher stress concentration in the column and the more the decrease in the total stress of the surrounding soft soil are which leads to more improvement in the behavior of the reinforced soft soil.

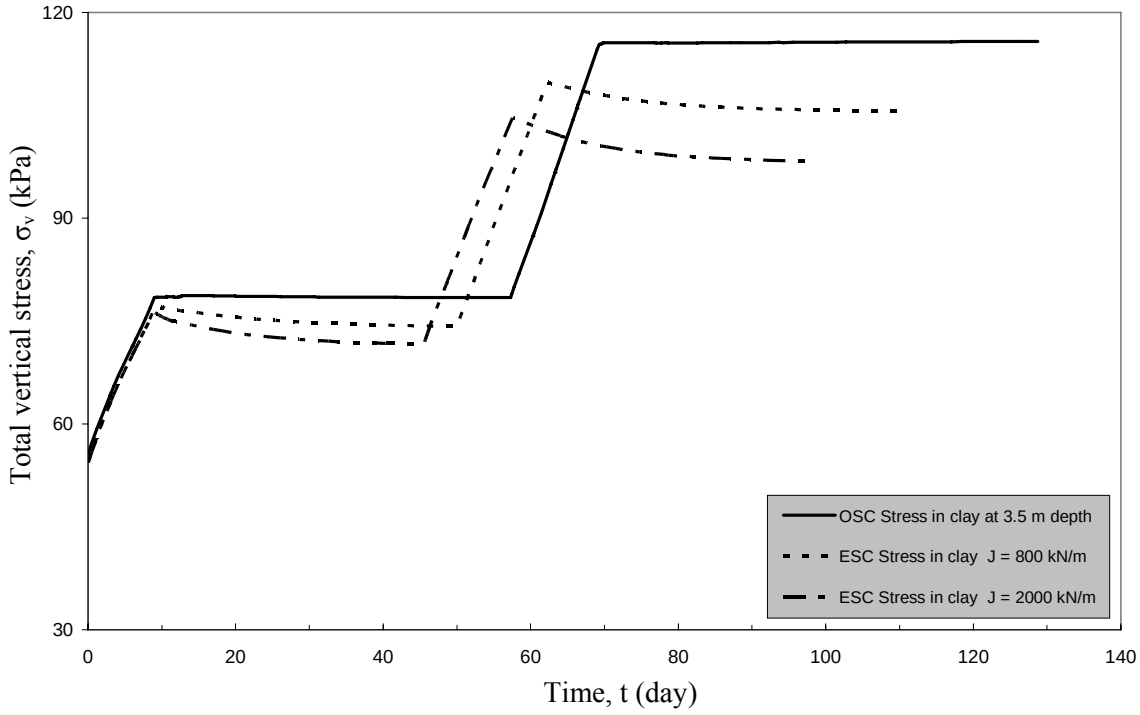

Fig. 9-14 Total vertical stress-time relationship for point Eat depths of 3.5 m

10 Summary

In the framework of the research on numerical analyses of the ordinary and encased stone columns reinforced soft soil, several parameters have been studied. The research can be divided into three main parts. The first part includes the direct loading of the stone column portion only. The second part contains the entire area loaded with fill of a highway embankment. The last part deals with the simulation of a case history of an embankment constructed on the reinforced soft soil with ordinary and encased stone columns. The finite element program Plaxis 9 has been used for the current analyses. Therefore, the most important findings from this research are summarized in the following paragraphs.

The first part of the current research contains the stone column loading only to study the effect of spacing between columns, column diameter, geogrid encasement, geogrid stiffness, and encasement depth on the behavior of the stone columns in undrained and drained conditions of the surrounding Bremerhaven clay, as outlined in Chapter 4. The “unit cell” analysis has been conducted for a column and the surrounding soft soil using axisymmetric conditions. The reinforced soft soil has a depth of 6.0 m. Based on the results; the following conclusions can be extracted to:

- The bulging of the stone column disappears in depths below approximately two times the column diameter in undrained conditions while the bulging implies values along the column in drained conditions. This phenomenon is attributed to stress transfer to greater depths when the columns are loaded in drained conditions.
- The bearing capacity increases and the bulging and the settlement of the stone column decrease with decreasing spacing distance between the columns and diameter of the column in undrained and drained loading conditions.
- The heave in undrained loading conditions as well as the settlement in drained loading conditions of the surrounding soft soil increase with decreasing spacing distance between columns.
- The differential settlement between the column and the soft soil and the heave decrease with decreasing stone column diameter.
- When the stone columns are encased with geogrid materials, a huge increase in the bearing capacity occurs and the lateral bulging is minimized.
- The stiffer the geogrid is, the higher the load capacity of the column is and the smaller the settlement, the differential settlement, the heave and the lateral bulging are.
- The hoop tension force increases with increasing geogrid encasement stiffness. The more the reduction in the horizontal and the vertical displacement of the encased stone column is, the more the tension forces are generated in geogrid encasement. In comparison with the undrained conditions, the hoop tension forces in drained conditions are greater and they extend to lower depths due to the stress transfer within downward direction.
- When the working load is applied on the encased stone columns in undrained conditions, the increase of the bearing capacity beyond an encasement depth that equals three times the column diameter is not significant. Therefore, the

encasement depth of three times the column diameter is sufficient to minimize the values of the settlement and lateral bulging of the stone column as well as the heave in the soft soil.

- As the working load is applied in drained conditions, the bearing capacity increases with increasing encasement depth. Hence, the deeper the encasement of the stone column is, the smaller the settlement, the differential settlement and the lateral bulging are.

In the second part, the non-reinforced and the reinforced clay with ordinary and encased stone columns have been loaded by an embankment fill. Two types of soft clay have been used which are the Bremerhaven clay and the Hamburg clay with a thickness of 6.0 m. The embankment fill has been constructed to a height of 5.0 m in two equal layers. The consolidation analyses are performed during and after each construction stage. The unit cell technique has been used. This part is divided into three categories. Firstly, the Bremerhaven and the Hamburg clay have been reinforced with ordinary stone columns with a diameter of 1.0 m and a spacing ratio of 2, as discussed in Chapters 5 and 6. The results showed that the Hamburg clay has a smaller bearing capacity, greater settlement and excess pore water pressure and a longer consolidation time than the Bremerhaven clay. This is attributed to the Hamburg clay has the smaller shear strength, the lower permeability and the higher compressibility. Either the Bremerhaven or the Hamburger clay needs a very long time to reach the consolidation end. Hence, the construction on these types of soil is impossible without using any soil improvement method. The comparison between the analysis of the loading of the non-reinforced soft soil with the analysis of the reinforced soft soil with ordinary stone columns leads to the following conclusions:

- The existence of the stone columns reduces the total settlement to approximately half of that of the non-reinforced clay and accelerates also the consolidation time to less than one-tenth of that of the non-reinforced clay.
- Using stone columns in soft clay reduces the production of the initial pore water pressure and accelerates its dissipation time.
- The stress concentration ratio increases with increasing load and consolidation time until it reaches higher values. Beyond the higher stress ratios, they decrease with increasing consolidation time until it reaches minimum values at the end. The steady state stress concentration ratios at various depths vary from 3.3 to 6.6 which agree with the field measurements range (2-9).
- The decrease in the stress concentration ratio during the consolidation is attributed to the column yielding and the increase in the strength of the surrounding soft soil. The yielding firstly starts at the top of the column and then it continues in the downward direction. The soft soil doesn't imply any yielding except the zone which is located very close to the column.
- The total vertical stress in the non-reinforced soft soil is constant during the consolidation process while the total vertical stress in the reinforced soft soil is variable and decreases with consolidation time. This is a result of the stress transfer from the surrounding soil and stress concentration in the column.
- The initial pore water pressure dissipates in the reinforced soft soil due to drainage and stress concentration in the stone column. The participation of the stress

concentration on the acceleration of consolidation can be computed by evaluate the reduction on the total stress in the reinforced soft soil during the consolidation and it is divided by the initial excess pore water pressure.

- The stress concentration on the stone column participates in the acceleration of the consolidation process by approximately quarter and one-seventh of the total consolidation in the Bremerhaven and Hamburg clay, respectively. Therefore, using stone columns in the Bremerhaven clay is more effective than in the Hamburg clay.

Secondly, the reinforced soft soils with stone columns have been loaded with the embankment fill to study the effect of spacing between the columns and column diameter on the behavior of the reinforced soft soils during and after the consolidation, as explained in Chapter 7. Depending on this analysis, the following conclusions can be made:

- The smaller the spacing distance between the columns is, the faster the consolidation is and the smaller the settlement is. The construction time of the reinforced clay decreases also with decreasing diameter of the column. But the settlement has no significant decrease with decreasing diameter of the stone column because the spacing ratio is constant for the different used diameters.
- At the spacing ratio of 2, the reinforced Bremerhaven and Hamburg clay with stone columns with a diameter of 0.6 m has the smallest settlement and the shortest consolidation time among the other studied cases. Using these stone columns reduces the total settlement to less than half of that of the non-reinforced clay and accelerates the total consolidation time to approximately 1 % of that of the non-reinforced clay.
- The lateral bulging along the stone column increases with increasing load causing more load transfer to the lower depths during the consolidation. The smaller the spacing distance and the column diameter are, the smaller the lateral bulging of the stone column and the excess pore water pressure production and the shorter the dissipation time are.
- The greater the spacing distance between the columns is, the higher the vertical stress in the stone columns, the higher the stress concentration ratio and the higher the vertical stress in the surrounding clay are. The stress concentration ratio also increases with increasing diameter of the column.
- the smaller the spacing distance and the column diameter are, the more the decrease and the more the reduction rate in the total stress of the surrounding soft soil is which leads to more participation percentage of the stress transfer in the acceleration of the consolidation.
- The reinforced clays using stone columns with a diameter of 0.6 m and a spacing ratio of 2 has the higher participation of the stress concentration in the consolidation acceleration. The stress concentration on thus stone column participates in the acceleration of the consolidation process by approximately half and quarter of the total consolidation in the Bremerhaven clay and the Hamburg clay, respectively.

Lastly, the analysis of the reinforced soft soils with encased stone columns has been performed. The encased stone column has a diameter of 0.6 m and a spacing ratio of 2. The reinforced soft soil has been loaded with the embankment fill to study the effect of geogrid encasement, geogrid stiffness and encasement depth on the behavior of the reinforced soft soil during and after the consolidation, as explained in Chapter 8. The findings of this analysis can be concluded as the following:

- Once the stone columns are encased with geogrid under embankment loads, the consolidation time and settlement of the reinforced soft clays are reduced with a high degree. Therefore, the encasement causes a huge increase in the bearing capacity of the reinforced clay. Further reduction occurs in the settlement with increasing stiffness of the encasement. In contrast, the encasement stiffness has no significant effect on the consolidation time.
- Using encased stone columns with encasement stiffness of 800 kN/m reduces the total settlement to approximately one-eighth and quarter of the settlement of the non-reinforced and the reinforced Bremerhaven clay with ordinary stone columns, respectively. Using thus encased stone columns reduces also the total settlement to approximately one-sixth and one-third of the settlement of the non-reinforced and the reinforced Hamburg clay, respectively.
- The settlement in the ordinary stone column and in the surrounding soft soil is constant while there is a differential settlement between the encased stone columns and the surrounding soft soil. The differential settlement increases with increasing encasement stiffness which is clearer in the Hamburg clay.
- When the stone column is encased in the soft soils, its bulging decreases largely and becomes organized along the stone column. The lateral bulging of the encased stone columns decreases and be more organized with increasing geogrid stiffness.
- The higher the stiffness of the geogrid encasement is, the more the generated radial tension forces in the encasement and the more the enhancement in the reinforced soils behavior are.
- The encasement increases the overall stiffness of the stone columns which leads to increase the stress concentration in the encased stone columns.
- The increase of the encasement depth leads to increase the bearing capacity and to decrease the consolidation time. The full encased stone columns have the smallest settlement and the shortest consolidation time in comparison with the partially encased stone columns.
- The bulging of the column reduces to minimum values in all depth of the column when the column is encased completely. When the stone column is partially encased, its bulging in the encased zone is slightly smaller than that of the full encased column case. But the non-encased zone has higher values of the column bulging. The shallower the encasement depth is, the higher the lateral bulging values in the non-encased zone of the stone column are.
- When the partial encased stone column is loaded, the radial tension forces are implied. The tension forces in the partial encasement of the stone column are smaller than those of the full encasement. While the end points of the partial encasements have peak values of tension force which are larger than that of the full encasement at the same location.

- The excess pore water pressure decreases and dissipates rapidly with increasing encasement depth. The reduction and the dissipation acceleration of the excess pore water pressure are more significant at depths more than the depth of three times the column diameter.
- The deeper the encasement depth is, the more the stress transfer from the surrounding soil and the more the stress concentration in the column are.
- The rate of the reduction in the total stress during each consolidation phase of the soft soil increases also with increasing encasement depth. The greater the rate of the reduction of the total stress during a consolidation phase leads to a higher participation percentage of the stress concentration in the acceleration of the consolidation. Hence, using full encased stone columns provides the best performance of the reinforced soft soil in comparison with the partial encased stone columns.

In the third part, a case history of an embankment constructed on the reinforced soft soil with ordinary stone columns has been chosen to be simulated. The stone columns have a diameter of 0.8 m and a spacing distance between columns of 2.4 m. The stone columns, arranged in a square grid, extend through the soft soil layer for a depth of 6 m above the layer of the stiff clay. Plane strain and axisymetric techniques are used to simulate the embankment parts. The field measurements and the FEM results have been compared. The encased stone columns have been also used to reinforce the soft soil in the FEM analyses to imply the influence of the encasement on the behavior of the stone columns-soft soil foundation, as discussed in Chapter 9. The following conclusions can be made:

- There is a good agreement between the FEM results and the field measurements. The axisymetric model induces better agreement with field measurements than that of the plane strain model.
- The reinforced soft soil with encased stone column has a smaller settlement and a shorter consolidation time than those of the reinforced soft soil with ordinary stone columns. The reduction in the settlement is more significant with developing consolidation time and with increasing load and encasement stiffness.
- The excess pore water pressure in the reinforced clay with encased stone column decreases and its dissipation consumes shorter time in comparison with the reinforced clay with ordinary stone columns. The excess pore water pressure and its dissipation time decrease with increasing stiffness of the encasement.
- The effective vertical stress and the stress concentration in the encased stone columns are higher than those in the ordinary stone columns. The higher the encasement stiffness is, the higher the stress concentration in the column and the more the reduction in the total stress of the surrounding soft soil are which leads to more improvements in the behavior of the reinforced soft soil.

11 References

Alamgir, M. Miura, N. Poorooshasb, H. B. and Madhav, M. R. (1996). Deformation analysis of soft ground reinforced by columnar inclusions. Journal of Computers and Geotechnics 18, No. 4, 261-290.

Ali, Z. and Abolfazle, E. (2005). Determining the geotechnical parameters of stabilized soils by stone column based on SPT results. Electronic Journal of Geotechnical Engineering, 10A.

Al-Joulani, N. A. (1995). Laboratory and analytical investigation of sleeve reinforced stone columns. Ph.D Thesis of Carleton University, Ottawa, Canada.

Ambily, A. P. and Gandhi, S. R. (2007). Behavior of stone columns based on experimental and FEM analysis. ASCE, Journal of Geotechnical and Geoenvironmental Engineering 133, No. 4, 405-415.

Andreou, P., Frikha, W., Frank, R., Canou, J., Papadopoulos, V. and Dupla, J.C. (2008). Experimental study on sand and gravel columns in clay. Journal of Ground Improvement 161, No. 4, 189-198.

Bae, W., Shin, B. and An, B. (2002). Behavior of foundation system improved with stone columns. Proc. of the 12th international Offshore and Polar Engineering Conference, the Int. Society of Offshore and Polar Engineering, Kitakyushu, Japan, 675-678.

Balaam, N. P. and Booker, I. R. (1981). Analysis of rigid rafts supported by granular piles. International Journal for Numerical and Analytical Methods in Geomechanics 5, 379-403.

Balaam, N. P. and Booker, I. R. (1985). Effect of stone column yield on settlement of rigid foundations in stabilized Clay. International Journal for Numerical and Analytical Methods in Ceomechanics 9, 331-351.

Bergado, D. T. and Long, P. V. (1994). Numerical analysis of embankment on subsiding ground improved by vertical drains and granular piles. Proceeding of the XIII ICSMFE, New Delhi, India, 1361-1366.

Bergado, D. T., Anderson, L.R., Miura, N. and Balasubramaniam, A. S. (1996). Soft ground improvement in lowland and other environments. ASCE press, New York, USA. 427 pp.

Bergado, D. T., Asakami, H., Alfaro, M. C. and Balasubramaniam, A. S. (1991). Smear effects of vertical drains on soft Bangkok clay. ASCE, Journal of Geotechnical Engineering 117, No. 10, 1509-1530.

Black, J., Sivakumar, V. and McKinley, J. (2007). Performance of clay samples

reinforced with vertical granular columns. Canadian Geotechnical Journal 44, No. 1, 89-95.

Black, J., Sivakumar, V., Madhav, MR. and McCabe, B. (2006). An improved experimental test set-up to study the performance of granular columns. Geotechnical Testing Journal 29, No. 3, 193-199.

Borges, J. L., Domingues, T. S. and Cardoso, A. S. (2009). Embankments on soft soil reinforced with stone columns: numerical analysis and proposal of a new design method. Journal of Geotechnical and Geological Engineering 27, No. 6, 667-679.

Bouassida, M., Ellouze, S. and Hazzar, L. (2008) Investigating Priebe's method for settlement estimation of foundation resting on soil reinforced by stone columns. Proceedings of the Second International Workshop on Geotechnics of Soft Soils, Scotland, 321-325.

Castro, J. (2007). Pore pressure during stone column installation, Proceedings of the 18th European Young Geotechnical Engineers Conference, Ancona, Italy.

Castro, J. (2008). Theoretical analysis of the consolidation and deformation around stone column. Ph.D Thesis, Cantabria University, Cantabria, Spain.

Castro, J. and Sagaseta, C. (2008a). Influence of stone column deformation on surrounding soil consolidation. Proceedings of the Second International Workshop on Geotechnics of Soft Soils, Scotland, 333-338.

Castro, J. and Sagaseta, C. (2008b). Consolidation around stone columns. Influence of column deformation. International Journal for Numerical and Analytical Methods in Geomechanics 33, No. 7, 851-877.

Castro, J. and Sagaseta, C. (2009). Field instrumentation of an embankment on stone columns. Proceeding of the 17th ICSMGE, Alexandrina, Egypt.

Cheung, K. and Wagner, C. (1998). Geogrid reinforced light weight embankment on stone columns. Roading Geotechnics Conference: Geotechnical Society Proceedings, Auckland, New Zealand, 273-278.

Cho, S., Kim, B., Kim, Y. and Lee, S. (2005). Effect of soil compaction piles on settlement reduction in soft ground. International Journal of Offshore and Polar Engineering 15, No. 3, 235-240.

Christoulas, ST., Bouckovalas, G. and Giannaros, CH. (2000). An experimental study on model stone columns. Soils and Foundations Journal 40, No. 6, 11-22.

Deb, K. (2007). Modeling of granular bed-stone column-improved soft soil. International Journal for Numerical and Analytical Methods in Geomechanics 32, No. 10, 1267-1288.

Dipty, S. and Girish, M. (2009). Suitability of different materials for stone column construction. Electronic Journal of Geotechnical Engineering, 14M.

Egan, D., Scott, W. and McCabe, B. (2008). Installation effects of vibro replacement stone columns in soft clay. Proceedings of the Second International Workshop on Geotechnics of Soft Soils, Scotland, 23-29.

Elshazly, H., Elkasabgy, M. and Elleboudy, A. (2008). Effect of inter-column spacing on soil stresses due to vibro-installed stone columns: Interesting Findings. Journal of Geotechnical and Geological Engineering 26, No. 2, 225-236.

Elshazly, H., Hafez, D. and Mossaad, M. (2006). Back-calculating vibro-installation stresses in stone-column-reinforced soils. Journal of Ground Improvement 10, No. 2, 47-53.

Elshazly, H., Hafez, D. and Mossaad, M. (2007). Settlement of circular foundations on stone column-reinforced grounds. Journal of Ground Improvement 11, No. 3, 163-170.

Geduhn, M. (2005). Geokunststoffummantelte Vacuum-säulen Ein Gründungsverfahren für sehr weiche bindige Böden. Ph.D Thesis of Duisburg-Essen University, Essen, Germany.

Geduhn, M., Raithel, M. and Kempfert, H. G. (2001). Practical aspects of the design of deep geotextile coated sand columns for the foundation of a dike on very soft soils. Proceedings of the Int. Symposium “Earth Reinforcement"; Kyushu, Fukuoka, Japan, 545-548.

Gniel, J. and Bouazza, A. (2007). Methods used for the design of conventional and geosynthetic reinforced stone columns. Proceedings of the 10th Australia New Zealand Conference on Geomechanics - Common Ground, Brisbane Australia, Vol. 2, 72-77.

Gniel, J. and Bouazza, A. (2008). Numerical modeling of small-scale geogrid encased sand column tests. Proceedings of the Second International Workshop on Geotechnics of Soft Soils, Scotland, 143-149.

Greenwood, D. A. and Kirsch, K. (1983). Specialist ground treatment by vibratory and dynamic methods. Proceeding of the International Conference on Advances in Piling and Ground Treatment for Foundation, London, England, 17-45.

Guetif, Z., Bouassida, M. and Debats, J.M. (2007). Improved soft clay characteristics due to stone column installation. Computers and Geotechnics Journal 34, No. 2, 104-111.

Han, J. and Ye, S. L. (1991). Field tests of soft clay stabilized by stone columns in coastal areas in China. Proc. of the 4th International Conference on Piling and Deep Foundations, Stresa, Italy, 243-248.

Han, J. and Ye, S. L. (1992). Settlement analysis of buildings on the soft clays

stabilized by stone columns. Proc. of the International Conference on Soil Improvement and Pile Foundations, Nanjing, China, 446-451.

Han, J. and Ye, S. L. (2001). Simplified method for consolidation rate of stone column reinforced foundations. ASCE, Journal of Geotechnical and Geoenvironmental Engineering 127, No. 7, 597-603.

Hughes, J.M.O. and Withers, N.J. (1974). Reinforcing of soft cohesive soils with stone columns, *Ground Engineering* Journal 7, No. 3, 42-49.

Keller Grundbau (2002). Die Tiefenrüttelverfahren. Firmenprospekt 10-02D

Kempfert, H. G. (1996). Embankment foundation on geotextile-coated sand columns in soft ground. Proceedings of the First European Geosynthetic conference EurGeo 1, Maastrict, Netherlands, 245-250.

Kempfert, H. G. (2003). Ground improvement methods with special emphasis on column-type techniques. Keynote lecture. Proc. Int. Workshop on Geotechnics of Soft Soils-Theory and Practice. Netherlands, 101-112.

Kempfert, H. G., Joup, A. and Raithel, M. (1997). Interactive behavior of flexible reinforced sand column foundation in soft soils. Proc. of the 13th International Conf. on Soil Mech. and Found. Eng. Hamburg 3, Germany, 1757-1760.

Kempfert, H. G., Mobius, W., Wallis, P., Raithel, M., Geduhn, M. and Mcclinton, R. G. (2002). Reclaiming land with geotextile encased columns. Geotechnical Fabric Report Journal 20, (6), 34-39.

Khabbazian, M., Kaliakin, V. N. and Meehan, C. L. (2009). 3D Numerical analyses of geosynthetic encased stone columns. Proc. of the International Foundations Congress and Equipment Expo (IFCEE09), Contemporary Topics in Ground Modification, Problem Soils, and Geo-Support, Geotechnical Special Publication 187, Orlando, ASCE, Reston, USA, 201-208.

Kirsch, F. (2004). Experimentelle und numerische Untersuchungen zum Tragverhalten von Rüttelstopfsäulengruppen. Ph.D Thesis of Braunschweig University, Braunschweig, Germany.

Kirsch, F. (2006). Vibro stone column installation and its effect on the ground improvement. Proc. of the International Conference on “Numerical Simulation of Construction Process in Geotechnical Engineering for Urban Environment”, Bochum, Germany 115-124

Kirsch, F. (2008). Evaluation of ground improvement by groups of vibro stone columns using field measurements and numerical analysis. Proceedings of the Second International Workshop on Geotechnics of Soft Soils, Scotland, 241-248

Kirsch, F. and Sondermann, W. (2003). Field measurements and numerical analysis of

the stress distribution below stone column supported embankments and their stability. Int. Vermeer et al. (Eds.) Geotechnics of Soft Soils - Theory and Practice, Essen: VGE, S., Germany, 595-600

Koerner, R. M. (2000). Emerging and future development of selected geosynthetic applications. ASCE, Journal of Geotechnical and Geoenvironmental Engineering 125, No. 4, 293-306.

Lee, J. S. and Pande, G. N. (1998) Analysis of stone-column reinforced foundations. International Journal for Numerical and Analytical Methods in Geomechanics 22, No.12. 1001-1020.

Li, G, Huang, W. and Ugai, K. (2000). Interactions between column inclusion and surrounding soil in composite ground. International Journal of Lowland Technology (IALT) 2, No. 1, 23-34.

Madhav, M.R., Alamgir, M. and Miura, N. (1994). Improving granular column capacity by geogrid reinforcement. Proceedings of the Fifth International Conference on Geotextiles, Geomembranes and Related Products, vol. 1, Singapore, 351-356.

Malarvizhi, S.N. and Ilamparuthi, K. (2004). Load versus settlement of clay-bed stabilized with stone and reinforced stone columns. Proceeding of the 3rd Asian Regional Conference on Geosynthetics, GEOASIA, Seoul, Korea, 322-329.

Malarvizhi, S.N. and Ilamparuthi, K. (2006). Modeling of geogrid encased stone column. Proceedings of the 2nd International Congress on Computational Mechanics and Simulation (ICCMS-06), IIT Guwahati, India.

Malarvizhi, S.N. and Ilamparuthi, K. (2007). Comparative study on the behavior of encased stone column and conventional stone column. Soils and Foundations Journal 47, No. 5, 873-885.

Mckelvey, D., Sivakumar, V., Bell, A. and Graham, J. (2004). Modelling vibrated stone columns in soft clay. Journal of Geotechnical Engineering 157, No. 3,137-149.

Mitchell, J. K. and Huber, T. R. (1985). Performance of a stone column foundation. Journal of Geotechnical Engineering 111, No. 2, 205-223.

Murugesan, S. and Rajagopal, K. (2006). Geosynthetic-encased stone columns: numerical evaluation. Geotextiles and Geomembranes Journal 24, No. 6, 349-358.

Murugesan, S. and Rajagopal, K. (2008). Performance of encased stone columns and design guidelines for construction on soft clay soils. Proceedings of the 4th Asian Regional Conference on Geosynthetics, Shanghai, China, 729-734.

Murugesan, S. and Rajagopal, K. (2009). Investigations on the behavior of geosynthetic encased stone columns. Proc. of the 17th ICSMGE, Alexandrina, Egypt.

NAUE GmbH & Co. KG, Espelkamp, Germany.

Plaxis Manual (2008). Finite Element Code for Soil and Rock Analysis Program, Version 9.

Poorooshasb, H. B. and Meyerhof, G. G. (1997). Analysis of behavior of stone columns and lime columns. Journal of Computers and Geotechnics 20, No. 1, 47-70.

Priebe, H. J. (1995). Design of vibro replacement. *Ground Engineering* Journal 28, No. 10, 31-37.

Raithel, M. (1999). Zum Trag- und Verformungsverhalten von Geokunststoffummantelten Sandsäulen. Ph.D Thesis of Kassel University, Kassel, Germany.

Raithel, M. and Kempfert, H. G. (2000). Calculation models for dam foundations with geotextile coated sand columns. Proceeding of the International Conference on Geotechnical and Geological Engineering, Melbourne, Australia.

Raithel, M., Küster, V. and Lindmark, A. (2004). Geotextile-encased columns - a foundation system for earth structures, illustrated by a dyke project for works extension in Hamburg. Nordic Geotechnical Meeting NGM, Ystad, Sweden.

Raju, V. R. (1997). The behaviour of very soft soils improved by vibro replacement. Ground Improvement Conference, London. England.

Raju, V. R. and Hoffmann, G. (1996). Treatment of tin mine tailings in Kuala Lumpur using vibro replacement. Proc. of the 12th South East Asian Geotechnical Conference, Kuala Lumpur, Malaysia.

Richwien, W. (1981). Das Formänderungs- und Festigkeitsverhalten weicher bindiger Böden. Mitteilungen Institut für Grundbau, Bodenmechanik und Energiewasserbau, Universität Hannover. Heft 18.

Samieh, A. M. (2002). Analyses of earth embankment constructed in soft clay reinforced by stone columns. Proc. of the 5th European Conference of Numerical Methods in Geotechnical Engineering, Paris, France, 471-478.

Saroglou, H., Antoniou, A. A. and Pateras, S. K. (2008). Ground improvement of clayey soil formations using stone columns: a case study from Greece. International Journal of Geotechnical Engineering 3, No. 4, 493-498.

Satibi, S. (2009). Numerical analysis and design criteria of embankments on floating piles. Ph.D Thesis of University of Stuttgart, Stuttgart, Germany.

Shahu, J.T. (2006). Non-uniform granular pile–mat foundations: analysis and model tests. Journal of Geotechnical and Geological Engineering 24, No. 4, 1065-1087.

Shahu, J.T., Hayashi, S. and Madhav, M.R. (2000). Analysis of soft ground reinforced by non-homogeneous granular pile-mat system. Lowland Technology International, Journal of International Association of Lowland Technology 2, No. 2, 71-82.

Sharma, R. S., Kumar, B. P. and Nagendra, G. (2004). Compressive load response of granular piles reinforced with geogrids. Canadian Geotechnical Journal 41, No. 1, 187-192.

Sivakumar, V., Glynn, D., Black, J. and McNeill, J (2007). A laboratory model study of the performance of vibrated stone columns in soft clay. Proc. of the 11th European Conference on Soil Mechanics and Geotechnical Engineering, Madrid, Spain, 1545-1550.

Sivakumar, V., McKelvey, D., Graham, J. and Hughes, D. (2004). Triaxial tests on model sand column in clay. Canadian Geotechnical Journal 41, No. 2, 299-312.

Stewart, D. and Fahey, M. (1994). An investigation of the reinforcing effect on stone columns in soft clay. Proc. of Settlement 94', In Vertical and Horizontal Deformation of Foundations and Embankments, ASCE, Geotechnical Special Publication, No. 40, 513-524

Tan, S. A., Tjahyono and Oo, K. K. (2008). Simplified plane-strain modelling of stone-column reinforced ground. ASCE, Journal of Geotechnical and Geoenvironmental Engineering 134, No. 2, 186-194.

Weber, T. (2006), Centrifuge modeling of ground improvement under embankments. Pollack Periodica Journal 1, No. 2, 3-15.

Weber, T. (2008). Modellierung der Baugrundverbesserung mit Schottersäulen. Ph.D Thesis of Geotechnical Engineering Institute of Zürich, Zürich, Switzerland.

Wehr, J., Karstunen, M. and others. (2007). Ground improvement and reinforcement. European Plaxis Users Meeting, Karlsruhe, Germany.

Wood, D., Hu, W. and Nash, D. F. T. (2000). Group effects in stone column foundations model tests. *Géotechnique* Journal 50, No. 6, 689-698.

Xu, X. T., Liu, H. L. and Lehane, B. M. (2006). Pipe pile installation effects in soft clay. Journal of Geotechnical Engineering 159, No. 4, 285-296.

Zhang, R. and Lo, S.R. (2008). Analysis of geosynthetic reinforced stone columns in soft clay. Proceedings of the Forth Asian Regional Conference on Geosynthetics, Shanghai, China, 735-740.